Theses and Dissertations | 1. Thesis and Dissertation Collection, all items

1996-09

Low-power high-speed dynamic logic families for complementary gallium arsenide (CGaAs) fabrication processes

Shehata, Khaled Ali

Monterey, California. Naval Postgraduate School

http://hdl.handle.net/10945/8639

NAVAL POSTGRADUATE SCHOOL
Monterey, California

DISSERTATION

LOW-POWER HIGH-SPEED
DYNAMIC LOGIC FAMILIES FOR
COMPLEMENTARY GALLIUM ARSENIDE (CGaAs)
FABRICATION PROCESSES

by

Khaled Ali Shehata

September 1996

Dissertation Advisor: Douglas J. Fouts

Approved for public release; distribution is unlimited.

REPORT DOCUMENTATION PAGE

Public reporting burden for this collection of information is estimated to average 1 hour per response, including the time reviewing instructions, searching existing data sources, gathering and maintaining the data needed, and completing and reviewing the collection of information. Send comments regarding this burden estimate or any other aspect of this collection of information, including suggestions for reducing this burden to Washington Headquarters Services, Directorate for Information Operations and Reports, 1215 Jefferson Davis Highway, Suite 1204, Arlington, VA 22202-4302, and to the Office of Management and Budget, Paperwork Reduction Project (0704-0188), Washington, DC 20503

1. AGENCY USE ONLY (Leave Blank)	2. REPORT DATE September 1996	3. REPORT TYPE AND DATES COVERED Ph.D. Dissertation

4. TITLE AND SUBTITLE

LOW-POWER HIGH-SPEED DYNAMIC LOGIC FAMILIES FOR COMPLEMENTARY GALLIUM ARSENIDE (CGaAs) FABRICATION PROCESSES

5.

6. AUTHOR(S)

Khaled Ali Shehata.

7. PERFORMING ORGANIZATION NAME(S) AND ADDRESS(ES)

Naval Postgraduate School
Monterey, CA 93943-5000

8. PERFORMING ORGANIZATION

9. SPONSORING/ MONITORING AGENCY NAME(S) AND ADDRESS(ES)

10. SPONSORING/ MONITORING AGENCY REPORT NUMBER

11. SUPPLEMENTARY NOTES

The views expressed in this dissertation are those of the author and do not reflect the official policy or position of the Department of Defense or the United States Government.

12a. DISTRIBUTION / AVAILABILITY STATEMENT

Approved for public release; distribution is unlimited

12b. DISTRIBUTION CODE

13. ABSTRACT (Maximum 200 words)

The design and evaluation of several different low-power, high-speed, high-density complementary gallium arsenide (CGaAs) dynamic logic families that are compatible with existing CGaAs fabrication processes and design tools are documented. Circuits studied include Domino logic, N-P Domino logic and Two-Phase Dynamic FET Logic (TPDL). The TPDL circuits have been implemented and fabricated. The dynamic circuits are evaluated and compared with typical static logic circuits for speed, power consumption and layout area.

Dynamic circuits are non-ratioed logic. Therefore, the transistor sizes can be minimized to reduce the layout area and the power dissipation of the circuits. Furthermore, dynamic circuits are faster than static circuits because they do not use PFETs for evaluation, only for precharging. Dynamic circuits consume less power than the static circuits because they have no short-circuit current and a reduced leakage current (only switching current flows in the dynamic circuits). This means that CGaAs dynamic logic circuits have higher speed than Directly-Coupled FET Logic (DCFL) and lower power consumption than complementary GaAs logic.

14. SUBJECT TERMS

GaAs, Dynamic Logic, CHIGFET, CGaAs, Two-Phase Dynamic FET Logic, TPDL, Clock Generator, Domino logic, N-P Domino logic, CLA, static logic.

15. NUMBER OF PAGES

281

16. PRICE CODE

17. SECURITY CLASSIFICATION OF REPORT Unclassified	18. SECURITY CLASSIFICATION OF THIS PAGE Unclassified	19. SECURITY CLASSIFICATION OF ABSTRACT Unclassified	20. LIMITATION OF ABSTRACT UL

13. The TPDL circuits designed for this dissertation are the fastest low-power logic circuits ever reported in this technology. The use of TPDL in CGaAs technology will enhance the CGaAs advantages by increasing the maximum speed and reducing the power dissipation. CGaAs TPDL is an excellent candidate for the next generation of high speed, high density and low power ICs and is ideal for digital signal processing and digital communication ICs.

LOW-POWER HIGH-SPEED
DYNAMIC LOGIC FAMILIES FOR
COMPLEMENTARY GALLIUM ARSENIDE (CGaAs)
FABRICATION PROCESSES

Khaled Ali Shehata
Lt. Col., Egyptian Air Force
B.S., Military Technical College, Cairo, Egypt, 1981
M.S., Cairo University, Cairo, Egypt, 1991

DOCTOR OF PHILOSOPHY IN ELECTRICAL
AND COMPUTER ENGINEERING

from the

NAVAL POSTGRADUATE SCHOOL
September 1996

ABSTRACT

The design and evaluation of several different low-power, high-speed, high-density complementary gallium arsenide (CGaAs) dynamic logic families that are compatible with existing CGaAs fabrication processes and design tools are documented. Circuits studied include Domino logic, N-P Domino logic and Two-Phase Dynamic FET Logic (TPDL). The TPDL circuits have been implemented and fabricated. The dynamic circuits are evaluated and compared with typical static logic circuits for speed, power consumption and layout area.

Dynamic circuits are non-ratioed logic. Therefore, the transistor sizes can be minimized to reduce the layout area and the power dissipation of the circuits. Furthermore, dynamic circuits are faster than static circuits because they do not use PFETs for evaluation, only for precharging. Dynamic circuits consume less power than the static circuits because they have no short-circuit current and a reduced leakage current (only switching current flows in the dynamic circuits). This means that CGaAs dynamic logic circuits have higher speed than Directly-Coupled FET Logic (DCFL) and lower power consumption than complementary GaAs logic.

The TPDL circuits designed for this dissertation are the fastest low-power logic circuits ever reported in this technology. The use of TPDL in CGaAs technology will enhance the CGaAs advantages by increasing the maximum speed and reducing the power dissipation. CGaAs TPDL is an excellent candidate for the next generation of high speed, high density and low power ICs and is ideal for digital signal processing and digital communication ICs.

TABLE OF CONTENTS

LIST OF FIGURES

xiv

LIST OF TABLES

LIST OF SYMBOLS AND ACRONYMS

BFL	Buffered FET Logic
CCL	Capacitor-Coupled FET Logic
CDFL	Capacitor-Diode FET Logic
CGaAs	Complementary Gallium Arsenide
CLA	Carry Lookahead Adder
CMOS	Complementary Metal Oxide Semiconductor
DCFL	Directly-Coupled FET Logic
DFET	Depletion-Mode FIeld Effect Transistor
ECL	Emitter Coupled Logic
EFET	Enhancement-Mode Field Effect Transistor
FET	Field Effect Transistor
GaAs	Gallium Arsenide
HFET	Hetrostructure Field Effect Transistor
HIGFET	Hetrostructure Isolated Gate Field Effect Transistor
IC	Integrated Circuit
JFET	Junction Field Effect Transistor
LSI	Large Scale of Integration
MESFET	Metal Semiconductor Field Effect Transistor
MODFET	Modulation Doped Field Effect Transistor
MOSFET	Metal Oxide Semiconductor Field Effect Transistor
MSI	Medium Scale of Integration
SBFL	Super-Buffer FET Logic
SCFL	Source-Coupled FET Logic
SDFL	Schottky Diode FET Logic
SSI	Small Scale of Integration
TPDL	Two-Phase Dynamic Logic
V_{DS}	Drain to Source Voltage
V_{GS}	Gate to Source Voltage
VLSI	Very Large Scale of Integration
VTN	Threshold Voltage of NFET
VTP	Threshold Voltage of PFET
Wn	NFET Gate Width
Wp	PFET Gate Width

ACKNOWLEDGEMENTS

I. INTRODUCTION

The objective of the research documented in this dissertation is to investigate different static and dynamic logic families that can be implemented in a GaAs Complementary Hetrostructure Isolated Gate (CHIGFET) process. Key points in the analysis of different designs are to maximize speed and minimize both consumed power and layout area. In addition, the logic circuits should be suitable for VLSI implementations. The dynamic logic families discussed in this dissertation include Domino logic, N-P Domino logic and Two-Phase Dynamic Logic (TPDL).

In this chapter, the history of the development of GaAs is introduced in Section A. A comparison between the electrical properties of GaAs and silicon is discussed in Section B. Section C discusses different GaAs devices. Section D discusses static logic families, while Section E explains well-known dynamic logic families. Section F outlines the rest of the dissertation.

A. HISTORICAL REVIEW OF GALLIUM ARSENIDE (GaAs)

Gallium Arsenide (GaAs) is a compound semiconductor that has been used since the 1960's for microwave amplifiers and optical-electronic devices. In the opto-electronic area, GaAs is used for light emitting diodes, solid state lasers, and optical sensors. GaAs transistors, both FET (Field Effect Transistor) and HBT (Hetrostructure Bipolar junction Transistor), are used for digital integrated circuits, primarily when the application requires very high speed and the delay and power requirements of silicon CMOS or bipolar ICs are too high. The high-frequency performance of GaAs digital ICs is excellent. The high electron velocity at moderate electric fields improves the high-frequency performance of GaAs transistors. The fast switching capabilities of these devices is based on their low internal capacitances and on their high electron velocity.

The use of GaAs for digital applications began in 1974 with some relatively high-power, high-speed SSI divider circuits and has developed over the years into a well-established LSI technology, with some inroads into the VLSI arena. Initially, GaAs

integrated circuits appeared in digital fiber-optic communication systems [1, 2, 3, 4, 5]. However, the demand for faster computers requires faster logic circuits. The feasibility of using GaAs technology to build the next generation of computers has been demonstrated. Experimental GaAs RAMs, parallel multipliers, microprocessors and other computer circuits with a cycle time of a few nanoseconds or less have been reported [6, 7, 8, 9].

B. COMPARISON BETWEEN GALLIUM ARSENIDE (GaAs) AND SILICON (SI) ELECTRICAL PROPERTIES

1. Electron Mobility

The resistivity of a doped semiconductor is dependent upon the doping density (the number of charge carriers present within the material) and also upon the ease with which these carriers can move under the application of an electric field. This later property is known as the carrier mobility, which is defined as the ratio of the carrier velocity to the electric field strength. The primary advantage of GaAs over Si is that the electron mobility of GaAs is approximately five times that of Si, which offers a higher speed of operation than that achievable using Si devices [3, 10, 11, 12, 13, 14]. The disadvantage of GaAs is the relatively high power dissipation per logic gate during low-speed operation, small logic swing and correspondingly narrow noise margins. Low logic density, as a result of layout restrictions and low manufacturing yield, are also disadvantages of GaAs logic.

Digital IC technologies are usually compared using a "power-delay product" parameter which is calculated by multiplying the logic gate delay by the power dissipated per gate. A high power delay product implies that either the gate power dissipation is high (limiting the integration density and increasing power consumption), or that the gate delay is high (limiting the speed performance of the technology). GaAs has a power-delay product advantage over Si in the vicinity of four to five times, which is principally determined by the high electron mobility.

2

2.   Semi-insulating Substrate

When semiconductor devices are fabricated together on an IC, it is important that any interaction between them which might negatively affect the performance of the complete circuit be kept to a minimum. Thus, the integrated components must be electrically isolated from each other. The resistivity of a semiconductor is dependent on the doping level. Silicon technologies generally use a doped N-type or P-type substrate with devices fabricated in oppositely doped "wells" to provide sufficient device isolation at relatively small separations. In comparison, the intrinsic resistivity of GaAs is several orders of magnitude higher, falling into the "semi-insulating" range [13, 15, 16]. This property allows GaAs devices to be fabricated in wells in un-doped substrate while still maintaining good isolation. The principal advantage of this is the reduced parasitic capacitance in GaAs ICs compared to that of silicon ICs [12, 13].

3.   Radiation Hardness

The immunity of an IC to damage from exposure to radiation is important for many applications. Military, space, and nuclear systems have certain requirements for radiation hardness. Other applications may also be affected if the IC is sensitive to radiation naturally occurring radiation from sources in the environment or packaging. GaAs has an advantage over silicon, depending on the type of radiation concerned. Radiation can ionize the atoms in a material. The total ionized charge produced depends on the total radiation dose. GaAs FETs have higher immunity than silicon ICs to total dose effects from ionizing radiation and only undergo a small change in their operating parameters [17]. GaAs has a high density of energy states at the surface which absorbs charge produced by radiation and thus minimizes changes in device parameters such as threshold voltage and parasitic resistance. It also prevents large surface leakage currents from occurring. The sensitivity of device characteristics to a radiation pulse is defined as the transient radiation hardness. The resulting transient radiation current may occur in two regions, within the active device or in the substrate [18]. In GaAs ICs, the dominant effects are due to substrate current. The

wider band gap of GaAs over that of Si (excluding Silicon On Sapphire-SOS) makes it harder to generate carriers and thus the sensitivity of GaAs to transient radiation is relatively low, provided that high quality, un-doped substrates are used.

4. Hole Mobility

The hole mobility of GaAs is lower than that of silicon by a factor of approximately five. Therefore, devices based upon the use of P-type GaAs will be slower than those based upon P-type silicon. Also, P-channel GaAs FETs have a higher channel resistance which degrades speed compared to silicon [13].

5. Other Properties

One of the major disadvantages of Complementary GaAs, compared to silicon, is the cost factor. This high cost occurs for several reasons. The biggest cause of the relatively high cost of Complementary GaAs ICs is the fact that yields are low and wafer sizes are small compared to silicon [13]. This means that there are fewer working devices per wafer over which the processing costs can be shared.The material costs are higher (GaAs crystals are difficult to grow and IC production sometimes uses gold-based metallization). In practice, this means the use of Complementary GaAs is restricted to high speed applications where high cost can be tolerated in order to obtain a degree of performance that is not available from silicon ICs.

Thermal conductivity is also an important property. High thermal conductivity is required to dissipate the heat generated by an IC during operation. GaAs has lower thermal conductivity than silicon. Thus, a GaAs IC runs hotter than a silicon IC when dissipating the same power. Also, thermal gradients across the surface of a GaAs chip are more severe. Thinning the substrate of GaAs ICs will aid in reducing this problem.

C. GaAs DEVICES

The Gallium Arsenide transistor with a diffusion gate structure, which was first reported in 1967, yields useful gain in the low megahertz frequency band. In 1969, the

silicon field effect transistor (FET) was developed with a 1 μm gate length. In 1971, a significant step was made when 1 μm gate length FETs on GaAs were developed with a useful gain up to 18 GHz.

Oxide growth has been tried on GaAs surfaces for more than 20 years. The quality of oxide grown on GaAs has been poor, and a high density of surface states results at the GaAs-insulator interface. These effects make it difficult to fabricate GaAs MOSFETs. Schottky barrier MESFETs and Junction Field Effect transistors (JFET) are examples of practical GaAs FETs. In many cases, these devices are fabricated by direct implantation into a GaAs semi-insulating substrate. Both enhancement and depletion MESFETs can be fabricated and each has advantages, depending on the application. The JFET is basically a voltage controlled resistor that employs a p-n junction as a gate to control the resistance, and thus the current that flows, between two ohmic contacts. The JFET has a lower switching speed than the MESFET because of the higher input edge capacitances in a planner JFET processes. The advantage of JFETs is that complementary logic is possible because n-p and p-n junctions can be fabricated on the same wafer.

The development of advanced epitaxial growth techniques such as Molecular Beam Epitaxy (MBE) in the 1970s has enabled the fabrication of useful high quality semiconductor hetrostructures. The original concept of hetrojunction FETs (HFETs) came from experimental observation of enhanced electron mobility in modulation-doped hetrostructures. The term modulation doping has led to the name MODFET for the first generation of HFETs.

1. Noise in Digital Circuits

Noise in a digital circuit can be classified as either internal or external. External noise is generated outside the integrated circuit of interest, such as power supply ripple or electrostatic discharge. Internal noise is generated inside the integrated circuit of interest, such as mutual inductance and/or capacitance (cross-talk) between signal lines, inductive and resistive voltage spikes, power supply and ground leed voltage drop, interconnect

reflections, etc. A practical IC must be able to tolerate both types of noise in order to operate successfully and reliably in the intended application.

The dc noise margins are the parameters that measure the ability of a circuit to operate error-free in a noisy environment. The noise margins of digital logic circuits can be measured in many different ways. Slope = -1 noise margin, intrinsic noise margin and maximum width noise margin are examples of the methods to measure noise margin of digital circuits. The factors that influence the noise margins are the voltage gain and the symmetry of the transfer characteristics of the circuit. As the voltage gain increases, the slope of the output voltage in the transition region increases and consequently the noise margins are increased. When the transfer curve of a digital circuit is symmetric, the noise margin low is equal to the noise margin high.

The dynamic noise margin refers to the ability of a circuit to maintain a constant output when a short-duration noise pulse is present on the input. It depends on both the width and the magnitude of the input pulse. As the width of the input pulse decreases, a greater magnitude will be required to upset the output of the circuit and vise versa.

2.   Power Dissipation in GaAs Circuits

When designing a GaAs digital circuit, the first parameters optimized are usually the noise margins. Then, the speed and the dissipated power can be optimized. GaAs digital circuits dissipate two types of power, static power and dynamic power. Static power is dissipated due to current flow from supply to ground or supply to supply during at least one logic state. Dynamic power is dissipated during switching due to the charging and discharging of the capacitive load. The total power dissipated by the circuit is the sum of both types.

3.   Depletion-Mode Logic Circuits

N-type depletion-mode FETs (DFETs) are ON when $V_{GS} = 0$ and require a negative V_{GS} to cut off the flow of drain current. V_{DS} is usually kept positive all the time. Logic circuits containing only DFETs are characterized by unequal input and output voltage

6

levels and the need for level shifting networks. Both negative and positive signals are required, thus two power supplies are needed, leading to an increase in power dissipation and system-level design complexity. The use of two power supplies also makes this type of logic more susceptible to backgating effects. The backgating effect is the phenomenon of depleting the back side of the channel from charges when the substrate is negative with respect to the source, causing an increase in the threshold voltage which decreases the drain current and subsequently reduces the switching speed. The main advantage of DFET-only logic is the increased voltage transition which increases both the noise margin and the yield.

4. Enhancement/Depletion Mode Logic Circuits

This logic family requires both enhancement and depletion-mode FETs. Its main advantage over DFET-only logic is the equal input and output voltage levels. Therefore, there is no need for level shifting networks, which saves layout area. It also requires only one power supply with a value less than that of depletion-mode only logic circuits. The small logic transition provided by this type of logic leads to a higher speed and lower power dissipation compared to depletion-mode logic families. The main drawback of this family is that the small logic transition makes it sensitive to parameter variations, especially the threshold voltage. Therefore, it requires a uniformity of threshold voltage between components and between wafers.

D. GaAs MESFET STATIC LOGIC CIRCUITS

MESFET static logic families are ratioed logic, meaning that their high and low logic levels are determined by the width and length ratios of the load and switching FETs. GaAs MESFET static logic families dissipate static power, due to the current flow from the supply voltage to ground. Therefore, their performance is tied to constant power-delay curves. The main property that distinguishes the design of GaAs FET circuits from CMOS circuits is the forward bias gate conduction that results from the Schottky barrier at the gate/channel junction of the FET. This gate conduction clamps the upper value of V_{GS} (gate to

source voltage) to about 0.7 volts, the voltage required to forward bias the Schottky barrier diode.

The design of GaAs digital logic circuits is a multidimensional problem. The circuit design problem is much more difficult than silicon MOS circuit design because there are few standards established for logic levels and supply voltages, and no preferred or obviously superior circuit topology has dominated design at the present time. The threshold voltages of both depletion and enhancement-mode FETs are different from one foundry to another, and a relatively wide variance from the mean threshold voltage is allowed. Therefore, the GaAs user must utilize a more general set of design methodologies than is necessary to complete the design of a standard NMOS or CMOS silicon IC [12].

The approach taken to optimize the design will depend on the application in which the circuit will be used. Speed and consumed power can be traded off over a range of about five to one for most circuits, without changing the threshold voltage. Speed and circuit tolerance to process variation, supply voltage or ground fluctuations, or temperature variations are also interchangeable to a degree because a circuit with a low logic transition will exhibit less delay than one that is designed with a larger logic transition and therefore is more robust in a digital system application [12]. The highest priority is assigned to the dc functionality of the circuit (noise margin and delay) over the expected range of process parameters and operating temperatures. Without satisfying this prerequisite, the maximum operating speed of the designed circuit has no significance. The following sections describe the relevant design details for the most commonly used static logic gate families.

1.   Directly-Coupled FET Logic (DCFL)

DCFL has the lowest power consumption and highest logic function density. It is also the simplest form of the static logic families. It uses an E-MESFET for the switch device and D-MESFET for the load device. Figure 1.1 shows a DCFL inverter whose output logic high voltage will move towards V_{DD} when the switch is off, but be clamped by the forward biased gate-channel Schottky diode at the input of the next switch device. This limits the

output high voltage to about 0.7 V ($V_{OH} = 0.7$ V) and reduces the noise margins of this family. The key point for correct operation is to decrease the output low voltage (V_{OL}) below the threshold voltage of the E-MESFET switch device. Design of the inverter involves scaling the device gate widths and lengths so as to get an acceptable logic low and a reasonable noise margin [2, 19, 20].

Due to its low noise margin, only basic logic gates can be reliably fabricated. NAND gates are not recommended in this logic family since they use two series E-MESFETs which degrades the noise margin.
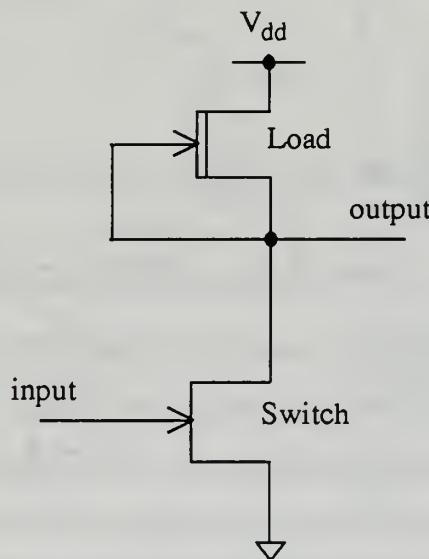
Figure 1.1: Directly-Coupled FET Logic (DCFL) Inverter

2.   Buffered FET Logic (BFL)

DCFL circuits are difficult to make due to the need to integrate enhancement and depletion mode MESFETs. The BFL family uses only D-MESFETs, Figure 1.2 shows a BFL inverter. The use of the D-MESFET as a switch device requires that the input voltage transition must be negative (below the threshold voltage) to turn the device off. Because the output of the inverter can not fall below zero, a level shifting stage (D1, D2, Q4) is used to shift the output negatively which requires another power supply (V_{ss}). Q3 is a source-

follower used to increase the drive capability and increase the speed of this logic family [21]. Unbuffered logic is derived from BFL by eliminating the source follower Q3 and connecting the drain of Q1 directly to D1. This can be done when the drive capability of BFL is not needed.

In comparison to DCFL, BFL has a much higher power dissipation due to the extra level shifting stage and the use of two voltage rails. The buffering circuit provides a lower propagation delay and higher drive capability. Also, fabrication of BFL circuits is easier than that of DCFL because it uses only D-MESFETs and has much better tolerance to variations in MESFET characteristics.
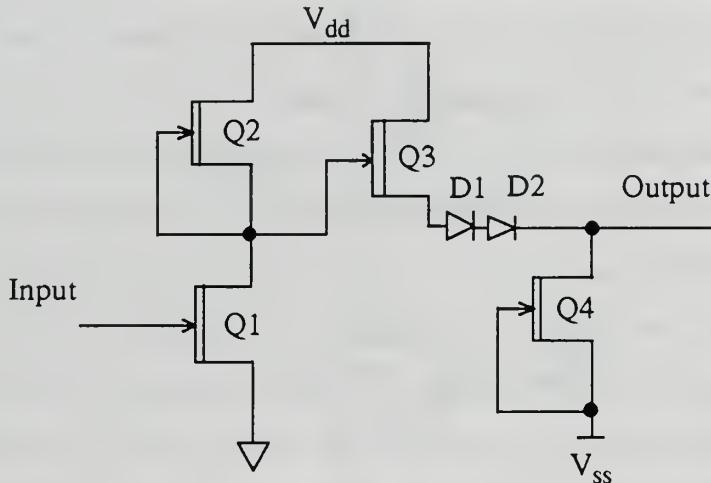
Figure 1.2: Buffered FET Logic (BFL) Inverter

3. Schottky Diode FET Logic (SDFL)

When the power dissipation of BFL is too high, the level shifting stage can be moved from the output to the input of the gate. The diodes can be used as switching elements rather than using them only for level shifting purposes, resulting in a new logic family called SDFL. The diodes have low capacitance, low series resistance and there is no minority carrier charge storage problems as with p-n junction diodes. Therefore, if used for switching, a saving in area is also possible. Figure 1.3 shows the circuit of a three inputs

SDFL NOR gate. In this family, the output of the level shifting stage will drive only one logic gate, less drive capability is required, much smaller devices can be used and correspondingly the power dissipation is reduced [22, 23, 24, 25].
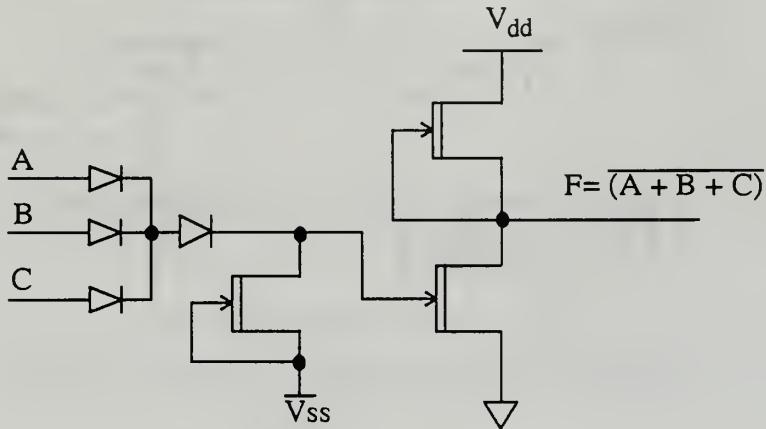
Figure 1.3: Three-input Schottky Diode FET Logic (SDFL) NOR Gate

4.   Source-Coupled FET Logic (SCFL)

Source Coupled FET Logic (SCFL) uses a differential gate topology as shown in Figure 1.4. It is analogous to bipolar emitter coupled logic (ECL). SCFL is the fastest form of GaAs MESFET logic [26]. It uses differential amplifier circuits which provide the benefit of good common-mode rejection. This property is advantageous because any wafer-to-wafer variation in the threshold voltage becomes a common mode voltage and will not affect the switching threshold of the circuit. This leads to a design tolerable to FET threshold variation when compared to DCFL. Another advantage of differential circuits is their high transconductance, g_m, leading to a high cut-off frequency and a better switching speed than DCFL. SCFL has good noise margins because it is differential. The circuit operates by steering a fixed current through a pair of switches and then using this current to develop a voltage drop across one of a pair of load devices [27]. The main drawback of SCFL is the high power consumption. Also, the differential circuit requires routing of all

variables and their complement, which increases the metallization and wiring area, leading to increases in the parasitic capacitances in the circuit.
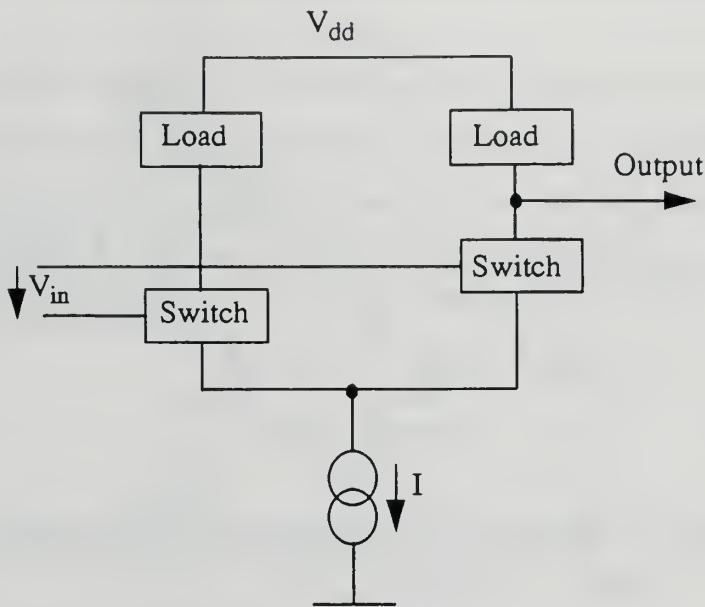
Figure 1.4: Source-Coupled FET Logic (SCFL) Inverter (Differential Inputs)

5. Alternative Logic Families

There are many families other than DCFL, BFL, SDFL, and SCFL with various levels of performance. In the following sections, these families are discussed very briefly.

a. Capacitor-Coupled Logic (CCL)

This logic family uses a coupling capacitor between stages to give the necessary level shifting to drive D-MESFET-only logic. CCFL offers lower power consumption than BFL and SDFL due to the absence of any power consuming level shifting stage [28]. The capacitance in CCL is implemented with a reversed biased Schottky diode [29]. Figure 1.5 shows the circuit diagram of two CCL cascaded inverters.
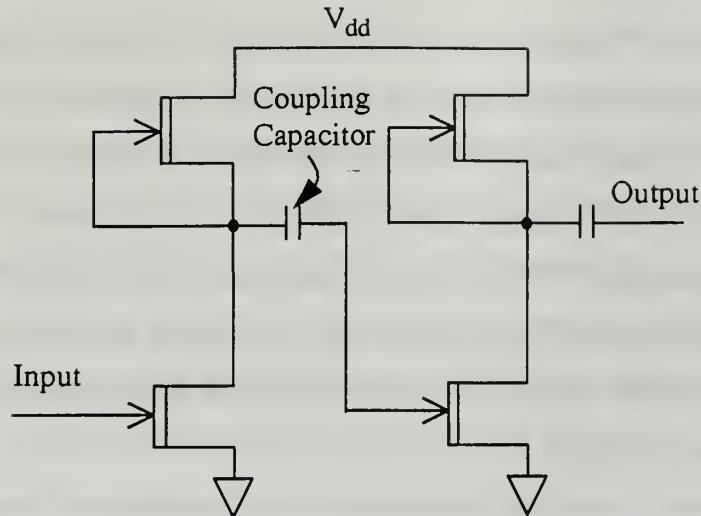
Figure 1.5: Capacitor-Coupled Logic (CCL) Inverters

b. *Capacitor Diode FET Logic (CDFL)*

In order to overcome the problem of dynamic only operation of the CCL family, capacitor diode FET logic has been devised. The dc level shifting stage is added in parallel with the capacitor. Since this stage is only required to provide coupling at low frequencies, the drive requirements are small and thus a very low power dissipation can be maintained in this extra stage [30]. The circuit diagram for this family is shown in Figure 1.6.
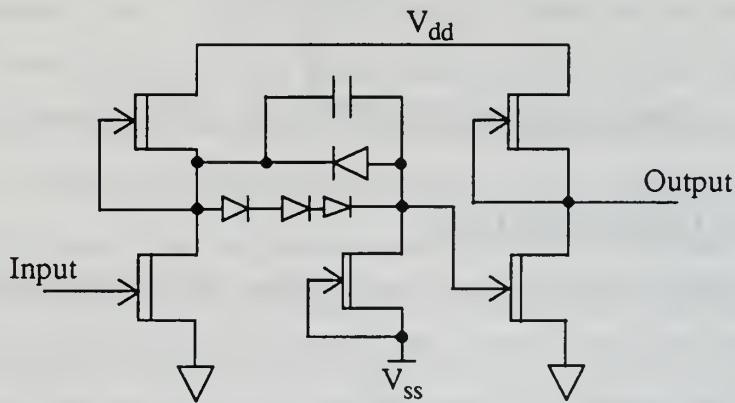
Figure 1.6: Capacitor Diode FET Logic (CDFL) Inverter

13

c. *Super-Buffer FET Logic (SBFL)*

The use of quasi-complementary output drivers (super-buffers) will give better current drive capability which improves the switching speed of DCFL family, providing a new circuit called super buffer FET logic (SBFL) [2, 31]. This family has a push-pull output stage to provide increased drive capability. The SBFL inverter is shown in Figure 1.7. The disadvantage of SBFL is the power and ground current spikes that occur when the output waveform switches from high to low. The reason for the spikes is that both the source follower and the pull down transistors are ON at the same time. Power consumption for SBFL is also very high.
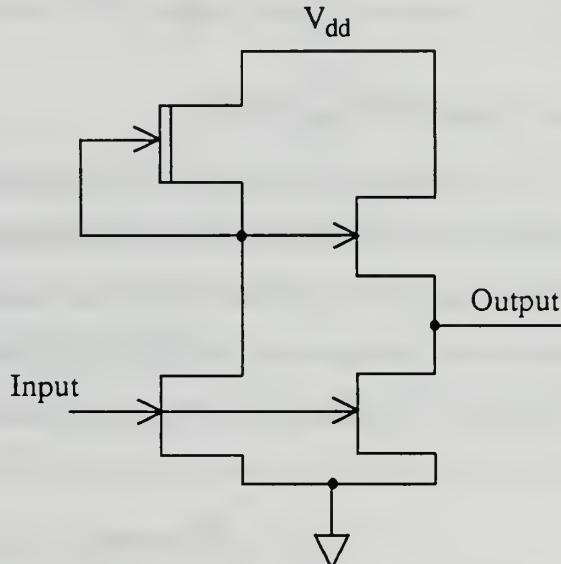
Figure 1.7: Super-Buffer FET Logic (SBFL) Inverter

E. DYNAMIC LOGIC CIRCUITS

Dynamic logic circuits have been used in silicon MOSFET technologies to decrease power dissipation and thus increase logic function complexity and circuit density. The basic dynamic gate consists of a N-channel transistor logic structure whose output node is precharged to V_{DD} through a clocked P-channel transistor and conditionally discharged to V_{SS} or ground through a switching N-channel transistor. Dynamic circuits require a clock

14

for proper operation. Dynamic logic is a non-ratioed logic, meaning that the logic levels are not determined by the width and length ratios of the load and switching transistors. This allows the design of dynamic logic circuits, in most cases, to use minimum device dimensions and results in a small layout area and high fan-in. The use of clocked transistors prevents the flow of current from power supply to ground at the same time, decreasing the static power dissipation. Dynamic circuits have two-phases of operation precharge and evaluation. In the precharge phase, the circuit nodes are charged or discharged to some reference level according to the design. Inputs of the gate can change only during the precharge phase. At the completion of the precharge phase, the path to V_{DD} is turned off and the path to ground is conditionally turned on by the clock signal. During the evaluation phase, these precharged nodes either float high or are pulled down according to the gate inputs.

The main drawback of dynamic circuits is the need to route the clock signal to every gate in the circuit which complicates the routing problem and increases the parasitic capacitance. Also, they have a minimum frequency of operation because of the leakage current from the precharged nodes to ground. This drawback can be eliminated in Domino circuits by using a weak pull up P-channel transistor or a feedback transistor. The routing delay of the clock signal across an IC must be considered to prevent clock skew and metastability problems. Finally, charge redistribution problems must be taken care of while designing any dynamic logic circuit. A strong limitation of the simple dynamic structure, which uses only one clock, is the impossibility of cascading the logic blocks to implement complex logic [32]. Figure 1.8 illustrates the situation when cascading two stages of the simple dynamic structure. When the gates are precharged, the output nodes are charged to V_{DD}. During the evaluation phase, the output of the first gate will conditionally discharge. Due to the finite pull-down time, the precharged node (N_1) can discharge the output node of the following gate (N2) before the output of the first stage is correctly evaluated, causing

an erroneous state as shown in Figure 1.8. This problem can be eliminated through careful design of cascaded dynamic logic gates, as explained in the following subsections.
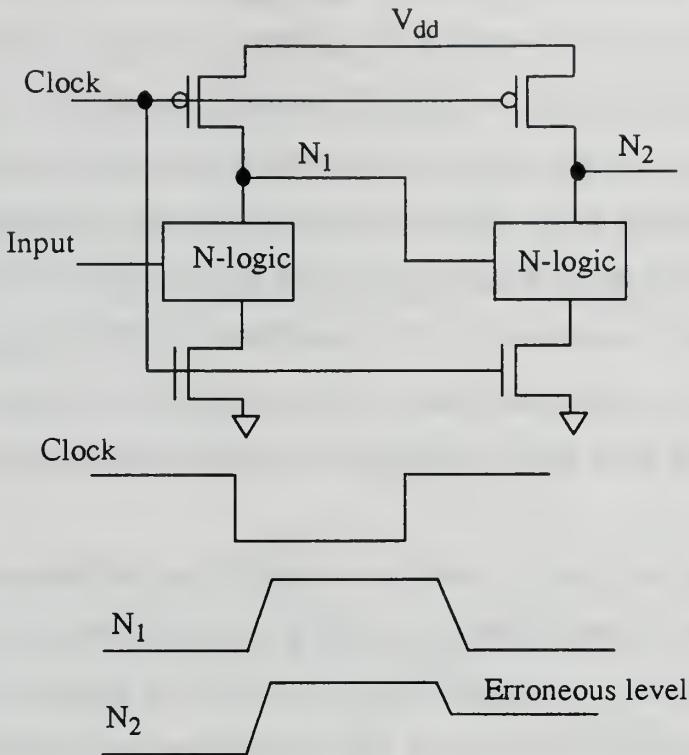
Figure 1.8: Erroneous Evaluation in Cascaded Dynamic CMOS Gates

1. **CMOS Dynamic Logic**

   a.   Domino Logic

   Domino logic modifies the simple dynamic structure by adding a static buffer (inverter) to each logic gate output. This allows a single clock to precharge and evaluate a cascaded set of dynamic domino logic blocks without entering an erroneous state [33]. The basic Domino logic gate is shown in Figure 1.9. The output of the dynamic gate goes only to the buffer and the output of the buffer is the logic gate output. During the precharge phase, the dynamic gate output is a logic high and the buffer output is a logic low. Also, all domino gate outputs are low, thus the transistors they drive are cutoff. During the evaluation phase, the domino logic gate output can only make a transition from low to high.

16

As a result, there can be no switching hazards at any node in the circuit because nodes can make at most a single transition and then must remain stable until the next precharge cycle. In a cascaded set of logic blocks, each stage evaluates and then causes the next stage to evaluate. Dynamic domino logic circuits have low power consumption because there is no dc path from V_{DD} to ground, except for the static buffer. Also, the full pull-down current is available to drive the output nodes. At the same time, the load capacitance is much smaller than complementary circuits because most of the P-channel transistors have been eliminated from the load. Domino circuits use a single clock which provides a simple operation and full utilization of the speed of each gate.

The limitation of this circuit technique is that all of the gates are non-inverting, meaning that it does not form a complete logic family. Another limitation is that each gate must be buffered by a static inverter, meaning that this technique is not completely dynamic and dissipates some static power. Finally, in common with all dynamic circuits, charge redistribution can be a problem.
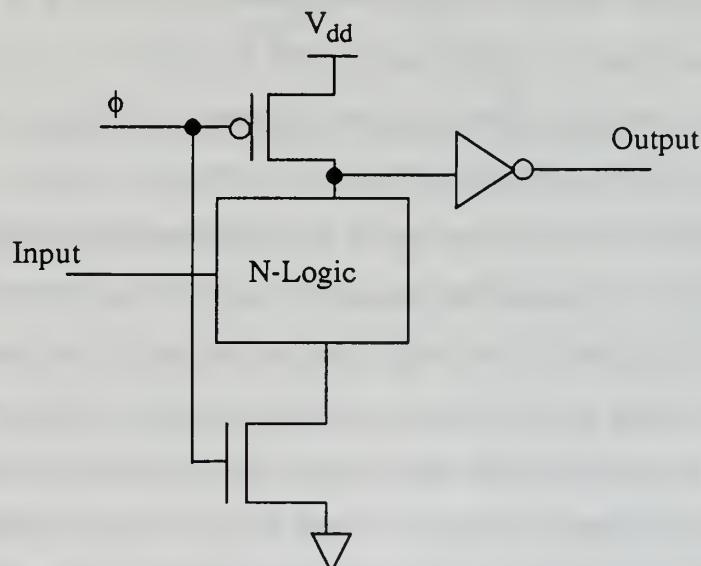
Figure 1.9: Dynamic Domino Logic Gate

17

To allow a lower frequency of operation and to avoid the risk of storing data on floating nodes, a low current, weak pull-up P-channel transistor can be added, in parallel with the main pull-up transistor. With the gate of the weak pull-up transistor grounded, the buffer input is pulled up during precharge. This will force the buffer output to be low, compensating for the leakage currents. The weak pull-up transistor must be small enough (small W/L) not to fight against discharging of the dynamic logic gate output node during evaluation. There is no significant impact on pull-down current and the power consumed during the evaluation phase is tolerable. In some applications, when the precharge time is long enough, the clocked P-channel transistor can be eliminated and substituted with the weak transistor [32]. Domino gates may also be made latching by including a feedback P-channel transistor from the output of the buffer to its input. This transistor is sometimes called a 'not to forget transistor'.

b.   *N-P Domino Logic*

The limitation of Domino logic is the lack of inverted logic functions. The combination of the dynamic block with a static inverter will give a non-inverted output signal. This decreases the logic flexibility and therefore may require more transistors per logic function. Another limitation in Domino circuits is the difficulty of pipelining multiple stages because all the logic blocks evaluate and precharge together.

N-P Domino circuits solve the above two problems. The logic functions in N-P Domino circuits are implemented using N-type and P-type dynamic blocks, as shown in Figure 1.10. The output of the N-type is fed to the input of the P-type logic block and the output of the P-type is fed to the input of the N-type logic block, and so on [34, 35]. The static buffer is used only if the output of one type of logic is fed to the input of the same type. This dynamic logic family requires both the clock and its complement to drive N-type and P-type blocks respectively. The N-type logic block will precharge to VDD and the P-type block will pre-discharge to ground during their precharge phase. That is why this

implementation is sometimes called 'zipper logic'[36]. During precharge phase, all the transistors in n-logic and p-logic blocks will be turned off.

The removal of the static inverter will reduce the static power dissipation and also make this family capable of producing inverted output. Zipper implementation make this family suitable for pipelining. The limitation of this logic family is the use of the slow P-channel transistors in evaluating the logic function. This will limit the maximum frequency of operation of the circuit, especially in gallium arsenide implementations.
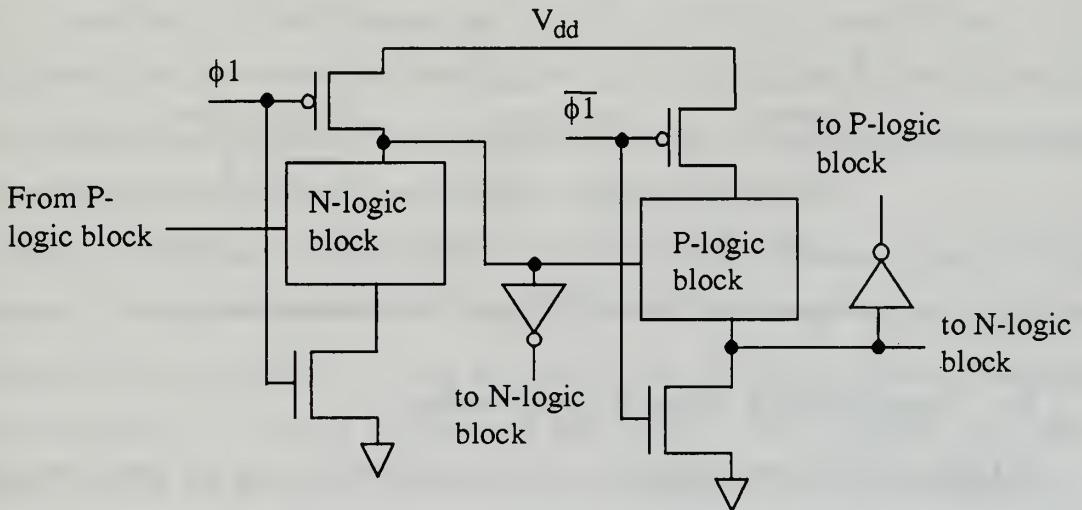
Figure 1.10: N-P Domino Dynamic Logic Gate

c. *Two-Phase Dynamic Logic*

This family uses only N-channel transistors in evaluating the function. As the first stage evaluates its output node, the second stage will be precharging and vise versa. The two successive blocks are fed from two non-overlapping clock phases. A pass gate is used between successive logic blocks to isolate the data stored at the input of the second block from corruption when the output of the first block is precharging. Clocking of two-phase logic is shown in Figure 1.11. The two clock phases ϕ_1 and ϕ_2 are non-overlapped in the logic high level [32]. The main disadvantage of this family is the use of extra metallization to run the two clock phases and their complements.
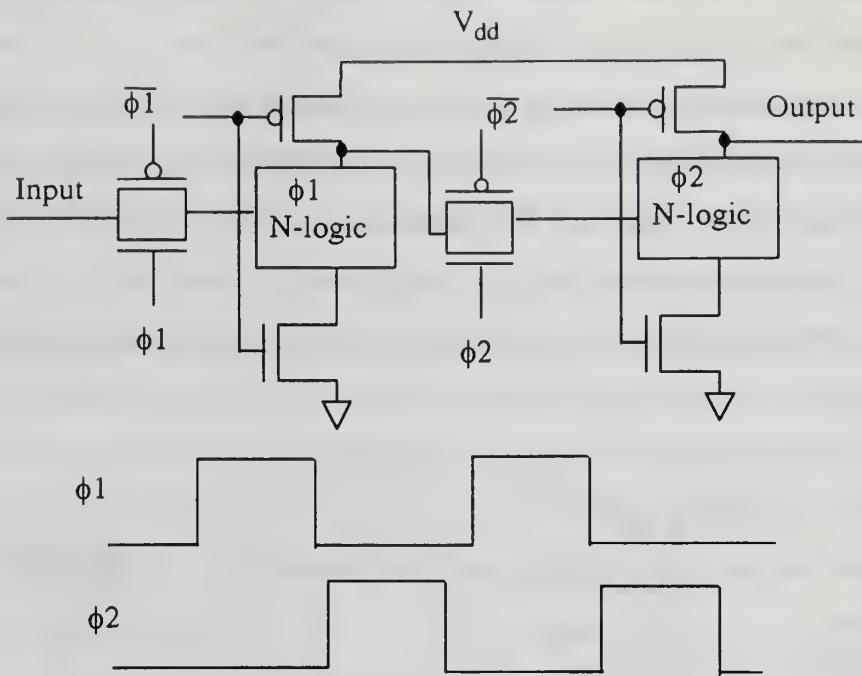
Figure 1.11: Clocking of Two-Phase Dynamic Logic

2. GaAs MESFET Dynamic Logic Families

In GaAs MESFET static logic circuits, direct current flows at all times from power supply to ground. Also, static logic is usually dependent on width ratios to control logic levels and noise margins. Therefore, these circuits are called 'ratioed logic'. The speed and power dissipation are inversely proportional to the device widths. In static logic circuits, decreasing the power supply voltage will reduce the dissipated power but will reduce the output voltage transition which decreases the noise margin. Also, reducing the supply voltage will reduce the current flow in the circuit which decreases the switching speed. Shrinking the transistor-gate widths will save some layout area but will sacrifice both the drive capability and the speed of the circuit by reducing the current.

Dynamic logic has been relatively un-exploited with GaAs FET technology. Earlier applications were mainly oriented toward very high speed SSI circuits such as divide by two and shift register circuits [37, 38, 39].

20

The first Domino circuit was demonstrated in reference 40 and is a four-input AND gate. It is shown in Figure 1.12. It consists of three stages, an input stage, an inverting stage, and a level shifting stage and is composed entirely of depletion mode MESFETs. It requires two power supplies and two in-phase clock signals, level shifted with respect to each other. If Q1 and Q2 are enhancement-mode transistors, there will be only one clock and one power supply required for this circuit. This will decrease the noise margin of the circuit and decrease the consumed power.

Another Domino circuit is presented in reference 41 and shown in Figure 1.13. It is called Capacitively Coupled Domino Logic (CCDL). It differs from that in Figure 1.12 in two regards. First, the order of the inverting and level shifting stages are reversed. Second, three different threshold MESFETs are required. However, current fabrication technology has enough difficulty controlling two different threshold MESFETs.

The third Domino circuit is called Trickle Transistor Dynamic Logic (TTDL) presented in reference 42 and shown in Figure 1.14. This Domino topology uses static level shifting rather than capacitive, trading off the need for two clock signals for increased power dissipation. The major drawback of this design is that it requires four power supplies. In all of the above AND gate circuits, the propagation delay was measured to be around 200 ps and the power dissipated per gate was about 0.5 mW. Due to the previously mentioned drawbacks of the Domino circuits, this topology has seen limited use.

The GaAs implementation of Two-phase Dynamic FET Logic (TDFL) is presented in references 43, 44, 45, 46 and 47. The schematic of two TDFL inverters in series is shown in Figure 1.15. The gates operate from a single power supply and two non-overlapping (in the logic high level) clocks. The precharge phase of the first gate is the evaluation phase of the second stage and vise versa. TDFL circuits are self latching and are suited for pipelined architectures. TDFL gates are non-ratioed which compacts the circuits layout.

Another topology used in GaAs dynamic circuits is pass transistor logic. Application of Si MOS pass transistor topologies in GaAs MESFET circuits is not straight forward. MESFET gate conduction limits the signal levels on control gates and also limits noise

margins. Gate conduction requires different logic transitions on gate nodes than that on drain and source nodes [48]. The circuits used to generate the control signal levels from the data signal levels are both area and power consuming, which limits the use of this topology.
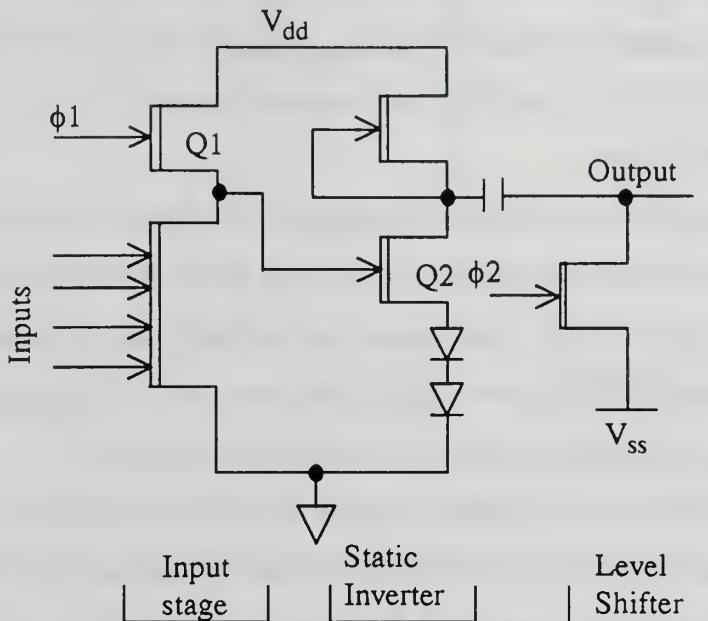
Figure 1.12: GaAs MESFET Domino 3-Input AND Gate
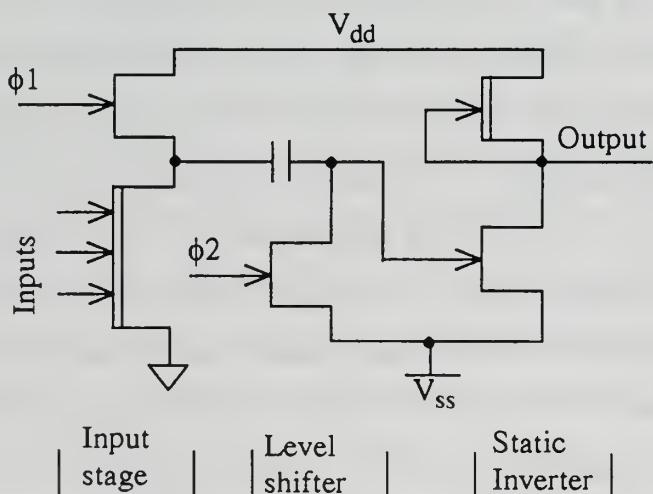
Figure 1.13: GaAs MESFET CCDL 3-Input AND Gate
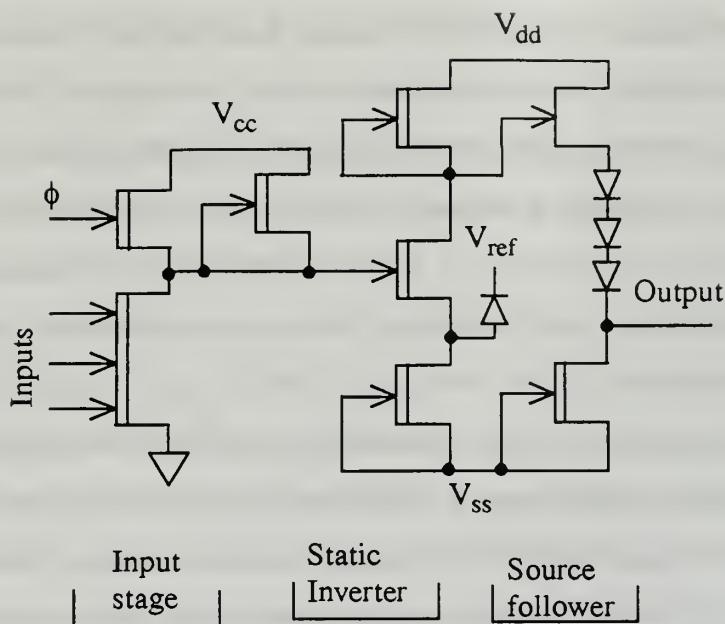
Figure 1.14: GaAs MESFET TTDL 3-Input AND Gate
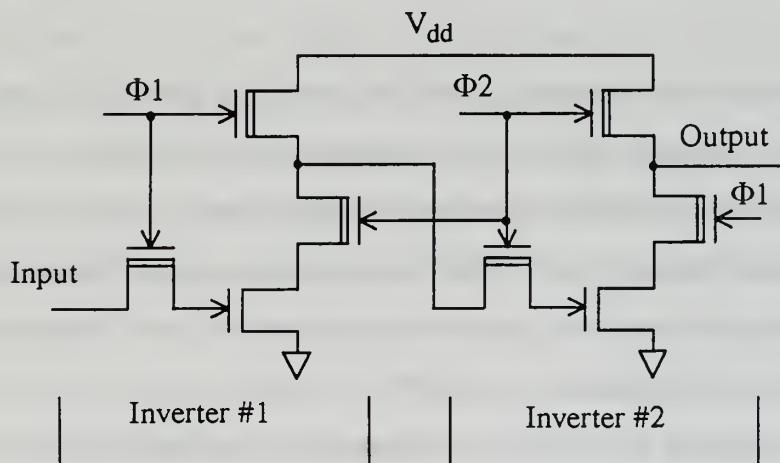
Figure 1.15: Two GaAs MESFET TDFL Inverters in Series

23

F. OUTLINE OF DISSERTATION

In this dissertation, the possibility of using dynamic digital logic circuits with Complementary GaAs (CGaAs) fabrication processes is explored. Different dynamic circuit configurations are presented. The main problem of exploring these dynamic logic families in NGaAs technology is the gate conduction of GaAs transistors, as well as the absence of the PFETs. This problem is eliminated (partially) when using isolated gate CGaAs technology. In this case, the charge can be stored on the gate capacitor of the transistor for a longer time.

Chapter I has been an overview of static logic families (ratioed logic), as well as dynamic logic families implemented in CMOS and NGaAs technologies. The theory of operation and the characteristics of the Complementary Hetrostructure Isolated Gate Field Effect Transistor (CHIGFET) is explained in Chapter II. The power consumption of the circuits implemented in CGaAs is much lower than the NGaAs technology, which introduces the CGaAs technology to the LSI and VLSI regions. The main problem of CGaAs logic is that the PFET is much slower than the NFET, which slows down this new technology.

Various dynamic logic families are designed, analyzed and/or implemented in the described research. In these dynamic logic families, the slow PFETs are used only to precharge the output nodes. PFETs are not used in the evaluation blocks, thus the speed of these dynamic logic families is much higher than the standard static CGaAs logic family. There is no direct path from the supply to the ground at any time. Therefore, the static power dissipation of these families is very low.

Chapter III discusses the design of the basic combinational logic gates (Inverter, NAND, NOR, XOR, XNOR gates) using both the static logic and the Two-Phase Dynamic FET Logic (TPDL). Also in this chapter, the comparison in speed, power consumption, and layout area between these two families is detailed [49]. The TPDL circuits require two non-overlapped clock phases and their complements for proper operation. The design and

analysis of a clock generator is also explained in this chapter. This chapter is the first section that details the original contributions of the described research.

Chapter IV explains the design of the basic sequential circuits (D-latch, D flip-flop and linear feedback shift register). The design of these circuits is performed using the static and TPDL logic families [49]. This chapter also contains the comparison in performance between the two different logic families.

In Chapter V, four different two-level functions are designed using static logic and all the well-known dynamic logic families. The dynamic logic families used are Domino logic, N-P Domino logic, and TPDL logic. These four circuits are simulated using HSPICE to differentiate among the different logic families in speed, power consumption and layout area. Based on the simulation results, it has been found that the performance of the TPDL family is superior to all the other static and dynamic logic families [50].

Chapter VI explores the feasibility of using the TPDL in practical circuit designs through implementation of complex functional blocks. In this chapter, a TPDL Four-Bit Carry Lookahead Adder (4-Bit CLA) is designed, optimized and analyzed [51]. The design of the same adder using the static logic and the pipelined static logic are completed. Also, a performance comparison among the three designed circuits is performed.

In Chapter VII, the implementations of the circuits designed and analyzed in the previous chapters is completed. Seven integrated circuits are implemented. All ICs are designed to drive a 50 Ω resistive load and a 15 PF parasitic capacitance. The design of the input receiver and output driver circuits, required for operation and testing of all the implemented ICs, is also explained. HSPICE simulation results of all the implemented chips, including the drivers, are also presented. The design data base of these chips is compatible with the Motorola Semiconductor CHIGFET fabrication process. HSPICE simulation files of all the implemented chips are included in Appendix A, while the circuit layout of these chips is presented in Appendix B.

Conclusions and suggestions for further work are explained in chapter VIII at the end of the dissertation. It summarizes the main contribution of this dissertation which is the

development and implementation of a new dynamic logic family, Two-Phase Dynamic FET Logic (TPDL), for complementary gallium arsenide (CGaAs) fabrication technologies. The TPDL family enhances the advantages of CGaAs technology by increasing the speed and decreasing the power consumption. It also reduces the layout area. The results of the described research allow CGaAs technology to be used for implementing VLSI ICs for the first time.

II. COMPLEMENTARY GALLIUM ARSENIDE (CGaAs) TECHNOLOGY

Complementary metal oxide semiconductor (CMOS) field effect transistors are now the dominant technology for VLSI integrated circuit. This dominance is due to the fairly high speed and low power consumption of CMOS logic circuits. CGaAs is the compound semiconductor analog of silicon CMOS technology. Also, CGaAs can be used as an alternative process for BiCMOS because it offers higher speed and lower speed than BiCMOS [52].

In this chapter, Complementary Hetrostructure Insulated Gate FET (CHIGFET) devices, provided by Motorola Semiconductor, are investigated for implementing dynamic logic circuits. Section A provides an overview of CGaAs technology, discussing the problems associated with this technology and their solutions. Section B discusses applications for this technology. The internal structure and the fabrication process of CHIGFETs is explained in Section C. Section D discusses the gate current in CHIGFET and associated limitations. Finally, Section E explains modeling of both N- and P-channel devises using HSPICE simulation tools and discusses their performance.

A. OVERVIEW OF COMPLEMENTARY GaAs

Several problems have to be solved before CGaAs technology will be more generally useful for a wide variety of applications. The first problem is the low hole mobility in GaAs, which diminishes the speed advantage of this technology because speed becomes limited by the speed of P-channel devices. The second problem is the gate leakage current that diminishes the advantage of low power consumption in CHIGFETs because it increases the consumed static power. Also, it limits the input gate voltage transition which leads to a small noise margin in complementary logic circuits. The third problem is the increased source series resistance which increases the gate to source voltage which in turns reduces the transconductance. The fourth problem is the subthreshold current needs to be reduced to reduce the power consumption in CHIGFETs and increase the scale of integration. A

reduction in the subthreshold current is important, especially in sub-micrometer structures, because the subthreshold current increases sharply for gate lengths less than 1 μm [53].

Solutions to the above problems have been tried through the use of CGaAs technology based on N-channel and P-channel AlGaAs/GaAs hetrostructure devices. These devices offer the high speed, ultra low power consumption and high noise margin suitable for VLSI circuits. Also, a quantum-well P-channel AlGaAs/InGaAs/GaAs HIGFET has been designed and fabricated to give better performance than AlGaAs/GaAs devices [53, 54]. The gate leakage current for both N- and P- channel AlGaAs/InGaAs /GaAs quantum-well devices is reduced because they have a larger valance and conduction band discontinuity at the AlGaAs/InGaAs interface, compared to AlGaAs/GaAs. Also, the energy band discontinuity at the InGaAs/GaAs interface helps to reduce the subthreshold current by confining the channel [55].

In the absence of dopants, the threshold voltage of the HIGFET is difficult to control. In order to change the threshold voltage in a controlled way, dopants must be introduced into the HIGFET structure [56]. Dopants can be placed into the wide band semiconductor separating the channel from the gate, as done in a MODFET. Also, they can be placed into the semiconductor behind the channel as done in an inverted MODFET. Finally, they can be placed directly into the channel as done in a doped channel HIGFET. The latest case has the advantage of having better control of the threshold voltage [57]. Also, the subthreshold current and output conductance are reduced in this latest case.

AlGaAs/InGaAs/GaAs Quantum well Doped Channel FETs have been documented in [58]. They have a large transconductance, a high mobility, a large scale of integration and can be used to implement logic gates with very short propagation delays. Delta-Doped CHIGFET are introduced in [59] and make use of a high InAs mole fraction in a pseudomorphic InGaAs channel along with a sub-channel delta-doped silicon layer to adjust the N-HIGFET and P-HIGFET threshold voltage. This results in a high transconductance value which increase the switching speed with low power consumption. Also, a high mole fraction in AlGaAs barrier layer is demonstrated in [60] and is used to reduce the gate leakage current of both N- and P-HIGFETs. In addition, the use of such a

high AlAs mole fraction results in reduced subthreshold currents and lowers the drain-to-gate leakage current in P-HIGFETs. Some test circuits have been fabricated using CHIGFET technology by Honeywell and Motorola and gave promising results.

B. APPLICATIONS FOR COMPLEMENTARY GaAs

Complementary GaAs (CGaAs) technology has already achieved $0.01\mu W/MHz/gate$ at 0.9 V [52]. By sacrificing some power dissipation, a 1 GHz signal processor has been made, as well as full-complementary digital ICs that operate at 500 MHz using the same process flow. These circuits have a speed/power measurement of $0.16~\mu W/MHz/gate$ [52]. The performance of 1 μm CGaAs has been shown to be superior to 0.5 μm CMOS or thin film SOI equivalents through the measurement of ring oscillator delay versus supply voltage for these technologies [52]. In addition, CGaAs circuits are more tolerable to threshold variations across the wafer and from wafer to wafer resulting in higher yield [61, 63, 64]. Due to the low threshold voltage of the CGaAs devices and high current drive, its performance is very good, even at low power supply voltages [52].

Complementary GaAs is finding applications where the required circuit performance is greater than CMOS can provide at a given power dissipation, or where additional speed is required when compared to existing CMOS devices. Significant power savings may be obtained for CGaAs at high clock rates. The types of applications where CGaAs can be used include high performance microprocessors, low-power RISC processors for portable applications, digital signal processors, and fast static memory. Complementary GaAs is also useful for space system applications due to its inherent total dose and dose rate radiation hardness.

C. GaAs CHIGFET STRUCTURE AND FABRICATION

The structure of a CHIGFET is analogous to that of a MOSFET with the un-doped AlGaAs taking the function of the oxide in CMOS. It is grown by molecular beam epitaxy (MBE) on a semi-insulating GaAs substrate as shown in Figure 2.1 (copied from reference [52] and not drawn in scale). In this structure, an un-doped GaAs buffer is grown on the semi-insulating substrate, followed by an InGaAs channel, then followed by an un-doped

AlGaAs dielectric and finally ending in a thin un-doped GaAs cap layer. A Wsi gate is then deposited on the structure, and serves as a self-aligned mask for the source and drain implants. After annealing the implant, ohmic contacts are deposited on both source and drain. The device may be either N-channel or P-channel depending on source and drain implants. The channel may also be delta-doped to control the threshold voltage. The rest of the structure is entirely un-doped. The fabrication process of CHIGFET requires only 13 masks [52].
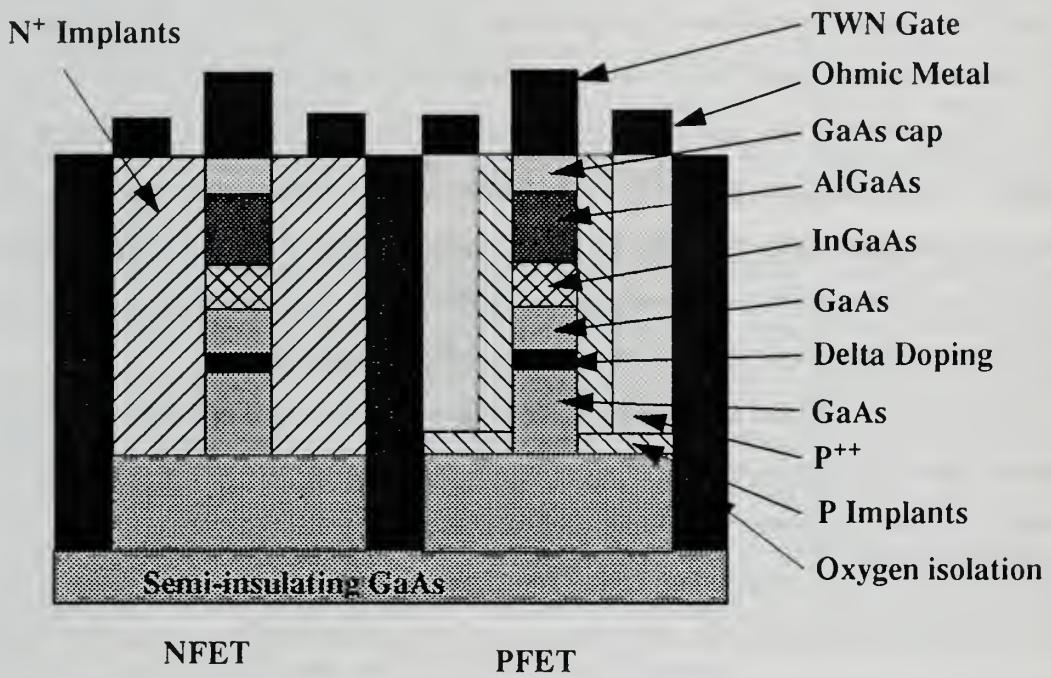
Figure 2.1: GaAs CHIGFET Transistor Structure

D. GaAs CHIGFET GATE CURRENT

GaAs CHIGFET structure is analogous to the MOSFET structure with the AlGaAs layer playing the role of the oxide. In silicon MOSFET technology, the charge carriers are confined to the channel by the silicon dioxide. On the other hand, the CHIGFET relies on the band discontinuity between the InGaAs channel and the AlGaAs dielectric to confine the charge carriers. Because this band discontinuity is considerably smaller than that in a Si-SiO$_2$ interface, the gate current in CHIGFET is significant, whereas it is negligible in most applications in silicon MOSFETs.

The gate current limits the usable range of gate voltage. If gate current is high, it creates an additional voltage across the source series resistance, which causes a sharp drop in the device transconductance. Also, increasing the gate voltage will increase the gate current, which dramatically increases the power consumed by the circuit without increasing the switching speed.

E. GaAs CHIGFET I-V CHARACTERISTICS

In this section, the GaAs CHIGFETs that can be fabricated by Motorola are simulated using HSPICE simulation tools. The transistor parameters can be found in [52] and have been supplied by Motorola. These parameters have been extracted from actual fabricated devices. Figures 2.2 through 2.5 show the drain current versus drain to source voltage for different width to length ratios of both N- and P-channel transistors. It is clear from these figures that the transistors have three regions of operations. The cut-off region where V_{GS} < V_T, the linear region where V_{GS}-V_T < V_{DS}, and the saturation region where V_{GS}-V_T > V_{DS} (same regions as the MOSFET transistors). As shown in these figures, the drain current increases with different rates as V_{GS} increases, the rate getting small as V_{GS} exceeds 2.0 volts. Therefore, the best region of operation for this transistor will be if V_{GS} is kept below 2.0 volts. It can be noticed that the drain current for the N-channel transistor is about three times that of the P-channel transistor for the same gate to source voltage (V_{GS}). Also, it can be noticed that the drain current is doubled when the width to length ratio of a transistor is doubled. These are the N- and P-channel transistor models that will be used in all the circuit designs in the following chapters. In our circuit designs in the following chapters, gate voltage transition will be limited to 1.75 volts to reduce the gate leakage current.

The transistors introduced in this chapter will be used in all the circuit designs presented in the following chapters. Chapter III includes the design and implementation of the basic combinational logic circuits using both TPDL and static logic. The performance comparison between both designs is also presented Chapter III.
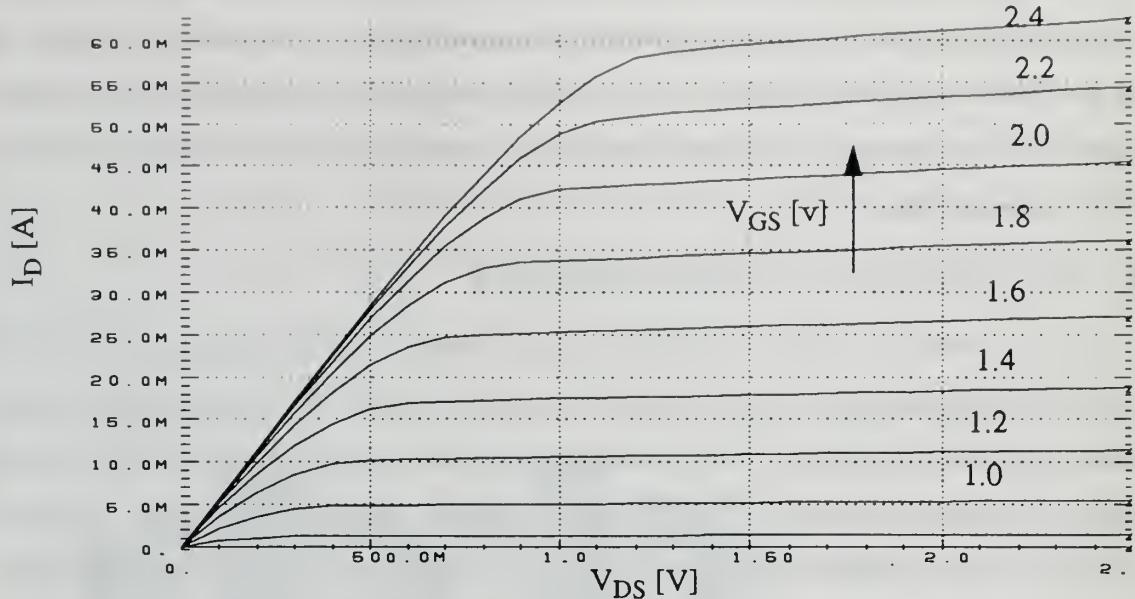
Figure 2.2: I-V Characteristics of N-Channel GaAs HIGFET Transistor (W=10 µm)
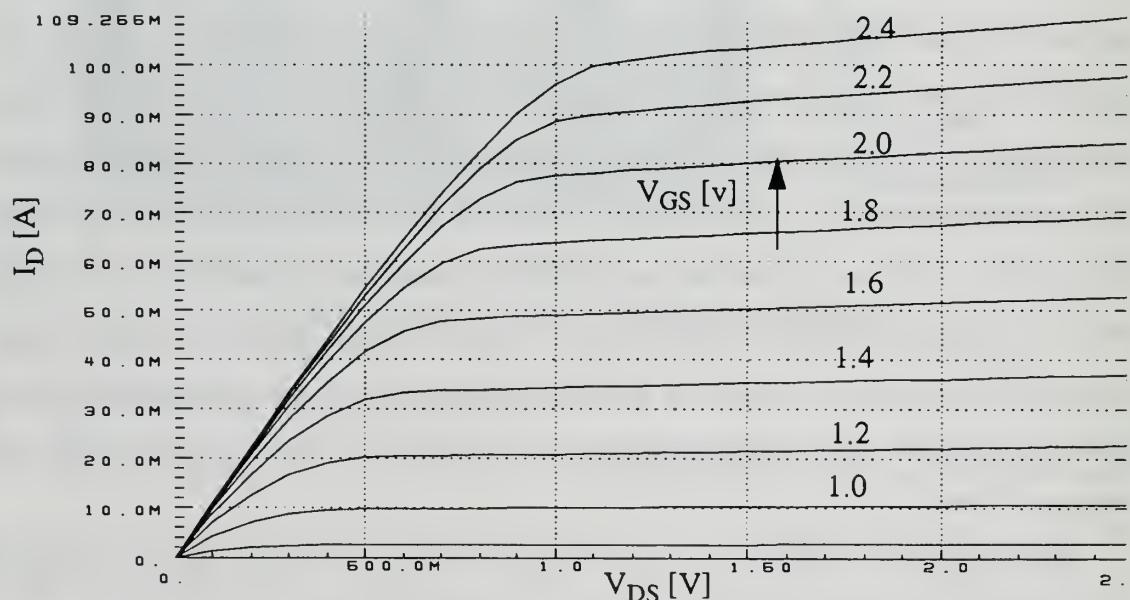
Figure 2.3: I-V Characteristics of N-Channel GaAs HIGFET Transistor (W=20 µm)
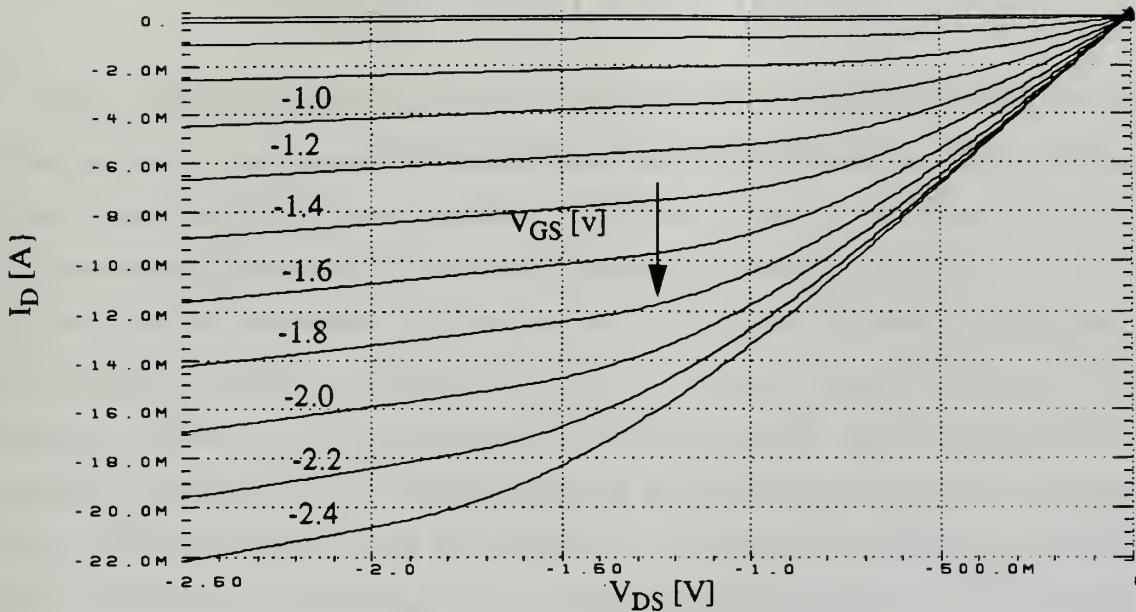
Figure 2.4: I-V Characteristics of P-Channel GaAs HIGFET Transistor (W=10 μm)
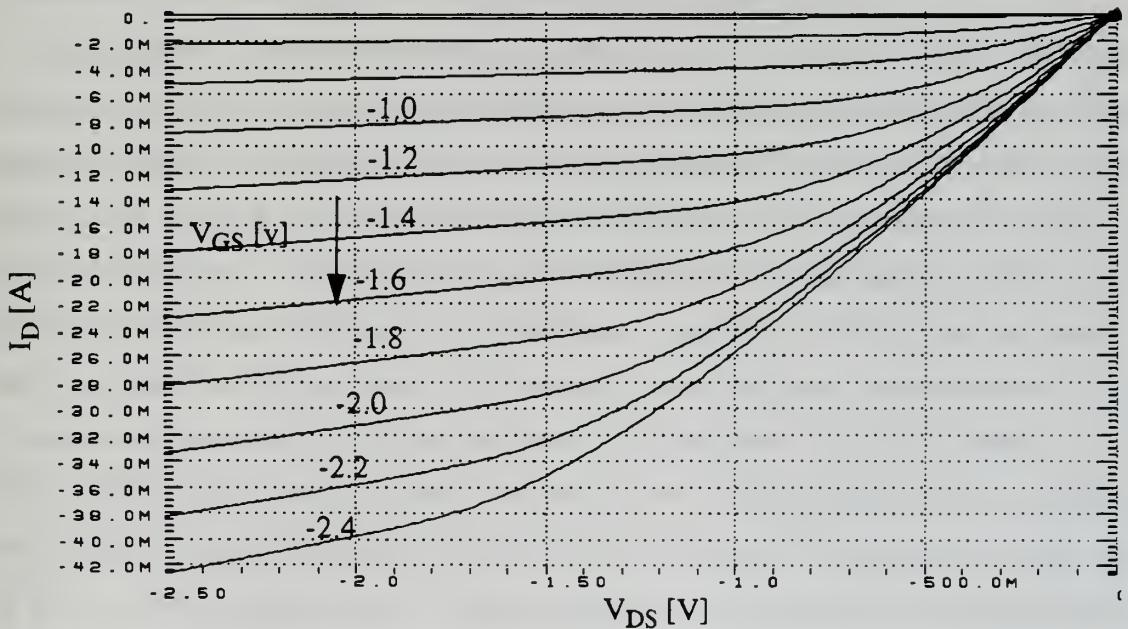
Figure 2.5: I-V Characteristics of P-Channel GaAs HIGFET Transistor (W=20 μm)

III. DESIGN AND ANALYSIS OF CGaAs STATIC AND DYNAMIC COMBINATIONAL LOGIC GATES

Logic circuits for digital systems may be combinational or sequential. A combinational circuit consists of logic gates with outputs that at any time are determined directly by the present combination of inputs, regardless of previous inputs. A combinational circuit performs a specific information-processing operation, fully specified logically by a set of Boolean functions. Sequential circuits employ memory elements in addition to logic gates. Their outputs are functions of inputs and the state of the memory elements. The state of the memory elements, in turn, are functions of the previous inputs. As a consequence, the outputs of a sequential circuit depend not only on the present inputs but also on the past inputs. The circuit behavior must be specified by a time-sequence of inputs and internal states. Combinational circuit designs are the subject of this chapter, while sequential circuit designs is discussed in the next chapter.

In the previous two chapters, previous work done by other people was reviewed and investigated. This chapter starts the new material of the dissertation.

In this chapter, the combinational logic gates, which are the basic building blocks of any logic circuit, are designed using both CGaAs static and dynamic circuit topologies. The principle dynamic logic family of interest in this chapter is Two-Phase Dynamic Logic (TPDL). This choice is based on the study of the different dynamic logic families, which is explained in Chapter V. The basic logic gates that will be discussed here are the Inverter, NAND gate, NOR gate, XOR gate and XNOR gate. In Section A, CGaAs static designs of these logic gates are studied. Also in this section, power and speed measurements of the CGaAs are carried out through the design of a ring oscillator. Section B explains the CGaAs TPDL deign of the same gates mentioned above. The loading and the power supply effects on the maximum operating frequency of these designs are also explained in each of the above sections. The design of a clock generator that generates two non-overlapped clock phases and their complements is explained in detail in Section C. These clock phases are required for the proper operation of the TPDL circuits. Section D explains the

comparison of the designed static gates and TPDL gates in speed, power consumed, and layout area.

Circuits designed in this dissertation are simulated using HSPICE simulation tools. The size of any circuit simulated by HSPICE is limited only by the virtual memory of the computer being used. HSPICE has a superior convergence and accurate modeling features. It produces a graph data file which is displayed by the Graphic Simulation Interface (GSI) tools. MEASURE statement is used in the HSPICE net-list file to measure the required circuit parameters (such as the average power consumption of a circuit). All average power consumption figures calculated in this dissertation are measured using the HSPICE MEASURE statement. The calculation is made by integrating the current drawn from the power supply over the simulation time (which is the total charge Q). Then, the total charge is divided by the simulation time (which gives the average current) and multiplied by the supply voltage.

A. CGaAs STATIC CIRCUIT DESIGN

The design methodology used in this section is for CGaAs static logic gates and is very similar to that of CMOS logic gates. The design priority emphasizes reliability over speed. Therefore, the noise margins are optimized. Equal low and high noise margins, if possible, will provide the best circuit reliability and should be the design goal. Width ratios of PFETs and NFETs are chosen for the best noise margins with a fan-out of two (two inverter load). Changing the gate widths of the transistors while keeping the same width ratio will effect the speed of the gates (pull-up and pull-down times).

1. Static Inverter Circuit Design

The schematic of a CGaAs static inverter is shown in Figure 3.1. All transistor gate lengths are 0.7 μm and transistor gate widths in microns are indicated on the diagram. The design of this gate has been tried for different width ratios of the NFET to the PFET (W_n/W_p) to get the best noise margin. Width to length ratios (W/L) of both the NFET and the PFET are changed, keeping a constant (W_n/W_p) to get the best drive capability of the circuit

with a fan-out of two. The inverter test circuit in Figure 3.2 consists of the inverter under test preceded by two inverters to serve as a pulse shaping circuit. The inverter under test is followed by two inverters as an output loading circuit. This test circuit was simulated in HSPICE and Figure 3.3 shows the DC transfer characteristic of the inverter from the HSPICE simulation program. This characteristic curve was generated at a supply voltage of 2.0 volts and input signal transitions are between 0.0 and 1.75 volts.
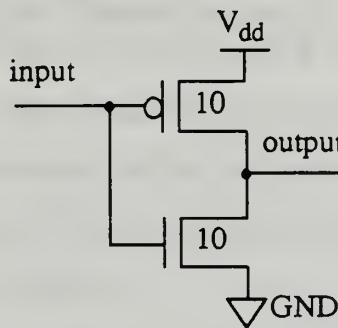
Figure 3.1: CGaAs Static Inverter
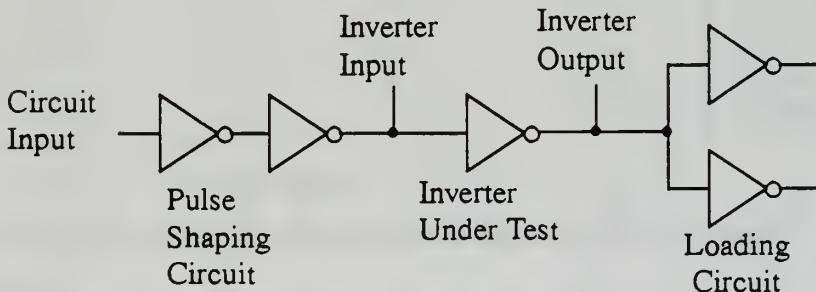
Figure 3.2: CGaAs Static Inverter Test Circuit

The inverter DC transfer curve shown in Figure 3.3 consists of five regions. The first region is characterized by $0 < V_{in} < V_{tn}$, where the NFET is cut off and the PFET is in the linear region. The second region is defined by $V_{tn} < V_{in} < V_{DD}/2$, where the PFET is still in the linear region and the NFET is in the saturation region. In the third region, both the NFET and the PFET are in the saturation region. In this region, the output switches from high to low. The value of the input voltage at which the inverter output is switched depends

on the width ratio between the NFET and the PFET (W_n/W_p). This is the region at which the inverter consumes short-circuit power because of the direct path of current from V_{dd} to ground through the ON transistors. The fourth region is described by $V_{DD}/2 < V_{in} < V_{DD} - |V_{tp}|$. The NFET is in the linear region and the PFET is in the saturation region. The last region is defined by $V_{in} > V_{DD} - |V_{tp}|$, where the NFET is in the linear region and the PFET is in the cut-off region. These five regions are identical to those for the CMOS inverter described in reference 32. V_{tn} and V_{tp} are the threshold voltages for N- and P-channel transistors respectively.
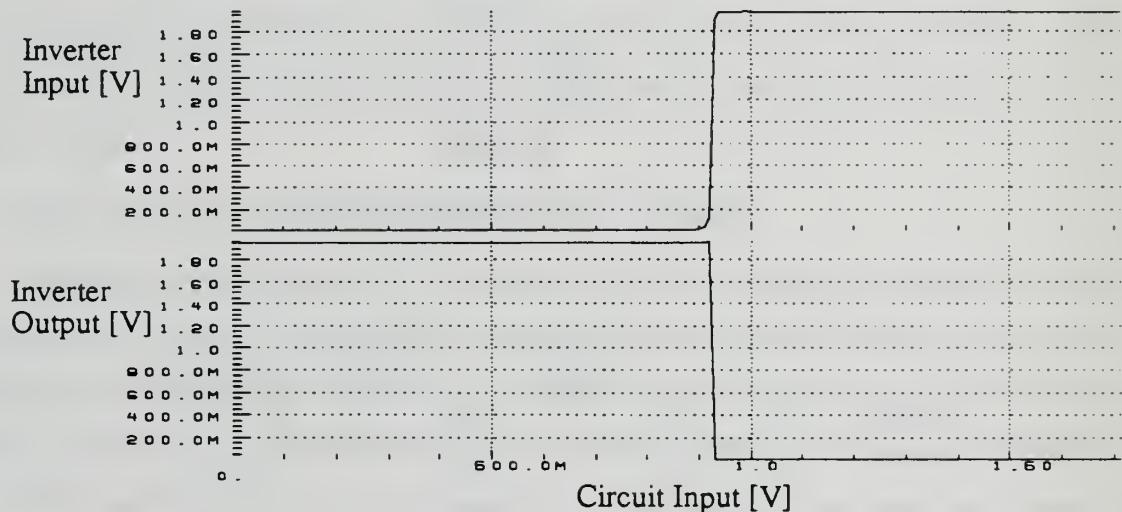
Figure 3.3: DC Transfer Characteristics of CGaAs Static Inverter

The best results for noise margins are obtained when both N- and P-FETs have the same gate widths ($W_n/W_p=1$), which agrees with the results mentioned in reference 61. From Figure 3.3, the noise margin high (NM_h) is measured to be 0.8 volts and the noise margin low (NM_l) is 0.9 volts at $W_n = W_p = 10$ µm and $L = 0.7$ µm with a fan-out of two. Figure 3.4 is the transient analysis of the same inverter which shows the switching speed. The pull-up and pull-down times, measured between 10% and 90% of the logic high level, are 0.29 ns and 0.16 ns respectively. The maximum frequency of operation of this inverter is 1.2 GHz with a fan-out of two. The average consumed power by the inverter at the

38

maximum frequency of operation is 2.17 mW from a 2.0 V power supply. The maximum operating frequency decreases as the loading increases because increasing the load will increase the output capacitance and consequently the pull-up and pull-down times. Also, the speed of the circuit and the power consumed are dependent on the power supply voltage. Increasing the supply voltage will increase the maximum frequency of operation but will also increase the consumed power (trade off). As the supply voltage exceed 2.0 volts, the consumed power increases dramatically due to the drain-to-source leakage current which creates a current flow from V_{DD} to ground. Also, increasing the input signal transition over 1.75 volts will increase the consumed power dramatically due to the gate leakage current, which is explained in detail in Chapter II. Therefore, the supply voltage of all designs in this chapter and following chapters will be limited to 2.0 volts and the input gate transition limited to 1.75 volts.
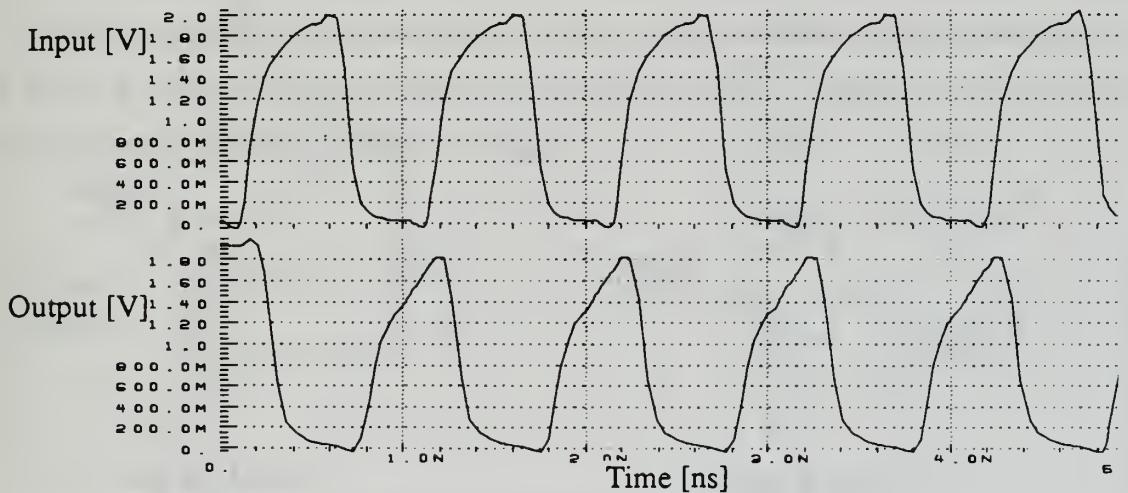
Figure 3.4: Transient Analysis of CGaAs Static Inverter

2.   Static NAND and NOR Gates Circuit Design

CGaAs Static NAND gate and NOR gate schematics are shown in Figure 3.5. The gate length of all transistors is 0.7 μm. The transistor gate widths in microns are indicated on the diagram. The given transistor sizes yield the best results for noise margins, drive capability

and speed. The DC transfer curves of both the NAND gate and the NOR gate, obtained from the HSPICE simulation, are shown in Figures 3.6 and 3.7, respectively. During simulation, each gate input was preceded by a pulse shaping circuit consisting of two cascaded inverters. The NAND gate DC transfer curve is obtained when the gate is powered with 2.0 volts. One input of the gate is tied to V_{dd} and the other input switches between 0.0 and 1.75 volts. The NOR gate DC transfer curve is obtained in the same way except the non ramped input is tied to ground to propagate the effect of the ramped input to the gate output. From these figures, the noise margin low and noise margin high of both the NAND gate and the NOR gate are the same and are equal to 0.8 volts. The transient analysis for both gates are also plotted in Figures 3.8 and 3.9, respectively, as an output of a HSPICE simulation. The circuit was powered from a 2.0 V power supply and input signals switch between 0.0 and 1.75 volts with a fan-out of two.

(a) NOR gate   (b) NAND gate
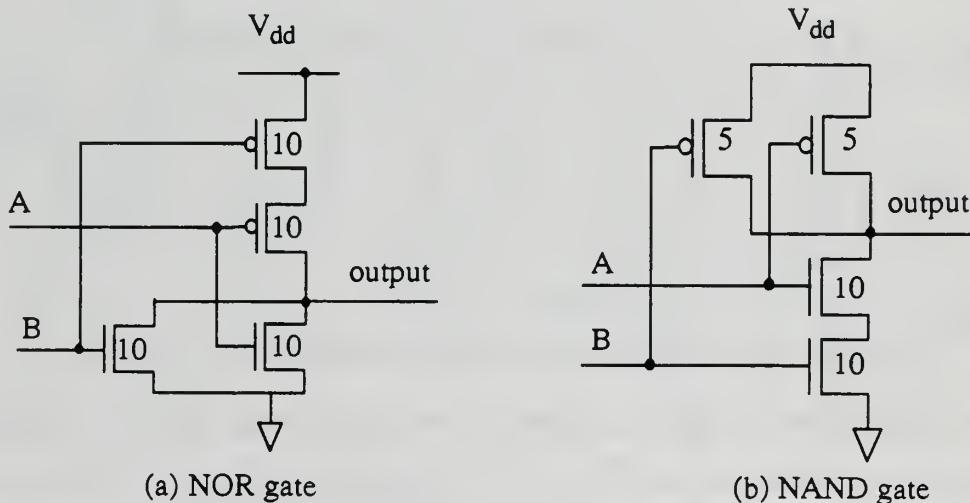
Figure 3.5: CGaAs Static NAND and NOR Gates

The power supply voltage of the NAND gate was changed from 2.0 V to 1.0 V in 0.25 V steps to study the effect of changing the power supply on the maximum operating frequency. Figure 3.10 shows the average consumed power by the NAND gate as a function of frequency at different power supply voltages. The maximum operating

frequency of the NAND gate is 1.22 GHz at a supply voltage of 2.0 V. It consumes 5.8 mW at this maximum frequency. Decreasing the power supply voltage will reduce both the maximum frequency of operation and the consumed power. Therefore, when working at a low frequency, the circuit can be operated from a lower power supply voltage to decrease the power consumed. The effect of increasing the output load on the maximum operating frequency of the NAND gate is also plotted in Figure 3.11. It is clear from this figure that the maximum frequency of operation decreases when the load increases because of the increased output capacitance.

For a CGaAs static NOR gate, the maximum frequency of operation is less than for a NAND gate because it contains two slow PFETs in series. In the NOR gate circuit, the PFET gate widths are increased to be 10 μm (compared to 5 μm for the NAND gate PFETs) to compromise for the above effect. The maximum frequency of operation of this gate is 0.82 GHz with a power supply of 2.0 V and the input signal switches between 0.0 V and 1.75 V. The average power consumed by the gate at the maximum operating frequency is 6.5 mW. It is worth mentioning that loading and power supply voltage effects on NOR gate performance is the same as for a NAND gate.
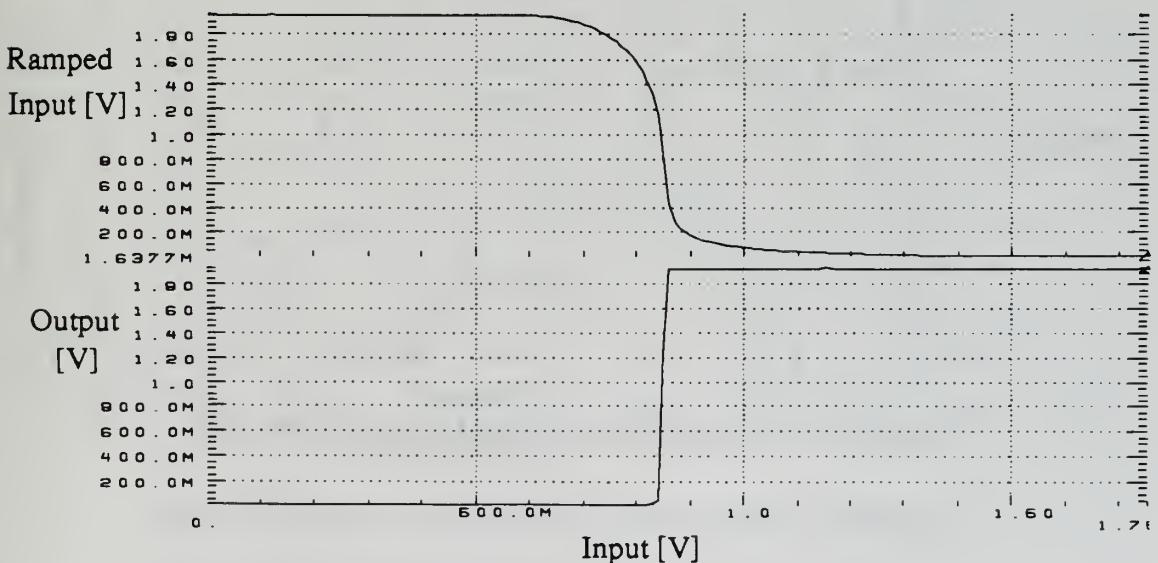
Figure 3.6: DC Transfer Curve of CGaAs Static NAND Gate
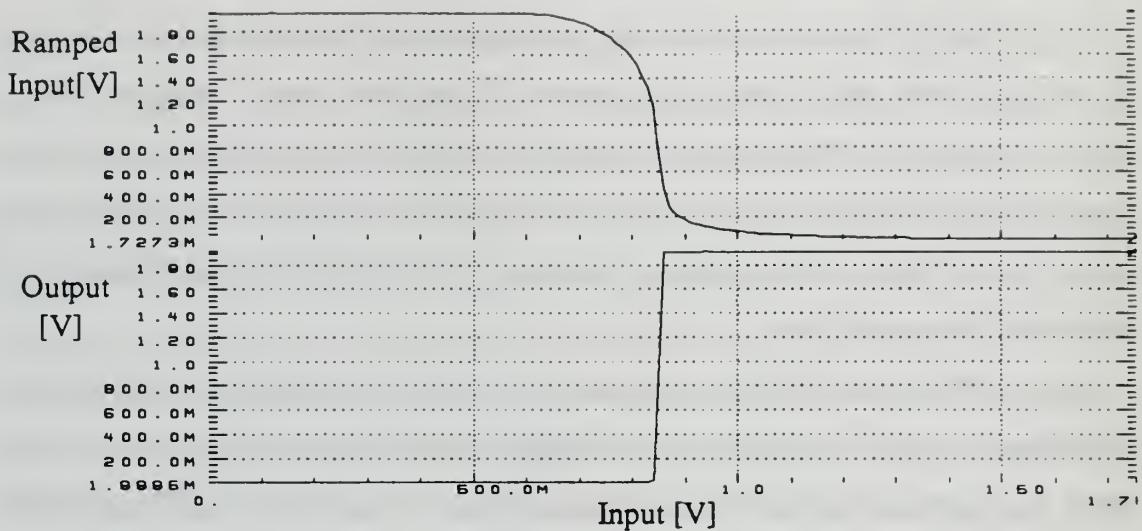
Figure 3.7: DC Transfer Curve of CGaAs Static NOR Gate
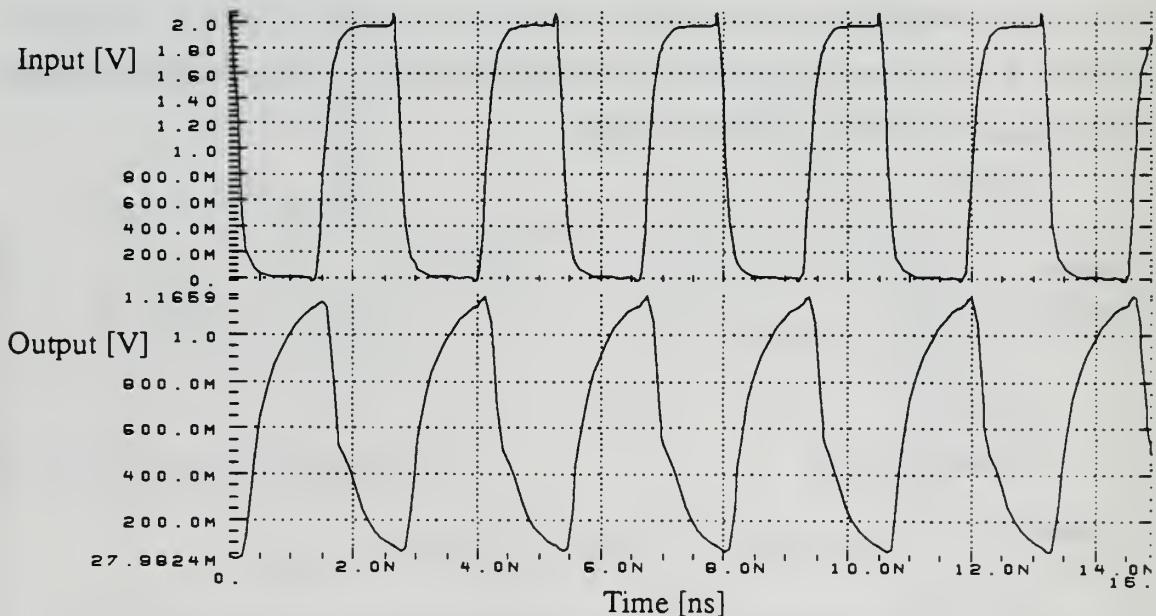
Figure 3.8: Transient Analysis of CGaAs Static NAND Gate

42
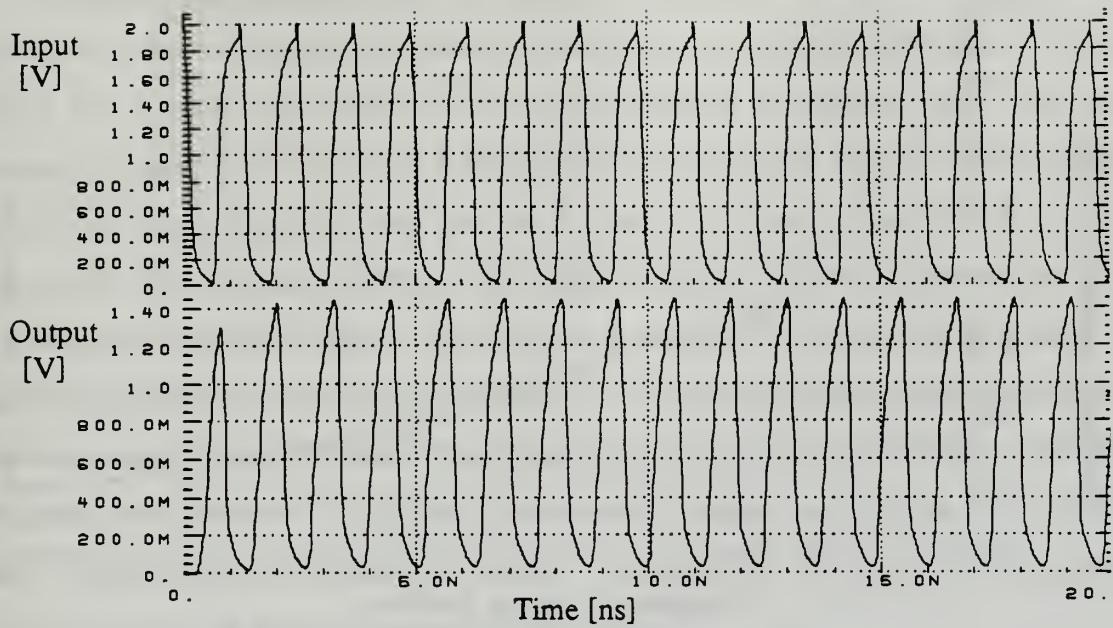
Figure 3.9: Transient Analysis of CGaAs Static NOR Gate
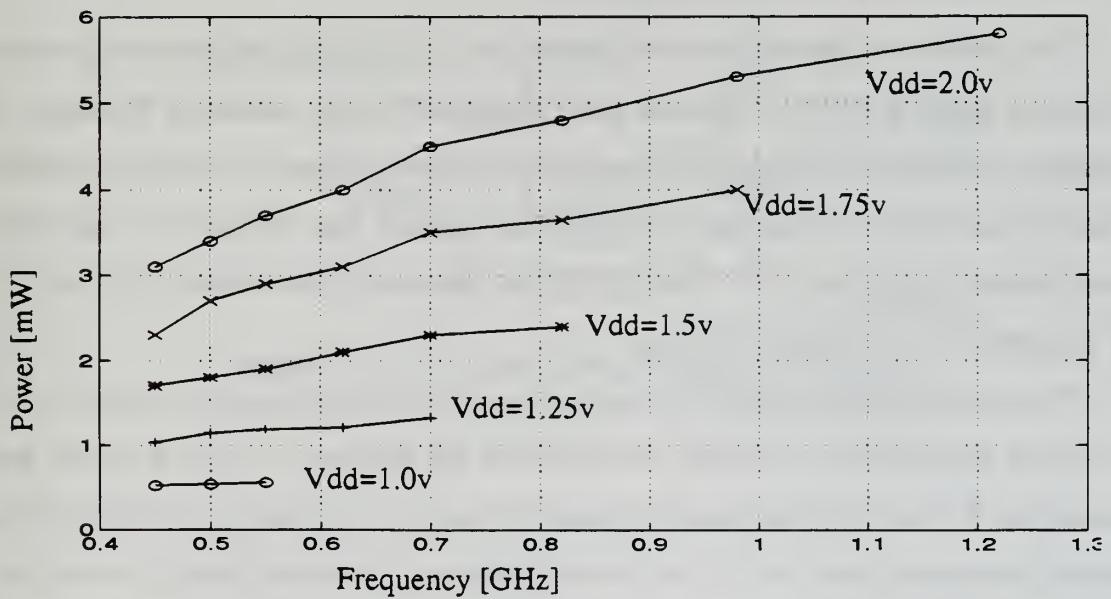
Figure 3.10: Power Consumption of CGaAs Static NAND Gate

43
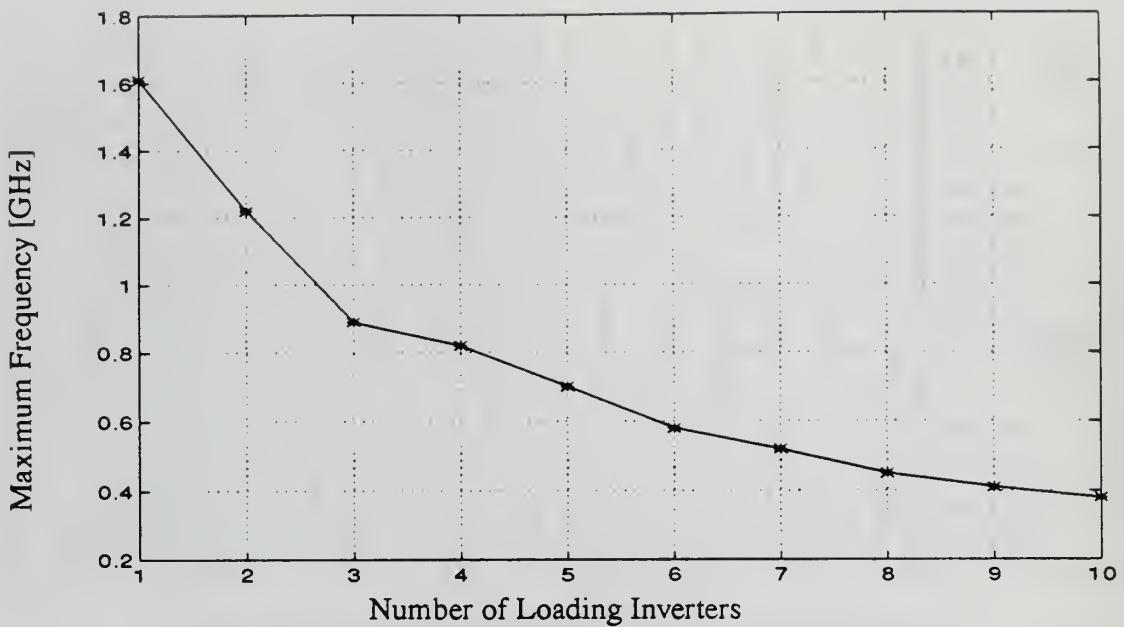
Figure 3.11: Loading Effects on CGaAs Static NAND Gate

3. Static XOR Gate Circuit Design

Two different implementations of CGaAs Static XOR gates have been designed and simulated using HSPICE to measure gate propagation delay, maximum frequency of operation and consumed power. The better design was then selected to be used as a building block in later circuits discussed in the following chapters. The simulation is carried out using a supply voltage of 2.0 V. The input signals were switched between 0.0 V and 1.75 V and a load of two inverters was used.

The first XOR gate consists of 6 transistors and the schematic is shown in Figure 3.12. Transistor gate widths in microns are written on the diagram, while all transistor gate lengths are 0.7 μm. The maximum operating frequency of this gate is 0.55 GHz with an average consumed power of 3.2 mW at that frequency. The second design consists of 8 transistors with the schematic shown in Figure 3.13. Maximum operating frequency of this gate is 0.7 GHz, which is higher than the maximum frequency of the first design. The average consumed power of this gate at the maximum frequency is 6.2 mW.

44

In a comparison between the two designs, the first gate has an advantage of fewer transistors and lower average power consumption compared to the second design. The first design has a major disadvantage of having asymmetrical propagation delay. I.E., the propagation delay from the A input to the output is not the same as from the B input to the output. Also, the propagation delay from the A input to the output depends on the B input logic level. The 8-transistor XOR gate has a higher maximum frequency of operation with a symmetrical propagation delay. Therefore, the 8-transistor XOR gate will be used as a building block in the circuits in the next chapters. A HSPICE simulation was performed for these two gates at different transistor gate widths to discover the optimum widths. Also, the simulation was conducted at different power supply voltages to study the effect of the power supply on the performance of the gates. This resulted in the same conclusion as for the NAND and NOR gate simulations obtained earlier.
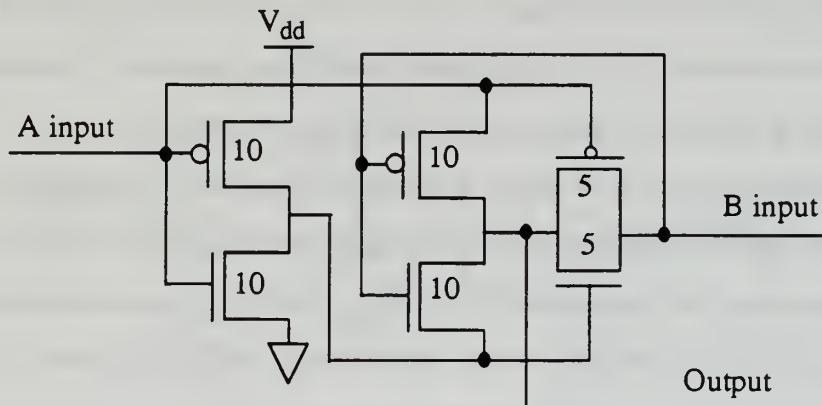
Figure 3.12: CGaAs Static Six-Transistor XOR Gate
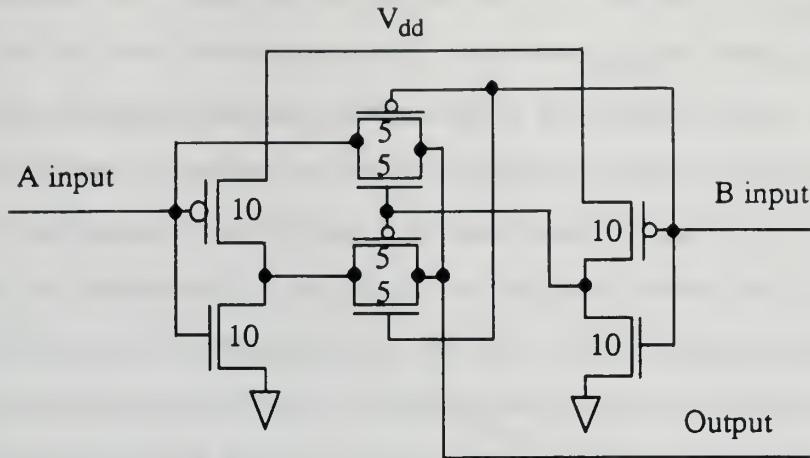
Figure 3.13: CGaAs Static Eight-Transistor XOR Gate

4. Static XNOR Gate Circuit Design

Following the same procedures conducted for XOR gate design in the previous subsection, two different XNOR gate circuits were simulated using HSPICE. The optimum design from the point of view of maximum frequency of operation, layout area and power consumption is selected for use in the circuits of the next chapter.

The schematic of the first design is shown in Figure 3.14 and contains 10 transistors. All transistor gate widths are 10 μm and transistor gate lengths are 0.7 μm. The maximum operating frequency of this gate is 0.7 GHz with an average power consumption of 11 mW at that frequency. The schematic of the second design shown in Figure 3.15 consists of 8 transistors. Transistor gate widths are in microns and are written on each transistor and gate lengths are 0.7 μm. The maximum frequency of operation of this gate is the same as that of the 8-transistor XOR gate and is 0.7 GHz. The average power consumed is 6.2 mW.

Comparing the two designs, the second design outperforms the first one because the layout area is smaller. Also, the average power consumption is less than that of the first one. Therefore, the 8-transistor XNOR gate will be used in the later chapters as a building block in the CGaAs Static circuits.
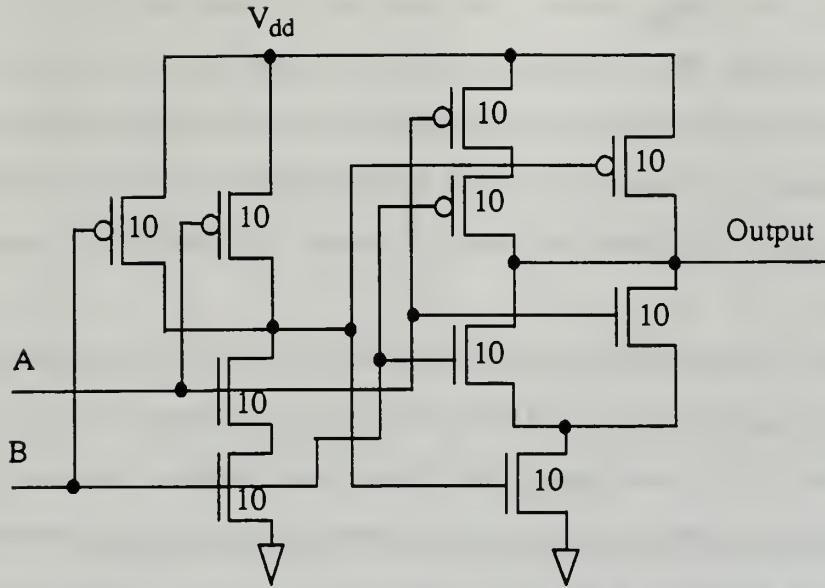
Figure 3.14: CGaAs Static Ten-Transistor XNOR Gate
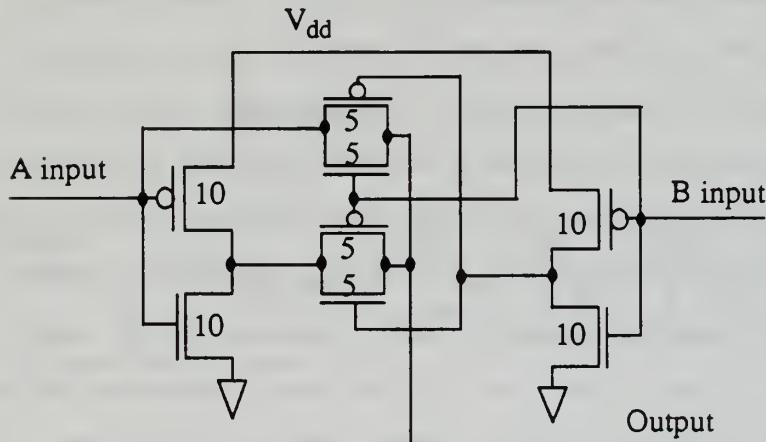
Figure 3.15: CGaAs Static Eight-Transistor XNOR Gate

5. CGaAs Ring Oscillator Design Using Static NOR Gates

The ring oscillator is an asynchronous test structure for propagation delay measurements. It is the easiest way to accurately measure the logic gate propagation delay. The ring oscillator in Figure 3.16 consists of an odd number (n) of inverting logic gates

connected in a closed loop. When the power is applied, the circuit will start to oscillate at a frequency $f = 1/(2nt_{pd})$, where n is the number of gates and t_{pd} is the average gate propagation delay. The propagation delay per gate can be found from a single measurement. A large number of gates should be used in this measurement to decrease the error in measuring the propagation delay. Increasing the number of gates will also reduce the measurement frequency and make it suitable for measure by conventional test equipment.

The ring oscillator designed here is shown in Figure 3.16 and it consists of eleven NOR gates. The output frequency is 149 MHz. It consumes an average power of 21.7 mW when powered from a 2.0 V power supply. All transistor-gate widths of the circuit are 10 μm and lengths are 0.7 μm. The input and output waveforms for this oscillator are shown in Figure 3.17. The first waveform is the applied reset pulse to start the oscillation and the second waveform is the output of the circuit. From the measured frequency, the propagation delay of one NOR gate is calculated to be 0.305 ns.
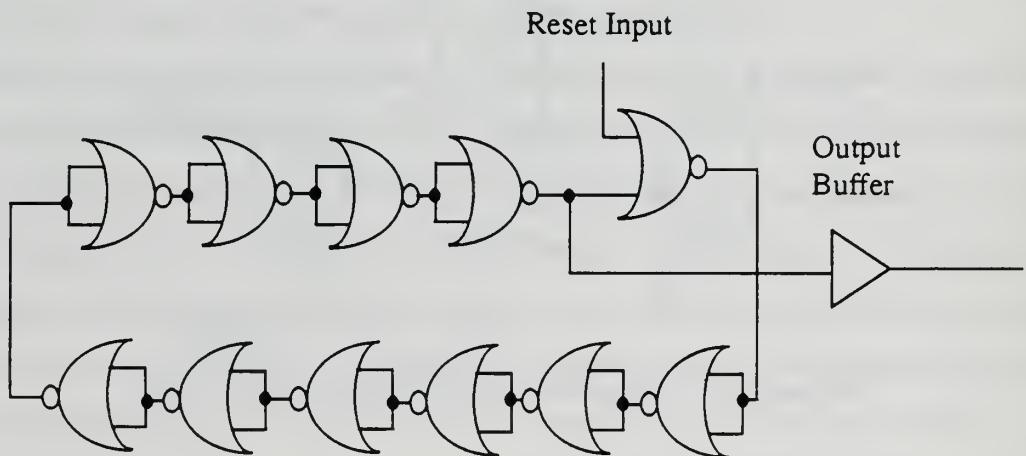
Figure 3.16: CGaAs Eleven NOR Gate Ring Oscillator
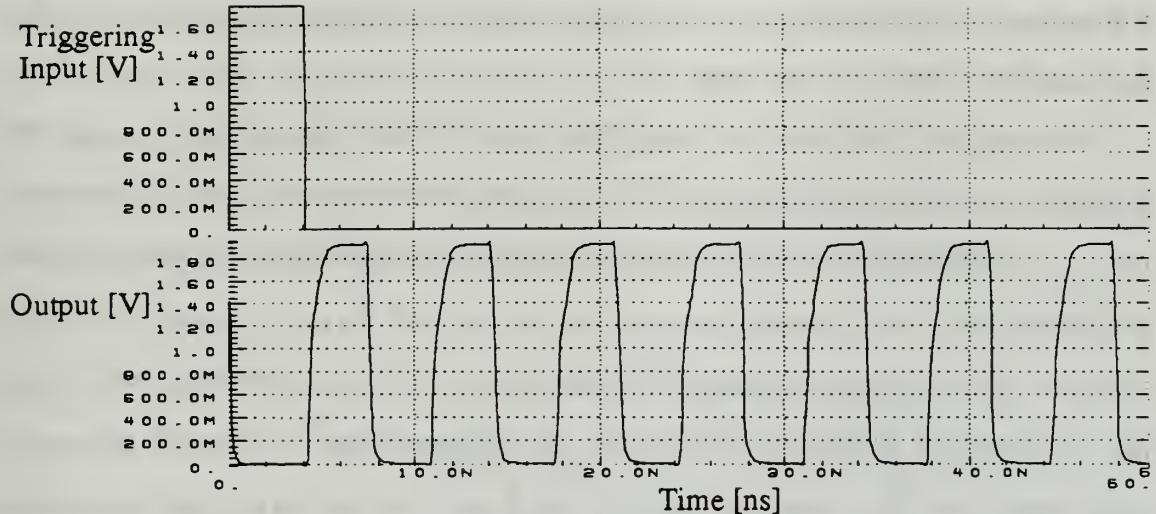
Figure 3.17: Output Waveforms of CGaAs Eleven NOR Gate Ring Oscillator

B. CGaAs TPDL CIRCUIT DESIGN

CGaAs Two-Phase Dynamic Logic (TPDL) circuits use only the fast N-channel transistors in evaluating a logic function. P-channel transistors are used only for precharging the output nodes. Also, there is no direct current path from supply voltage to ground at any time, which eliminates static and short-circuit power consumption in this logic family. The evaluating transistor block (NFETs) can be designed using minimum size transistors (in most cases) without affecting the noise margins or the speed. This will reduce both the layout area and the consumed power. Increasing the sizes of the evaluating transistor block will increase the drive capability of the circuit, but will increase the output capacitance which decreases the maximum operating frequency (trade off). Decreasing the power supply voltage will decrease both the power consumption and the power-delay product, but will also decrease the noise margin (trade off). As the number of transistors in the evaluating transistor block increases, the size of the clocked PFET needs to be increased to be able to quickly charge the output node.

The basic circuit topology of this family is shown in Figure 3.18. The circuits consist of two main blocks, a ϕ_1 block and a ϕ_2 block. Each block consists of pass gates, a clocked

precharge PFET, a clocked discharge NFET and an N-transistor logic block. The output of a ϕ_1 stage can not be connected to the input of another ϕ_1 stage or fed back to itself. The same condition applies to a ϕ_2 stage.

The detailed operation of the circuit is as follows. When ϕ_1 is low and ϕ_2 is high, the ϕ_1 stage is precharging its output node N1 through the ON transistor Q1. At the same time, the input data is passed to the N-transistor logic block through the ON ϕ_1 pass gates. The precharged output of this stage is isolated from the inputs of the next ϕ_2 stage by the off ϕ_2 pass gate. The ϕ_2 stage is evaluating the data stored on the N-transistor logic block inputs (ϕ_2 is high and Q3 is OFF while Q4 is ON). The evaluated output is passed to the next ϕ_1 stage through the ON ϕ_1 pass gate. When ϕ_1 is high and ϕ_2 is low, the ϕ_1 stage is evaluating the data stored on the input of the N-transistor logic block. The output (node N1) is fed to the next ϕ_2 stage through the ON ϕ_2 pass gate. At the same time, the ϕ_2 stage is precharging the output which is isolated from the next ϕ_1 stage by the off ϕ_1 pass gate. When both ϕ_1 and ϕ_2 are high at the same time (they are non overlapped in the logic low), both stages (ϕ_1 and ϕ_2) will be evaluating the inputs stored on the N-transistor logic block. The outputs of both stages will be isolated from the next stage by the off pass gates so there is no corruption of data. The two phases must be non overlapped in the low state to prevent data corruption. If this condition is not satisfied and both phases are low at the same time, both stages will precharge their output nodes and the precharged outputs will be passed to the inputs of the next stage. When either ϕ_1 or ϕ_2 switches to logic low, the corresponding stage will start to evaluate the erroneous inputs (pre-charged outputs of the previous stages) and give an erroneous output. If any input to a ϕ_1 stage is supplied from another circuit (non-TPDL circuit), it has to be stable (unchanging) during ϕ_1 logic low. Similarly, if any input to a ϕ_2 stage is supplied from a non-TPDL circuit, this input has to be stable during ϕ_2 logic low. Another condition that must be satisfied is that ϕ_1 stage outputs can only be connected to ϕ_2 stage inputs and ϕ_2 stage outputs can only be connected to ϕ_1 stage inputs. This is similar to Si CMOS "zipper" logic [36].

An inverter, NAND gate and NOR gate are implemented here because they are the main building blocks of any logic family. Figure 3.19 shows the N-transistor logic block representation of these gates. The following sections show the simulation results of these TPDL gates as well as for TPDL XOR and XNOR gates using HSPICE circuit simulation tools. HSPICE simulation results outline that the TPDL logic family is superior to the static logic family, as will be explained in the comparison section later in this chapter.
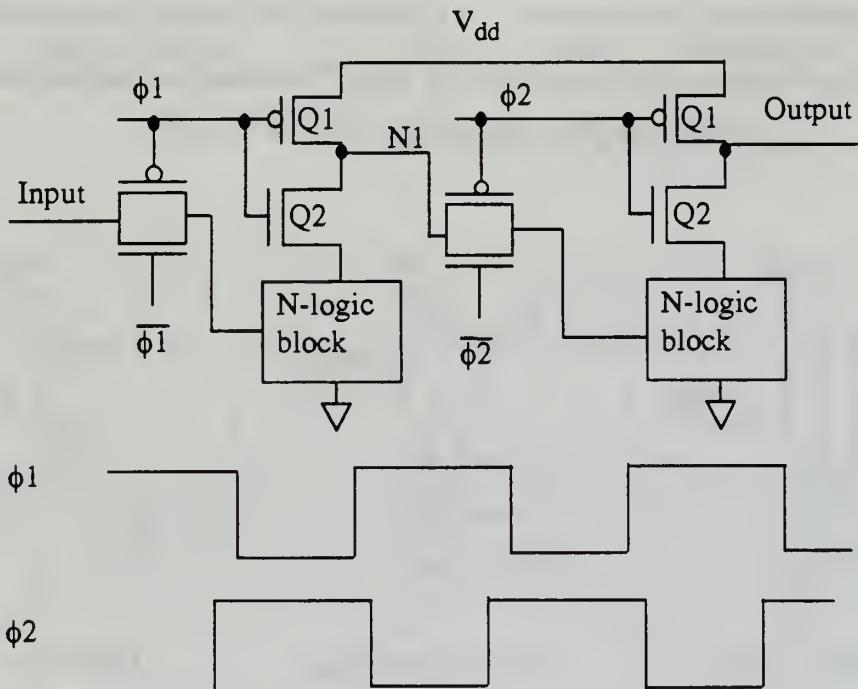
Figure 3.18: Basic Circuit Topology of CGaAs TPDL Gate

1.   TPDL Inverter Circuit Design

The TPDL inverter circuit shown in Figure 3.19 has been inserted in the test circuit shown in Figure 3.20. The test circuit was then simulated using HSPICE to test the TPDL inverter performance. HSPICE simulation results show that this TPDL inverter has a maximum frequency of 2.38 GHz with a fan-out of two when powered from a supply voltage of 2.0 V. The input signal switches between 0.0 V and 1.75 V. The average power consumed by the inverter at the maximum frequency is 1.7 mW. Input and output

waveforms for the inverter operating at a frequency of 2.38 GHz are shown in Figure 3.21. The first waveform is the input signal applied to the ϕ_1 section of the circuit. This signal must be stable during ϕ_1 low because during this time the input signal is passed through the ϕ_1 pass gate to the ϕ_1 section evaluating block. Therefore, for the evaluation to be correct, this signal has to be stable. The second waveform is the ϕ_1 clocking signal, while the third waveform is the inverter output. The output of this inverter can only be applied to a ϕ_2 section input because it is an output of a ϕ_1 section. The inverter output precharges when ϕ_1 is low and evaluates the input during ϕ_1 high. Thus it can be sampled at the end of ϕ_1 evaluation phase (at the end of ϕ_1 high period).
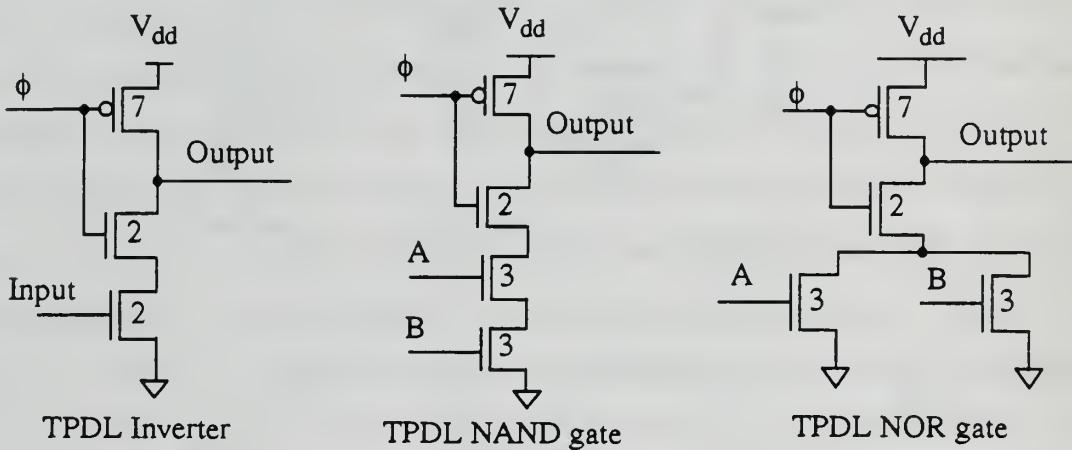
Figure 3.19: CGaAs TPDL Combinational Logic Gates

52
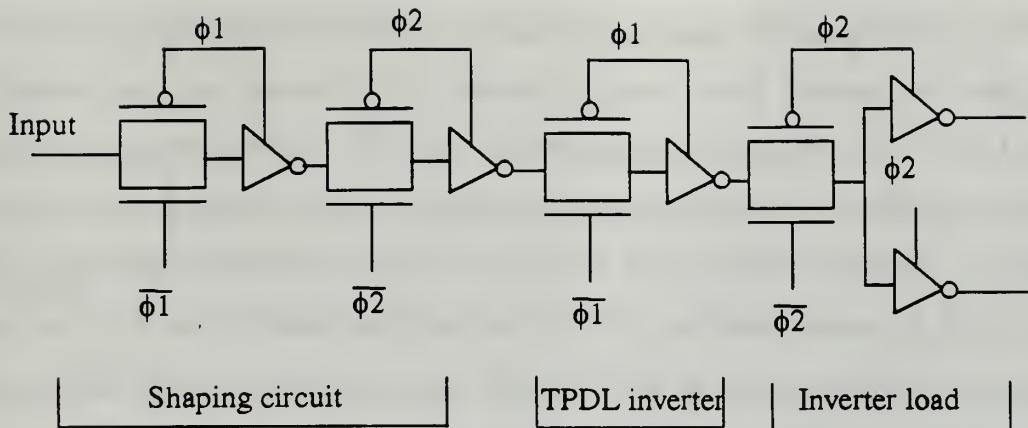
Figure 3.20: CGaAs TPDL Inverter Test Circuit
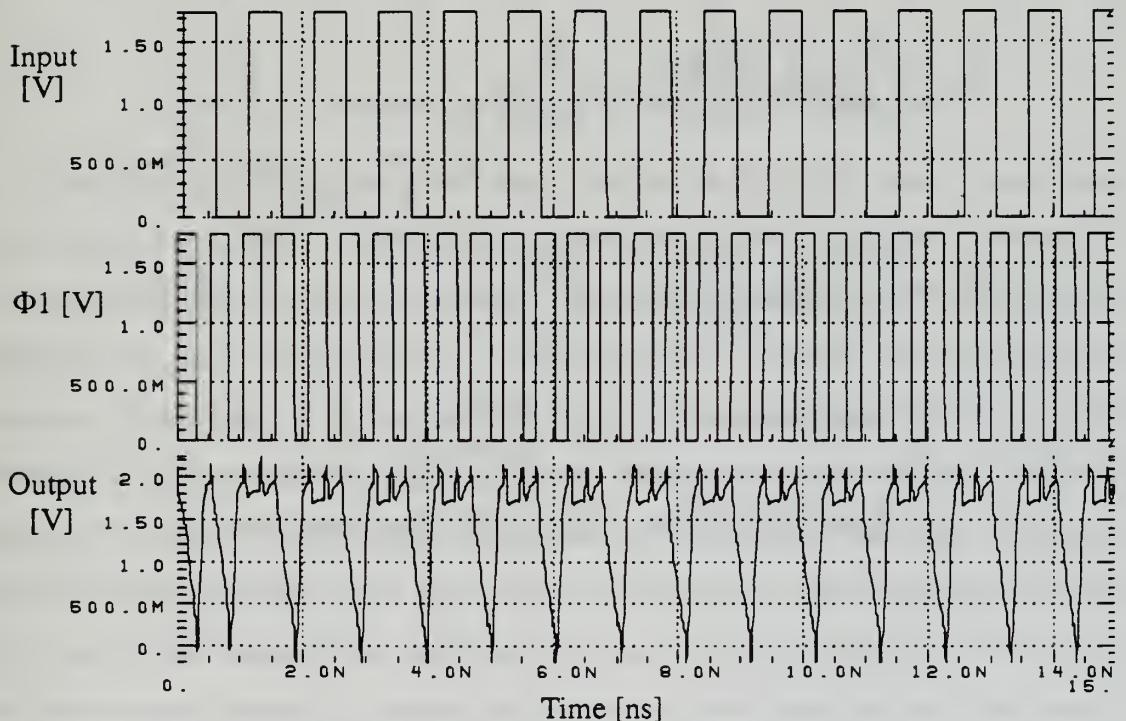
Figure 3.21: Input-Output Waveforms of CGaAs TPDL Inverter

2. TPDL NAND Gate Circuit Design

The TPDL NAND gate shown in Figure 3.19 was inserted in a test circuit to study its performance for the comparison of this logic family with static logic. The circuit shown in

53

Figure 3.22 is the complete test circuit simulated using HSPICE to test the performance of the TPDL NAND gate. The maximum frequency of operation achieved by this circuit is 2.38 GHz when powered from a supply voltage of 2.0 V. The input switches between 0.0 V and 1.75 V. The average power consumed by this TPDL NAND gate at the maximum frequency is 1.98 mW. The input and output waveforms of the NAND gate are shown in Figure 3.23. The first waveform is the A input of the NAND gate while the B input is held at logic high, the second waveform is the ϕ_1 clocking signal, while the last waveform is the gate output. As shown in Figure 3.23, the input signal is applied to the ϕ_1 section and is stable (unchanged) during ϕ_1 low to insure correct operation of the circuit.
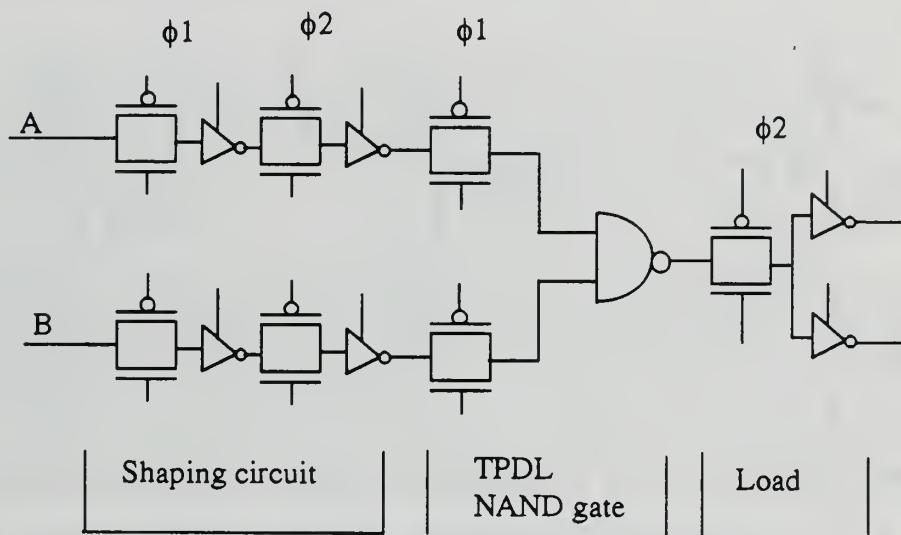
Figure 3.22: CGaAs TPDL NAND Gate Test Circuit
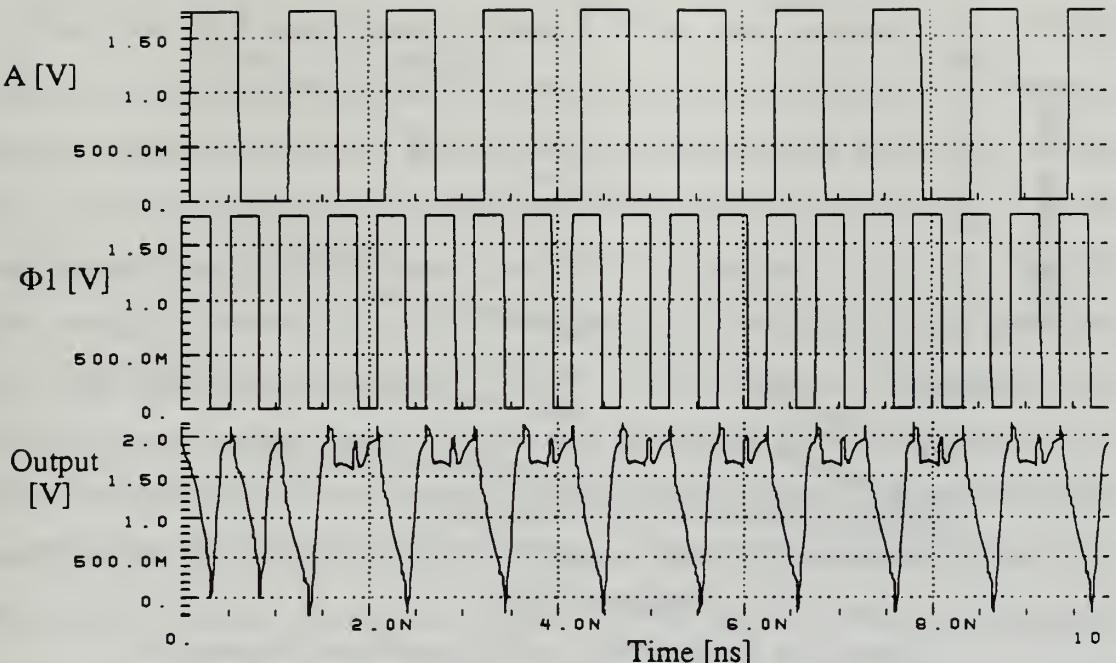
Figure 3.23: Transient Analysis of CGaAs TPDL NAND Gate

The effect of changing the power supply voltage on the NAND gate average power consumption and maximum frequency of operation was also studied. Figure 3.24 shows the average power consumption as a function of the operating frequency for different supply voltages and input transitions. The consumed power is linearly proportional to the frequency of operation. Also, the consumed power increases with the increase in the supply voltage due to the increase in the drain-source leakage current and the gate conduction current. The effect of increasing the output load on the maximum operating frequency of the NAND gate, powered from a 2.0 V power supply, is also studied and plotted in Figure 3.25. As the load increases, the maximum frequency of operation decreases. The decrease in the maximum frequency is not very much (compared with that of the static logic family) because the load is separated from the driving circuit by the pass gate. The effect of loading on the maximum frequency is due to the charge redistribution problem which ia a common problem in all dynamic logic families.
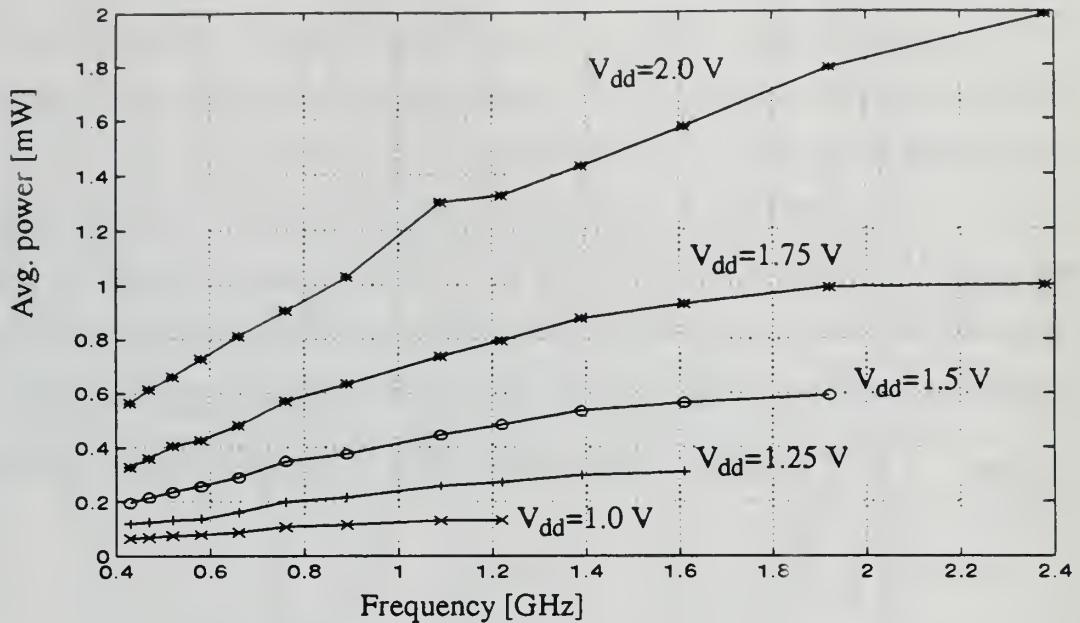
Figure 3.24: CGaAs TPDL NAND Gate Power Consumption
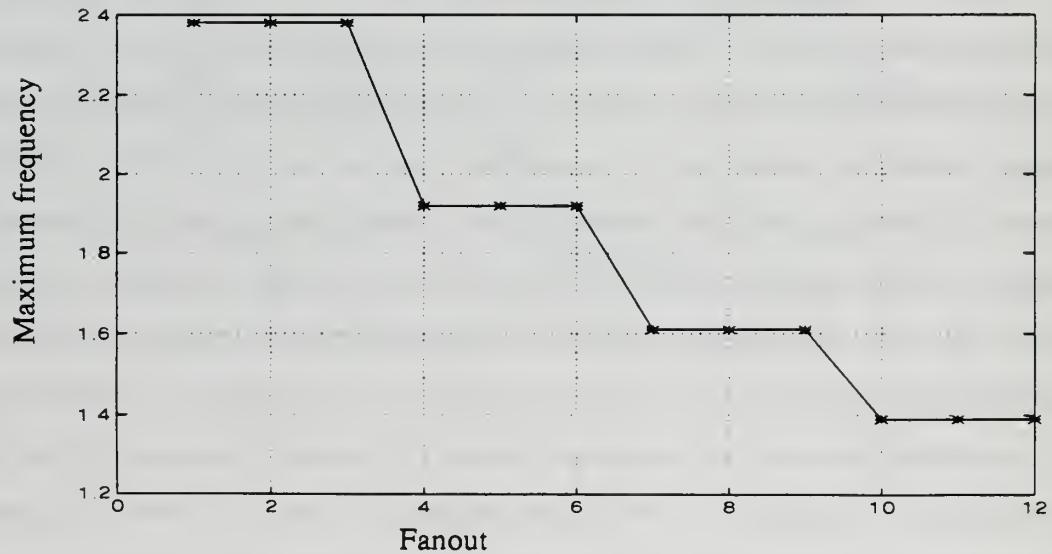
Figure 3.25: Loading Effects on CGaAs TPDL NAND Gate

3. TPDL NOR Gate Circuit Design

The TPDL NOR gate shown in Figure 3.19 has been simulated using HSPICE simulation tools. The test circuit used to accomplish this is shown in Figure 3.26. Maximum operating frequency of this logic gate is 2.38 GHz (same as NAND gate) when powered from a 2.0 V power supply, and the input signal switches between 0.0 V and 1.75 V. The average power consumed by the gate at the maximum frequency is 2.01 mW. When the supply voltage decreases to 1.75 V, the same maximum frequency can be approached but the average consumed power drops to 1.04 mW. This drop is due to the decrease in both the drain-source leakage current and the gate conduction current. Input and output waveforms of the circuit, when simulated in HSPICE, are shown in Figure 3.27. The first waveform is the input applied to one input of the gate while the other input is held at 0.0 V. The second waveform is the ϕ_1 clocking signal and the last waveform is the logic gate output. As mentioned before, the input signals are allowed to switch between the logic levels only when the corresponding ϕ clock is logic high.
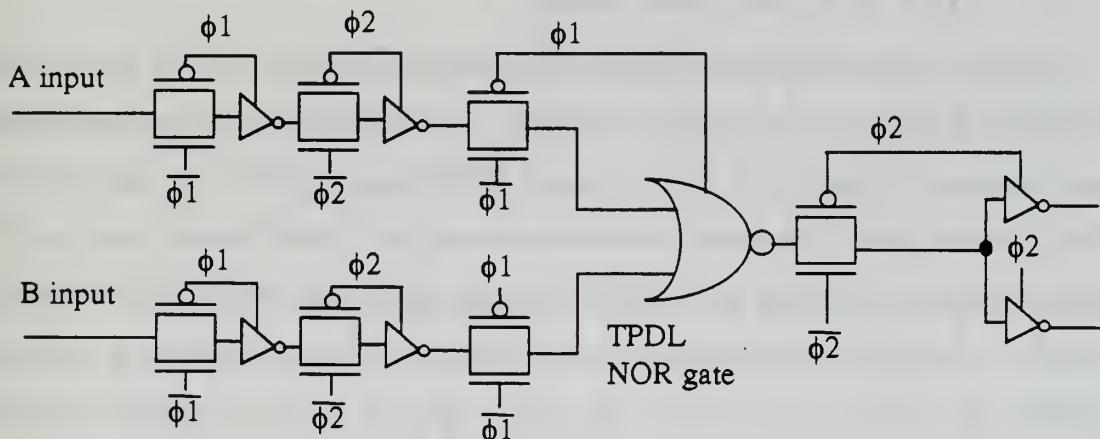
Figure 3.26: CGaAs TPDL NOR Gate Test Circuit

57
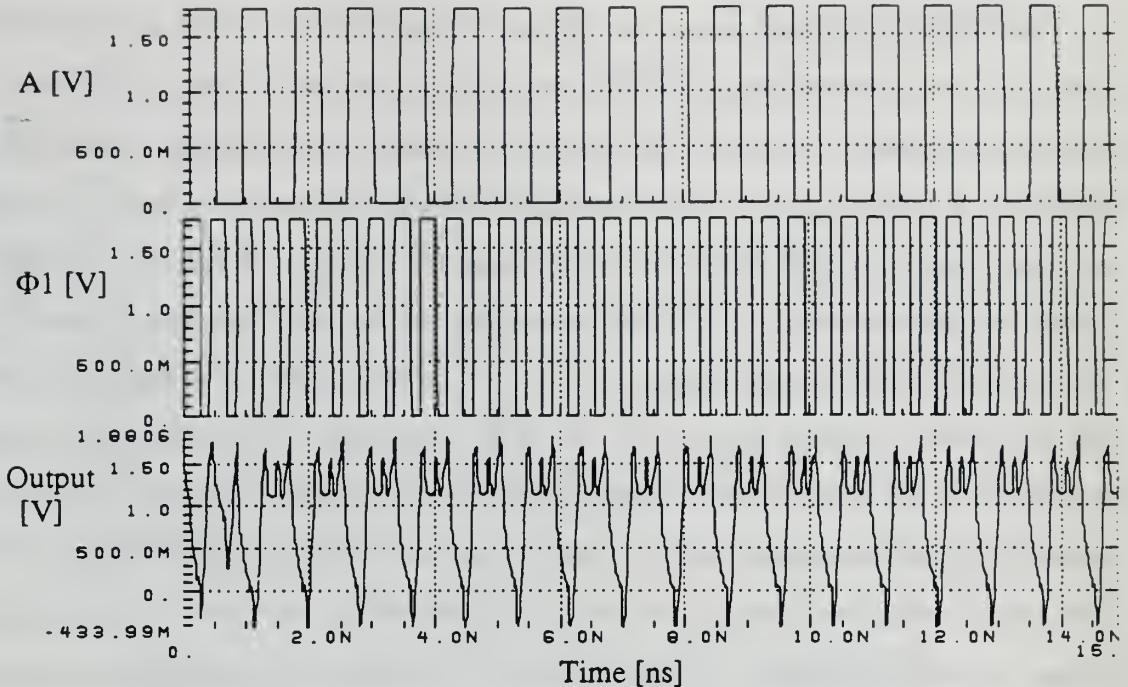
Figure 3.27: Input-Output Waveform of CGaAs TPDL NOR Gate

4.   TPDL XOR Gate Circuit Design

A useful complex logic gate in many combinational circuits is the XOR gate. A TPDL CGaAs XOR gate has been designed using three TPDL NAND gates and one static NAND gate as shown in Figure 3.28. X1 is the static NAND gate, while X2, X3 and X4 are the TPDL NAND gates. The circuit was simulated using the HSPICE simulation tool. The input and output waveforms at the maximum operating frequency with a fan-out of two are shown in Figure 3.29. Maximum operating frequency of this logic gate, according to HSPICE simulations, is 1.61 GHz when powered from a 2.0 V power supply and with an input signal transition between 0.0 V and 1.75 V. The average power consumed by the TPDL XOR gate at the maximum operating frequency is 4.8 mW when one of the inputs is switching and the other input is tied to 1.75 V. When one input of the gate is switching and the other input is tied to 0.0 V, the average consumed power drops to 3.98 mW. The TPDL XOR gate maximum frequency of operation is higher than that of the static gate. The

58

average consumed power is lower than that for the static gate and will be explained in detail in the comparison between TPDL and static logic, Section D.
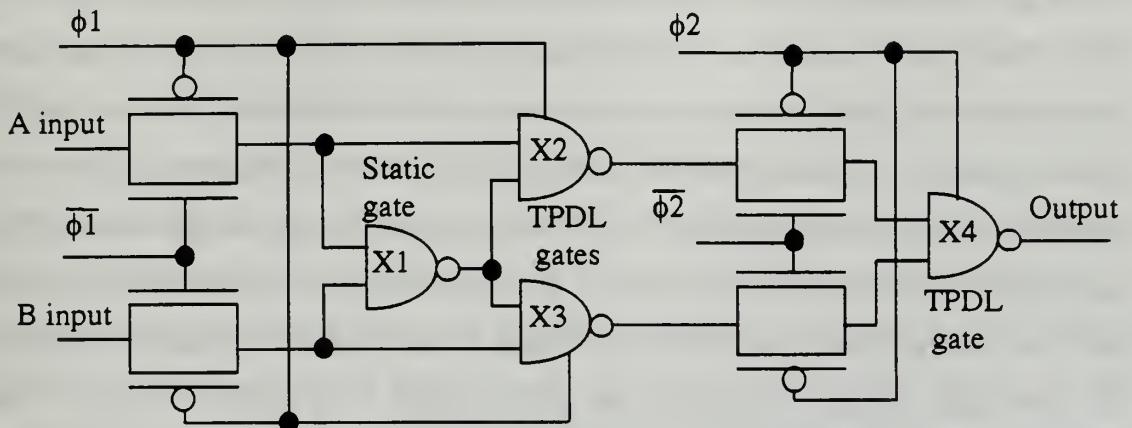
Figure 3.28: CGaAs TPDL XOR Gate
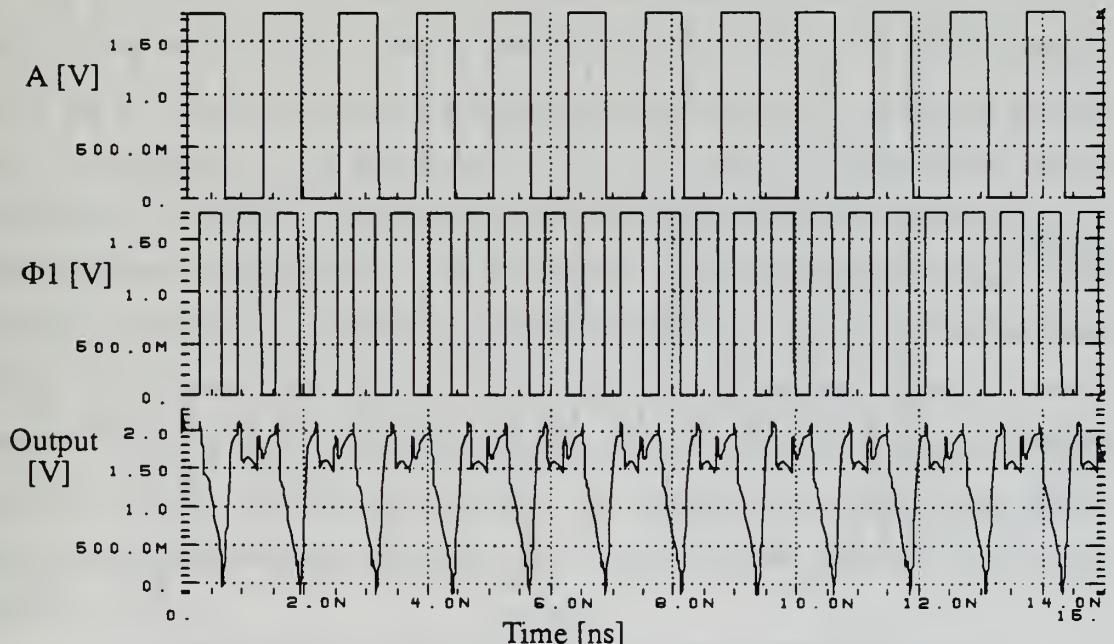
Figure 3.29: Input-Output Waveforms of CGaAs TPDL XOR Gate

5. TPDL XNOR Gate Circuit Design

The XNOR gate is also a useful complex combinational logic gate. A TPDL CGaAs XNOR gate has been designed using three TPDL NOR gates and one static NOR gate. The TPDL XNOR gate is similar to the circuit shown in Figure 3.28 but all NAND gates are replaced by NOR gates. This circuit was simulated using HSPICE simulation tools. The input and output waveforms of the simulated circuit are shown in Figure 3.30. Maximum frequency of operation of the circuit is 1.91 GHz at a power supply voltage of 2.0 V. The input signal switches between 0.0 V and 1.75 V with a load of two inverters (fan-out of two). The average power consumption of the gate at the maximum operating frequency is 7.61 mW when one input is switching and the other input is tied to 0.0 V. When the other input is tied to 1.75 V, the average consumed power drops to 6.27 mW.
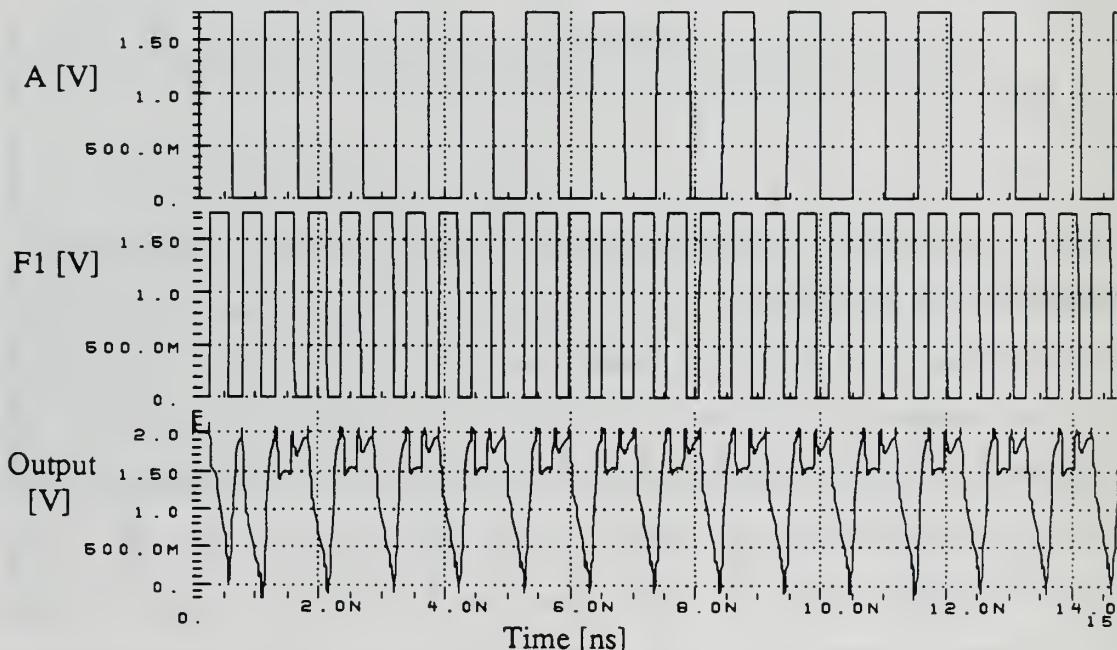
Figure 3.30: Input-Output Waveforms of CGaAs TPDL XNOR Gate

C. DESIGN OF CGaAs TWO PHASE NON-OVERLAPPING CLOCK GENERATOR

The operation of TPDL circuits requires two clock phases and their complements. This motivates the design of such clock generator. The latest design of a two-phase clock generator was found in reference 43. It has a maximum frequency of operation of 0.5 GHz. The average power consumed by this generator is 52 mW from a 1.5 V power supply. This clock generator generates only the two non-overlapped clocks without their complements, which is half of the described design as will be seen later in this section. The design in reference 43 was fabricated using a N-MESFET process which is faster than the CGaAs process but consumes much higher power. In this section, design, simulation and performance tests of the circuit that generates two non-overlapping clocks and their complements are explained.

The two-phase non-overlapping clock generator consists of two main parts. The first part generates the two-phases ϕ_1 and ϕ_2 from the input clock signal. The output of the first part is fed to the second part which generates the complements. The key to the design is that the two generated clock phases need to be non overlapped in the logic low level (a requirement of the TPDL circuits). Also, the complements of the two-phases need to be non-overlapped in the logic high level. This implies that each phase and its complement need to be 180 degrees out of phase. As the frequency increases, the clock period decreases, which make the phase error crucial. The logic diagram of the generator circuit is shown in Figure 3.31. The circuit diagram of the generator is shown in Figure 3.33. Transistor gate widths, in microns, are indicated in Figure 3.33, while transistor-gate lengths are 0.7 μm.The transistor-gate widths of the pass-gate transistors in this figure are 2 μm for both NFETs and PFETs.

61
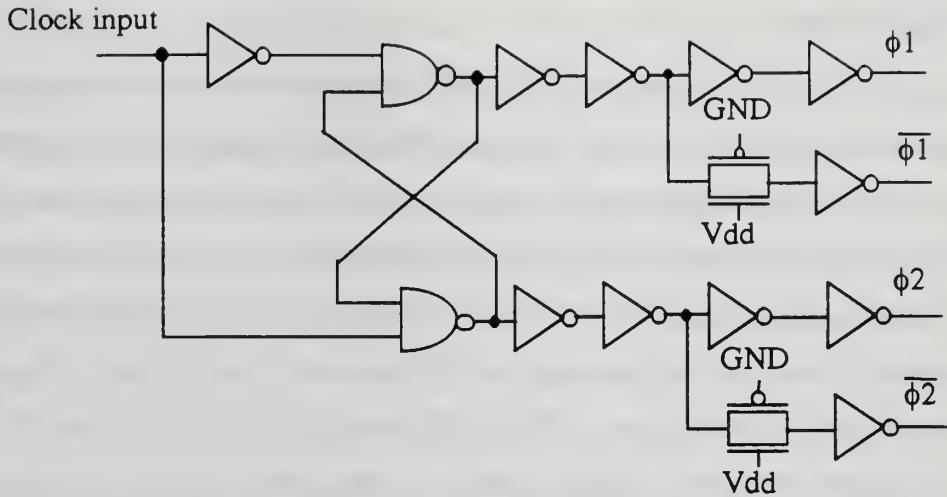
Figure 3.31: Logic Diagram of Two-Phase Clock Generator

The generator circuit was designed, then simulated using HSPICE simulation tools and finally implemented using CADENCE tools to be fabricated in the Motorola fabrication process line. Its gate layout area is 77.7 μm^2. When the circuit is powered from 2.0 V and the clock input switches between 0.0 V and 1.75 V, the maximum operating frequency of the circuit is 1.0 GHz for a fan-out of two. The average power consumed by the circuit at the maximum operating frequency is 25.8 mW. Figure 3.32 shows the input and output waveforms of the clock generator at 1.0 GHz. The generated clock phases, ϕ_1 and ϕ_2, are non-overlapped in the logic low level. The effect of increasing the load on the maximum operating frequency of the circuit is also studied and plotted in Figure 3.34. As seen from this figure, maximum frequency of operation of the circuit decreases with increasing load. To drive a high capacitive load, a driver circuit for each phase is required to reduce the effect of the load on the maximum frequency of operation. Also, as the frequency increases, the power consumption of the circuit increases due to the increase in the dynamic power consumption which is frequency dependent. The average power consumed by the circuit, as a function of frequency, is plotted in Figure 3.35. The power dependence on the frequency is linear.
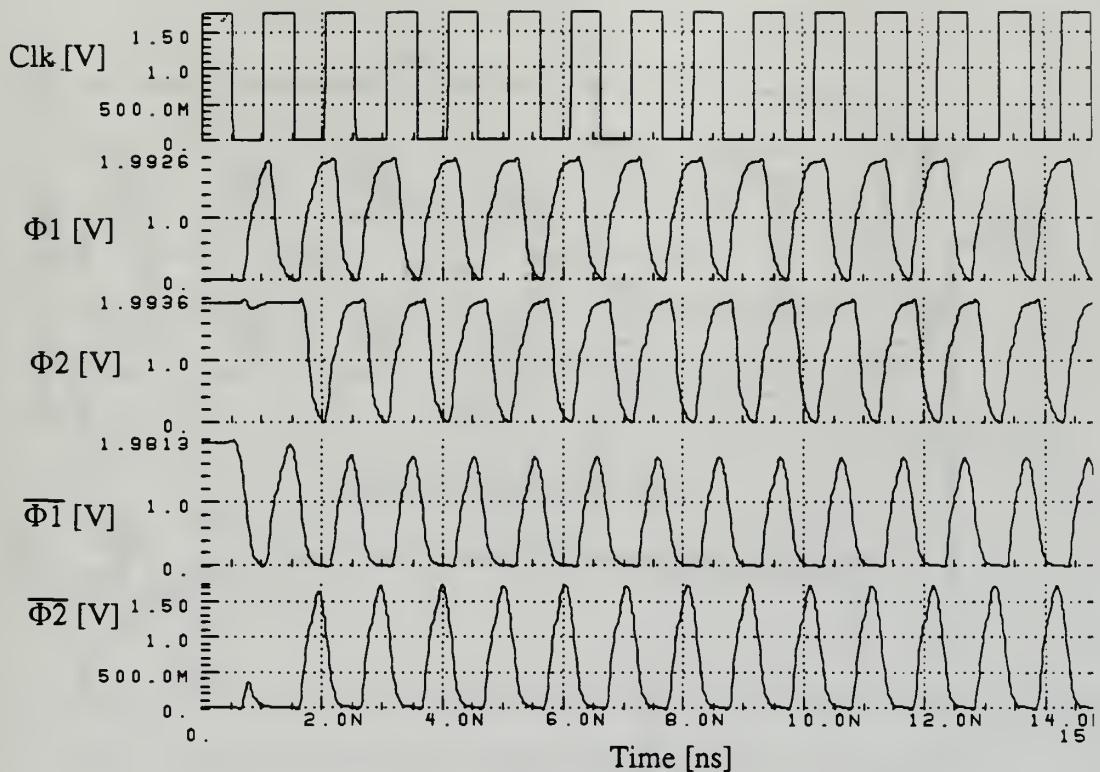
Figure 3.32: Input-Output Waveforms of Clock Generator
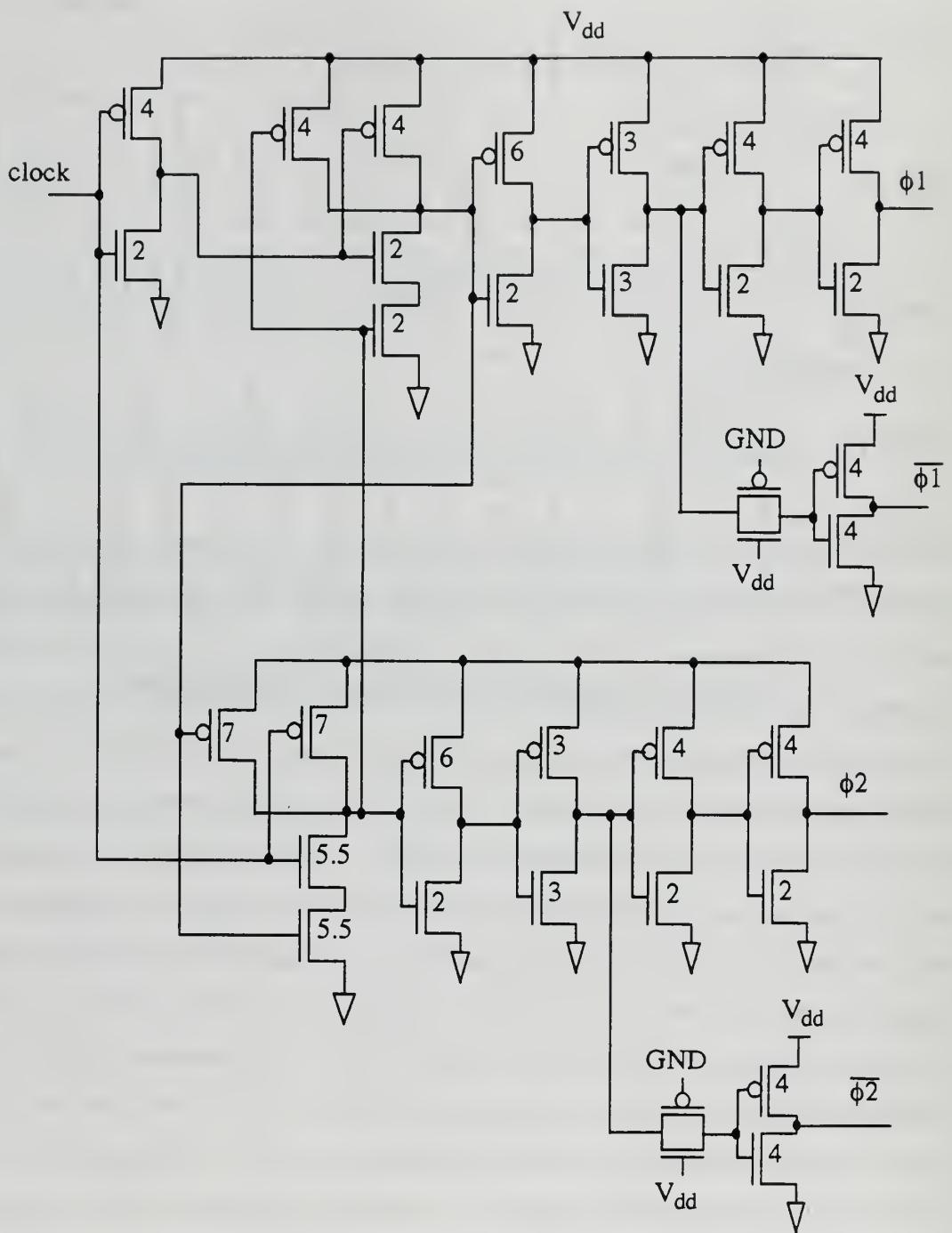
Figure 3.33: Circuit Diagram of Two-Phase Clock Generator

64
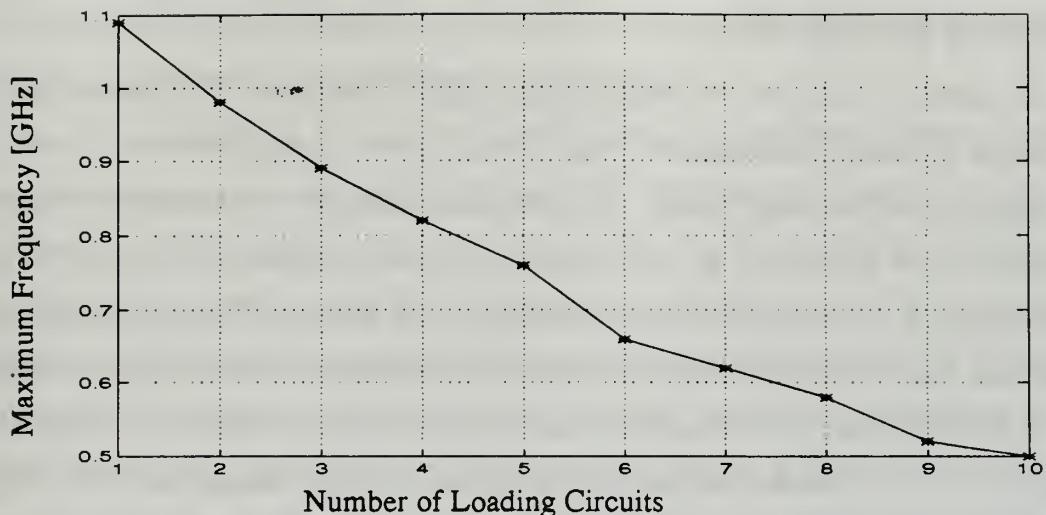
Figure 3.34: Loading Effects on Clock Generator
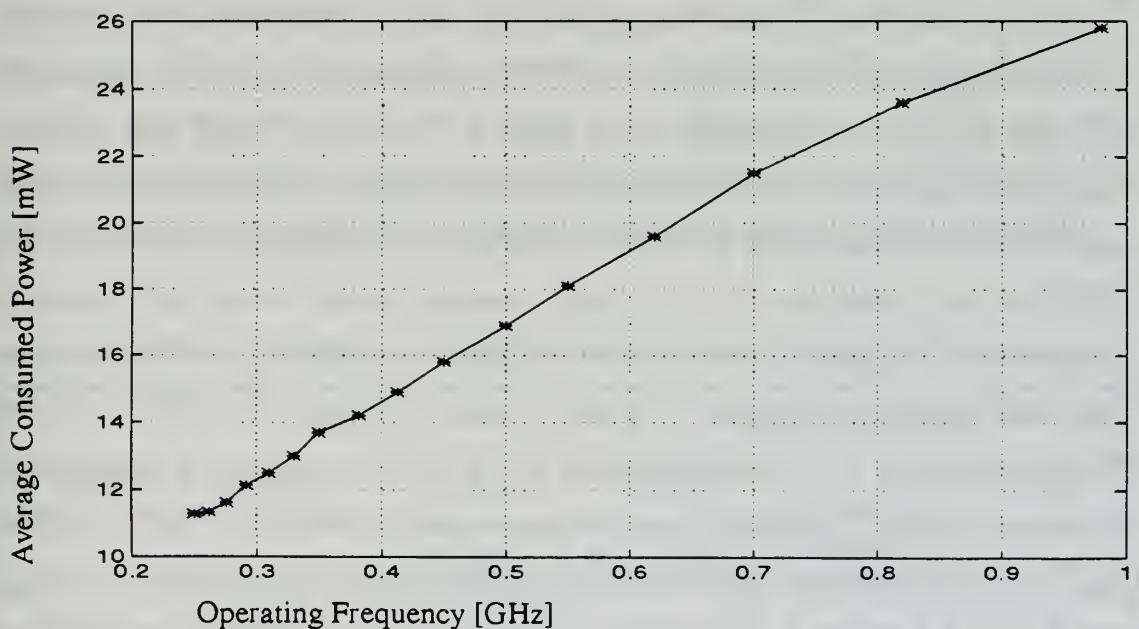
Figure 3.35: Power Consumption of Clock Generator

D. COMPARISON BETWEEN CGaAs STATIC AND TPDL COMBINATIONAL LOGIC CIRCUIT DESIGNS

In Sections A and B, the design of both CGaAs Static and TPDL logic gates are explained in detail. The design of TPDL circuits is very complicated, but it has many advantages over the static design. The maximum frequency of operation is higher, it consumes lower power and the layout area is less than that of the static design. Its main disadvantage is the need for two non-overlapped clock phases and their complements for operation. Also, it has a more complex logic and circuit design. The two clock phases have to be non-overlapped in the logic low level to prevent data corruption, as explained in Section C. Table 3.1 shows the comparison between static logic designs and TPDL designs [49]. As seen from the table, TPDL circuits have a maximum frequency of operation about double that of the static circuits. Also, the consumed power at the maximum frequency is always less than that of the static circuits.

For the power consumption comparison to be fair, two factors must be considered. First, the average consumed power of both TPDL and static circuits must be calculated at the same frequency. For example, from Table 3.1, the static NAND gate maximum frequency of operation is 1.2 GHz and the power consumption at that frequency is 5.8 mW, while the power consumed by the TPDL NAND gate at 2.38 GHz is calculated to be 1.98 mW. The fair comparison for the average consumed power, when both powers are calculated at 1.2 GHz, are 5.8 mW for the static gate and 1.4 mW for the TPDL gate when both gates are connected to the same power supply. However, the TPDL circuit will function properly at 1.2 GHz when powered from a 1.0 V power supply with much lower power consumption. The average consumed power is then reduced to 0.15 mW. Therefore, at 1.2 GHz, the comparison between static and TPDL average consumed power will be 5.8 mW to 0.15 mW, which is over thirty-eight times. Second, for the comparison to be fair, the layout area and the power consumed by the two-phase non-overlapping clock generator must be considered. The gate layout area of the clock generator is 77 μm^2 and it consumes 25 mW at its maximum operating frequency. If the clock generator explained in previous section drives a hundred combinational logic gates, its power consumption and the layout

66

area should be distributed over these driven gates. Dividing the layout area and the power consumption of the clock generator over the driven gates will increase theirs by less than 10%. Thus, this factor has a small effect on the comparison.

For the comparison to be clear, the NAND gate will be taken as a study case. The power consumption versus the operating frequency at different power supply voltages for both static and TPDL designs is shown in Figure 3.36. This figure actually combines the two graphs for both static and TPDL NAND gates plotted previously. The power delay product for the TPDL and static logic NAND gates is also plotted in Figure 3.37. The power delay product decreases as the power supply decrease because of the decrease in the leakage current. Also, loading effects on both designs are shown in Figure 3.38. This figure shows that the loading effect has less influence on the TPDL gate maximum frequency of operation than for the static gate. This is because the load of the TPDL gate is isolated from the output node by the pass gate. Loading effects on the static design are due to the increased output capacitance, while loading effects on the TPDL design are due to the charge redistribution problem, which is a common problem for all dynamic logic circuits.

This concludes the combinational logic circuit design using both TPDL and static logic. In the next chapter, the design and implementation of the sequential logic circuits is presented. Also, the performance comparison between the two techniques is discussed.

Table 3.1: CGaAs Static and TPDL Combinational Circuit Performance

Designed Logic Gate	Circuit Topology	Circuit performance			
		Maximum Frequency [GHz]	Average Power @ F_{max} [mW]	Number of Transistors	Total Layout Area [μm^2]
Inverter	Static	1.2	2.17	2	14
	TPDL	2.38	1.7	3	7.7
NAND	Static	1.2	5.8	4	28
	TPDL	2.38	1.98	4	10.5

Table 3.1: CGaAs Static and TPDL Combinational Circuit Performance

Designed Logic Gate	Circuit Topology	Circuit performance			
		Maximum Frequency [GHz]	Average Power @ F_{max} [mW]	Number of Transistors	Total Layout Area [μm^2]
NOR	Static	0.82	6.5	4	28
	TPDL	2.38	2.01	4	10.5
XOR	Static	0.55 0.7	3.2 6.2	6 8	35 42
	TPDL	1.61	4.8	24	48.3
XNOR	Static	0.7 0.7	6.2 11	8 10	42 70
	TPDL	1.91	7.61	24	48.3
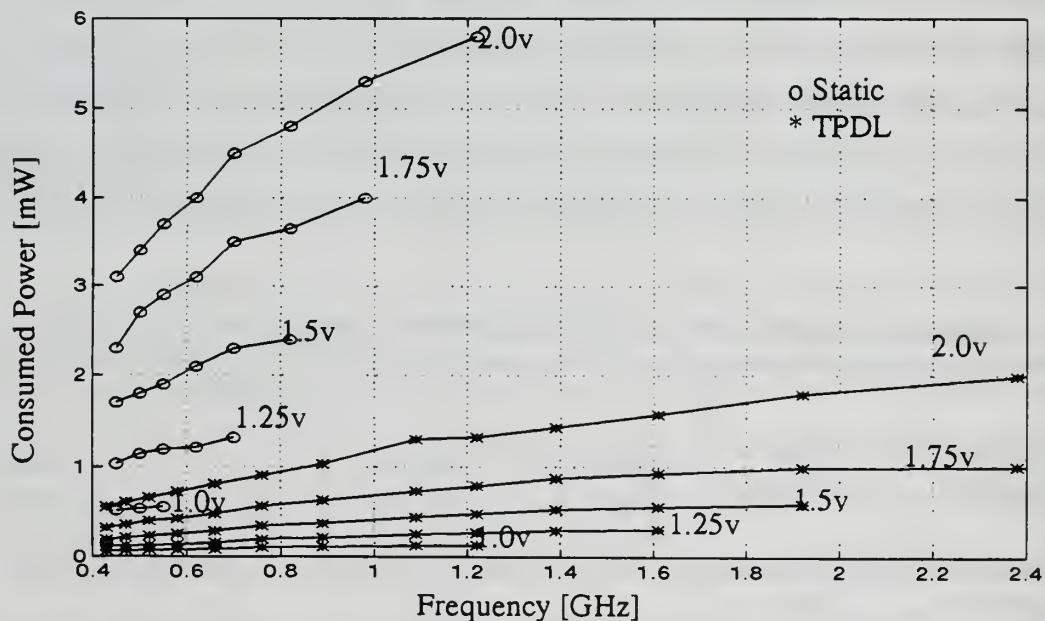
Figure 3.36: CGaAs Static and TPDL NAND Gate Power Consumption
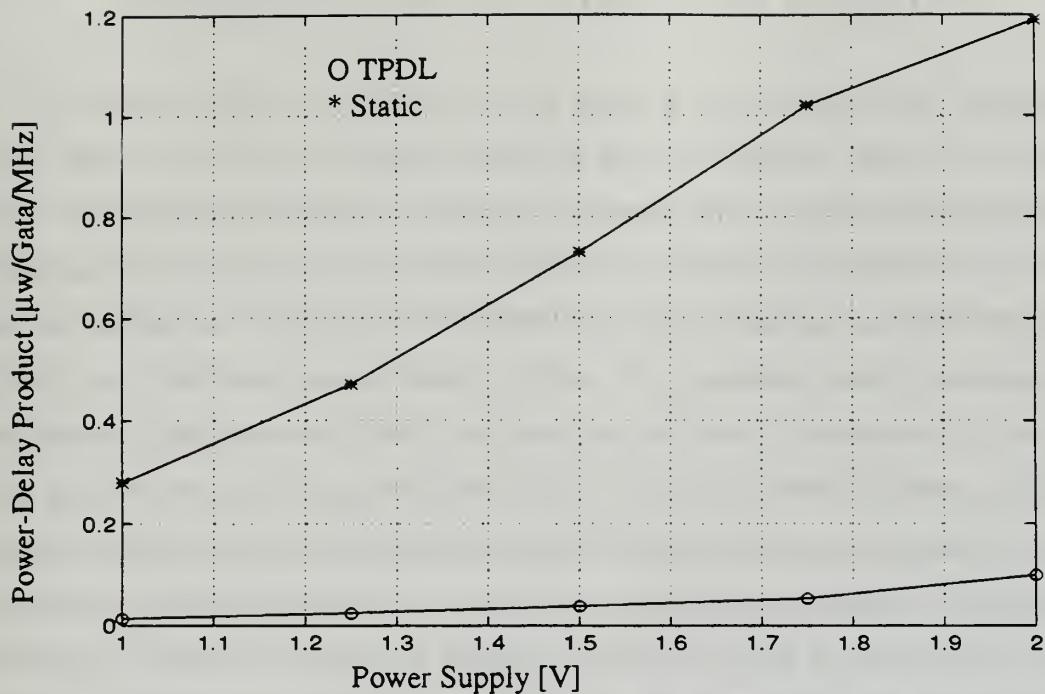
Figure 3.37: CGaAs Static and TPDL NAND Gate Power-Delay Product
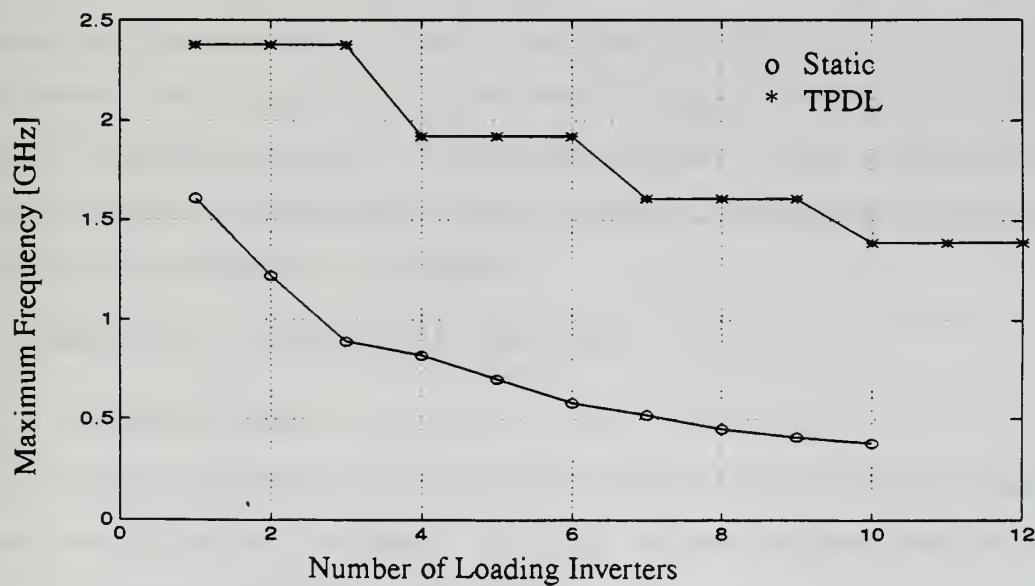
Figure 3.38: Loading Effects on CGaAs Static and TPDL NAND Gates

IV. DESIGN AND ANALYSIS OF COMPLEMENTARY GaAs STATIC AND DYNAMIC SEQUENTIAL CIRCUITS

A sequential circuit is a circuit where the output is a function of either the previous inputs (state) or the previous inputs (state) and the current inputs. There are two major classes of sequential circuits, pulse-mode sequential circuits and fundamental-mode sequential circuits. Pulse-mode sequential circuits are often called synchronous circuits because their action is synchronized with the pulse input. Fundamental-mode sequential circuits are often called asynchronous circuits. To guarantee proper operation of a fundamental-mode sequential circuit, only one input is allowed to change at any given time. Also, an input can only change when the circuit is internally stable. Fundamental-mode analysis is more complex than pulse-mode analysis because it requires tracking all changes of internally stored signals. Also, the necessity of avoiding critical races in fundamental-mode circuits makes the process of assigning internal variables to internal states rather complex. Moreover, the initial determination of the flow table and the process of minimizing the number of internal states requires care.

The purpose of this chapter is to design different pulse-mode sequential logic functions using Complementary GaAs (CGaAs) static and TPDL circuit topologies, then compare between their performances. The functions designed in this chapter are: D-latch, D flip flop, divide-by-two circuit, 3-Bit Linear Feedback Shift Register (3BLFSR), and 4BLFSR. Section A discusses the design of these functions using static circuits, while in Section B, the same functions are designed using TPDL. In Section C, the comparison between static and TPDL circuit performance is established.

A. CGaAs STATIC SEQUENTIAL CIRCUITS

1. D-Latch Circuit

A CGaAs D-latch static circuit is shown in Figure 4.1. It consists of ten transistors (three inverters and two pass gates). The circuit has been designed, simulated using HSPICE and then analyzed and optimized in layout area to achieve the highest frequency of operation. All transistor gate lengths used in this design are 0.7 μm, while the gate widths

are 10 μm for the inverter transistors and 5 μm for pass-gate transistors (both NFETs and PFETs). Pass gates do not regenerate the input logic levels and increasing the transistor gate widths will not increase the speed of the circuit. The circuit speed will decrease because of the increased loading on the previous stage. Maximum operating frequency of the designed circuit is limited by the propagation delay of the signal through the entire circuit. The circuit was simulated with a power supply of 2.0 volts and the input signal transitions between 0.0 volts and 1.75 volts. Maximum clock frequency of the gate is 0.82 GHZ and the average consumed power at this frequency is 12.32 mW when loaded by two inverters (fan-out of two). D input and clock signals applied to the circuit have a rise and fall time of 0.01ns. The time required to pull up the output to a logic high level measured from 50% of the clock pulse rising edge to 50% of the output signal rising edge (T_{plh}) is 0.75 ns. The time required to pull down the output to a logic low level measured from 50% of the clock pulse rising edge to 50% of the output signal falling edge (T_{phl}) is 0.45 ns. Input and output waveforms of the D-Latch circuit at a frequency of 0.82 GHz are shown in Figure 4.2. The top waveform is the clock pulse applied to the circuit while the second waveform is the D-input and the bottom waveform is the circuit output.
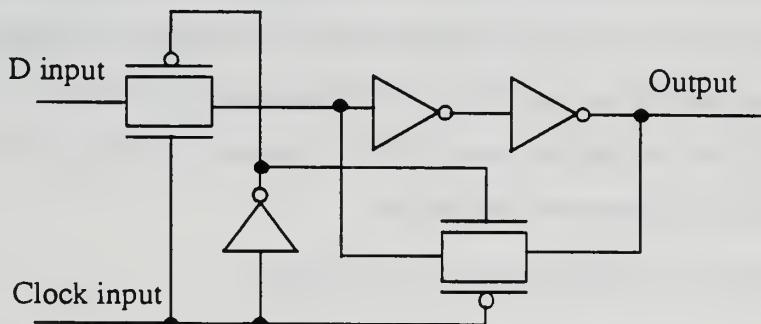
Figure 4.1: CGaAs Static D-Latch Circuit
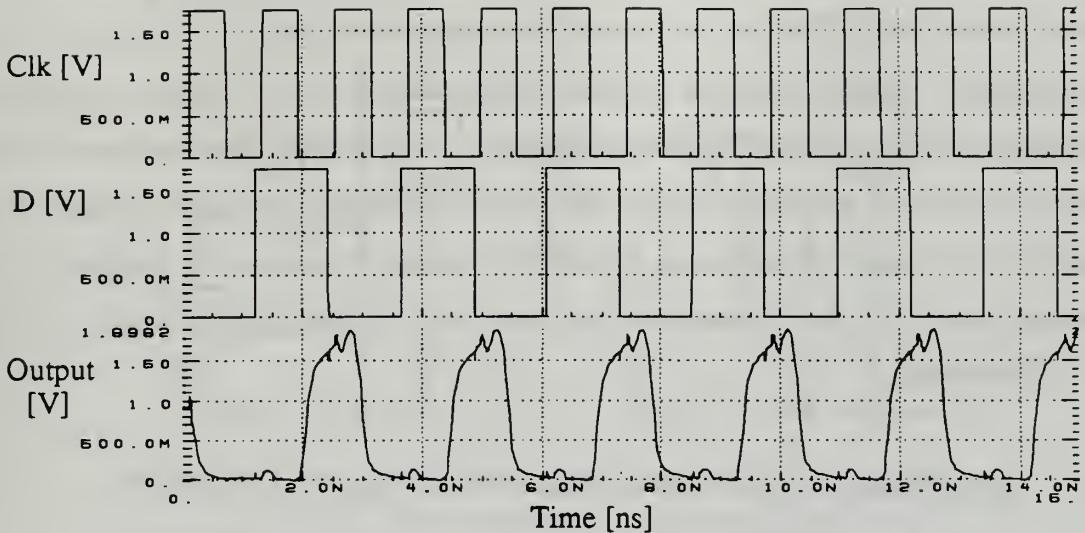
Figure 4.2: Input-Output Waveform of CGaAs Static D-Latch

2. D Flip Flop (D-FF) Circuit Design

A negative edge-triggered D-FF is shown in Figure 4.3 which contains 20 transistors. Actually, this design is a master-slave flip flop. It consists of two D-latch gates, with $\overline{Q}$ output of the first latch connected to the D input of the second latch. Transistor sizes are the same as for the D-latch circuit (designed in the previous subsection). Maximum operating frequency of this circuit is 0.82 GHz with a power supply voltage of 2.0 volts. Input signals switch between 0.0 volts and 1.75 volts and the circuit has a fan-out of two. The average power consumed by the circuit at the maximum operating frequency is 20.8 mW. The pull-up time of the flip flop is 0.83 ns, measured from 50% of the clock-falling edge (after the input changes to a logic level high) to 50% of the output rising edge. Pull-down time is 0.58 ns, measured from 50% of the clock-falling edge (after the input changes to a logic level low) to 50% of the output-falling edge. Input and output waveforms of the D-FF at a clock frequency of 0.82 GHZ are shown in Figure 4.4.

73
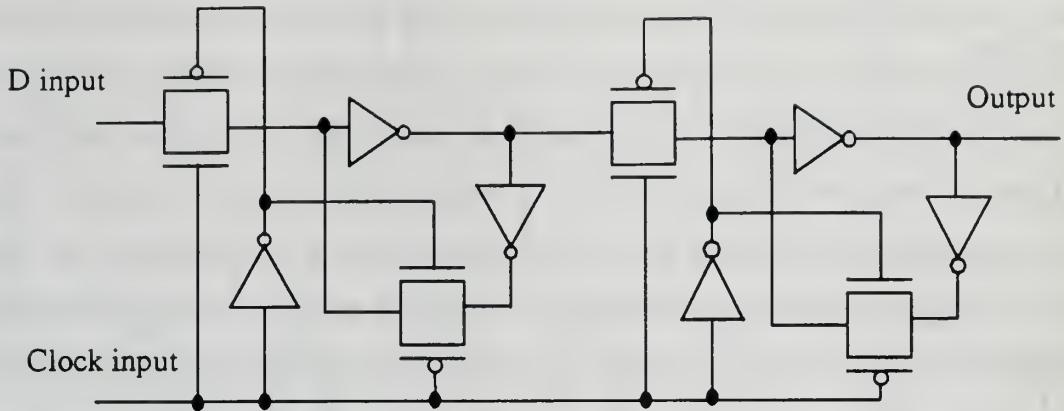
Figure 4.3: CGaAs Static Negative-Edge Triggered D Flip Flop

Time [ns]
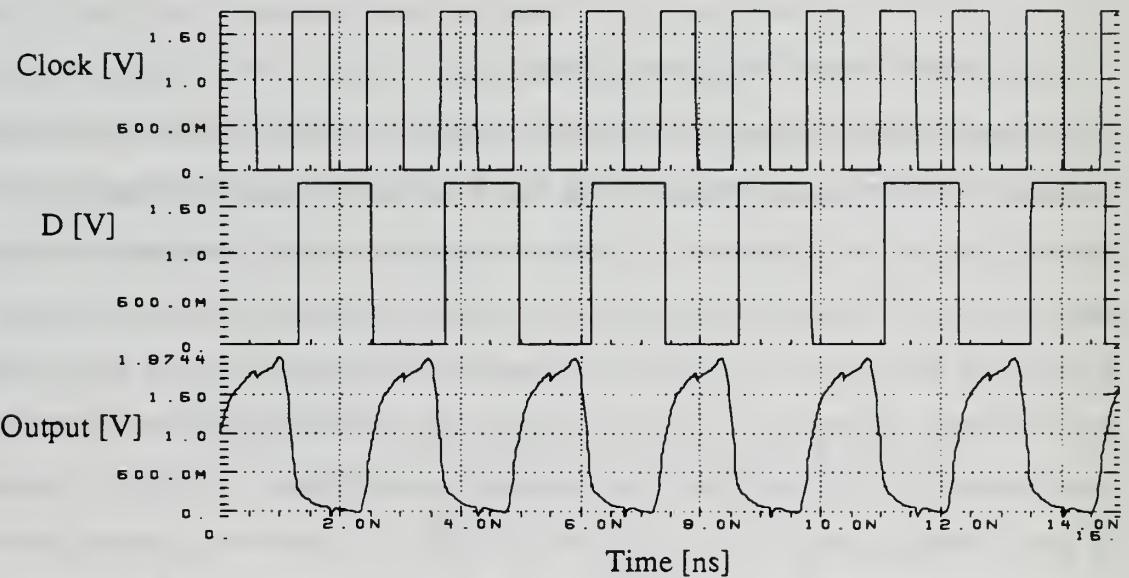
Figure 4.4: Input-Output Waveforms of CGaAs Static D Flip Flop

3. Divide-By-Two Circuit Using D Flip Flops

The CGaAs divide-by-two static circuit design is based on the D flip flop circuit described in the previous subsection. When the $\overline{Q}$ output of the D flip flop is fed back to the D input, the frequency of the output will be the input clock frequency divided by two. The logic diagram for this divider is shown in Figure 4.5. The circuit was designed, then

74

simulated using HSPICE to measure the performance. Maximum operating frequency of this divider is 0.82 GHz, same as the maximum frequency of the D-FF, when powered from a 2.0 V power supply. The input clock signal transitions between 0.0 V and 1.75 V with a load of two inverters (fan-out of two). Average power consumed by the divider circuit at the maximum frequency of operation is 22.5 mW. Input and output waveforms of the circuit operating at maximum frequency (0.82 GHz) are plotted in Figure 4.6. The top waveform in this figure is the input clock, while the bottom waveform is the circuit output.
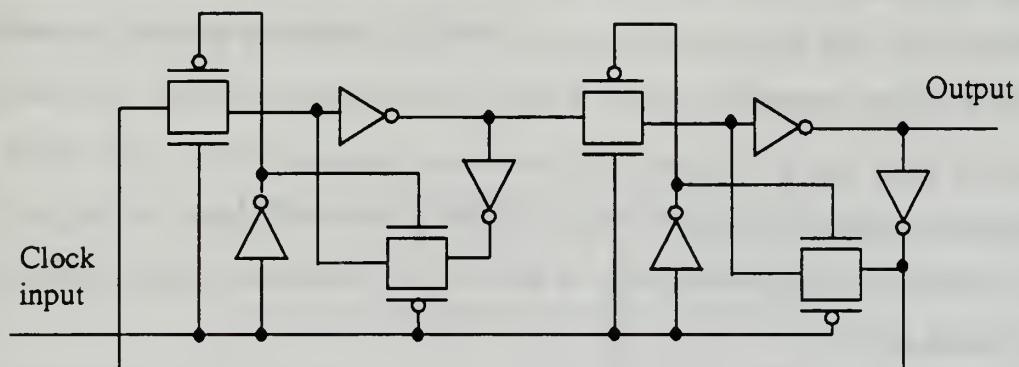
Figure 4.5: CGaAs Static Divide-By-Two Circuit
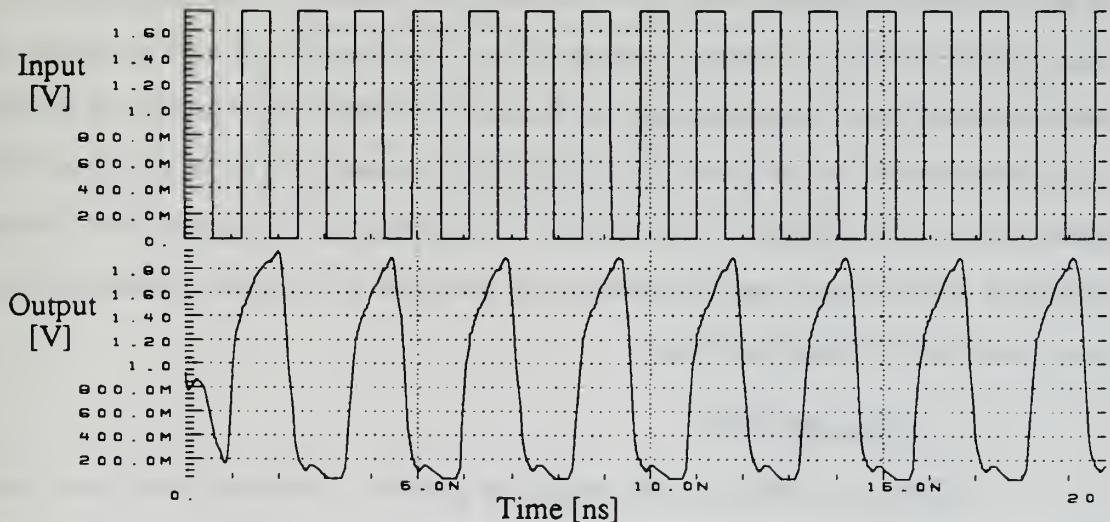
Figure 4.6: Input-Output Waveform of CGaAs Static Divide-By-Two Circuit

4. Linear Feedback Shift Registers (LFSRs)

A LFSR is a logic network constructed from the following basic components: unit delay or D Flip Flop, modulo-2 adder, or modulo-2 scalar multiplier. Such a circuit is considered to be linear because it preserve the principle of superposition. Its response to a linear combination of stimuli is the linear combination of the responses to the individual stimuli. LFSR circuits are used extensively as sources of pseudorandom binary test sequences. These sequences have many properties similar to random sequences but they are periodic and deterministic, thus they are pseudorandom instead of random. LFSR circuits are autonomous, they have no inputs except for a clock. Also, they are cyclic in the sense that when clocked repeatedly, they go through a fixed sequence of states. The maximum number of states that an n-stages LFSR circuit can generate is $2^n - 1$. The LFSR that generates the maximum number of states is called a maximum length shift register. If a LFSR generates a cyclic state sequence of length k, then the output sequence repeats itself every k clock cycles.

The LFSRs designed here are of maximum length and will be used to generate a test sequence for testing the performance of circuits described in later chapters. The motivation for using LFSRs is to reduce the number of input/output terminals for the designed circuits. This number needs to be reduced because of the limited number of high frequency test probes that can be used simultaneously and because of the difficulty in generating off-chip, multi-bit test vectors at high speed. A 3-Bit LFSR will be used in the circuits that need three inputs, while a 4-Bit LFSR will be used in the circuits that need four inputs. During testing, all circuits will have only one input (clock) and the LFSR will internally generate the test vector required for testing the circuit.

a. Three-Bit LFSR

A Three bit LFSR has been deigned to generate a maximum-length test vector for the circuits having three inputs. The circuit schematic is shown in Figure 4.7. The circuit consists of three D Flip Flops and one 8-transistor XOR gate. The LFSR will generate the

sequence listed in Table 4.1 (all states except for state 000). If the state 000 is reached, the circuit will stay in this state forever (the layout contains a triggering input to force the circuit to start in a state other than 000). The 3-Bit LFSR circuit was designed and simulated using HSPICE. The power supply is 2.0 volts and the input clock switches between 0.0 volts and 1.75 volts. When the circuit output is loaded by two static inverters, the maximum clock frequency is 0.55 GHz. The maximum speed of the circuit is limited by the maximum speed of the static XOR gate (0.55 GHz). Average power consumed by the circuit at the maximum frequency is 40 mW. The generated output sequence is shown in Figure 4.8 and is similar to the sequence listed in Table 4.1.

Table 4.1: 3-Bit LFSR Generated Sequence

Q2	Q1	Q0
1	1	1
1	1	0
1	0	0
0	0	1
0	1	0
1	0	1
0	1	1
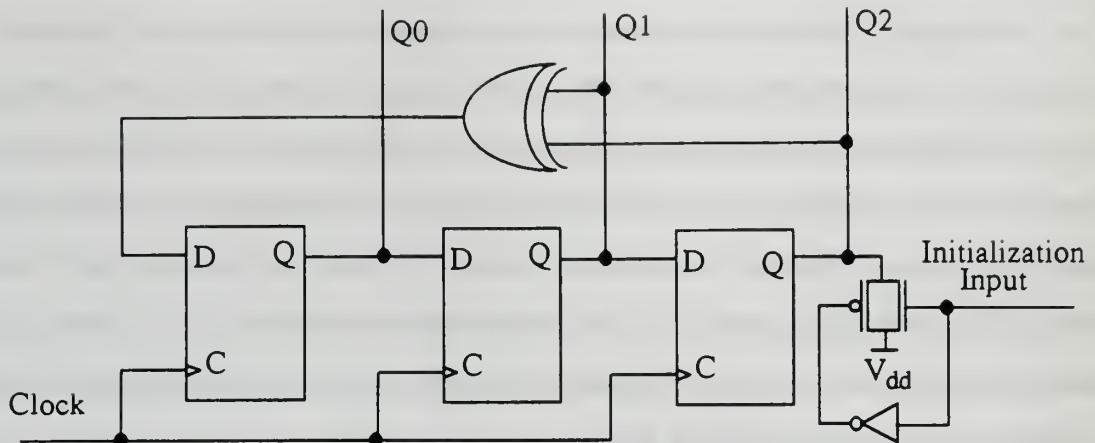
Figure 4.7: CGaAs Static 3-Bit LFSR Circuit
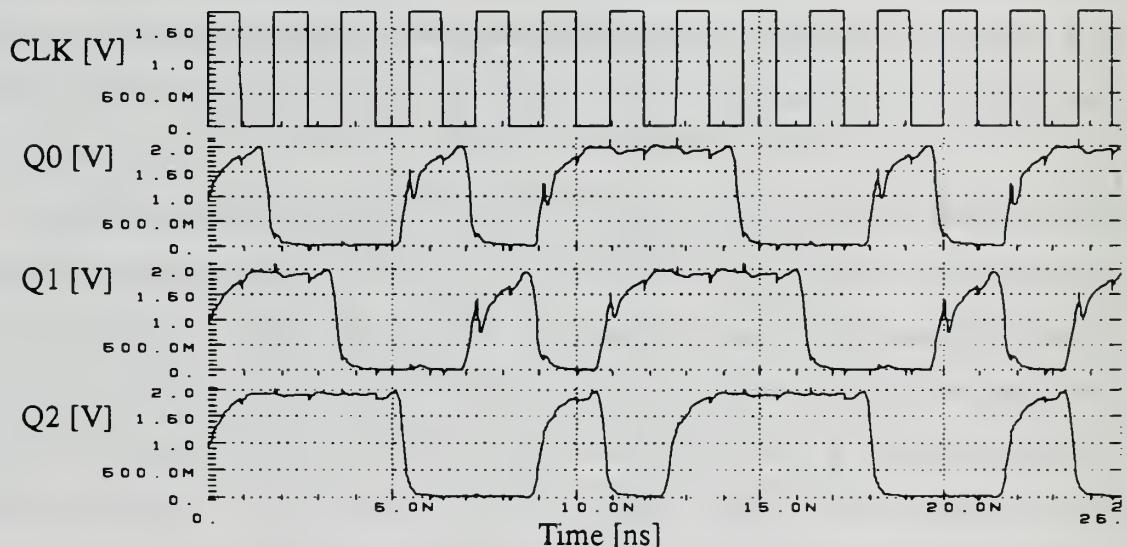
Figure 4.8: Input-Output Waveforms of CGaAs Static 3-Bit LFSR

b.   Four-Bit LFSR

A four-bit LFSR of maximum length was also designed. The schematic diagram is shown in Figure 4.9. The circuit consists of four D Flip Flops and one 8-transistor XOR gate. The four-stage circuit generates all the states except the state 000. The generated sequence for the four outputs is listed in Table 4.2 (state 0000 is un-reachable). When using a XNOR gate instead of a XOR gate, the un-reachable state will be 1111 instead of 0000.

78

The circuit has been simulated using HSPICE simulation tools. The power supply voltage is 2.0 volts and the clock input switched between 0.0 volts and 1.75 volts. Maximum operating frequency of the circuit is 0.55 GHz when the output is loaded by two static inverters. Average power consumed by the circuit at the maximum frequency is 48.2 mW. The generated output sequence of the circuit is shown in Figure 4.10. The circuit was also simulated at different operating frequencies to measure the average consumed power as a function of frequency. The increase in the average power consumed by the circuit is approximately linearly proportional to the increase in the operating frequency, as shown in Figure 4.11.

Table 4.2: 4-Bit LFSR Generated Sequence

Q3	Q2	Q1	Q0
1	1	1	1
1	1	1	0
1	1	0	0
1	0	0	0
0	0	0	1
0	0	1	0
0	1	0	0
1	0	0	1
0	0	1	1
0	1	1	0
1	1	0	1
1	0	1	0
0	1	0	1
1	0	1	1
0	1	1	1
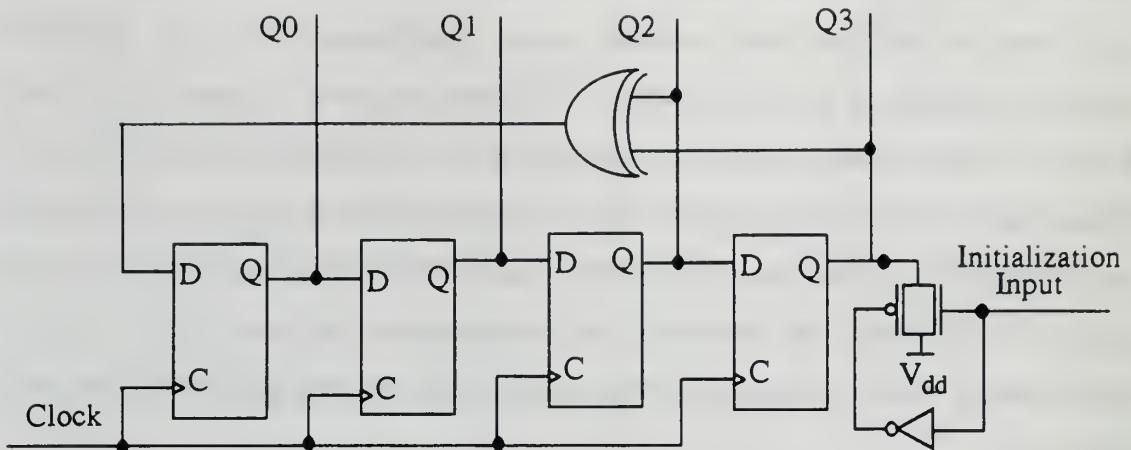
Figure 4.9: CGaAs Static 4-Bit LFSR Circuit
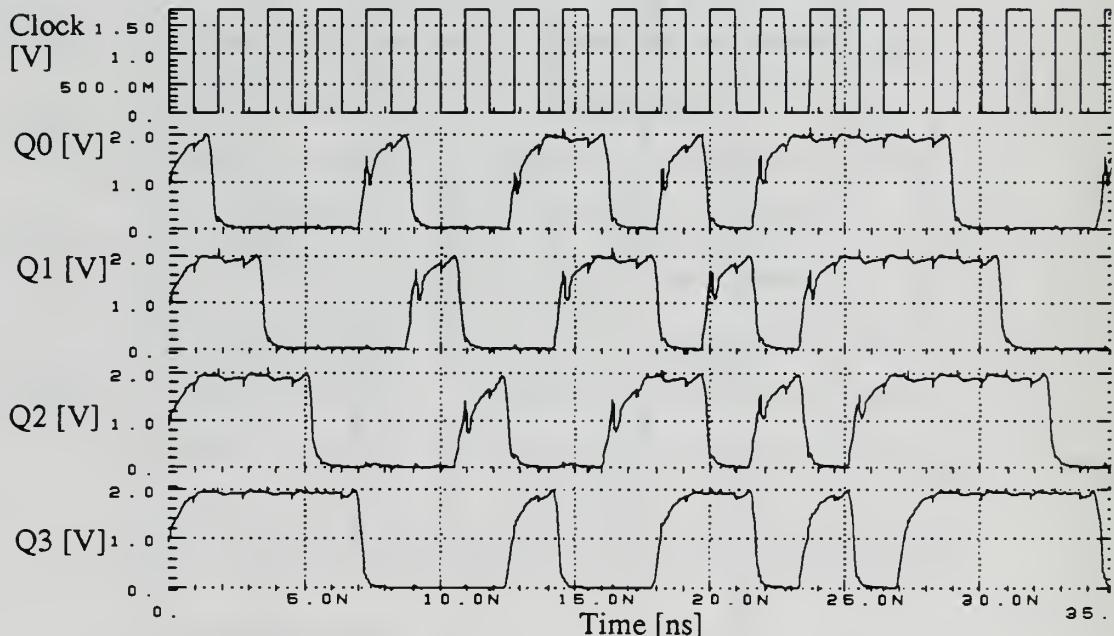
Figure 4.10: Input-Output Waveforms of CGaAs Static 4-Bit LFSR
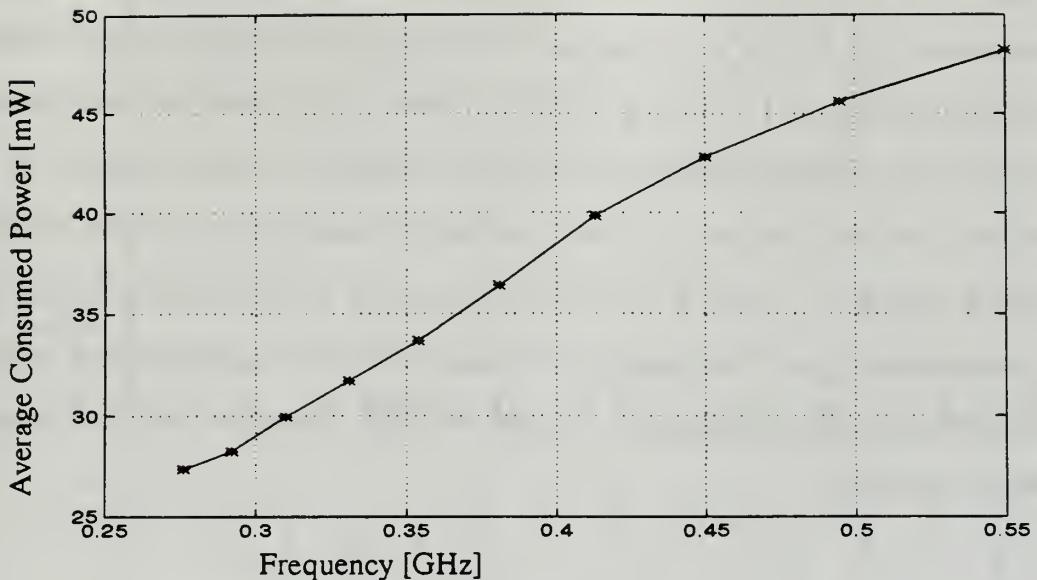
Figure 4.11: CGaAs Static 4-Bit LFSR Power Consumption

B. CGaAs TPDL SEQUENTIAL CIRCUITS

The CGaAs TPDL sequential circuits designed here will be used as building blocks in the circuits of the next chapters. The designed circuits are the D Flip Flop, 3-Bit LFSR and 4-Bit LFSR. The operation of these circuits requires two non-overlapped clock phases and their complements. The clock phases ϕ_1 and ϕ_2 have to be non overlapped in the logic low level, as explained in Section B, Chapter III. These clock phases are generated using the clock generator designed in Chapter III, Section C.

1. D Flip Flop (DFF) Circuit

A CGaAs TPDL D Flip Flop circuit diagram is shown in Figure 4.12. The circuit consists of two pass gates and two TPDL inverters, a total of 10 transistors. The transistor gate lengths are 0.7 μm while the transistor gate widths are written on each transistor in the diagram. The D Flip Flop circuits have been designed and simulated using the HSPICE simulation tool. The circuit was powered from a 2.0 volt power supply. The D-input and four clock phases switch between 0.0 volts and 1.75 volts. The maximum operating

81

frequency of the circuit is 2.0 GHz when loaded by two-TPDL inverters. Average power consumption is 4.54 mW at the maximum operating frequency. Input-output waveforms are shown in Figure 4.13. The first waveform is the ϕ_1 clock phase, the second waveform is the D-input, while the third is the flip flop Q output. The D-input is applied to the ϕ_1 section of the circuit and should be stable (unchanged) during ϕ_1 logic low (as explained in detail in Chapter III, Section B). The output of the circuit is taken from the ϕ_2 section, so it is precharged to V_{dd} during ϕ_2 logic low (ϕ_1 logic high) and evaluated during ϕ_2 logic high. This D Flip Flop will be used in the design of the TPDL Linear Feedback Shift Register in the next subsection.
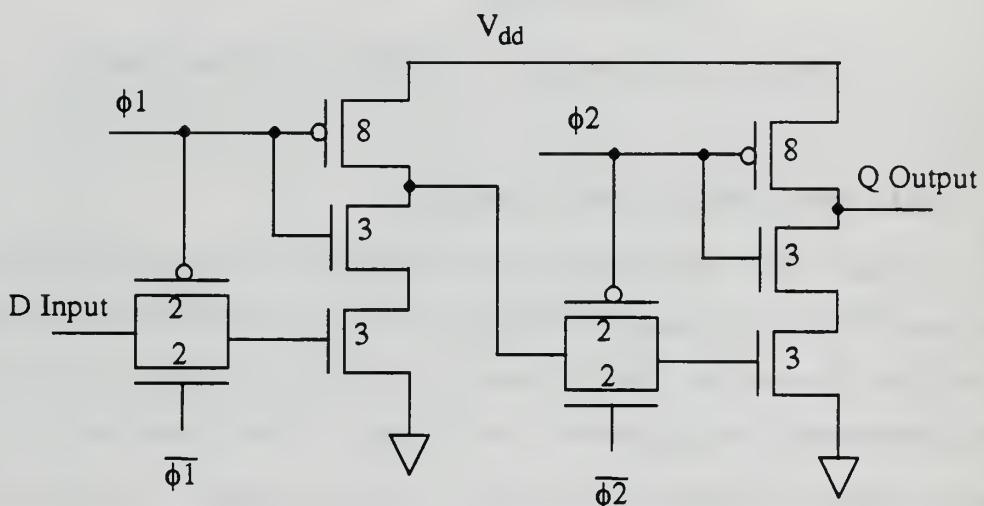
Figure 4.12: CGaAs TPDL D Flip Flop Circuit
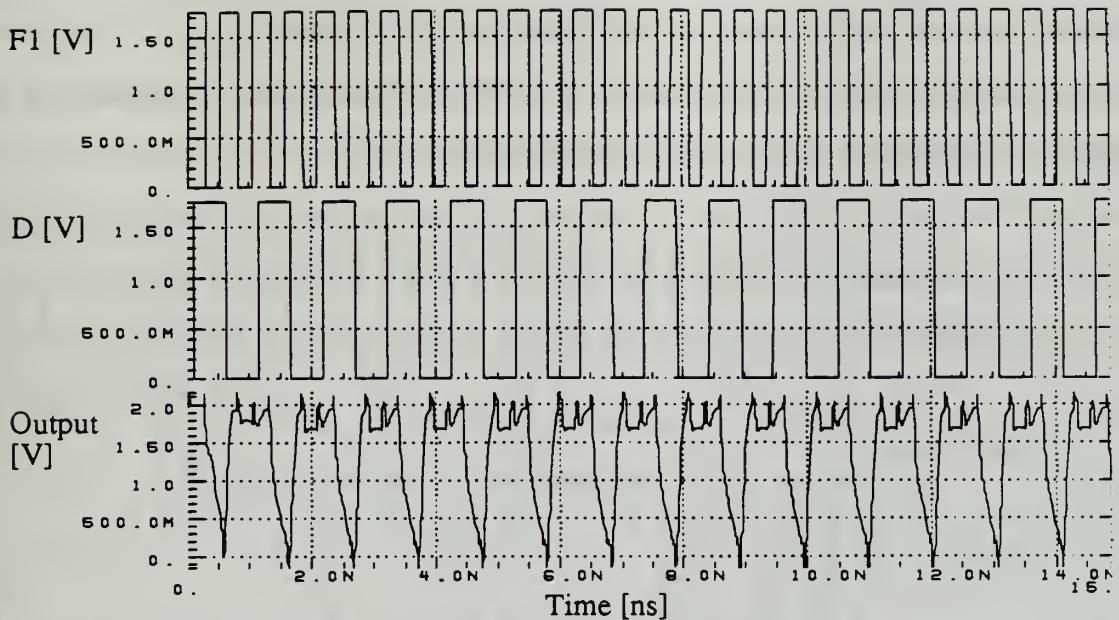
Figure 4.13: Input-Output Waveform of CGaAs TPDL D Flip Flop

2. Linear Feedback Shift Registers (LFSR)

The Linear Feedback Shift Registers designed here will be of maximum length to be functionally identical to the static LFSRs designed in Section A of this chapter.

a. Three-Bit LFSR

The CGaAs TPDL 3-Bit LFSR designed here consists of two TPDL D Flip Flops (designed in the previous subsection) and one TPDL XOR gate (designed in Chapter III, Section B). The outputs of the two D Flip Flops, Q_0 and Q_1, are applied to the XOR-gate inputs. The XOR-gate output is fed to the D_0 input. The TPDL XOR gate output is clocked, thus it can be used as a separate stage. The sequence generated by this LFSR is identical to that generated by the Static LFSR designed in Section A and listed inTable 4.1. The TPDL 3-Bit LFSR circuit has been designed and simulated using the HSPICE simulation tool to test the circuit performance. Maximum operating frequency of the circuit is 1.2 GHz when powered from a 2.0 volt power supply. The input clock signal transitions between 0.0 volts and 1.75 volts and every Q output of the circuit is loaded by two TPDL inverters (fan-out

83

of two). Average power consumed by the circuit at the maximum operating frequency is 10.5 mW. Q_0, Q_1, and Q_2 outputs of the circuit are shown in Figure 4.14. All Q outputs are taken from the ϕ_2 sections of the circuit. Therefore, they precharge to V_{dd} when the ϕ_2 phase is logic low and evaluate when it is logic high.
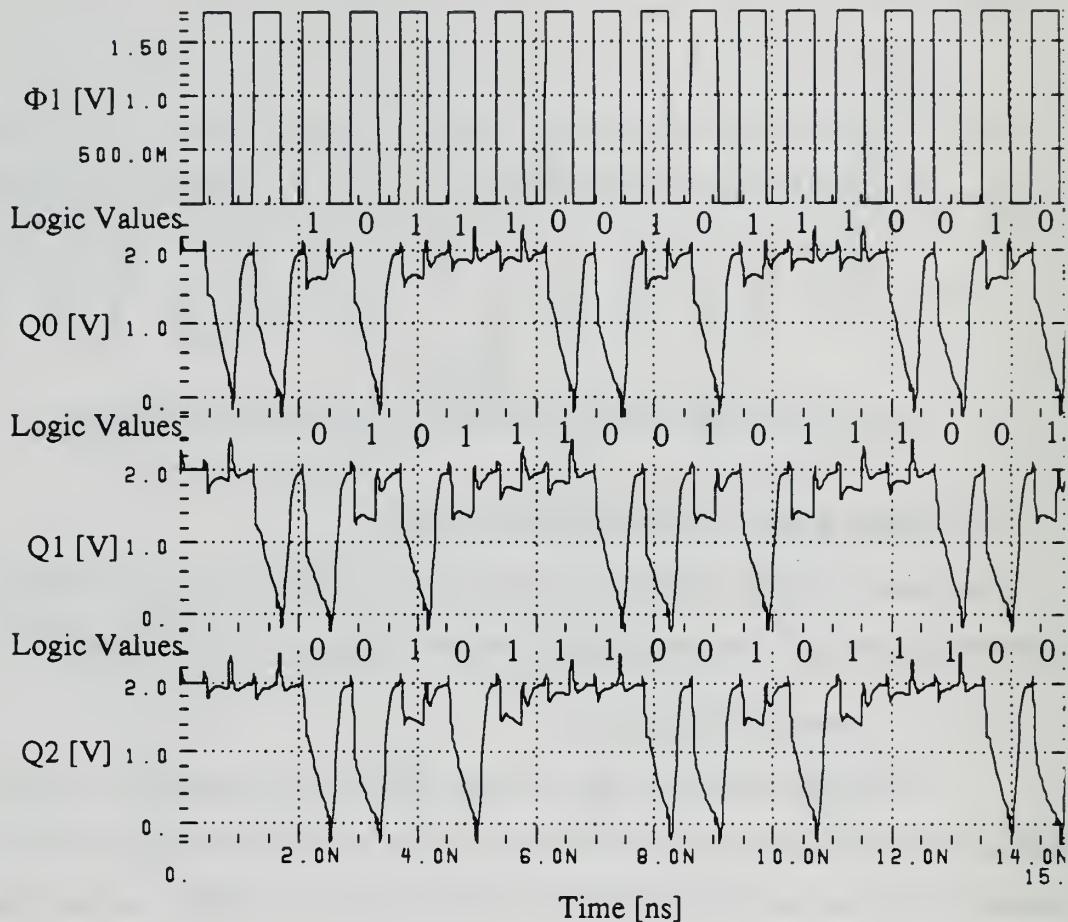
Figure 4.14: Input-Output Waveform for CGaAs 3-Bit LFSR

b.   Four-Bit LFSR

The CGaAs TPDL Four-Bit LFSR has been designed and simulated using HSPICE simulation tools. It consists of three D Flip Flops and one XOR gate. Maximum clock frequency of the circuit is 1.2 GHz when powered from a 2.0 volt power supply. The input clock signal switches between 0.0 volts and 1.75 volts and all Q outputs are loaded

by two TPDL inverters (fan-out of two). The circuit consumes an average power of 15.89 mW at the maximum frequency. The sequence generated by this LFSR circuit is identical to that generated by the Static 4-Bit LFSR and listed in Table 4.2. The four Q outputs are shown in Figure 4.15. All Q outputs precharge during ϕ_2 logic low and evaluate during ϕ_2 logic high because they are outputs from ϕ_2 sections of the circuit. The generated sequence can also be read directly from Figure 4.15. Also, the consumed power dependence on the operating frequency of the circuit was studied and found to be approximately linear, as plotted in Figure 4.16.
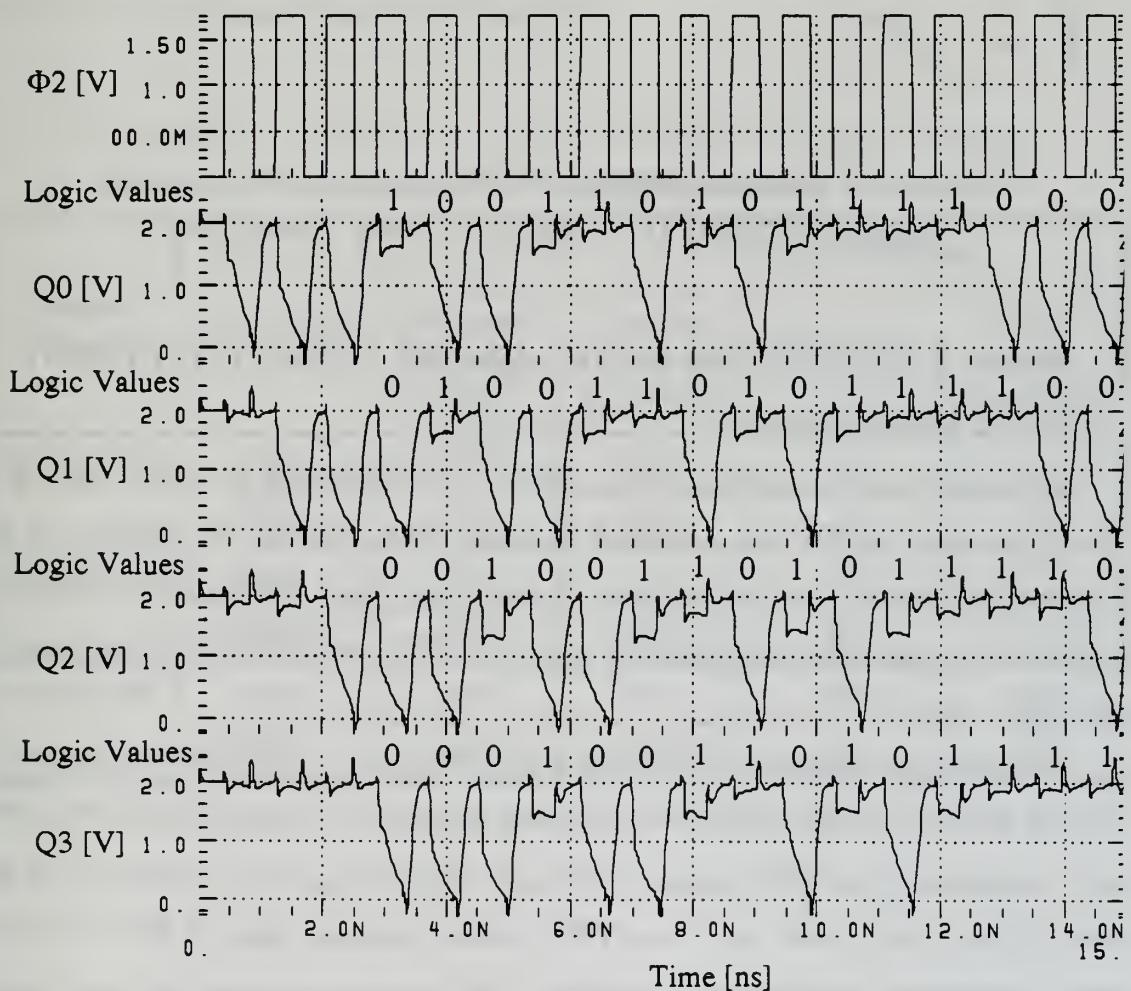
Figure 4.15: Input-Output Waveform for CGaAs 4-Bit LFSR

85
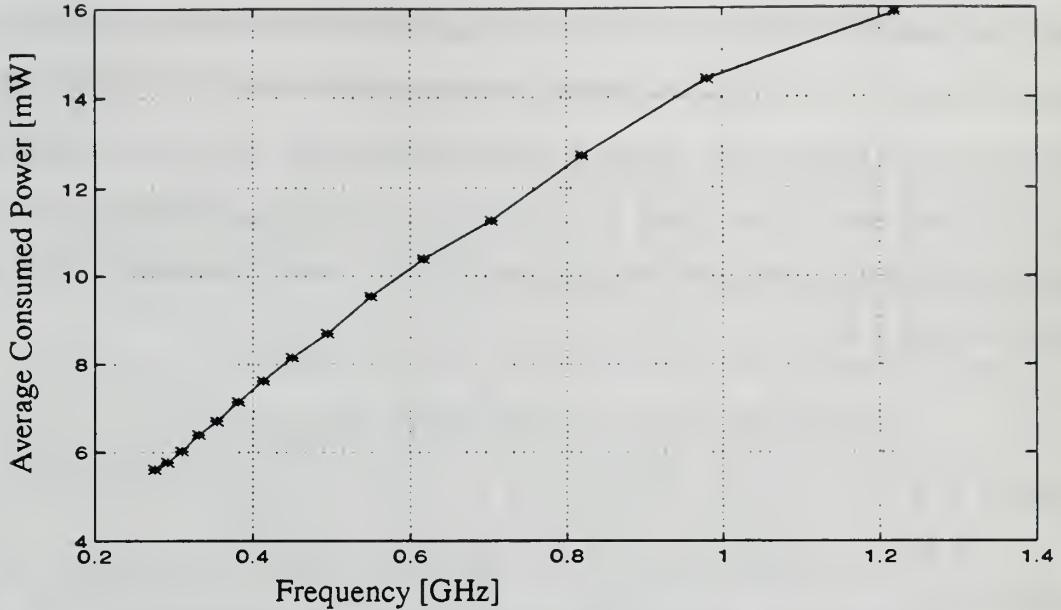
Figure 4.16: CGaAs TPDL 4-Bit LFSR Power Consumption

C. COMPARISON BETWEEN STATIC AND TPDL SEQUENTIAL CIRCUIT SIMULATION RESULTS

In the previous two sections, design, analysis and simulation of CGaAs static and TPDL sequential circuits are explained in detail. These circuits are designed to be functionally identical for the purpose of comparing their performance. Table 4.3 summarizes the performance of both the static and TPDL sequential circuits designed in this chapter [49].

The maximum frequency of operation is 0.55 GHz for the static 4-Bit LFSR and 1.2 GHz for the TPDL circuit. Layout area (transistor-gate area) of the static 4-Bit LFSR is 490 μm^2, while that of the TPDL circuit is 143 μm^2. Also, average power consumed by the static circuit is 48.2 mW, while the TPDL circuit consumes only 15.89 mW at the maximum frequency of operation. Therefore, TPDL circuits outperform the static design in maximum frequency of operation, average consumed power and total layout area. As

mentioned in Chapter III, for the comparison to be fair, two factors must be considered. First, power consumed by the clock generator required for TPDL circuit operation must be considered, which increases the actual power consumption and layout area of the TPDL designs. But, the clock generator can drive many TPDL circuits and the consumed power will be divided over all the driven circuits. Therefore, the increase in the power consumption and layout area of the TPDL circuits due to the clock generator is minimal as explained in Chapter III, Section D. Second, the comparison should be accomplished at the same operating frequency. Figure 4.17 shows the average power consumed by both static and TPDL 4-Bit LFSR circuits at different frequencies. The fair comparison can be read directly from this figure at any given frequency.

Table 4.3: CGaAs Static and TPDL Sequential Circuit Performance

| Designed Circuit | Circuit Type | Circuit performance | | | |
		Maximum frequency [GHz]	Average Power @ F_{max} [mW]	Number of Transistors	Total Layout Area [μm^2]
D Flip Flop	static	0.82	20.8	20	112
	TPDL	2.0	4.54	10	23.8
3-Bit LFSR	static	0.55	40	68	378
	TPDL	1.2	10.55	44	95.9
4-Bit LFSR	static	0.55	48.2	88	490
	TPDL	1.2	15.89	54	143.5
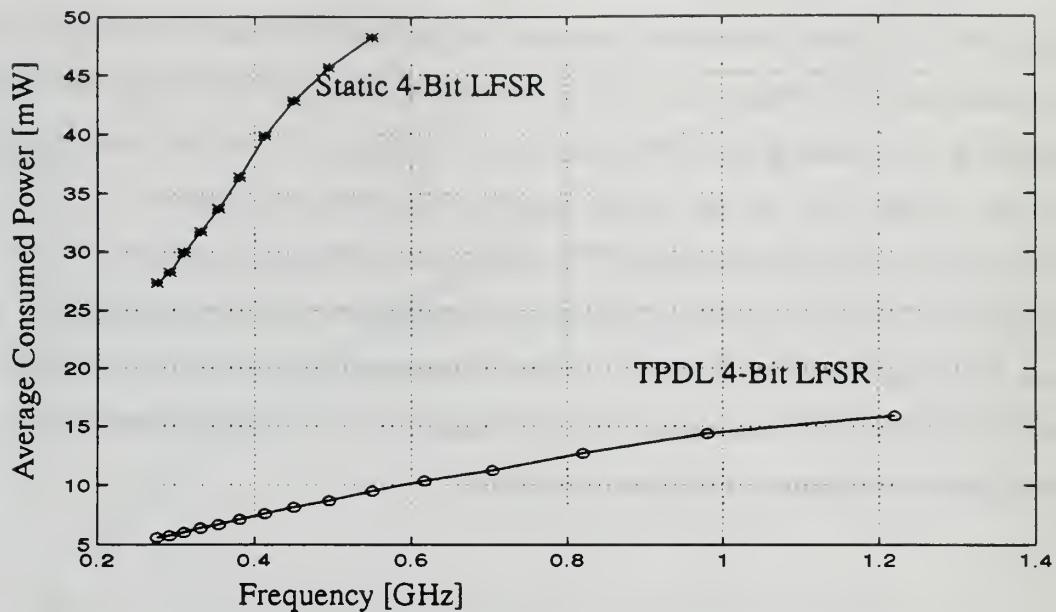
Figure 4.17: CGaAs TPDL and Static 4-Bit LFSR Power Consumption

V. DESIGN OF TWO-LEVEL LOGIC FUNCTIONS USING COMPLEMENTARY GaAs STATIC AND DYNAMIC LOGIC FAMILIES

A two-level logic circuit is a circuit which can be divided into two separate consecutive logic blocks. A two-level logic function is a logic function which requires a two-level logic circuit for implementation. In Chapter III, the design of one-level functions (inverter, NAND gate and NOR gate) using Complementary GaAs (CGaAs) static and TPDL circuits were discussed in detail. In this chapter, four different logic functions are selected for simulation and implementation using static and dynamic logic families. Dynamic logic families discussed in this chapter are Domino logic, N-P Domino logic and TPDL. These functions were selected because they are representative of typical two-level logic functions. The selected functions are as follows:

$$F_1 = (\overline{(\overline{A+B})+C})$$ (5.1)

$$F_2 = (\overline{(\overline{A \bullet B}) \bullet C})$$ (5.2)

$$F_3 = (\overline{(\overline{A+B}) \bullet C})$$ (5.3)

$$F_4 = (\overline{(\overline{A \bullet B})+C})$$ (5.4)

Section A discusses the design and simulation of the selected functions using static logic circuits. The design and simulation of the same logic functions using Domino logic is explained in Section B. Section C discusses N-P Domino circuits for implementing the above four logic functions. TPDL circuits generating the same logic functions are discussed in Section D. The comparison between the performance of all the above logic families is explained in Section E. The effect of increasing the load on the maximum operating frequency of all these logic families is discussed in Section F. In Section G, the effect of changing the power supply voltage on the performance of all logic families is explained. In all the above sections, the circuits designed are tested exhaustively to ensure their correct functionality.

A. CGaAs STATIC LOGIC CIRCUIT DESIGN

CGaAs static logic circuit designs discussed in this chapter are similar to static CMOS logic circuit designs that implement the same logic functions. They dissipate a small amount of static power in addition to the dynamic power dissipated. Transistor gate widths have been chosen according to DC transfer curves to get the optimal noise margin. Transistor gate lengths for all circuits are 0.7 μm. In this section, the design and HSPICE simulations of four different logic functions are performed.

The CGaAs static circuit that generates the logic function $F_1 = (\overline{(A + B) + C})$ is shown in Figure 5.1. All transistor gate widths of the circuit are 10 μm. Maximum operating frequency of the circuit is 0.62 GHz when powered from to a 2.0 volt power supply and with input variable transition between 0.0 volts and 1.75 volts. The maximum frequency is achieved when the circuit output is loaded by two static inverters (fan-out of two). Average power consumed by the circuit at the maximum operating frequency is 8.69 mW when the A input is connected to a pulse generator and both the B and the C inputs are tied to 0.0 volts to propagate the A input to the circuit output. Increasing the P-transistor width will not increase the maximum operating frequency but will increase the power dissipation. Input-output waveforms of the circuit operating at the maximum frequency are shown in Figure 5.2.

The CGaAs static circuit that generates the logic function $F_2 = (\overline{(A \bullet B) \bullet C})$ is shown in Figure 5.3. Analysis of the circuit was performed with the same power supply, input transitions and load as the circuit that generates logic function F_1. Input-output waveforms of the circuit are shown in Figure 5.4. Maximum operating frequency of the circuit is 0.83 GHz. The circuit consumes an average power of 10.39 mW at the maximum operating frequency. It should be noted that the maximum operating frequency of this circuit is higher than for the circuit that generates logic function F_1 because the later has two series P-channel transistors which slow its speed. Also, the power consumption of this

circuit is higher than the circuit that generates logic function F_1 because it operates at higher frequency, thus consumes more dynamic power (frequency dependent).

The CGaAs static circuit that generates the logic function $F_3 = (\overline{(A + B) \bullet C})$ is shown in Figure 5.5. The circuit is analyzed at the same power supply, input transitions and load as the previous two circuits. Maximum operating frequency of the circuit is 0.62 GHZ and the power consumption at this frequency is 9.49 mW. Input-output waveforms of the circuit operating at the maximum frequency is shown in Figure 5.6.

Finally, the CGaAs static circuit that generates the logic function $F_4 = (\overline{(A \bullet B) + C})$ is shown in Figure 5.7. Analysis of the circuit was performed with the same above conditions. Input-output waveforms of the circuit are shown in Figure 5.8. The circuit has a maximum frequency of operation of 0.62 GHZ and consumes an average power of 8.73 mW at the maximum frequency.

Table 5.1 summarizes the maximum operating frequency, the average power consumption at maximum frequency of operation and the layout area of the static logic circuits designed in this section. The layout area listed in this table is just the transistor gate area. It does not include the area of interconnect between the transistors.

Table 5.1: CGaAs Static Logic Circuit Performance

Generated Function	Maximum Frequency [GHz]	Average Consumed Power [mW]	Transistor Count	Layout Area [μm^2]
F1	0.62	8.69	8	56
F2	0.83	10.39	8	56
F3	0.62	9.49	8	56
F4	0.62	8.73	8	56
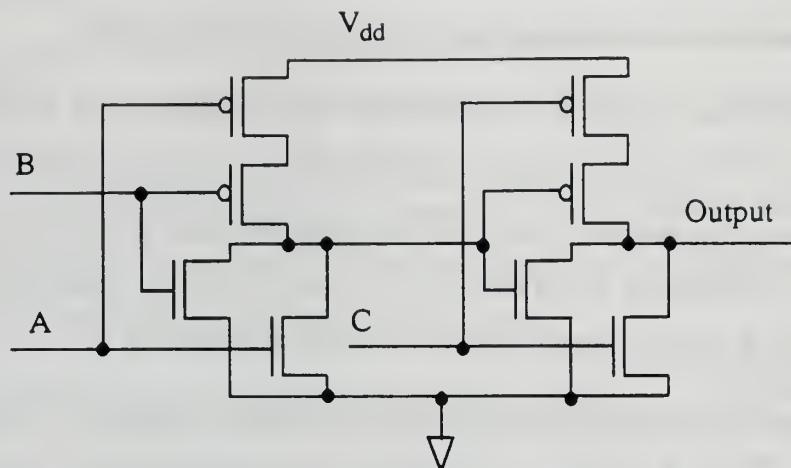
Figure 5.1: CGaAs Static Logic Circuit to Generate Function F1
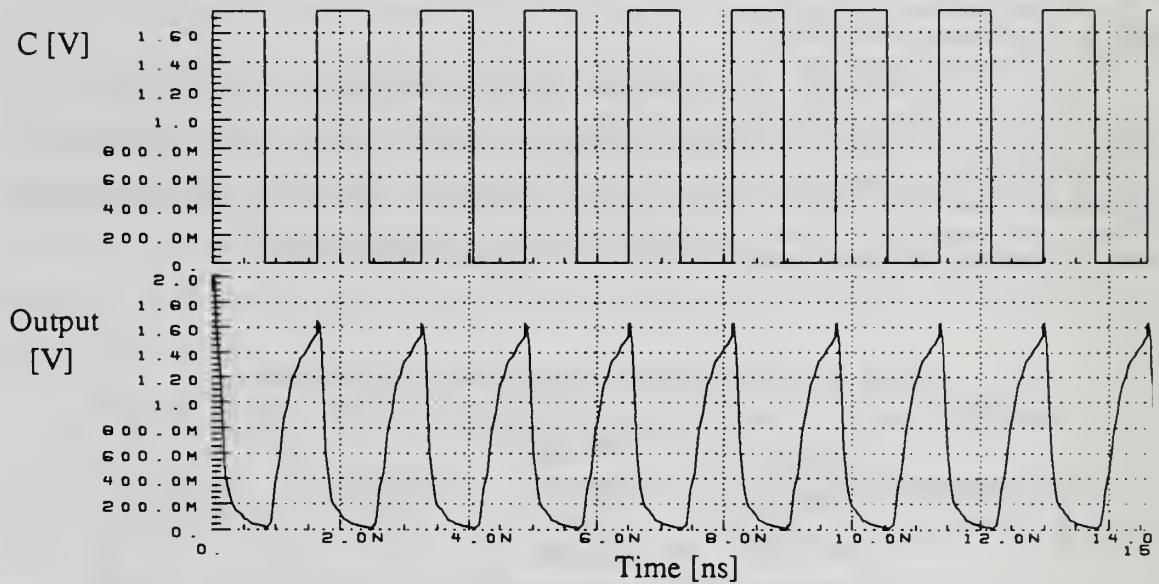
Figure 5.2: Input-Output Waveform of CGaAs Static F_1 Generator
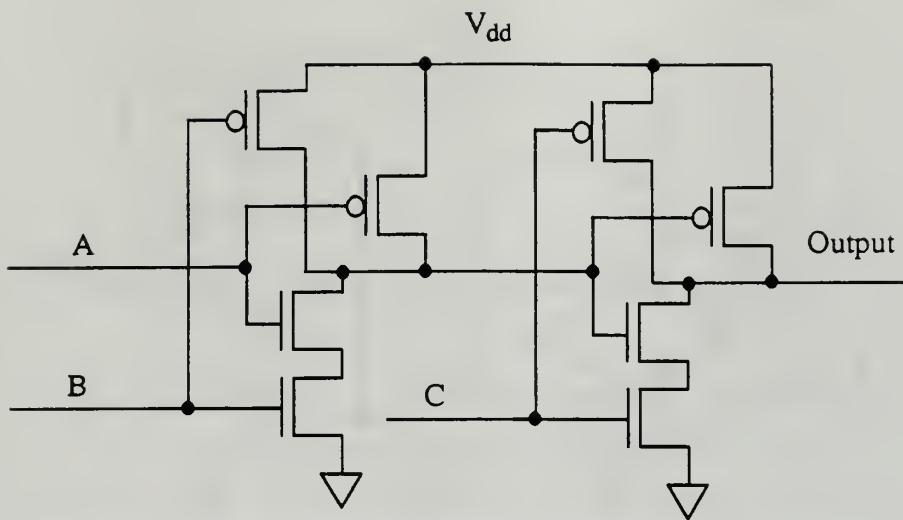
Figure 5.3: CGaAs Static Logic Circuit to Generate Function F2
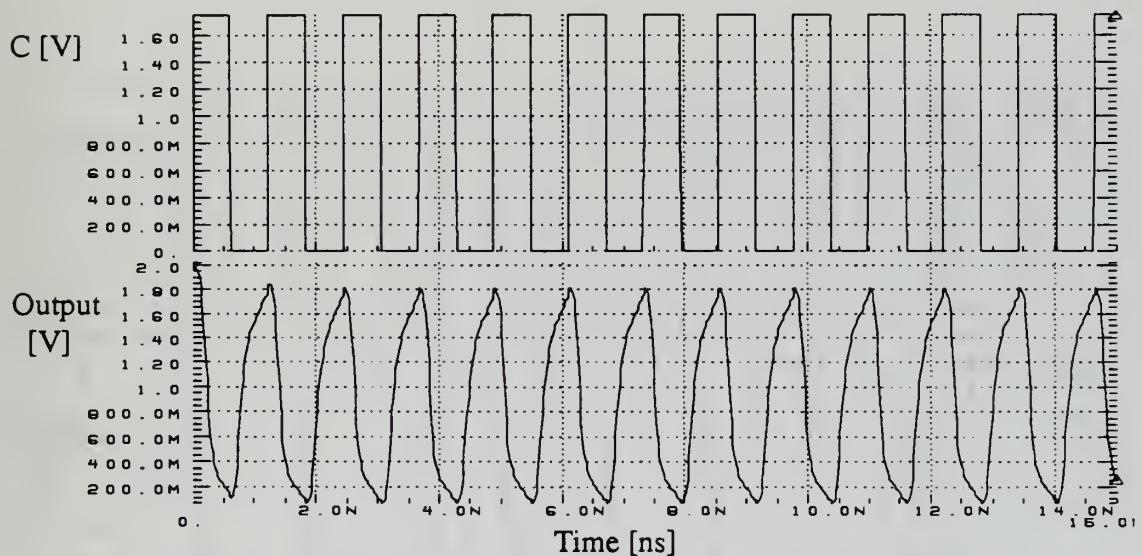
Figure 5.4: Input-Output Waveform of CGaAs Static F_2 Generator
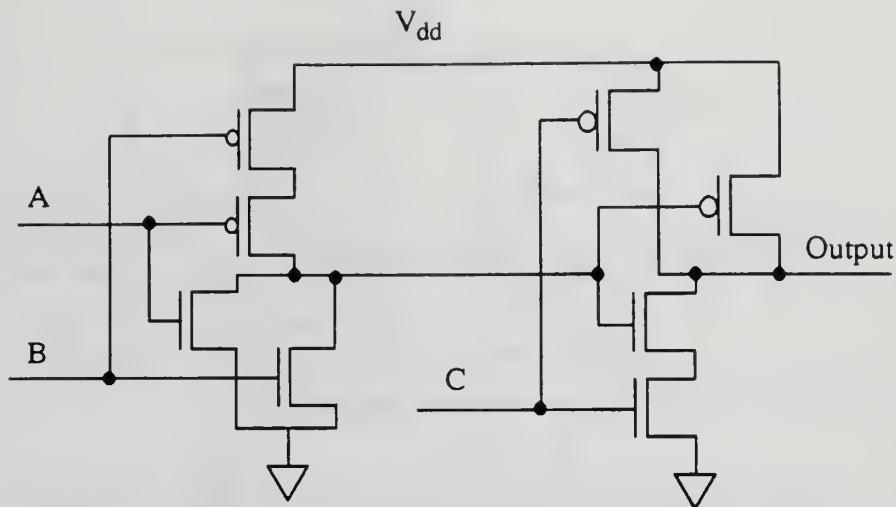
Figure 5.5: CGaAs Static Logic Circuit to Generate Function F3
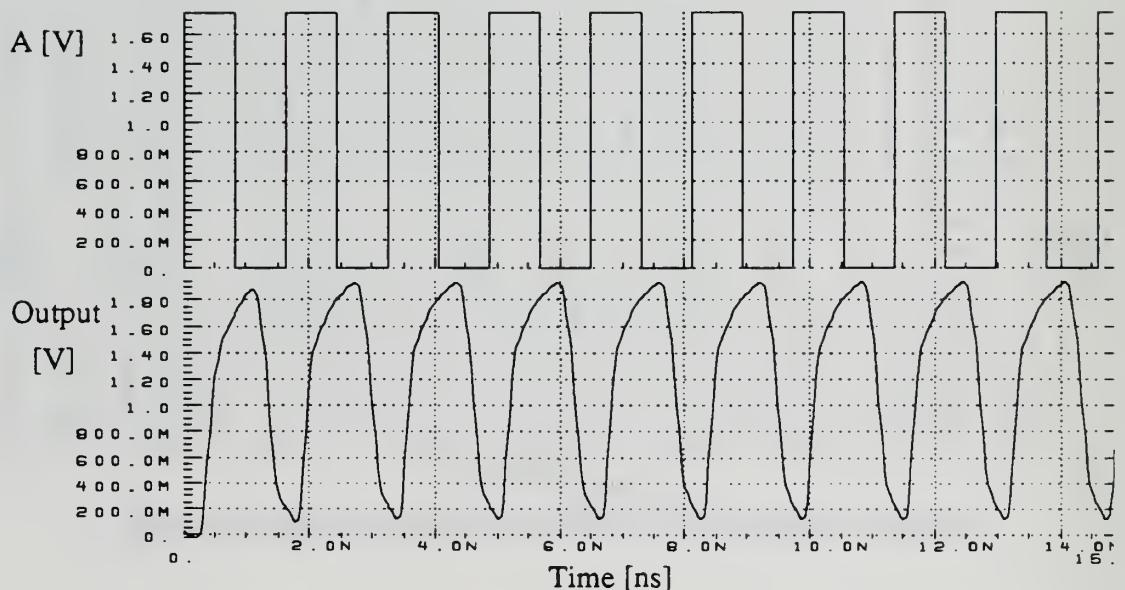
Figure 5.6: Input-Output Waveform of CGaAs Static F_3 Generator

94
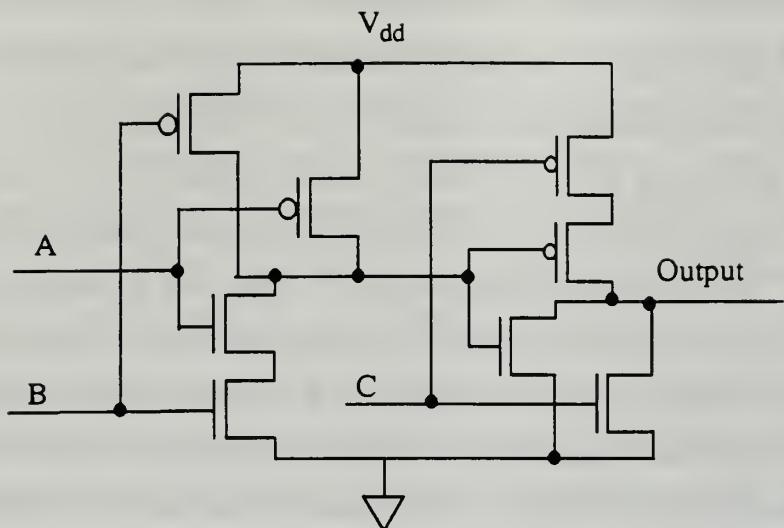
Figure 5.7: CGaAs Static Logic Circuit to Generate Function F4
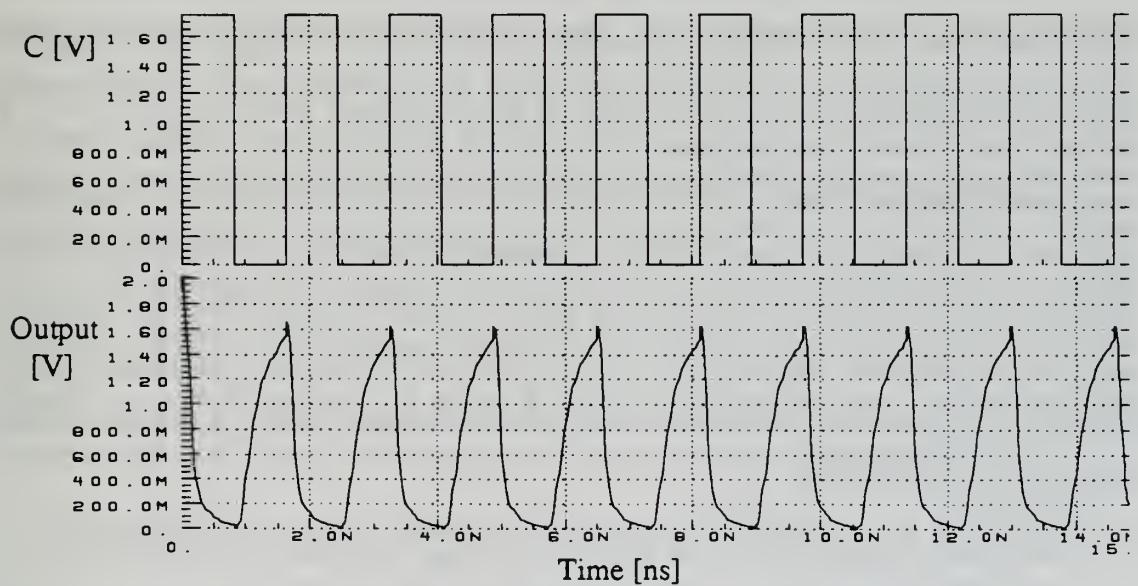
Figure 5.8: Input-Output Waveform of CGaAs Static F_4 Generator

95

B. CGaAs DOMINO LOGIC CIRCUIT DESIGN

Domino circuits consist of a dynamic N-transistor logic block followed by a static inverter. When the input clock signal is logic low (pre-discharge phase), the circuit output will discharge to the logic low level. When the clock switches to logic high (evaluation phase), the N-transistor logic block will evaluate the input signals and perform the specified logic function. The circuit output either stays at a logic low or charges to logic high (according to the input variables) through the output static inverter. Thus, the output will have at most one transition during evaluation, which prevents erroneous output states that can occur in simple dynamic logic schemes. Domino is not a complete logic family because it does not generate inverted functions. Also, Domino circuits are not completely dynamic because they contain static inverters. Inverted logic functions have to be re-expressed in a non-inverted expression to be represented in Domino logic. The principal of operation of Domino dynamic logic circuits is explained in Chapter I, Section E.

In this section, the four logic functions mentioned in the beginning of the chapter are designed using CGaAs Domino logic, then simulated using HSPICE simulation tools. Maximum operating frequency of each logic circuit and the average power consumption at the maximum frequency are the parameters measured. All circuits are simulated using a 2.0 volt power supply and inputs switch between 0.0 volts and 1.75 volts. Also, simulations are performed with the circuits loaded by two inverters (fan-out of two). Gate lengths for all transistors in the circuits are 0.7 µm. Gate widths of each transistor have been chosen to optimize the maximum frequency of the circuit and are written on the schematic. During simulation and operation, all inputs must be stable (unchanged) during the evaluation phase to prevent data corruption.

The CGaAs Domino circuit that generates the logic function $F_1 = (\overline{(A + B) + C})$ is shown in Figure 5.9. This inverted function must be converted to a non-inverted expression to be represented in Domino logic (inverted functions can not be represented in Domino logic family). The new expression for the function will be $F_1 = ((A + B) \cdot \overline{C})$. The highest frequency of the circuit is obtained for transistor gate widths written on each

transistor of Figure 5.9. Transistor gate widths for the static inverters are 2 µm for N-channel transistors and 4 µm for P-channel transistors. Maximum operating frequency of the circuit is 1.61 GHZ. Average power consumed by the circuit at the maximum operating frequency is 3.54 mW when the C input is switching and both the A and B inputs are tied to 1.75 volts (logic high level) to propagate the effect of the C input to the circuit output. When the C input switches, the static inverter at this input will switch between logic levels and consume dynamic (switching) power in addition to the static power consumed. Thus, the total power consumption of the circuit increases when the C input switches. Input-output waveforms for the circuit at the maximum frequency of operation with the C input switching between logic levels is shown in Figure 5.10. It can be seen from the waveforms that the circuit output always pre-discharges to logic low when the clock input is low (pre-charge phase). When the clock input is high (evaluation phase) the circuit evaluates the output node according to the input signals that are present.

The CGaAs Domino circuit which generates the logic function $F_2 = (\overline{(A \bullet B) \bullet C})$ is shown in Figure 5.11. The non-inverting expression for the function is $F_2 = ((A + B) \bullet \overline{C})$ for implementation in Domino logic. The maximum frequency of operation for the circuit is obtained for the transistor gate widths written on each transistor of Figure 5.11, while transistor gate widths for the static inverters are 2 µm for N-channel transistors and 4 µm for P-channel transistors. The maximum operating frequency of the circuit is 1.92 GHz and the average consumed power at this frequency is 4.1 mW when the C input is switching and both the A and B inputs are tied to logic low level. Input-output waveforms for the circuit at the maximum operating frequency are shown in Figure 5.12.

The CGaAs Domino logic circuit which generates the function $F_3 = (\overline{(A + B) \bullet C})$ is shown in Figure 5.13. Because Domino is a non inverting logic, the function has to be converted to a non-inverted expression to match the characteristics of the Domino logic family. The non-inverted expression of the function is $F_3 = ((A + B) + \overline{C})$. The maximum operating frequency of the circuit is 1.92 GHz and the average consumed power

97

at this frequency is 3.97 mW when the C input is switching and both the A and B inputs are connected to logic level low. Input-output waveforms for the circuit at the maximum operating frequency are shown in Figure 5.14.

The CGaAs Domino circuit which generates the logic function $F_4 = (\overline{(A \bullet B) + C})$ is shown in Figure 5.15. The non-inverted expression for the logic function is $F_4 = ((A \bullet B) \bullet \overline{C})$. Maximum frequency of operation of this circuit is 1.62 GHz and the average consumed power at this frequency is 3.6 mW when the C input transitions between logic levels and the A and B inputs are connected to a logic level high to propagate the effect of the C input to the circuit output. Input-output waveforms for the circuit at the maximum operating frequency are shown in Figure 5.16. Table 5.2 summarize the performances of all Domino logic circuits designed in this section.

Table 5.2: CGaAs Domino Logic Circuit Performance

Generated Function	Maximum Frequency [GHz]	Average Consumed Power [mW]	Transistor Count	Layout Area [μm^2]
F1	1.61	3.54	9	19.6
F2	1.92	4.104	9	21
F3	1.92	3.97	9	19.6
F4	1.61	3.6	9	22.4
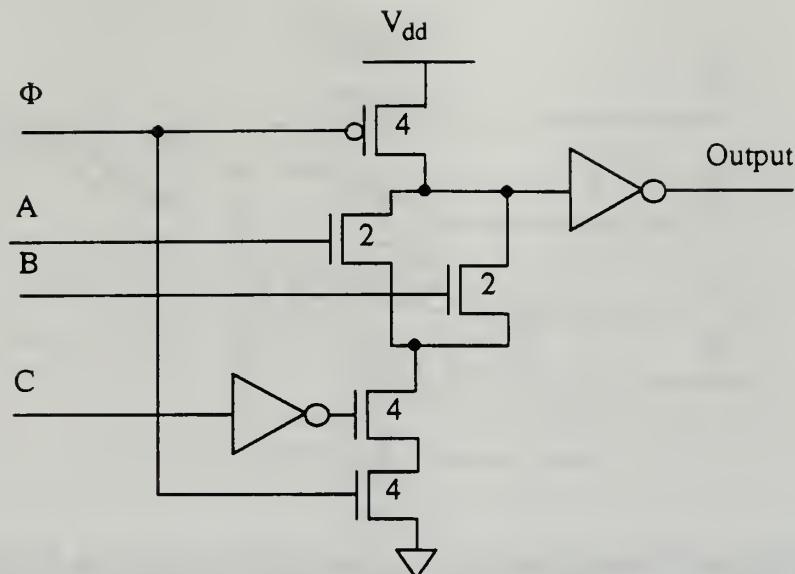
Figure 5.9: CGaAs Domino Logic Circuit to Generate Function F1
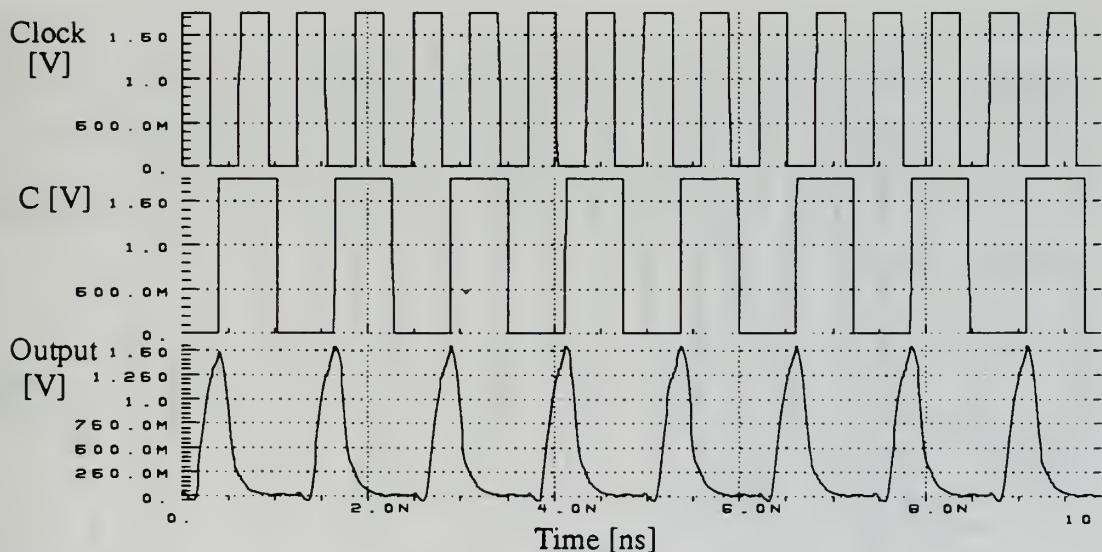
Figure 5.10: Input-Output Waveform of CGaAs Domino Logic F_1 Generator

99
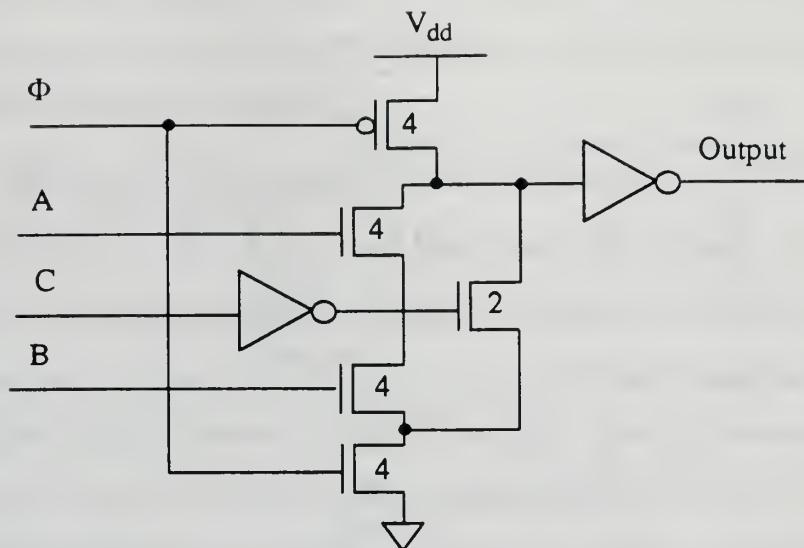
Figure 5.11: CGaAs Domino Logic Circuit to Generate Function F2
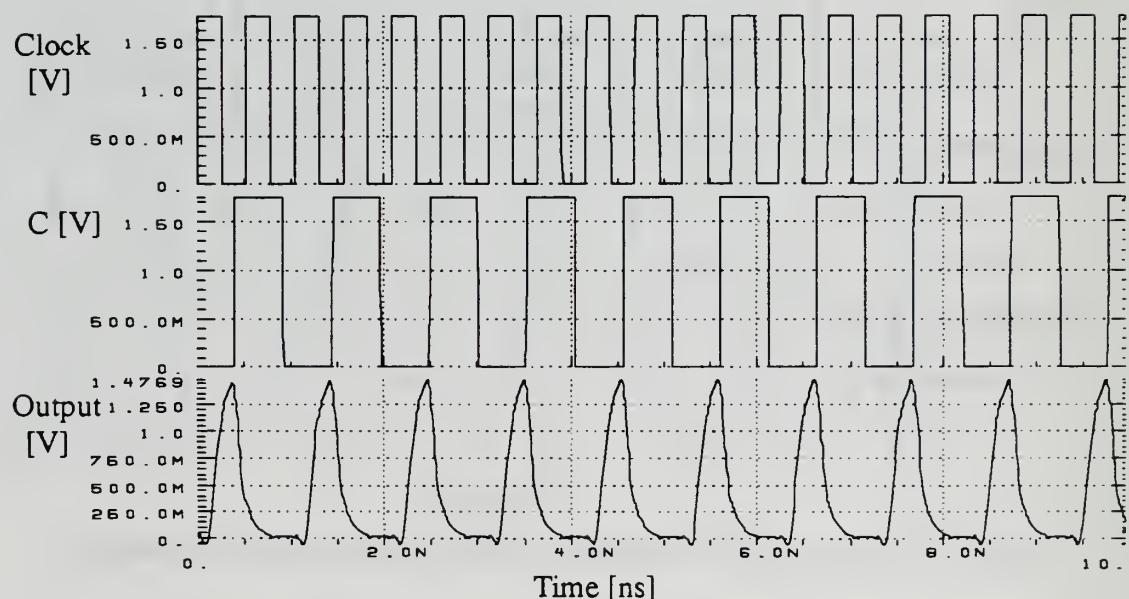
Figure 5.12: Input-Output Waveform of CGaAs Domino Logic F_2 Generator
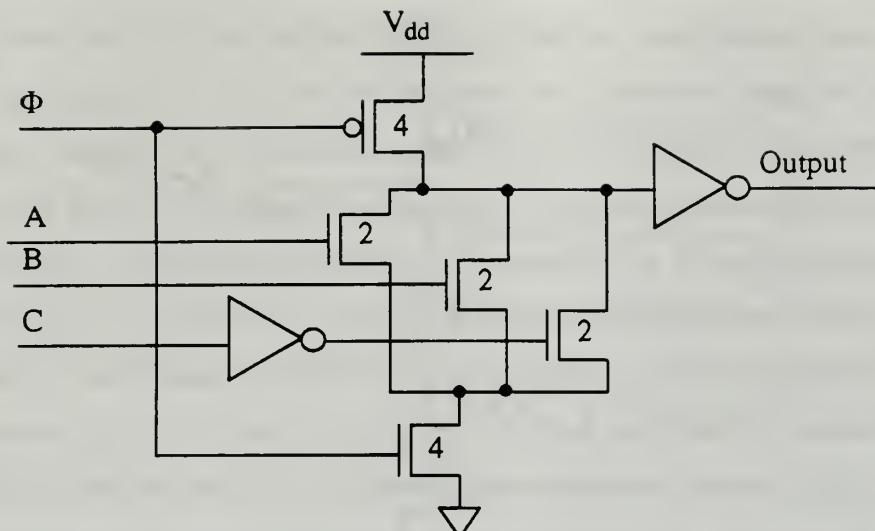
Figure 5.13: CGaAs Domino Logic Circuit to Generate Function F3
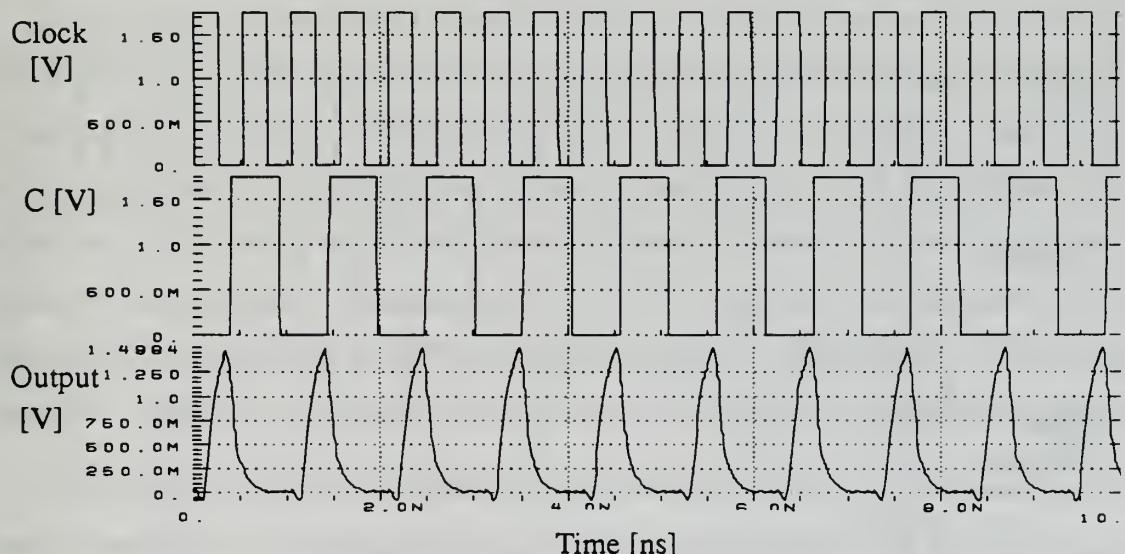
Figure 5.14: Input-Output Waveform of CGaAs Domino Logic F_3 Generator
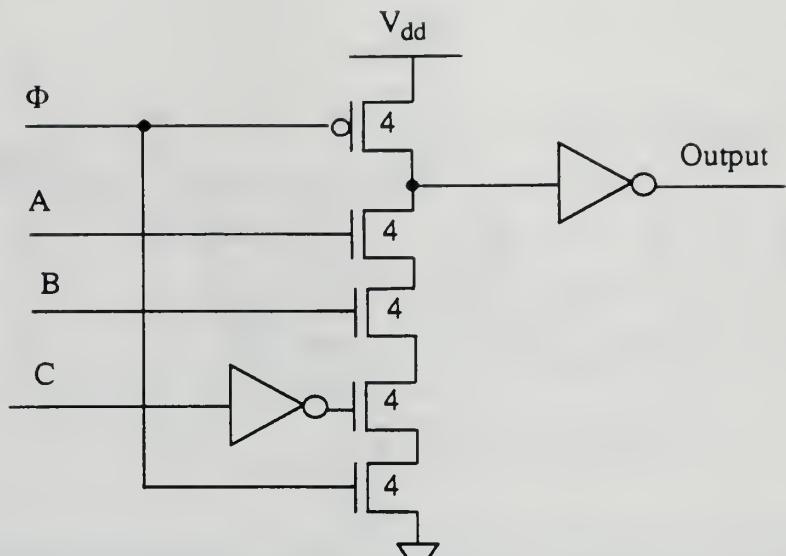
Figure 5.15: CGaAs Domino Logic Circuit to Generate Function F4

Time [ns]
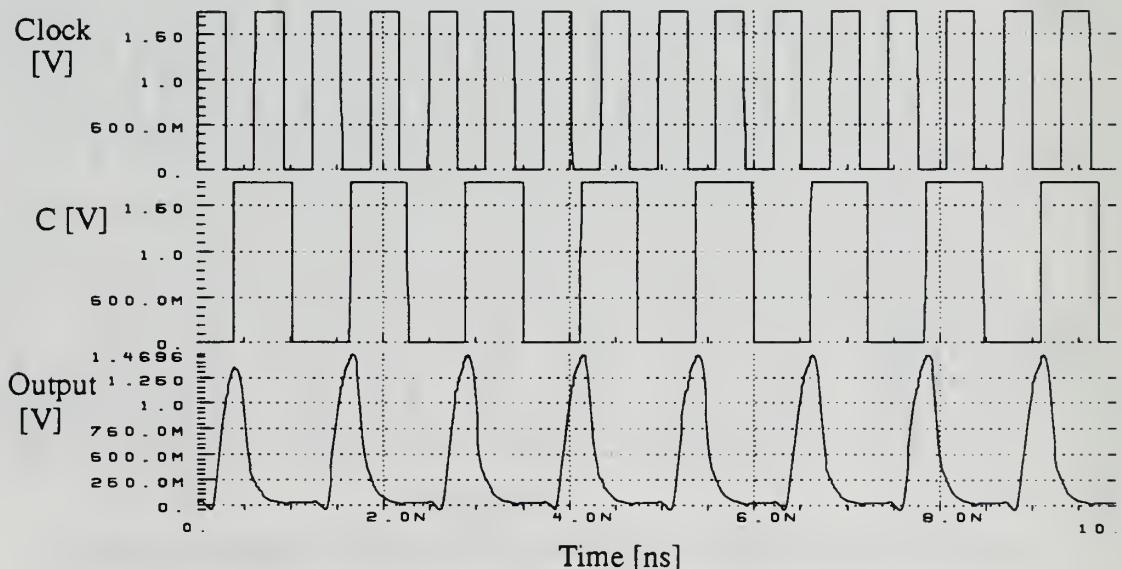
Figure 5.16: Input-Output Waveform of CGaAs Domino Logic F_4 Generator

C. CGaAs N-P DOMINO LOGIC CIRCUIT DESIGN

N-P Domino logic circuits use both N-channel transistors and P-channel transistors to evaluate a logic expression. N-P Domino logic gates are implemented using N-type and P-type transistor blocks. N-type transistor block outputs precharge to V_{DD} while P-type transistor block outputs pre-discharge to zero volts during their precharge phases (zipper operation). During the precharging phase, all transistor gates of the n-logic blocks are discharged to ground and they are turned off through the preceding p-logic blocks. Also, the transistors of the p-logic blocks will be turned off by the preceding n-logic blocks. Unlike Domino logic, N-P Domino logic is a complete logic family because inverted functions can be implemented. It is required that all inputs to N-transistor logic blocks be stable (unchanging) during the evaluation phase (clock is high). Also, all inputs to P-transistor logic blocks are required to be stable during the evaluation phase of P sections ($\overline{\text{clock}}$ is high). A complete explanation and basic operations for N-P Domino logic family is presented in Chapter I, Section E.

In this section, the four logic functions selected previously are designed using CGaAs N-P Domino logic gates. These circuits are simulated using HSPICE simulation tools to evaluate their performance. The maximum frequency of operation and power consumption are the parameters measured. Because P-channel transistors are used in evaluating the expression, it is expected that the maximum frequency of operation of this logic family should be less than that of Domino logic circuits. Gate lengths of all transistors in the designed circuits are 0.7 µm. In HSPICE simulations, only one input changes at a time. The other two inputs are set to propagate the effect of the switching input to the circuit output.

A CGaAs N-P Domino circuit that generates the logic function $F_1 = (\overline{(A + B) + C})$ is shown in Figure 5.17. Transistor gate widths are in micrometers and written on each transistor of the figure. If this circuit is inserted in a chain of N-P Domino logic gates and its inputs are driven from another N-P Domino circuit, the transistors Q1 and Q4 can be removed. In this case, it is guaranteed that all transistors of the N-transistor logic (p-logic) are turned off during the precharge phase and there is no current path from V_{DD} to ground.

The designer has to make sure that inputs of P-sections are driven only from outputs of N sections. If an output of a N section (P section) is required to be connected to an input of another N section (P section), it has to go through a static inverter. The circuit in Figure 5.17 has three series P transistors in its P section which causes the output to charge very slowly during the evaluation phase. The widths of these P-transistors have to be increased to compensate for the slow charging, which increases the power consumption. Maximum operating frequency of the circuit is 0.82 GHz. The average power consumption at the maximum operating frequency is 1.646 mW. Input-output waveforms of the circuit at the maximum operating frequency are shown in Figure 5.18.

A CGaAs N-P Domino circuit that generates the logic function $F_2 = (\overline{(\overline{A \bullet B}) \bullet C})$ is shown in Figure 5.19. The maximum frequency of operation of the circuit is 1.2 GHz and the average power consumption at this frequency is 1.863 mW. Maximum operating frequency of this circuit is higher than the circuit in Figure 5.17 because it has only two series P transistors in the P-section, compared to three for the other circuit. Also, the power consumption is less than that of Figure 5.17 due to the use of narrower P-channel transistors. Input-output waveforms of the circuit at the maximum operating frequency are shown in Figure 5.20.

A CGaAs N-P Domino circuit that generates the logic function $F_3 = (\overline{(\overline{A + B}) \bullet C})$ is shown in Figure 5.21. Transistor gate widths are in micrometers and written on each transistor in the figure. The maximum operating frequency of this circuit is 1.2 GHz and it consumes an average power of 1.682 mW at this frequency. Input-output waveforms of the circuit at the maximum operating frequency are shown in Figure 5.22.

A CGaAs N-P Domino circuit that generates the logic function $F_4 = (\overline{(\overline{A \bullet B}) + C})$ is shown in Figure 5.23. The maximum frequency of operation of this circuit is 0.82 GHz and it consumes an average power of 2.484 mW at this frequency. The maximum frequency of the circuit is low because it has three series P-channel transistors in the P section. Input-output waveforms of the circuit at the maximum operating frequency are shown in Figure

5.24. The performance of all CGaAs N-P Domino logic circuits designed in this section are summarized in Table 5.3.

Table 5.3: CGaAs N-P Domino Logic Circuit Performance

Generated Function	Maximum Frequency [GHz]	Average Consumed Power [mW]	Transistor Count	Layout Area [μm^2]
F1	0.82	2.487	8	22.4
F2	1.2	1.863	8	19.6
F3	1.2	1.682	8	16.8
F4	0.82	2.484	8	23.8
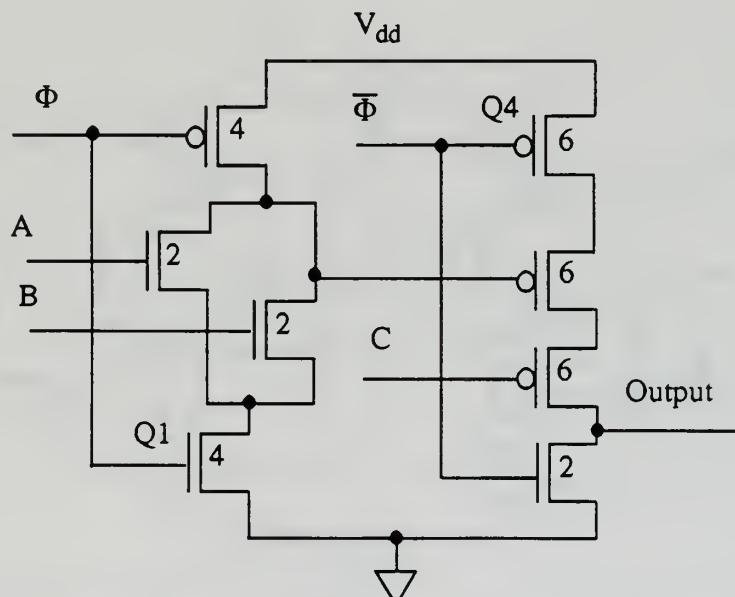
Figure 5.17: CGaAs N-P Domino Logic Circuit to Generate Function F1
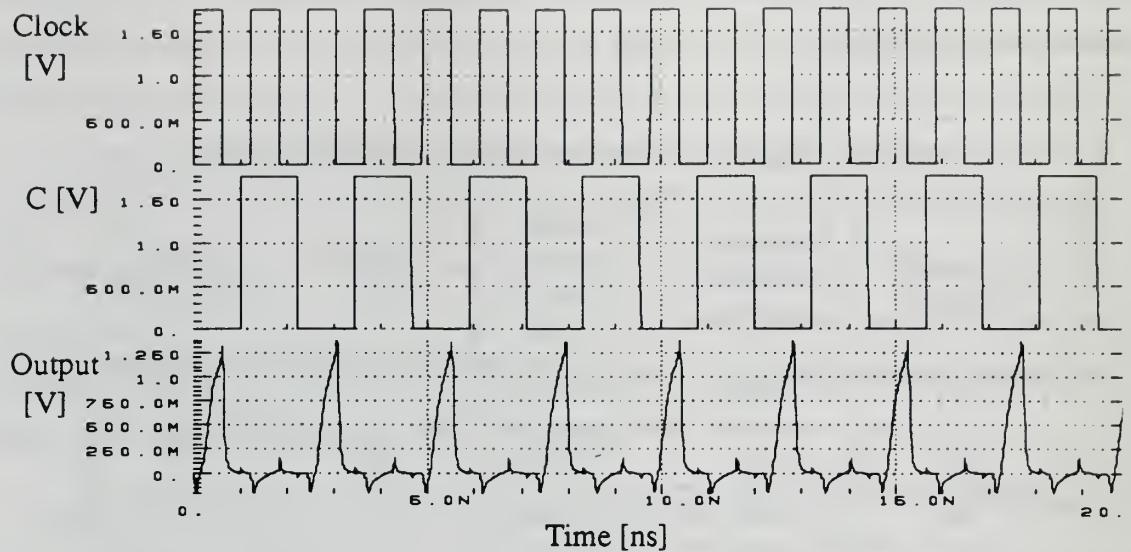
Figure 5.18: Input-Output Waveform of CGaAs N-P Domino F_1 Generator
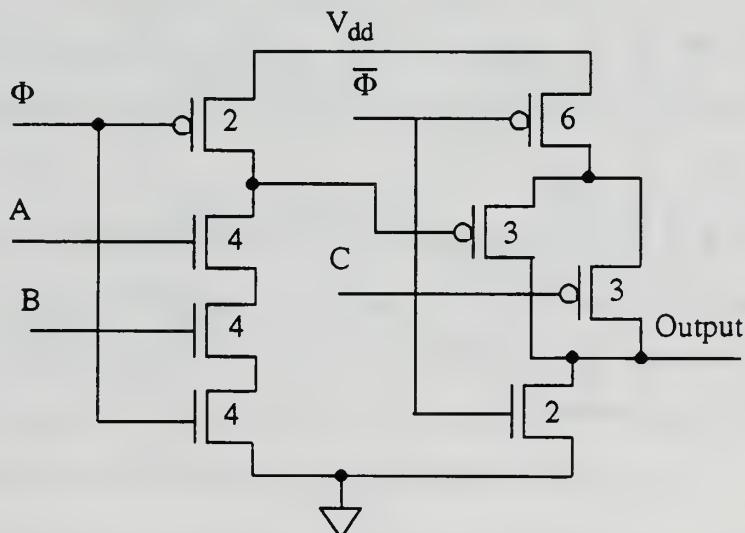
Figure 5.19: CGaAs N-P Domino Logic Circuit to Generate Function F2

106
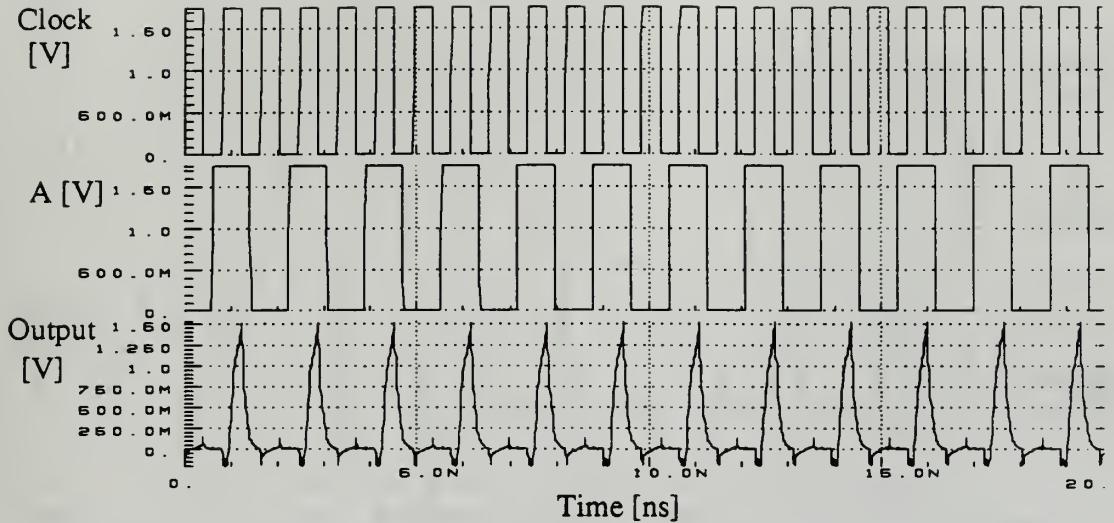
Figure 5.20: Input-Output Waveform of CGaAs N-P Domino Logic F_2 Generator
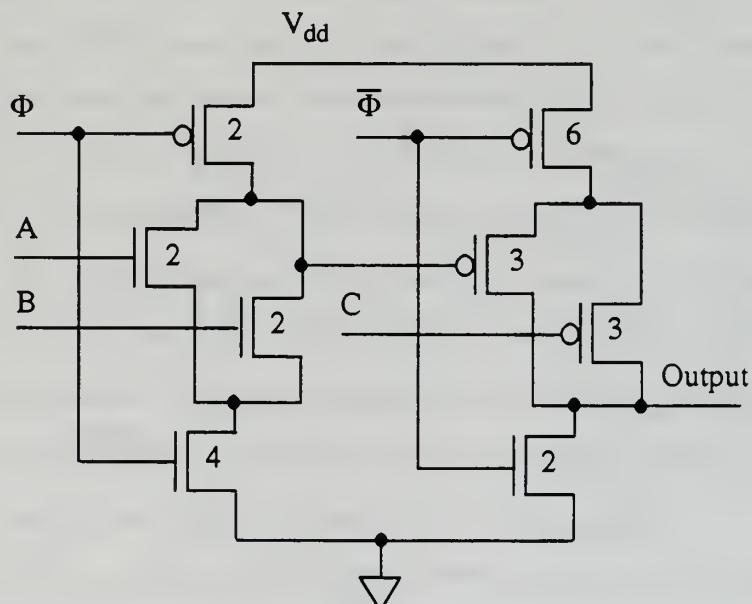
Figure 5.21: CGaAs N-P Domino Logic Circuit to Generate Function F3

107
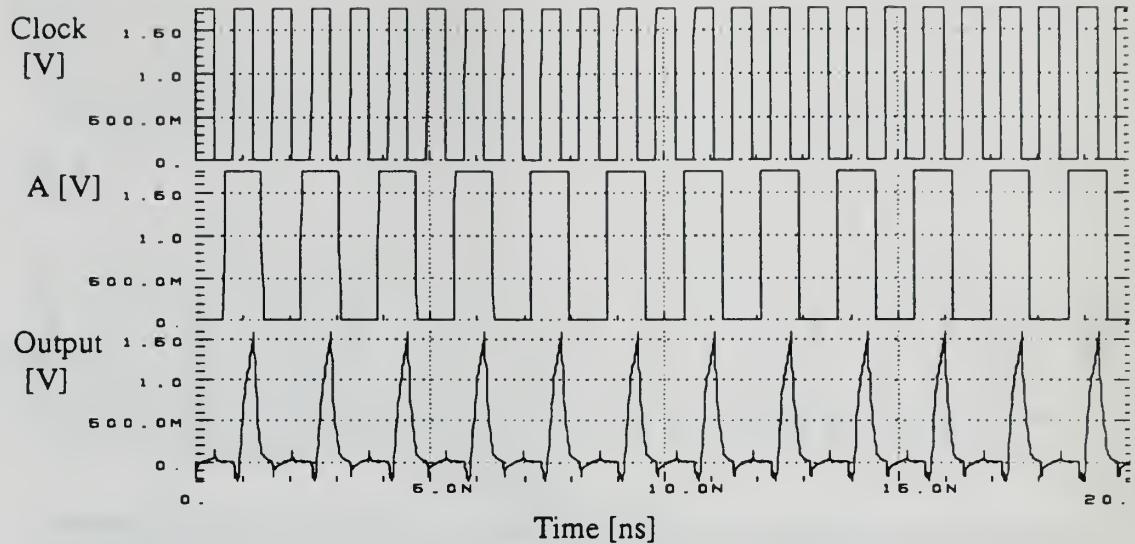
Figure 5.22: Input-Output Waveform of CGaAs N-P Domino Logic F_3 Generator
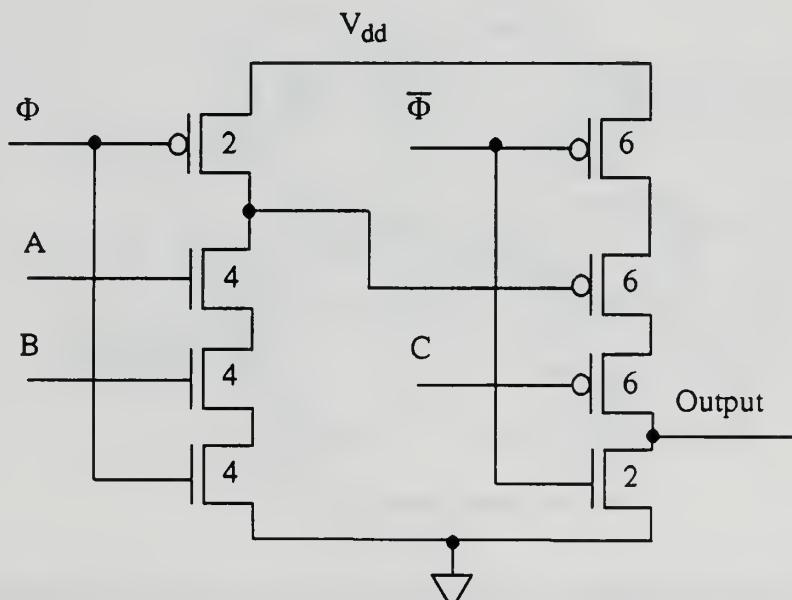
Figure 5.23: CGaAs N-P Domino Logic Circuit to Generate Function F4
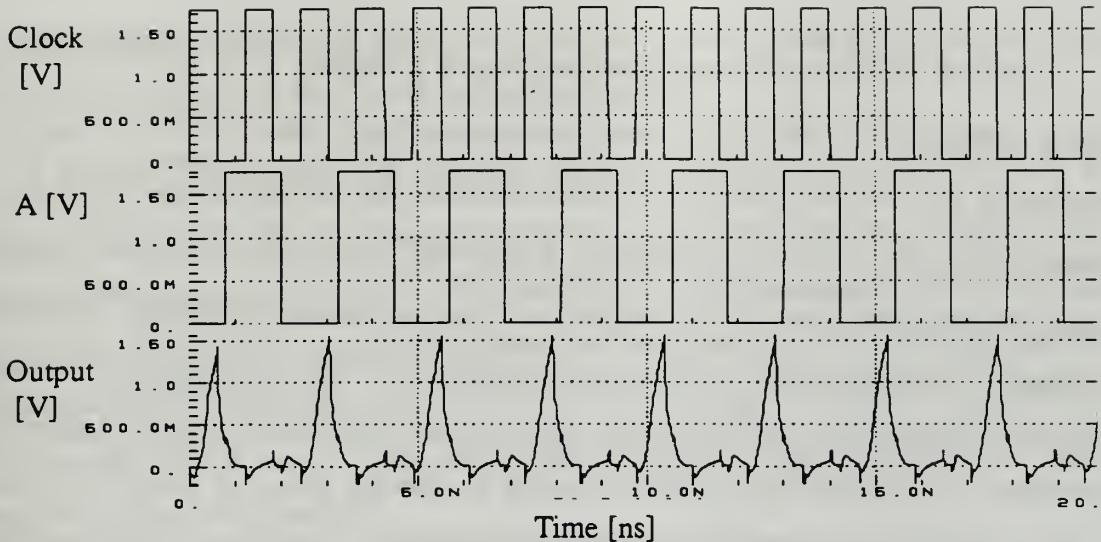
Figure 5.24: Input-Output Waveform of CGaAs N-P Domino Logic F_4 Generator

D. CGaAs TWO-PHASE DYNAMIC LOGIC (TPDL) CIRCUIT DESIGN

TPDL logic is similar to N-P Domino logic because of its 'zipper' operation. Unlike N-P Domino logic, TPDL uses only N-channel transistors in the evaluation part of the circuit. P-channel transistors are used only for precharging the output nodes. TPDL logic requires two clock phases (ϕ_1 and ϕ_2 non-overlapped in the logic low level) and their complements for proper operation. TPDL circuits consist of ϕ_1 logic-blocks and ϕ_2 logic-blocks. Each logic-block is preceded by one pass gate at each input. The output from each logic block can be sampled (read) at the end of its evaluation phase. Output of a ϕ_1 (ϕ_2) block can not be connected to an input of another ϕ_1 (ϕ_2) block or fed back to itself. The ϕ_1 clock phase and its complement control the operation of ϕ_1 logic blocks, while the ϕ_2 clock phase and its complement control the operation of ϕ_2 logic blocks.

In this section, the design and simulation of the previously selected four two-level functions are completed using CGaAs TPDL logic. The circuits are simulated with a 2.0 volt power supply and inputs transition between 0.0 volts and 1.75 volts. Gate lengths of all transistors are 0.7 μm. The precharging P-channel transistors have gate widths of 4 μm, while all N-channel transistors in the evaluation block have gate widths of 2 μm. Pass gate transistor widths are 2 μm for both N- and P-channel transistors.

A CGaAs TPDL circuit which generates the logic function $F_1 = \overline{((A + B) + C)}$ is shown in Figure 5.25. The A and B inputs are applied to a ϕ_1 block, while the C input is applied to a ϕ_2 block. The A and B inputs must be stable (unchanged) during the evaluation phase of the ϕ_1 logic-block (ϕ_1 clock phase is logic high), while the C input must be stable during the evaluation phase of the ϕ_2 logic-block (ϕ_2 clock phase is logic high). The circuit of Figure 5.25 was designed and simulated using HSPICE. The circuit output is available after one complete clock cycle from applying the inputs. Maximum operating frequency of the circuit is 2.38 GHz. The circuit consumes an average power of 1.998 mW at the maximum frequency of operation. Input-output waveforms of the circuit, when operating at the maximum frequency, are shown in Figure 5.26. The A input switches while both the B and C inputs are logic low to propagate the effect of the A input to the circuit output. The circuit output is precharged to V_{DD} when ϕ_2 is logic low and is evaluated when ϕ_2 is logic high (the output is taken from the ϕ_2 logic block).

The limitation on the maximum frequency of operation occurs when the output node is not pulled up to V_{DD} during the precharge phase. this is usually caused by a large capacitive load on the output node. This problem can be solved by increasing the time period in which the output is pulled high (ϕ_1 and ϕ_2 precharge times). This will increase the clock period and decrease the operating frequency. Increasing the width of the precharging P-channel transistors will solve the above problem but will increase the power consumption of the circuit (trade off). Using pass transistors instead of pass gates at logic-block inputs have been tried. N-channel transistors are poor in transmitting a logic 1 and P-channel transistors are poor in transmitting a logic 0. Using either type by itself will decrease the operating voltage range and consequently decrease the operating frequency.

A CGaAs TPDL circuit that generates the logic function $F_2 = \overline{((A \bullet B) \bullet C)}$ is shown in Figure 5.27. The maximum operating frequency of the circuit is 1.92 GHz and the average power consumption is 1.82 mW at that frequency. Input-output waveforms for the circuit at the maximum frequency of operation are shown in Figure 5.28. In this figure, the

C input switches between logic levels while both the A and B inputs are tied to logic low to propagate the effect of the C input to the circuit output.

A CGaAs TPDL circuit that generates the logic function $F_3 = (\overline{(A+B) \bullet C})$ is shown in Figure 5.29. The maximum operating frequency of the circuit is 1.92 GHz and it consumes an average power of 1.75 mW at that frequency. Input-output waveforms for this circuit at the maximum frequency of operation are shown in Figure 5.30. In this figure, the A input switches between logic levels, the B input is tied to logic low and the C input is tied to logic high. The B and C inputs are chosen to propagate the effect of the A input transitions to the circuit output.

A CGaAs TPDL circuit that generates the logic function $F_4 = (\overline{(A \bullet B) + C})$ is shown in Figure 5.31. The maximum frequency of operation for the circuit is 1.92 GHz and it consumes an average power of 1.82 mW at that frequency. Input-output waveforms for the circuit at the maximum frequency of operation are shown in Figure 5.32. In this figure, the A input switches between logic levels, the B input is held constant at logic high and the C input is logic low. The B and C inputs are chosen to propagate the effect of the A input transitions to the circuit output.

Table 5.4 summarizes the performances of the TPDL circuits designed in this section. During simulation, one input of the circuit is switching while the other two inputs are chosen to propagate the effect of the switching input to the circuit output.

Table 5.4: CGaAs TPDL Circuit Performance

| Generated Function	Maximum Frequency [GHz]	Average Consumed Power [mW]	Transistor Count	Layout Area [μm^2]
F1	2.38	2.38	16	25.2
F2	1.92	1.82	16	25.2
F3	1.92	1.75	16	25.2
F4	1.92	1.82	16	25.2
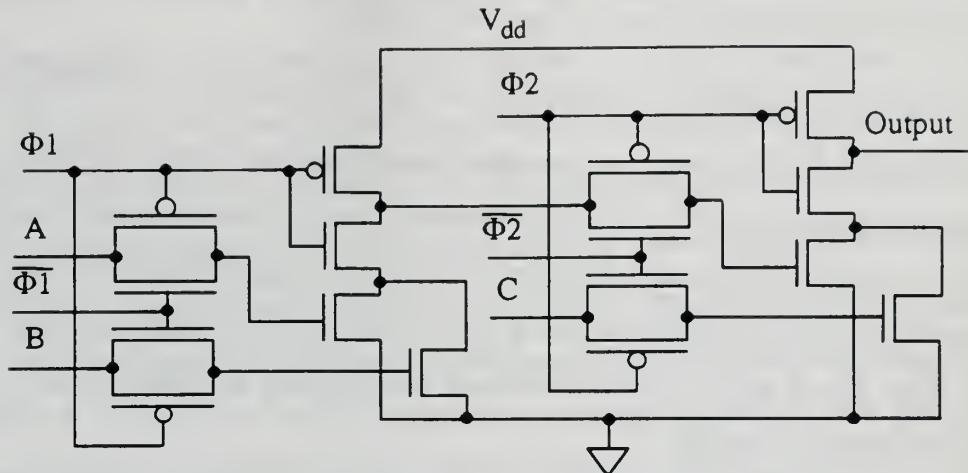
Figure 5.25: CGaAs TPDL Circuit to Generate Function F1
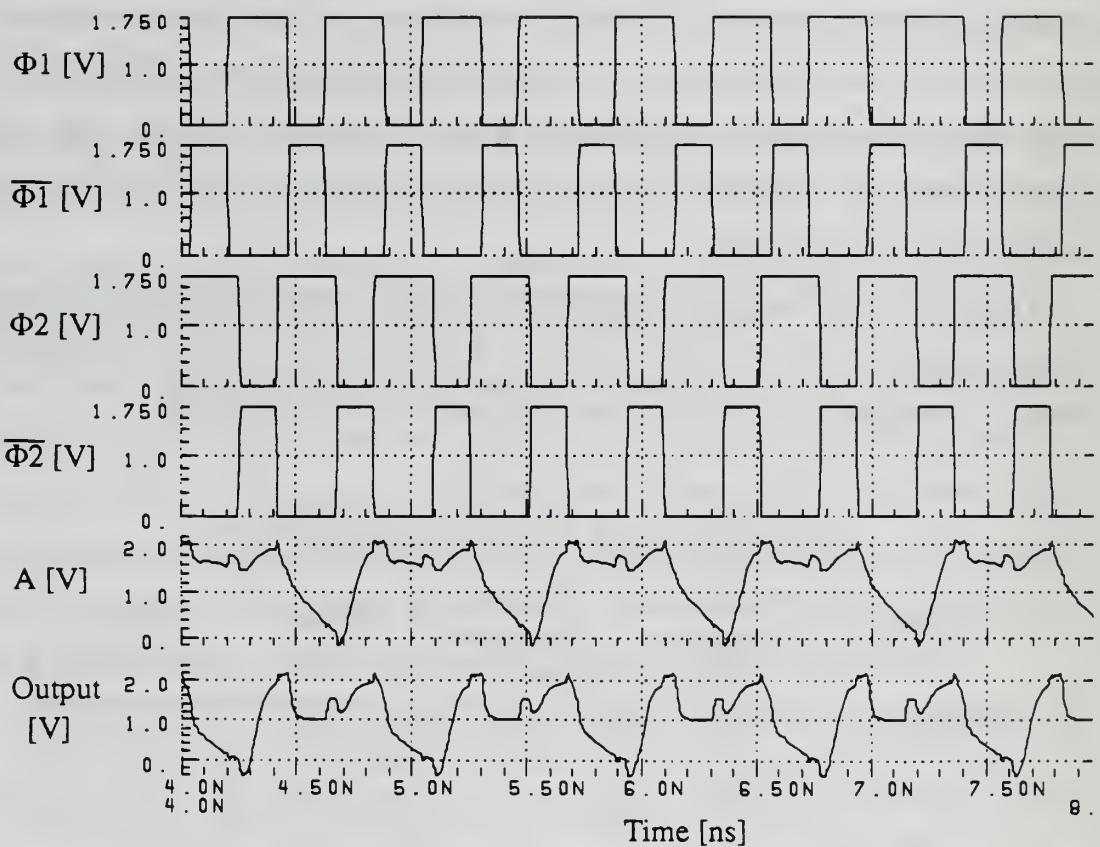
Figure 5.26: Input-Output Waveform of CGaAs TPDL F_1 Generator

112
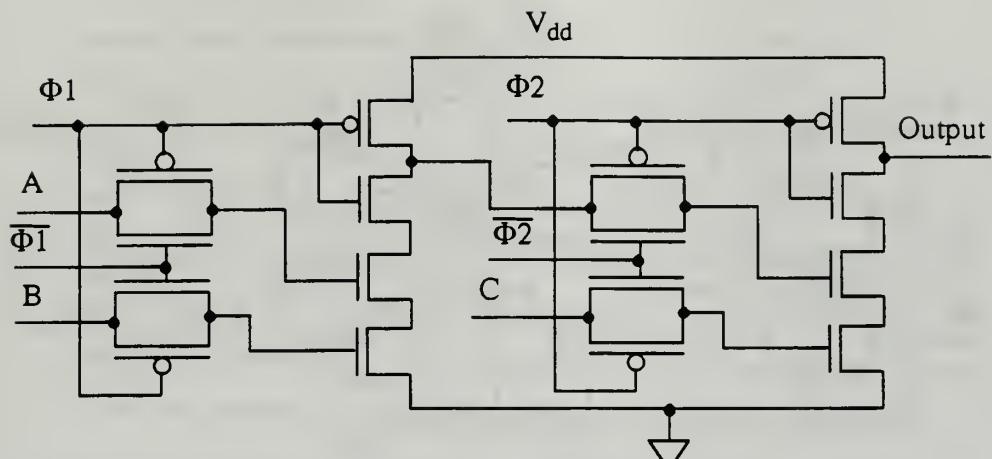
Figure 5.27: CGaAs TPDL Schematic Circuit To Generate Function F2
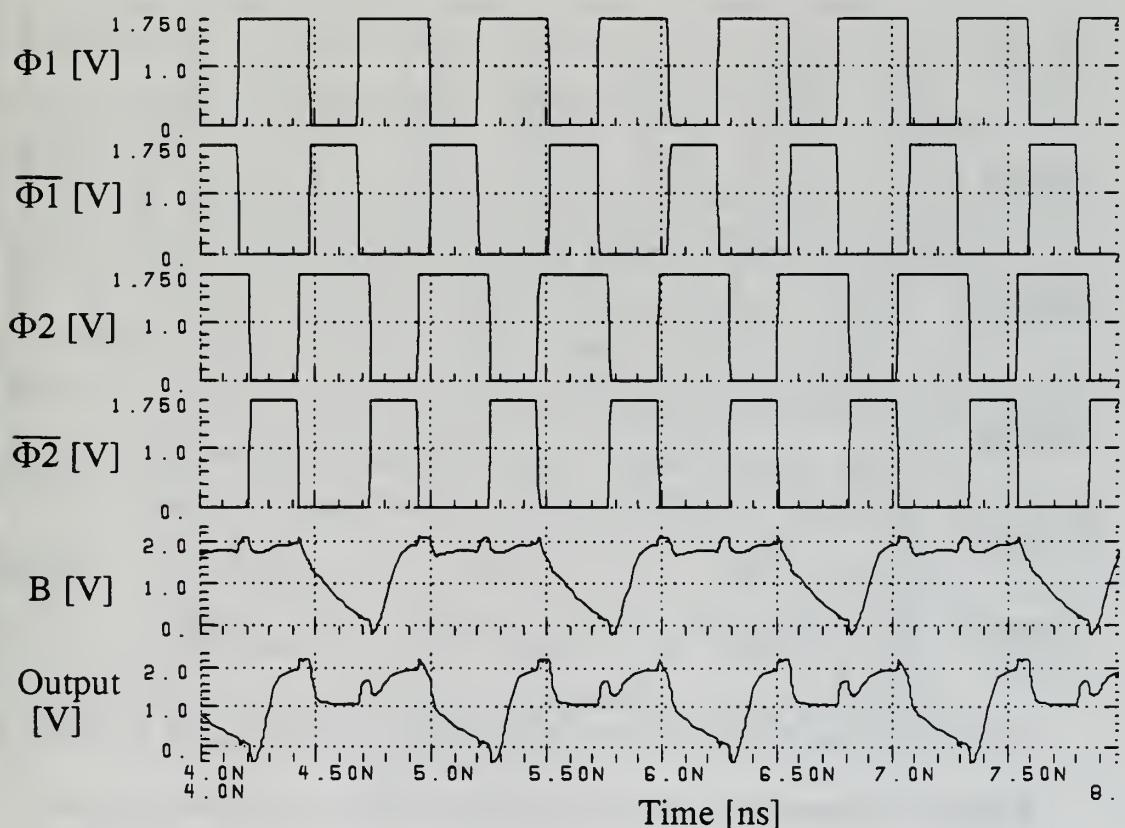
Figure 5.28: Input-Output Waveform of CGaAs TPDL F_2 Function Generator

113
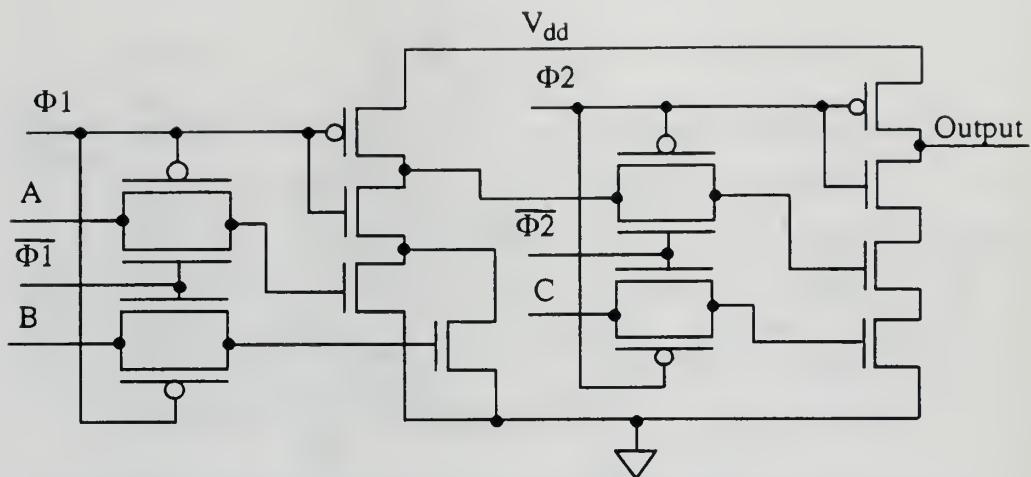
Figure 5.29: CGaAs TPDL Logic Circuit to Generate Function F3
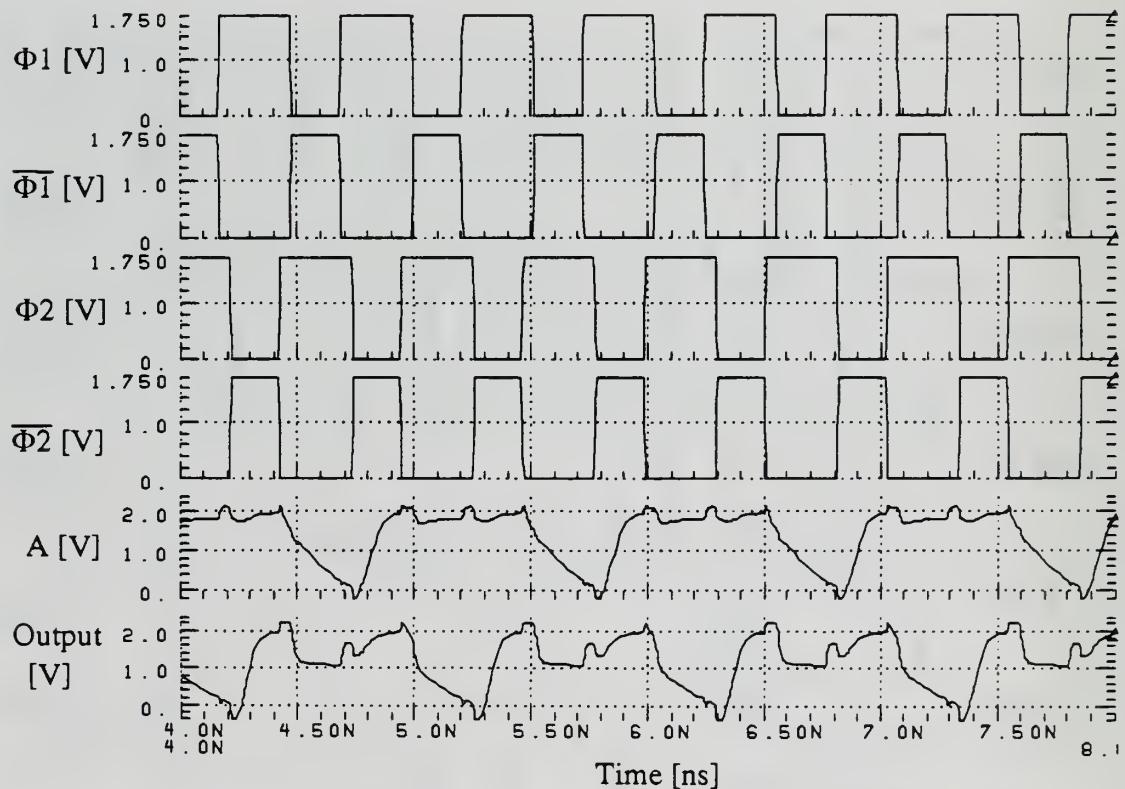
Figure 5.30: Input-Output Waveform of CGaAs TPDL F_3 Function Generator

114
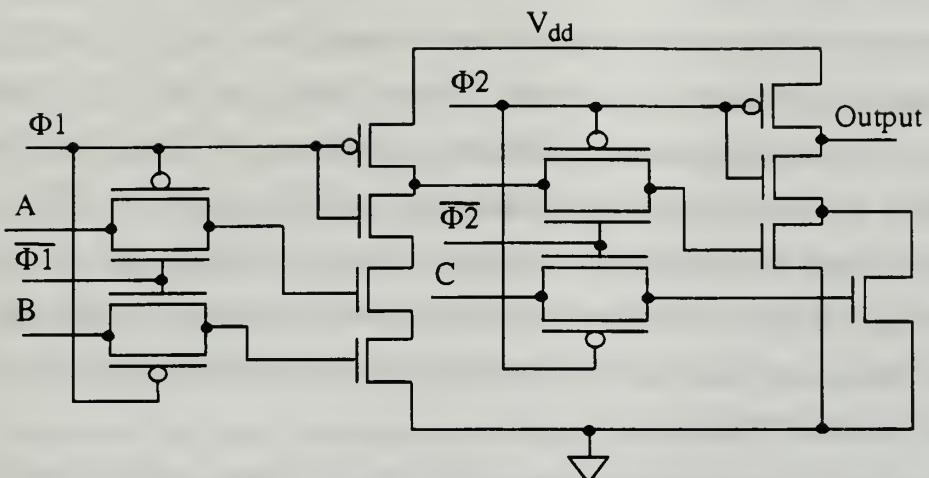
Figure 5.31: CGaAs TPDL Logic Circuit to Generate Function F4

Time [ns]
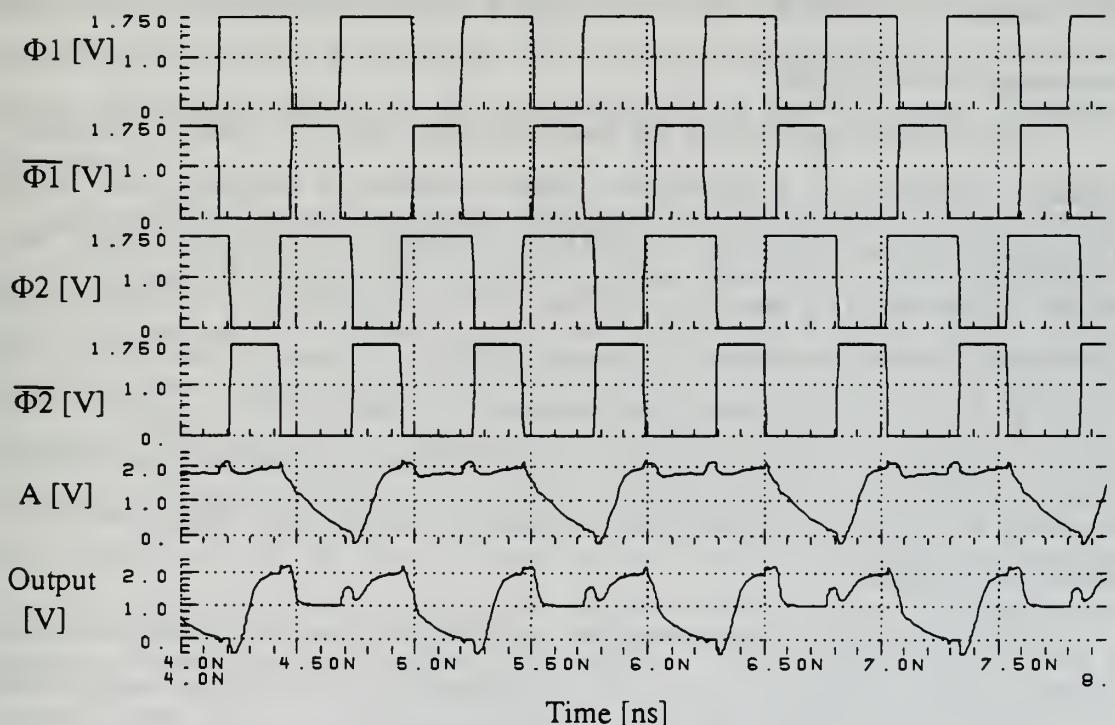
Figure 5.32: Input-Output Waveform of CGaAs TPDL F_4 Function Generator

115

E. COMPARISON BETWEEN CGaAs LOGIC FAMILIES

In the previous sections, the design and simulation of four two-level functions was performed using four different logic families. The logic families studied in this chapter are Static logic, Domino dynamic logic, N-P Domino dynamic logic and Two-Phase Dynamic Logic (TPDL). Due to the excellent performance of the TPDL circuits, the TPDL circuit performing the logic function F1 was implemented using CADENCE tools. This circuit will be fabricated to test its performance, as will be seen in Chapter VII. Also, the static logic circuit for the same function is laid implemented and will be fabricated and tested for comparison with the TPDL circuit.

In this section, a comparison between the studied CGaAs logic families is performed. Maximum operating frequency, average power consumption and layout area are compared. The function $F_1 = (\overline{(A + B) + C})$ will be taken as a study case and Table 5.5 summarizes the comparison results [50].

In CGaAs static logic circuits, the transconductance ratio of N-channel transistors to P-channel transistors has to be properly adjusted to achieve an acceptable noise margin. The design of the static logic circuit is quite easy and similar to the design of Silicon CMOS circuits implementing the same logic function. The drive capability of this family is quite low because the load capacitance is connected directly to the output. Thus, transistor gate widths of the driver circuit have to be increased to increase the drive capability, which increases the power consumption and the layout area. Static logic has the lowest maximum frequency of operation, the highest power consumption and the largest layout area of all the studied logic families.

CGaAs Domino logic is not a complete logic family because inverted functions can not be implemented in this family. Also, it is not completely dynamic because a static inverter is required at each gate output. Its design is more complicated than the static circuit design. Also, it requires a clock signal for proper operation. Domino circuits consist of a dynamic logic block followed by a static inverter. Transistor gate widths in the dynamic logic block can be chosen for minimal size because they only drive the static inverter. The main

disadvantage of Domino logic is that it is not suitable for pipelined system architectures. The maximum frequency of operation is more than double that of the static circuits. Also, the layout area is about one-third of the static circuit layout area and the power consumption is much less than that of static circuits implementing the same logic function.

CGaAs N-P Domino dynamic logic is a complete logic family and is completely dynamic (has no static inverters). It uses both N-channel and P-channel transistor evaluation blocks. Using the slow P-channel transistors in evaluating the logic reduces the speed of this family. N-P Domino logic requires a clock signal and its complement for proper operation. The power consumption and the layout area shown in Table 5.5 does not include the clock generator and driver power consumption and layout area. N-P Domino logic maximum frequency of operation is much lower than that of the Domino logic due to the use of slow P-channel transistor in evaluating the logic. Layout area for both Domino and N-P Domino circuits is comparable. N-P Domino power consumption is lower than that for the Domino circuit due to the reduction in the dynamic power (frequency dependent).

CGaAs TPDL logic has the highest maximum operating frequency, close to double that of Domino and about four times that of static logic. The layout area is comparable to that of Domino and N-P Domino logic and less than half that for static circuits. Even though the power consumption listed in Table 5.5 is the power consumed at the maximum frequency, TPDL circuit power consumption is significantly below that of the static circuit (less than one third). TPDL logic uses only the fast N-channel transistors in evaluating a logic function and uses the slow P-channel transistors only for precharging the output nodes. It does not consume any static power except for a small amount of leakage power (which decreases when lowering the supply voltage). Most of the consumed power is dynamic power. This logic family requires two clock phases and their complements for proper operation. Power consumption and layout area listed in Table 5.5 does not include those for the clock generator and driver circuits. Also, this family requires routing the four clock signals (two clock phases and their complements) to all the circuits, which increases the interconnect area and the design complexity.

For a fair comparison, the power consumption should be calculated at the same frequency. If this is done, TPDL power consumption at the static-circuit maximum operating frequency will be much lower than the value listed in Table 5.5. Moreover, at this low frequency, related to the maximum frequency of TPDL circuits, TPDL circuits would be powered from a lower power supply voltage and would be operated with lower input and output signal transitions, which reduces the consumed power. Also, for the power consumption comparison to be fair, power consumed by the clock generator (to generate ϕ_1, ϕ_2 and their complements required for TPDL circuits) should be considered.

The power consumption as a function of frequency for all the studied logic families implementing the function F1 are shown in Figure 5.33. This figure illustrates the low power consumption of the TPDL design compared to all other designs. Looking at the above comparison, one can conclude that TPDL circuits are the best logic family for building the next generation of high density circuits. CGaAs TPDL circuits are also suitable for pipelined architectures. When used in pipelined architectures, they do not require storage elements between stages. Logic levels are stored on transistor gates of the N-channel transistor logic blocks during the precharging phase. During the precharging phase, the pass gates preceding the logic-blocks are turned off to protect the stored data from corruption.

Table 5.5: Comparison of CGaAs Logic Families

Logic Family	Maximum Frequency [GHz]	Average Power [mW]	Layout Area [μm^2]
Static	0.62	8.69	56
Domino	1.61	3.54	19.6
N-P Domino	0.82	2.487	22.4
TPDL	2.38	2.38	25.2
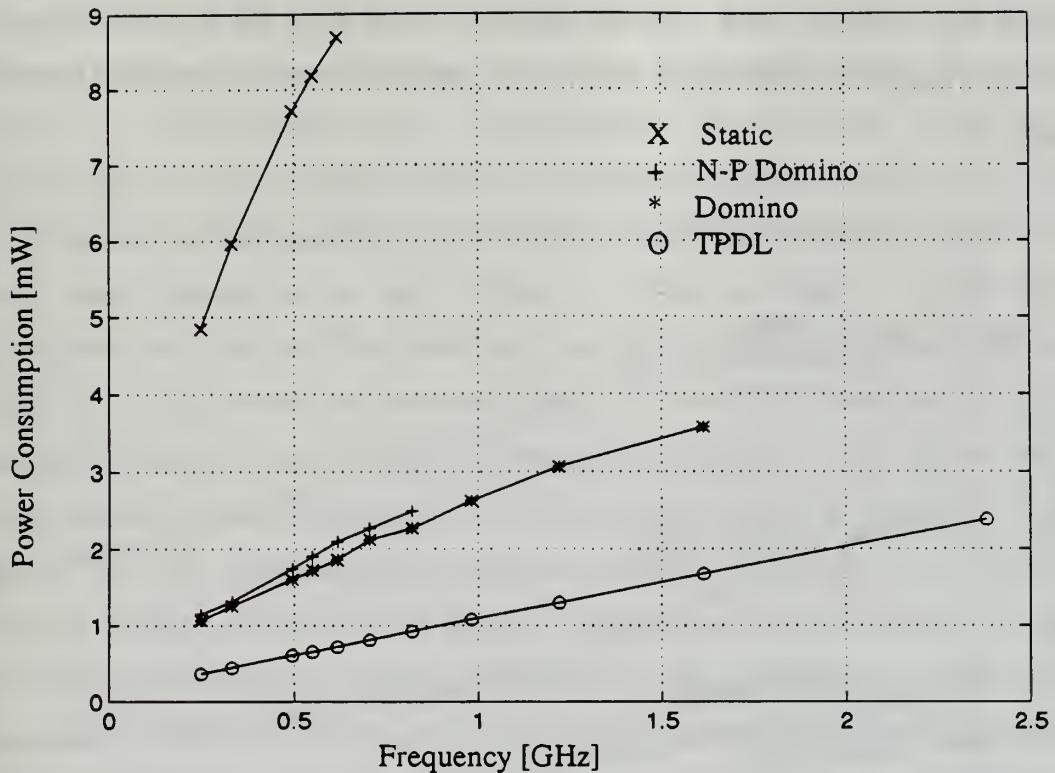
Figure 5.33: Power Consumption of Logic Circuits Implementing Function F1

F. LOADING EFFECTS ON CGaAs LOGIC FAMILIES

In this section, the effect of increasing the output load on the performance of the different CGaAs logic families will be discussed. The four logic families studied are static logic, Domino logic, N-P Domino logic and TPDL. The function $F_1 = (\overline{(A + B) + C})$ discussed in the previous sections will be used again. All logic circuits will be powered from the same power supply (2.0 volts). Also, the same input transitions will be applied to all circuits (input transitions between 0.0 volts and 1.75 volts). The maximum operating frequency, as a function of the number of loads, is plotted in Figure 5.34 for all logic families. From this figure, it can be seen that the maximum frequency of operation is inversely proportional to the number of loads in a nonlinear relation. The maximum

operating frequency of the TPDL family is always the highest frequency over all the studied logic families. Also, when the number of loads is 10 for the TPDL circuit, its maximum frequency is still higher than that for the static circuit with one load (about two times).
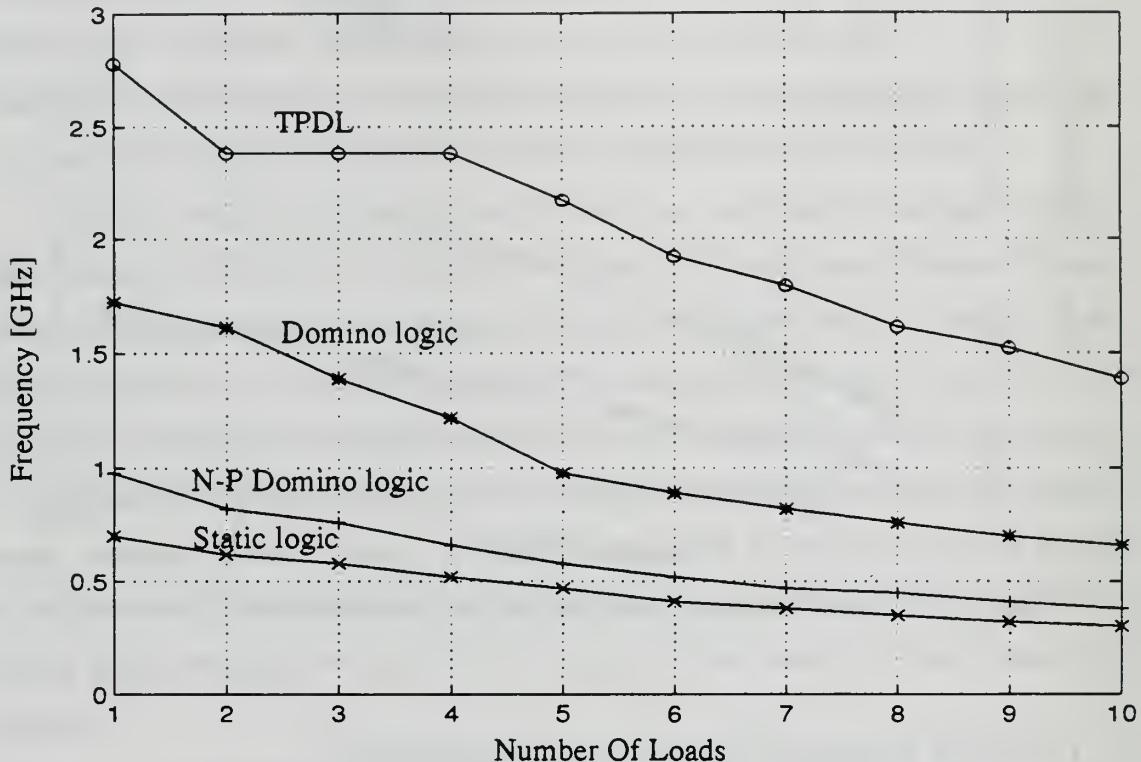
Figure 5.34: Loading Effects on the Logic Families

G. EFFECT OF POWER SUPPLY VOLTAGE ON CGaAs LOGIC FAMILIES

In this section, the effect of changing the power supply and input signal voltage on the maximum operating frequency and power consumption of all CGaAs logic families is studied. This will stress the advantage of the TPDL family over the other logic families.

The logic function $F_1 = (\overline{(\overline{A + B}) + C})$ will be used as a study case.

CGaAs circuits implementing the logic function F_1 have been designed and simulated using all four logic families. Simulations were accomplished with HSPICE when all circuits were loaded by two inverters (fan-out of two). The power supply voltage at which

120

all circuits were simulated were 2.00, 1.75, 1.50, 1.25 and 1.00 volts. When the power supply voltage was 2.0 volts, the input signal transition was 1.75 volts peak-to-peak. Otherwise, the power supply voltage was equal to the peak-to-peak input signal transition. The highest power supply voltage applied to the circuit was limited by the transistor drain-to-source leakage current. The highest gate voltage transition was limited by the transistor gate leakage current. The maximum operating frequency, as a function of power supply voltage for all logic families, is plotted in Figure 5.35. The power consumption, as a function of the power supply voltage for all logic families, is plotted in Figure 5.36. It can be seen from these two figures that the TPDL family has the highest maximum operating frequency with the lowest power consumption. This agrees with the results obtained in the previous sections. When the power supply is decreased from 2.0 volts to 1.75 volts, while keeping input signal-transitions at 0.0 volts to 1.75 volts, the maximum operating frequency of all dynamic logic families are not decreased, while for static logic it does decrease, as shown in Figure 5.35. Also, decreasing the power supply from 2.00 to 1.75 volts will decrease the power consumption for all logic families, as shown in Figure 5.36. Decreasing the power supply voltage and the input swings beyond 1.75 volts will reduce both the maximum frequency and the average power consumption of all logic families.

From this section and the previous two sections, one can conclude that the performance of TPDL logic is superior to all other dynamic and static logic families. The TPDL family will be chosen for designing and implementing the circuits of the following chapters.
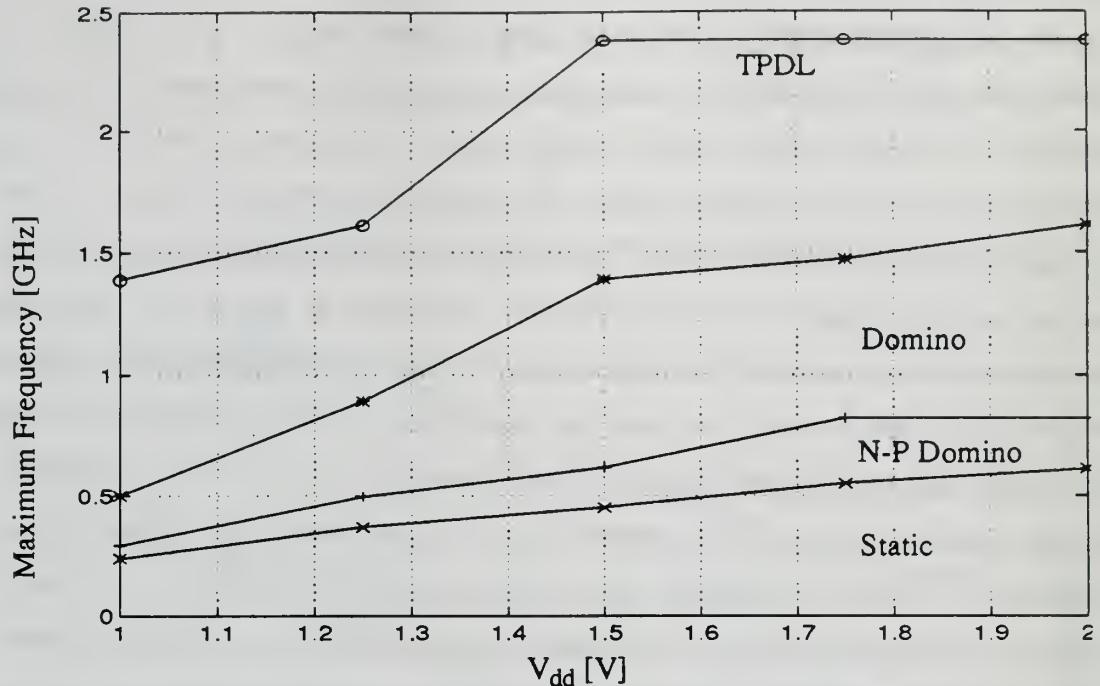
Figure 5.35: Maximum Operating Frequency of Logic Families
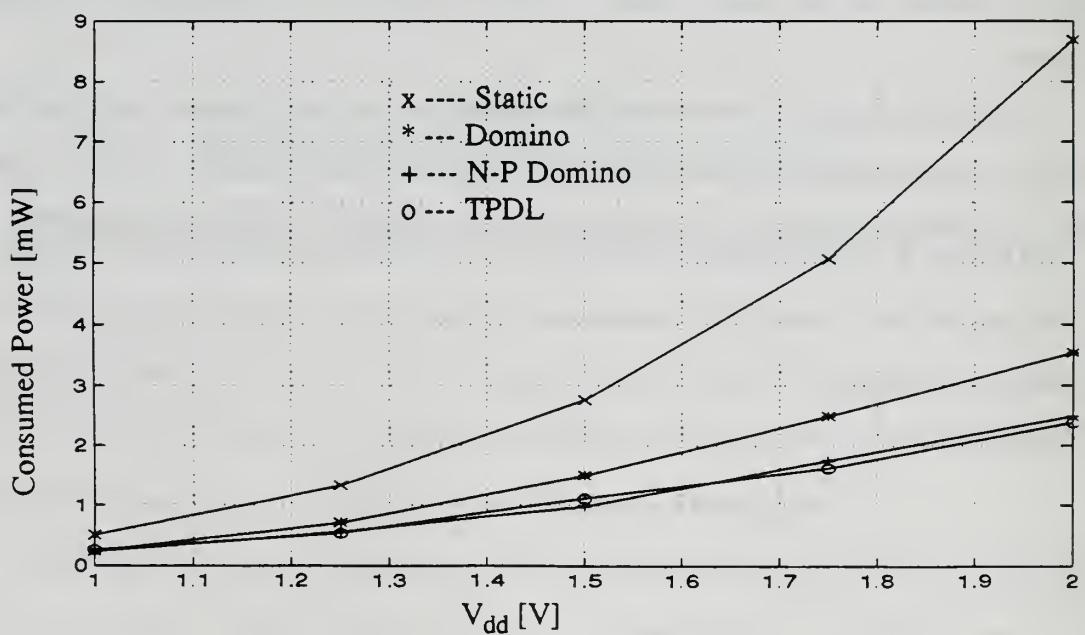
Figure 5.36: Power Consumption of Logic Families

122

VI. DESIGN OF COMPLEMENTARY GaAs MULTI-LEVEL TPDL AND STATIC LOGIC CIRCUITS

A multi-level logic circuit is a block of logic that can be divided into subblocks such that each subblock can be considered as a separate circuit. A multi-level logic function is a function that has multiple inputs and outputs and that requires a multi-level circuit for implementation. A Four-Bit Carry Lookahead Adder (4Bit-CLA) is an example of a multi-level logic function. In this chapter, a 4-Bit CLA will be designed and implemented using a multi-level logic circuit. In Chapter V, it was shown that Two-Phase Dynamic Logic (TPDL) is the optimal dynamic logic family. It has the highest maximum operating frequency and the lowest power consumption of all the studied dynamic logic families. The low power consumption of TPDL logic allows complementary dynamic GaAs circuits to enter the LSI and VLSI era. In this chapter, TPDL is the only dynamic logic family that will be used in circuit designs and implementations. However, circuits designed and implemented using TPDL will also be designed and implemented in static logic for comparison purposes.

In this chapter, an optimal designs for 4-Bit CLAs using static logic and TPDL logic are performed. A comparison is then performed between the two designs for maximum speed, total power consumption and layout area. Section A gives an overview of the carry lookahead adder and the arithmetic equations. The design and analysis of the CGaAs 4-Bit CLA, using static logic and piplined static logic, is explained in Section B. Section C shows the design and analysis of the same adder using TPDL. The comparison between the static logic and TPDL designs for speed, power consumption and layout area is explained in Section D.

A. CARRY-LOOKAHEAD ADDER OVERVIEW

All of the various arithmetic operations (add, subtract, multiply and divide) can be implemented by appropriate combinations of the add function. Thus, addition is the universal data operation for a computer Arithmetic Logic Unit (ALU). In the following

subsections, the basic design and the operation of different adder configurations will be discussed.

1.   Basic Add/Subtract logic

A Full Adder (FA) is the basic cell that is normally used to perform addition. In this subsection, a one-bit FA, that can be used to implement a n-bit adder, is described. A one-bit full adder adds two binary digits, A_i and B_i, and one carry input C_i, to produce a sum output S_i and a carry output C_{i+1}. The sum output has the same significance as the three inputs, while the carry output is one bit more significant. The two outputs are related to the three inputs by the following boolean Equations:

$$S_i = A_i \oplus B_i \oplus C_i \tag{6.1}$$

$$C_{i+1} = A_i B_i + B_i C_i + C_i A_i \tag{6.2}$$

The basic adder cell can be modified to become a 4-input Controlled Add/Subtract cell (CAS) by adding another input P which is used to control the add (P = 0) or subtract (P = 1) operations. In the case of subtraction, input C_i is called borrow-in and the C_{i+1} output is called borrow-out. The input-output relationship of a CAS cell is specified by the following pair of Boolean Equations.

$$S_i = A_i \oplus B_i \oplus P \oplus C_i \tag{6.3}$$

$$C_{i+1} = ((A_i + C_i) \cdot (B_i \oplus P)) + A_i C_i \tag{6.4}$$

When P = 0, $B_i \oplus P = B_i$ and the two sets of Equations (6.1/ 6.2 and 6.3/ 6.4) are identical.

When P = 1, $B_i \oplus P = \bar{B}_i$ and Equations 6.3 and 6.4 become

$$S_i = A_i \oplus \bar{B} \oplus C_i \tag{6.5}$$

$$C_{i+1} = A_i \bar{B}_i + A_i \bar{B}_i + A_i C_i \tag{6.6}$$

Any number of FA cells can be cascaded to form n-bit ripple adder. The carry in of a cell is driven from the carry out of the next least significant cell. Carry in to the least significant cell is driven from the carry input to the circuit. Carry out of the most significant

cell is the carry output of the whole adder. Each full adder has a latency of two gate-delays. Thus, the n-bit adder will have a *2*n*gate delay*. For large values of n, the latency of the ripple adder is very high, which slows the speed of computations. There are many techniques to reduce the adder latency. One of these techniques is the use of carry lookahead, which will be discussed in the following subsection.

2. Carry Generate, Propagate and Lookahead Functions

The speed of a digital arithmetic processor depends on the speed of the adders used. The carry lookahead adder described here is used to speed up carry propagation in the addition operation. The carries entering all bit positions of a parallel adder are generated simultaneously using additional logic circuits. This results in a constant addition time independent of the adder length. However, for long words, carry lookahead is usually performed in 4-bit groups to reduce implementation costs.

Let the vectors $A=A_{n-1}A_{n-2}......A_1A_0$ and $B=B_{n-1}B_{n-2}....B_1B_0$ be the augend and addend inputs to n-bit adder. Let C_{i-1} be the carry input to the ith bit position. The carry input to the least significant bit position is denoted as C_{-1}. Let S_i and C_i be the sum and carry outputs of the ith stage, respectively. Two auxiliary functions are defined as follows:

$$G_I = A_i \cdot B_i \qquad (6.7)$$

$$P_i = A_i \oplus B_i \qquad (6.8)$$

The carry generate function G_i reflects the condition that the carry originates at the ith stage. The function P_i, called carry propagate, is true when the ith stage will pass the incoming carry C_{i-1} to the next higher stage. Substituting P_i and G_i into Equations 6.1 and 6.2 (before reduction) to obtain S_i and C_i in terms of P_i and G_i.

$$S_i = (A_i \oplus B_i) \oplus C_{i-1}$$

$$S_i = P_i \oplus C_{i-1} \qquad (6.9)$$

$$C_i = A_i \cdot B_i + (A_i \oplus B_i) \cdot C_{i-1}$$

$$C_i = G_i + P_i \cdot C_{i-1} \qquad (6.10)$$

The above Equations reveal the fact that all P_i and G_i for $i = 0, 1,\ldots\ldots, n-1$ can be generated simultaneously from the external inputs A and B. Also, all S_i and C_i can be generated simultaneously. The recursive formula of P_i can be applied to Equation 6.10 to obtain all C_i as follows:

$$C_0 = G_0 + C_{-1} \cdot P_0 \qquad (6.11)$$

$$C_1 = G_1 + C_0 \cdot P_1$$

$$C_1 = G_1 + G_0 \cdot P_1 + C_{-1} P_0 P_1 \qquad (6.12)$$

$$C_2 = G_2 + C_1 \cdot P_2$$

$$C_2 = G_2 + G_1 \cdot P_2 + G_0 \cdot P_1 \cdot P_2 + C_{-1} \cdot P_0 \cdot P_1 \cdot P_2 \qquad (6.13)$$

$$C_{n-1} = G_{n-1} + G_{n-2} P_{n-1} + \ldots + C_{-1} P_0 P_1 \ldots P_{n-1} \qquad (6.14)$$

These equations can be implemented using a carry lookahead unit.

For n=4, two additional terminal functions called block carry generate G^* and block carry propagate P^* can be used to form an additional circuit. This new design allows the connection of 4-bit adder "slices" to be connected together to form an 8-bit or multiple 4-bit adder. This design is called Block Carry Lookahead Adder (BCLA).

$$P^* = P_0 \cdot P_1 \cdot P_2 \cdot P_3 \qquad (6.15)$$

$$G^* = G_3 + G_2 \cdot P_3 + G_1 \cdot P_2 \cdot P_3 + G_0 \cdot P_1 \cdot P_2 \cdot P_3 \qquad (6.16)$$

$$C_{out} = G^* + P^* \cdot C_{in} \qquad (6.17)$$

Where C_{in} and C_{out} are the carry in and carry out of the 4-Bit adder slice, respectively.

The block diagram of a 4-bit carry lookahead adder is shown in Figure 6.1. The propagate and generate block is the circuit that produces the propagate and generate carry (P_i and G_i) required for the consecutive blocks. P_i is generated using an XOR gate while G_i is generated using an AND gate. The C_i and S_i blocks generate the summation and signals

out signals, respectively, according to the above equations. The detailed design of these blocks, using both static logic and TPDL, will be explained in the next two sections.
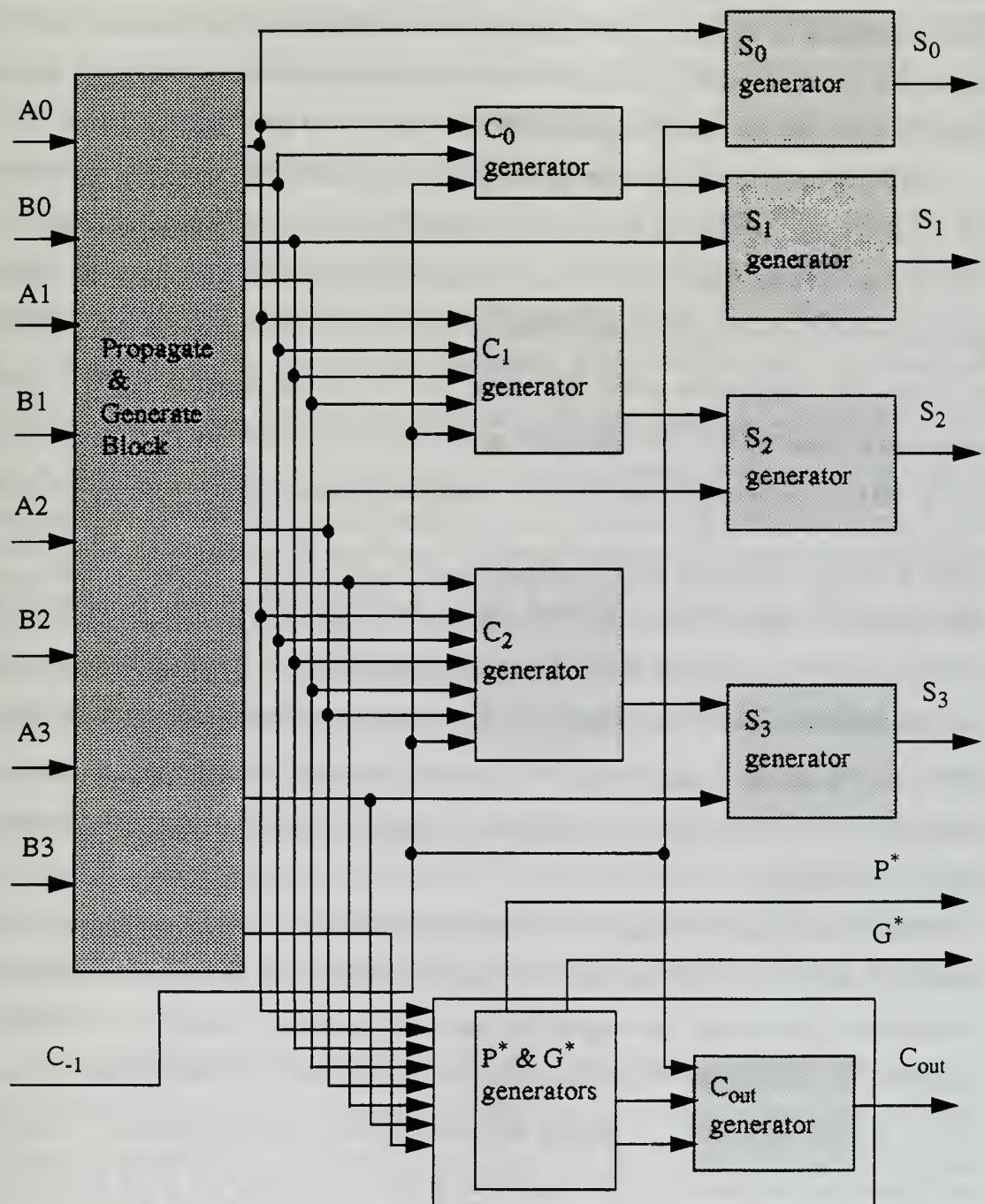
Figure 6.1: CGaAs 4-Bit Blocked CLA Logic Diagram

B. CGaAs STATIC 4-Bit CLA CIRCUIT DESIGN

In this section, the design of a 4-Bit CLA circuit using static logic will be explained in detail. The circuit in Figure 6.1 was designed and simulated using HSPICE simulation tools. Each block of the circuit is designed and simulated separately and then optimized for layout area and maximum operating frequency. Finally, all blocks are integrated to form the 4-Bit CLA. All the transistors used in these blocks have a gate length of 0.7 μm.

AND gates are used to generate the carry-generate signals (G_i) according to Equation 6.7. An AND gate consists of a NAND gate followed by an inverter. The design of the static NAND gates and the static inverters are discussed in Chapter III. XOR gates are used to generate the carry-propagate signals (P_i), according to Equation 6.8, and are also explained in Chapter III. Summation terms (S_0, S_1, S_2 and S_3) are generated using XOR gates, according to Equation 6.9. The circuit that generates the carry function C_0 from the inputs P_0, G_0 and C_{-1} is shown in Figure 6.3. The C_1 generator circuit is shown in Figure 6.4, while the C_2 generator circuit is shown in Figure 6.5. According to Equation 6.15, P^* requires a four-input AND gate which is designed using a four-input NAND gate followed by an inverter, as shown in Figure 6.6. The circuit that generates the G^* function is similar to the one that generates C_2, shown in Figure 6.5. The circuit to generate C_{out} from the inputs C_{-1}, P^* and G^* is similar to that in Figure 6.3, which generates C_0. Transistor gate widths are written on each transistor in all the schematics. These circuits are all designed similarly to static CMOS circuits.

The above circuits are integrated to form the static 4-Bit CLA shown in Figure 6.1. An exhaustive test structure has been used to check the functionality of the CLA. Input-output waveforms of the circuit, running at the maximum operating frequency, are shown in Figure 6.2. The simulation test structure was chosen such that all the summation (S_0, S_1, S_2 and S_3) and the carry out (C_{out}) outputs are switching for every input transition. Figure 6.2 was plotted for the following input signal test structure: $A_3A_2A_1A_0 = 1010$, $B_3B_2B_1B_0 = 0101$. The carry in signal is generated from a pulse generator which switches between logic

low and logic high. Propagation delay, measured from the time of applying the input pulses to the time the outputs switch, determines the maximum operating frequency of the circuit. For the selected test structure, when the input carry in switches from logic low to logic high, all summation signals switch from high to low and the carry out signal switches from low to high. The CGaAs 4-Bit CLA was simulated with a 1.75 volt power supply. Each output of the circuit was loaded by two static inverters (fan-out of two). The input logic-low level is 0.0 volts while the logic-high level is 1.75 volts.

Due to the difference in the propagation paths of all the summations and carry out signals, they have different propagation delays. Therefore, the maximum frequency is limited by the longest signal path (longest propagation delay). The longest propagation delay is for the output S_3. The measured propagation delay, when the carry in switches from logic high to logic low until the time when the summation output S_3 switches from logic low to logic high, is 1.45ns. The propagation delay measured from the change in carry in, from logic low to logic high, to the change in the summation output S_3, from logic high to logic low, is 1.9ns. The duty cycle of the applied input signal should be equal to or longer than the longest propagation delay of the circuit to prevent race conditions. This will limit the maximum frequency of the input signal to 260 MHz (1/(2*1.9ns)). The 4-Bit CLA circuit consumes an average power of 26 mW at the maximum operating frequency.

The summation and the carry out signals do not arrive at the circuit output simultaneously. Thus, the circuit requires a register at the output to hold the information and apply it to the next stage simultaneously. This will add circuitry and increase the layout area, the transistor count and the power consumption of the circuit. Also, the maximum operating frequency of the circuit will be decreased due to the added delay through the register file.

The piplined static 4-Bit CLA solves the above problems. A piplined adder increases the maximum frequency of operation but at the same time increases the transistor count, the power consumption and the layout area. The logic diagram of a three-stage, piplined, static, 4-Bit CLA is shown in Figure 6.7. Three stages of pipeline registers are added to overcome the problem of propagation delay. A pipeline register consists of static D Flip-

Flops, one for each bit. The design and analysis of a CGaAs static D Flip-Flop is presented in Chapter VI, Section A. The use of these pipeline registers will assure that all summation and carry out output signals will be delivered to the output terminals simultaneously. The number of transistors used in the pipelined adder circuit is 460. The circuit was simulated using HSPICE to measure its performance. The maximum frequency of operation is limited by the longest stage delay. The simulation power supply voltage was 1.75 volts and the input signals switch between 0.0 volts and 1.75 volts. All the circuit outputs are loaded by two static inverters (fan-out of two). The maximum operating frequency of the circuit is 550 MHz (more than double that for the static design). The power consumption of the circuit is 77.4 mW at the maximum frequency of operation. The input-output waveforms of the circuit at the maximum frequency are shown in Figure 6.8.
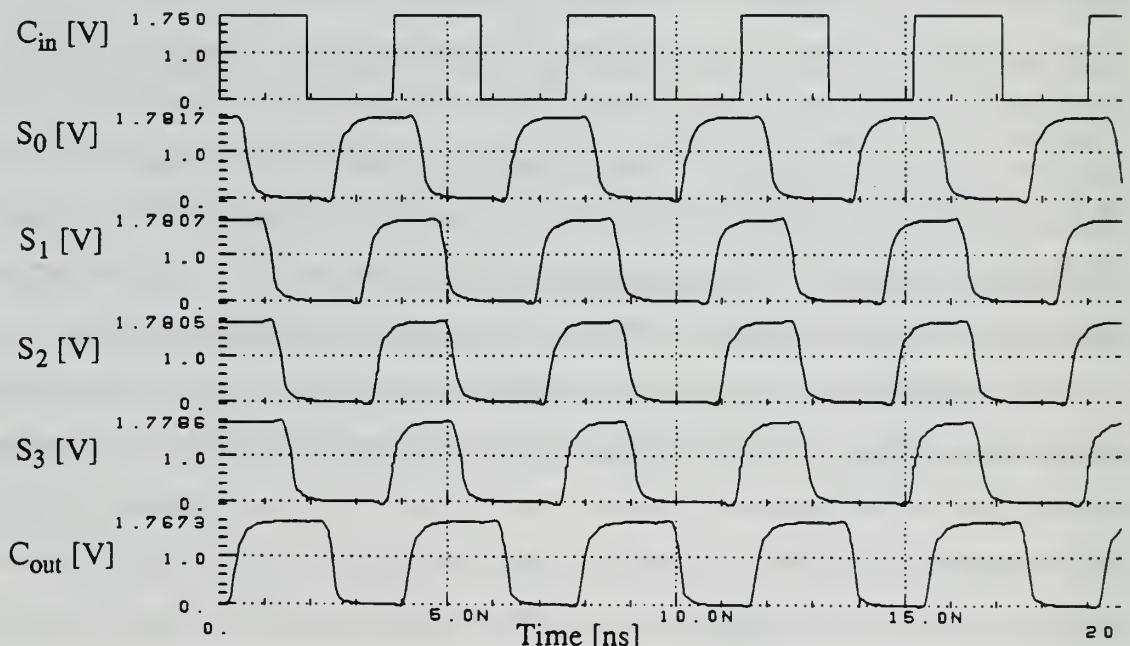
Figure 6.2: Input-Output Waveforms of CGaAs 4-Bit Static CLA
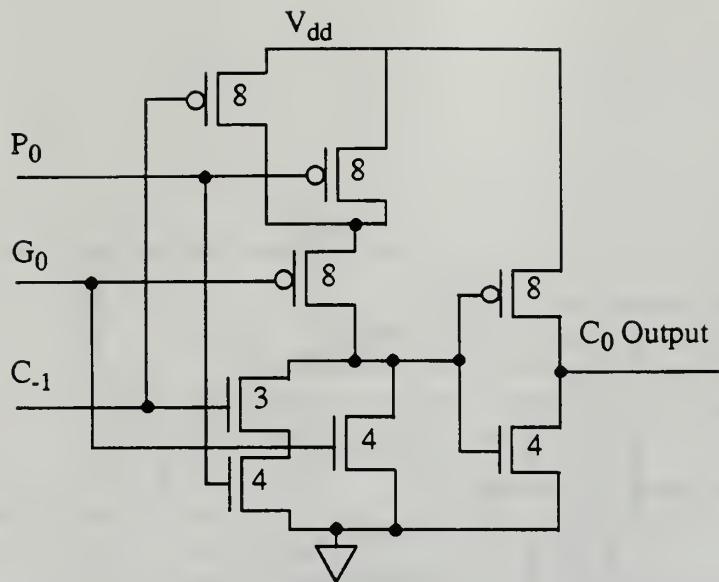
Figure 6.3: CGaAs Static Circuit for Generating the Function C_0
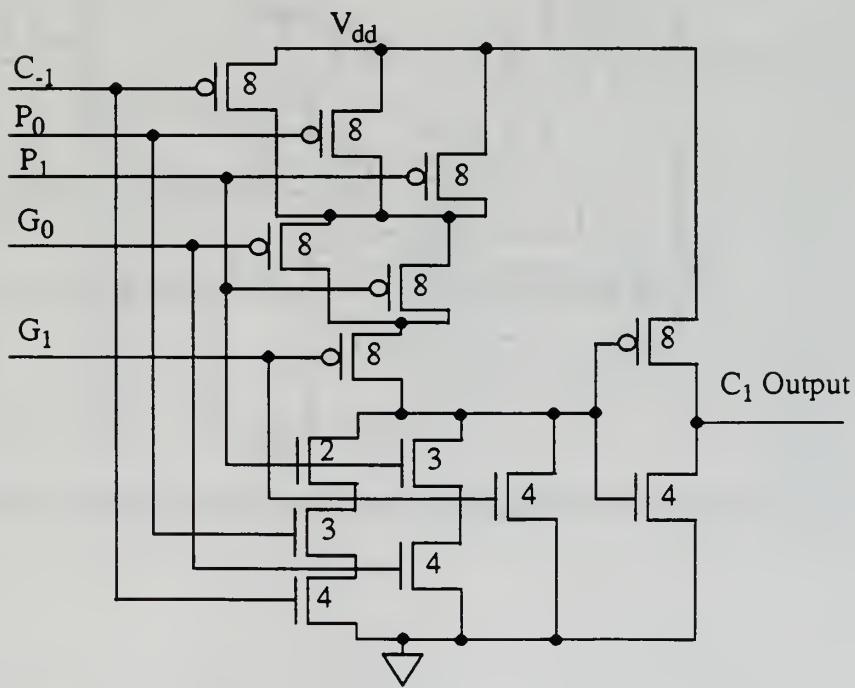
Figure 6.4: CGaAs Static Circuit for Generating the Function C_1
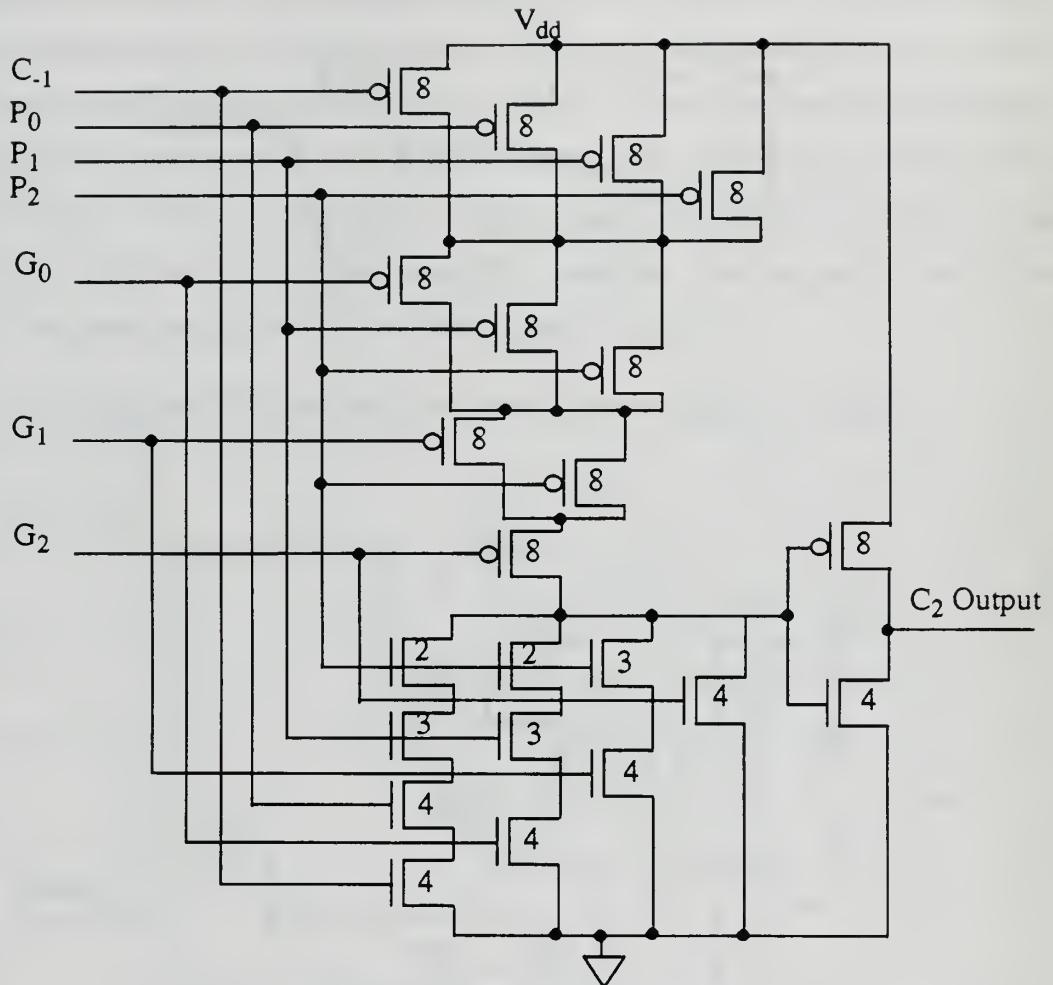
Figure 6.5: CGaAs Static Circuit for Generating the Function C_2

132
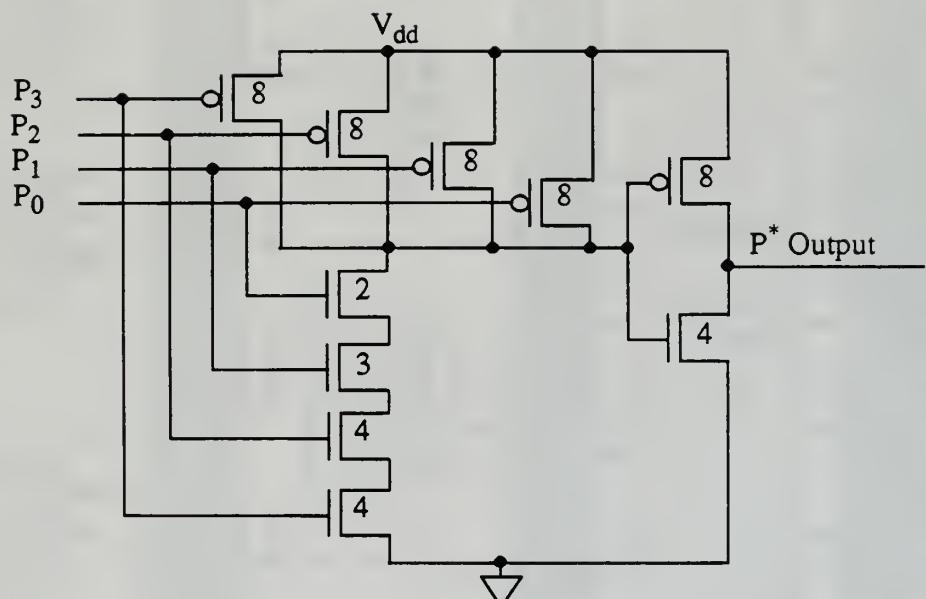
Figure 6.6: CGaAs Static Circuit for Generating the Function P*
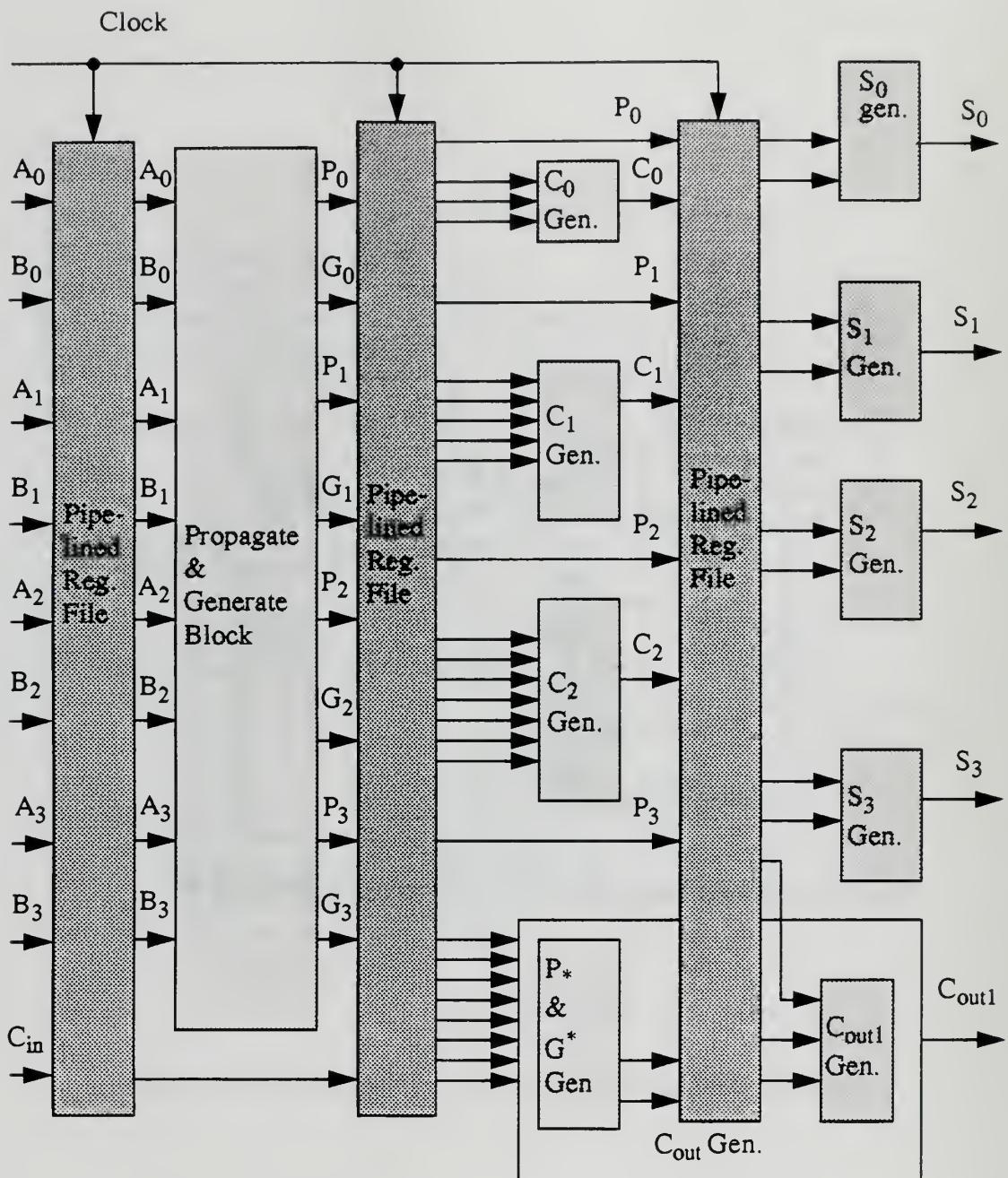
Figure 6.7: CGaAs Pipelined Static 4-Bit CLA Logic Diagram

134
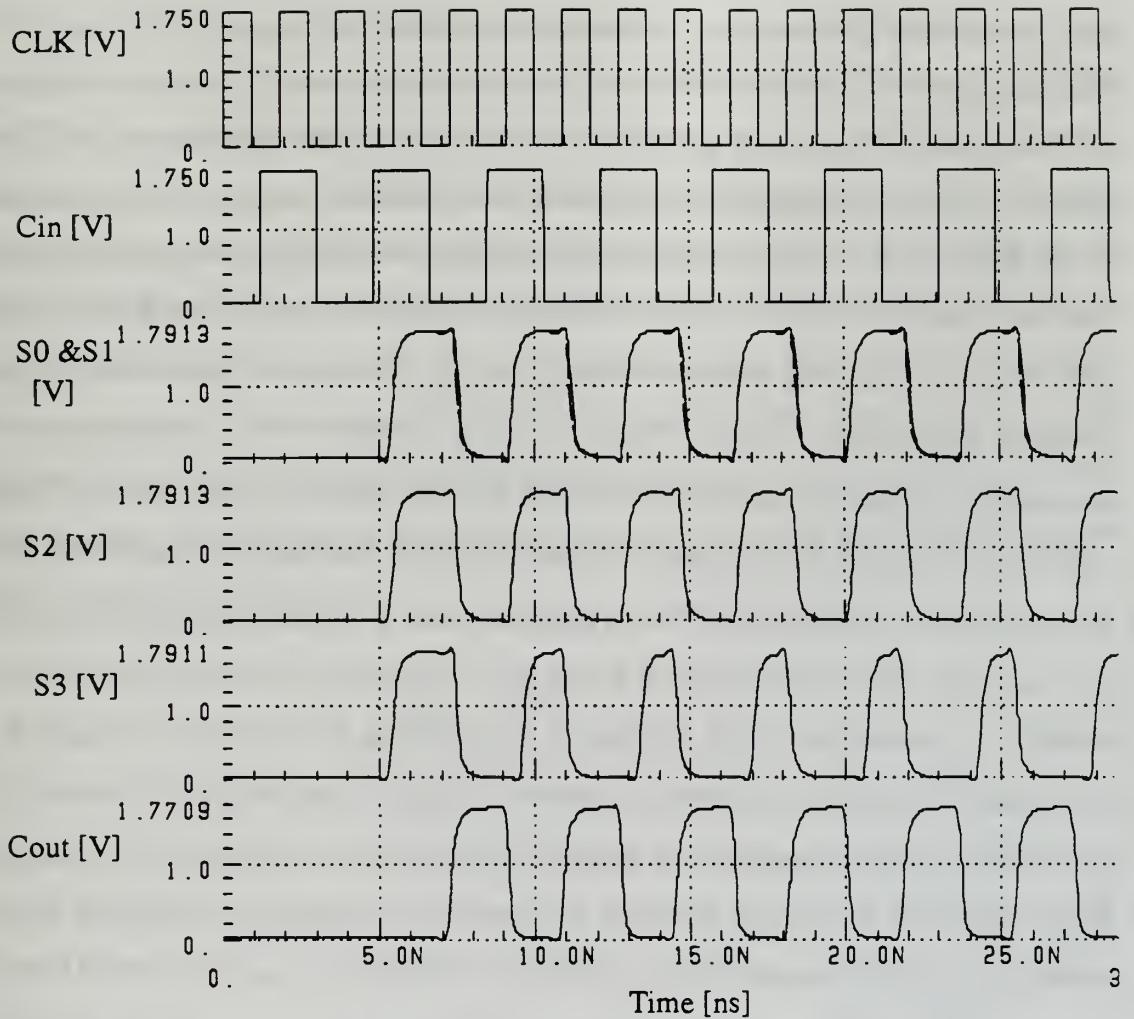
Figure 6.8: Input-Output Waveforms of CGaAs Pipelined Static 4-Bit CLA

C. CGaAs TPDL 4-Bit CLA CIRCUIT DESIGN

Using TPDL increases the throughput of the CGaAs 4-Bit CLA circuit. The logic diagram of the CGaAs TPDL 4-Bit CLA is shown in Figure 6.9. All the logic blocks of this figure will now be explained in detail. The carry generate signals (G_0, G_1, G_2 and G_3) are created according to Equation 6.7 using TPDL AND gates. A TPDL AND gate consists of a TPDL NAND gate followed by a TPDL inverter. Both gates are explained in Chapter III.

According to Equation 6.8, the carry propagate signals (P_0, P_1, P_2 and P_3) are generated using TPDL XOR gates which are also explained in detail in Chapter III. Both the TPDL AND gate and TPDL XOR gate have a fill time of one clock cycle. I.E., all carry-propagate and carry-generate signals are generated one clock period after the inputs A_i and B_i are applied. A one-clock delay TPDL D Flip-Flop is explained in Chapter IV, Section B. The D Flip-Flop output is delayed by one clock period and used to align the input signals of the next logic block to be in phase. P_i and G_i signals arrive at the C_i inputs delayed by one clock from the time of applying the input vectors A_i and B_i. The carry in signal is applied to C_i through a delay block, as shown in Figure 6.9, to be in phase with all P_i and G_i signals. A one clock period delay is applied to both inputs of the S_0 generator block to force all adder outputs to be in phase. The S_i generator blocks in Figure 6.9 are designed using TPDL XOR gates according to Equation 6.9. The C_0 generator block is designed according to Equation 6.11 using the TPDL logic circuit of Figure 6.11. The TPDL circuit which generates the signal C_1 is designed as shown in Figure 6.12, according to Equation 6.12. Figure 6.13 shows the TPDL logic circuit used to generate the signal C_2, according to Equation 6.13. The TPDL circuit that generates the function P*, according to Equation 6.15, is shown in Figure 6.14. The circuit that generates the function G*, according to Equation 6.16, is similar to the circuit that generates C_2 and shown in Figure 6.13. C_{out} is generated from the inputs C_{in}, P^* and G^*, according to Equation 6.17, using a circuit similar to the one that generates C_0 and is shown in Figure 6.11. All these TPDL logic circuits are designed and optimized for layout area and speed before integration into the adder circuit. The P* and G* blocks are added for two reasons. The first reason is to turn the circuit into a block adder. The second reason is to reduce the number of series N-channel transistors in the circuit P_2 which uses a four-input AND gate instead of a five input AND gate. This increases the maximum operating frequency of the circuit.

The fill time of the TPDL 4-Bit CLA circuit is 3 clock periods (the outputs are available three clock periods after applying the inputs). The circuit was simulated with

HSPICE to measure the performance. The power supply voltage used in the simulation was 1.75 volts. Input logic low and logic high levels were 0.0 volts and 1.75 volts, respectively. All output terminals of the circuit were loaded by two TPDL inverters (fan-out of two). The circuit was tested exhaustively to examine its functionality. The maximum operating frequency of the circuit is 1.22 GHz and it consumes an average power of 61.79 mW at that frequency. Input-output waveforms of the circuit are shown in Figure 6.10. In this figure, the following test vector is applied: $A_3A_2A_1A_0=1010$, $B_3B_2B_1B_0=0101$. The carry in signal is alternating between logic low and logic high levels. The selected input vectors force all outputs of the circuit to switch between logic states for each input change. All summations and carry out outputs precharge when ϕ_2 is logic low because they are taken from ϕ_2 gates. The effects of the input changes appear at the outputs after three clock cycles (the fill time of the circuit).

Figure 6.9: CGaAs TPDL 4-Bit CLA Logic Diagram

138
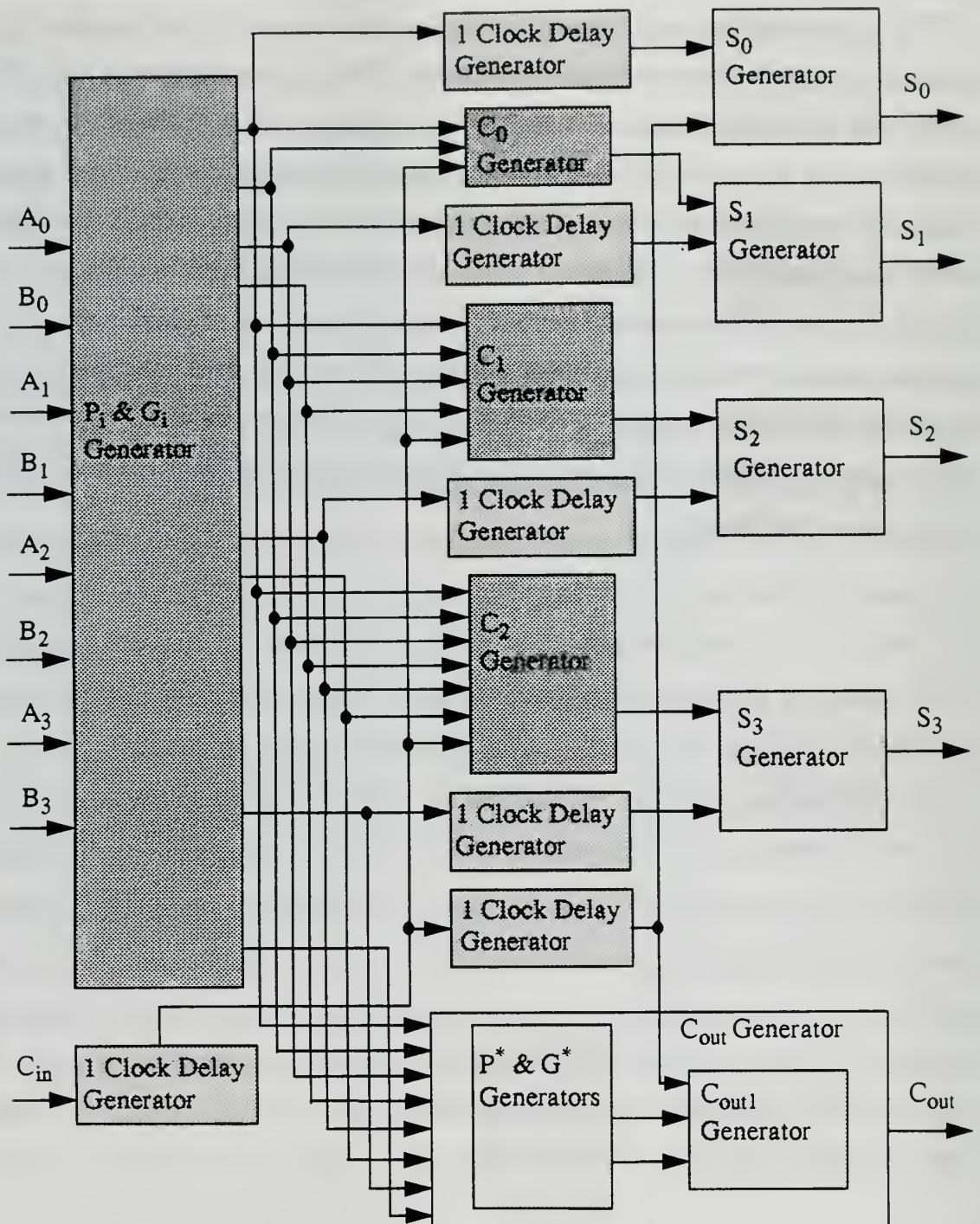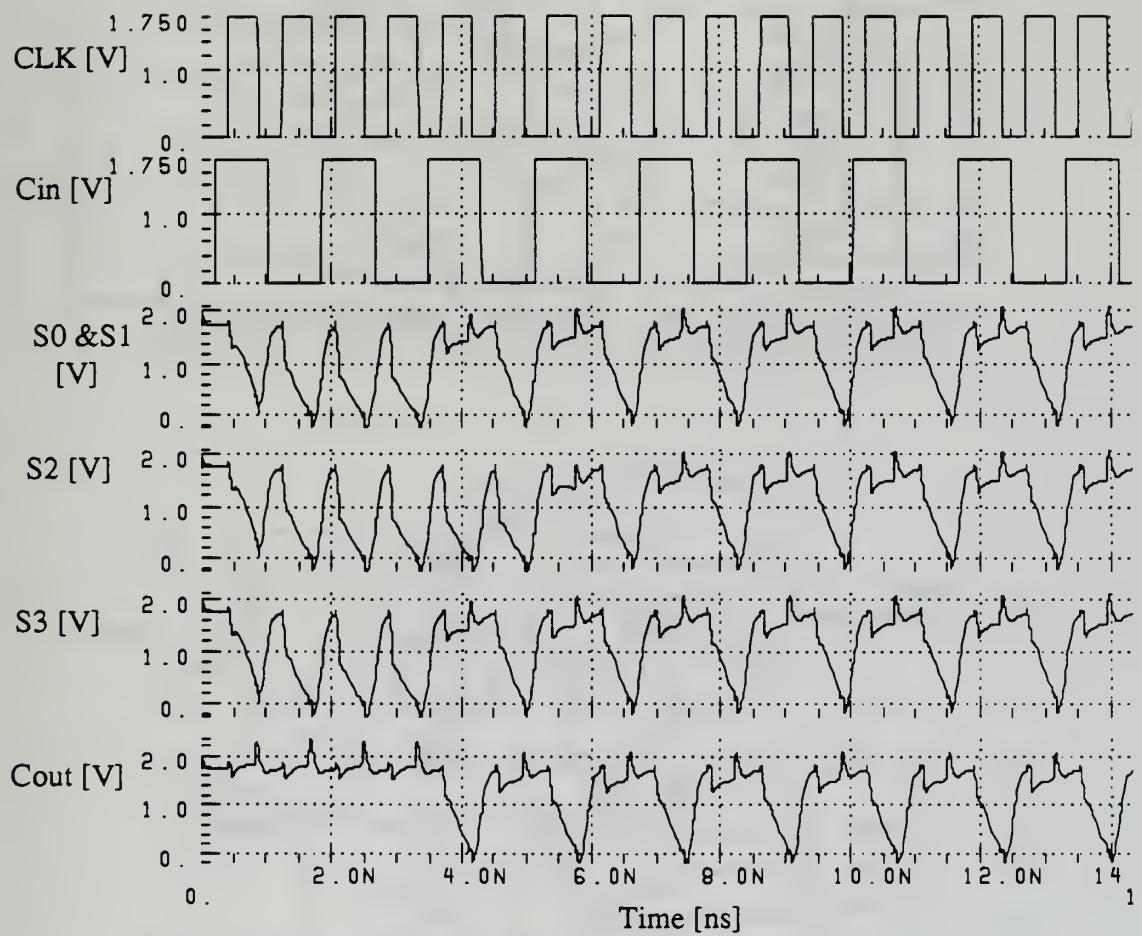
Figure 6.10: Input-Output Waveforms of CGaAs TPDL 4-Bit CLA

139
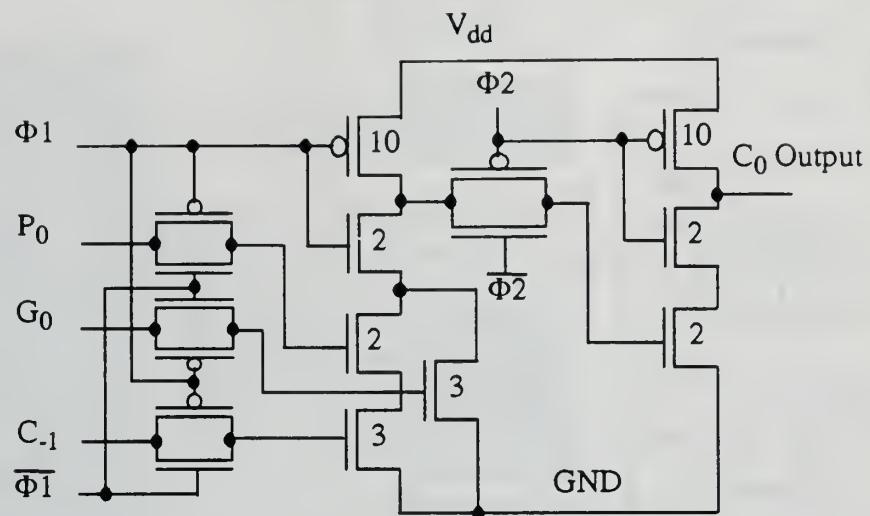
Figure 6.11: CGaAs TPDL Circuit for Generating Function C_0
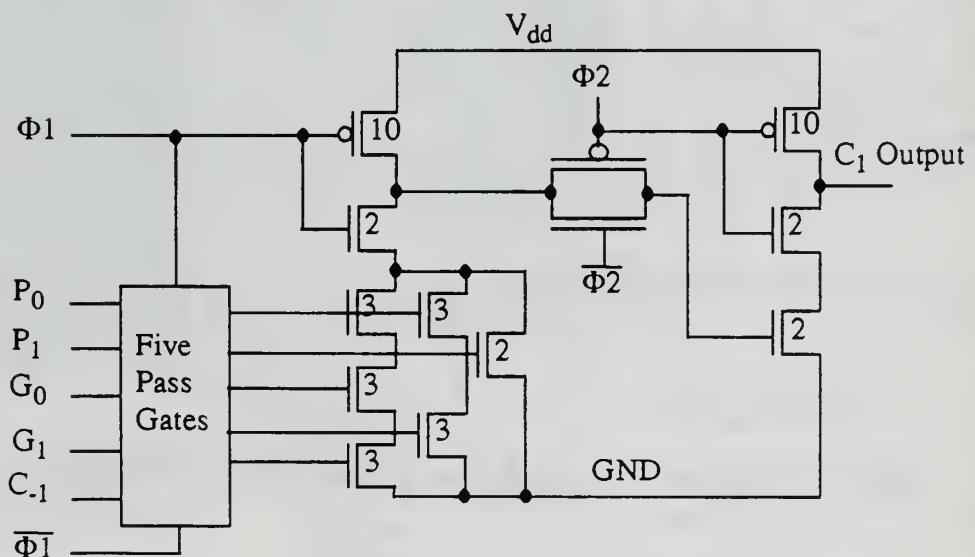
Figure 6.12: CGaAs TPDL Circuit for Generating Function C_1
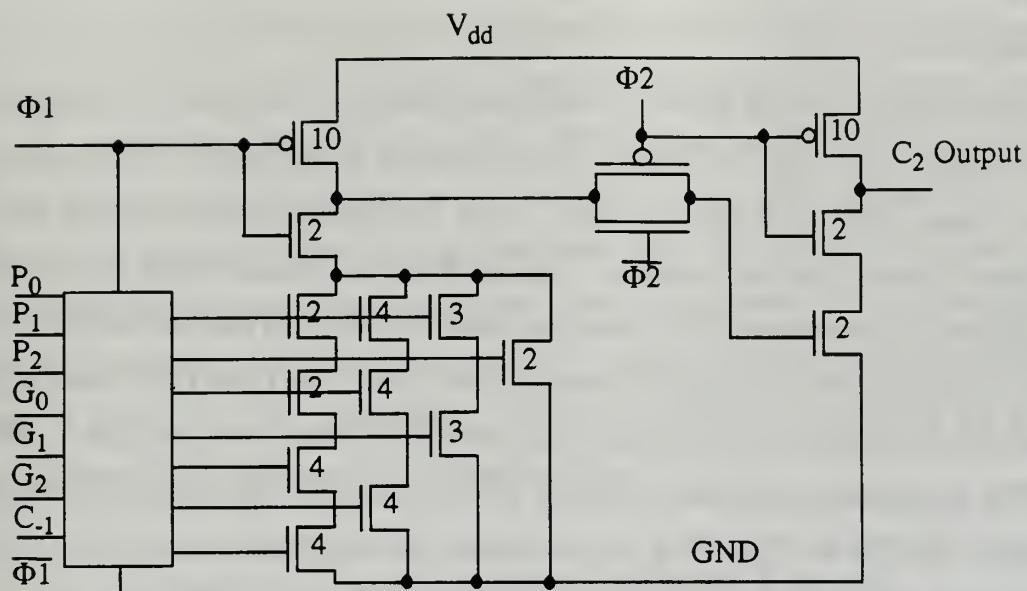
Figure 6.13: CGaAs TPDL Circuit for Generating Function C_2
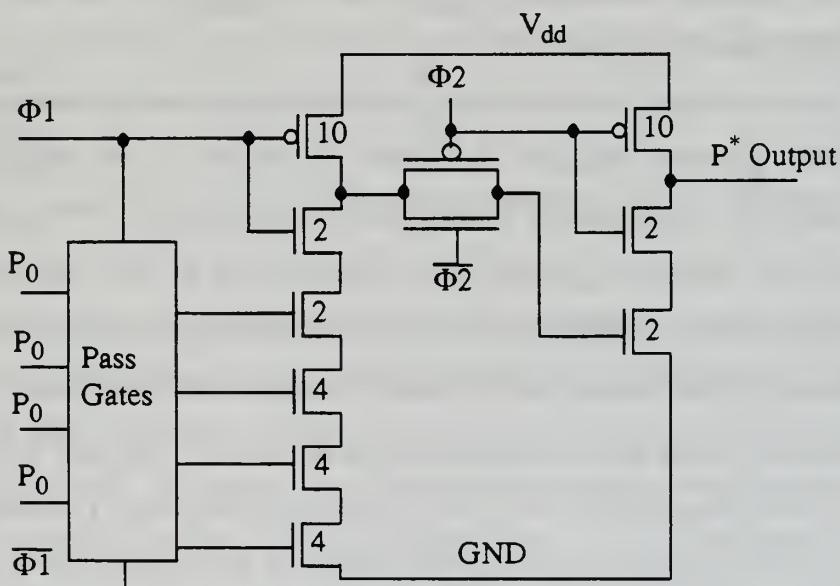
Figure 6.14: CGaAs TPDL Circuit for Generating Function P*

D. COMPARISON BETWEEN CGaAs STATIC, PIPLINED STATIC AND TPDL 4-Bit CLA

In the previous sections, the design and HSPICE simulation of a 4-Bit CLA using static logic, piplined static logic and TPDL were completed. In this section, the comparison between these different designs for speed, power consumption and layout area will be performed. Table 6.1 lists the maximum operating frequency of each design and the power consumption at that frequency [51]. Also, the number of transistors used and the layout area of each circuit are listed in the table. The layout area listed in the table is the transistor gate are and does not include the interconnect area between the transistors. Also, layout area of the TPDL design does not include the area of the clock generator that is required for proper operation. The CGaAs TPDL CLA has the highest operating frequency of all the studied CGaAs CLA logic designs. The maximum frequency is more than double that of the piplined static adder and more than four times that of the static adder. The power consumption at the maximum frequency is less than the power consumed by the piplined adder at half of the maximum frequency.

For the comparison to be fair, the layout area and the power consumption of the non-overlapped clock generator designed in Chapter III, Section C and required for the operation of the TPDL circuits, should be added to the layout area and power consumption of the TPDL adder. The clock generator has a layout area of 81 μm^2 and consumes an average power of 12 mW at 300 MHz and 25 mW at 1.0 GHz (power consumption of the clock generator at different frequencies is plotted in Figure 3.35). The transistor count for the TPDL adder will be 484 transistors and its layout area will be 1190 μm^2. It is important to compare the power consumption of all circuits at the same frequency. The average power consumption of static, piplined static and TPDL adders at 0.26 GHz are 26 mW, 42.74 mW and 23.82 mW, respectively. At 550 MHz, the piplined static adder consumes 77.4 mW while the TPDL adder consumes 43.66 mW. The static adder will not work at all at this frequency.

Figure 6.15 shows the power consumption of the three adder designs and the frequency range of their operation. From this figure, it can be seen that power consumption increases

as the frequency increases for the static adder and the TPDL adder. However, the rate at which power increases for the static circuit is greater than for the TPDL circuit. The power consumption increase for the static adder is linear with the increase in frequency. The rate of power consumption increase for the TPDL adder decreases as the frequency increases and approximates a logarithmic function. At any frequency, the power consumption of the TPDL adder is about half of that for the piplined static adder. It is also noted from the figure that the maximum frequency of the static adder is very low compared to that for the piplined or the TPDL designs. The delay-power product of both the static and the TPDL adders is plotted in figure 6.16. The power-delay product decreases with decreasing the power supply because of the decrease in the leakage current.

TABLE 6.1: Comparison of CGaAs 4-Bit CLA Designs

Used Logic Family	Maximum Frequency [GHz]	Power Consumption [mW]	Layout Area [μm^2]	Transistor Count
Static	0.26	26	989	236
Piplined Static	0.55	77.4	1853	516
TPDL	1.22	61.79	1109.5	450

Loading effects on the performance of the designed CLA circuits have also been studied. The three designs (static, piplined static and TPDL) of the CLA have been simulated in HSPICE with a 1.75 volt power supply. The input signals switch between 0.0 volts and 1.75 volts. The output load was varied to measure the maximum operating frequency of the circuit when driving different loads. For the static and piplined static adder, the loads were static inverters. For the TPDL adder, the loads were TPDL inverters. The number of loads changed from one to ten and the maximum operating frequency of each adder was recorded for each load. Figure 6.17 shows HSPICE simulation results of the maximum frequency of operation for the three adders driving different loads.

143

For the static adder, the limiting parameter for the maximum frequency of operation is the propagation delay through the entire adder. Increasing the load will increase the output capacitance of the adder which increases the charging and discharging times of the output nodes. Therefore, the maximum frequency of the circuit decreases linearly with increasing output load from one to ten.

For the piplined static adder, the limiting parameter for the maximum frequency of operation is the longest stage propagation delay. Fortunately, the longest delay of the three stages is for the middle stage. Increasing the load will only limit the maximum frequency of the last stage. Therefore, increasing the load from one to six will not affect the maximum frequency of the adder. As the load increases to seven, the propagation delay through the last stage becomes longer than for the middle stage and the last stage delay becomes the critical delay, which limits the maximum frequency of operation. Beyond a fan-out of seven, the maximum frequency decreases linearly with increasing load.

For the TPDL adder, the load capacitance is separated from the output by a transmission gate. Thus, increasing the load capacitance will not increase the output capacitance of the TPDL circuit. The limiting factor for the maximum operating frequency is the charge redistribution problem. This problem is common for all the dynamic circuit designs. This adds another advantage for the TPDL designs.

The power supply and input signal levels have also been varied to study their effect on the maximum operating frequency and the power consumption of the different logic designs of the 4-Bit CLA. The highest power supply voltage used in the HSPICE simulations is limited by the source-drain leakage current, while the highest input voltage level is limited by the gate leakage current of the transistors. The power supply and the peak-to-peak input voltage are varied from 1.75 volts to 1.00 volt in 0.25 volt steps. The maximum frequency of operation for each circuit, and its power consumption at that frequency for each power supply voltage, are listed in Table 6.2. The TPDL adder can function properly up to 292 MHz at a power supply of 1.00 volt. The power consumption is 2.1 mW, which is less than one-tenth of the power consumed by the static adder for proper functioning at the same frequency.

This concludes the circuit level design for both the static and dynamic circuits used in this research. The following chapter implements the designed circuits in this chapter and the previous chapters. Seven different integrated circuits have been implemented. The performance of all the implemented ICs is also included in Chapter VII.
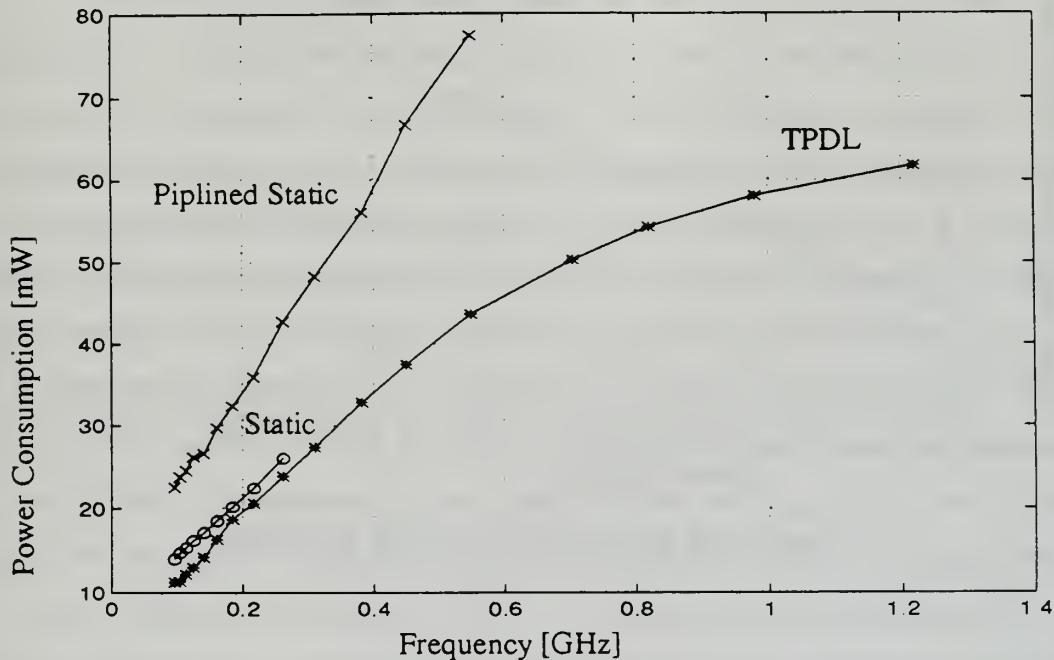
Figure 6.15: Power Consumption of 4-Bit CLAs

TABLE 6.2: Performances of CGaAs 4-Bit CLA Designs

Power Supply [V]	Static Design		Piplined Static		TPDL Design	
	F_{max} [GHz]	P_{av} [mW]	F_{max} [GHz]	P_{av} [mW]	F_{max} [GHz]	P_{av} [mW]
1.75	0.262	26.00	0.55	77.40	1.22	61.79
1.5	0.217	12.00	0.413	34.1	1.09	30.07
1.25	0.151	4.82	0.262	12.0	0.758	12.39
1.0	0.091	1.56	0.135	3.25	0.292	2.10
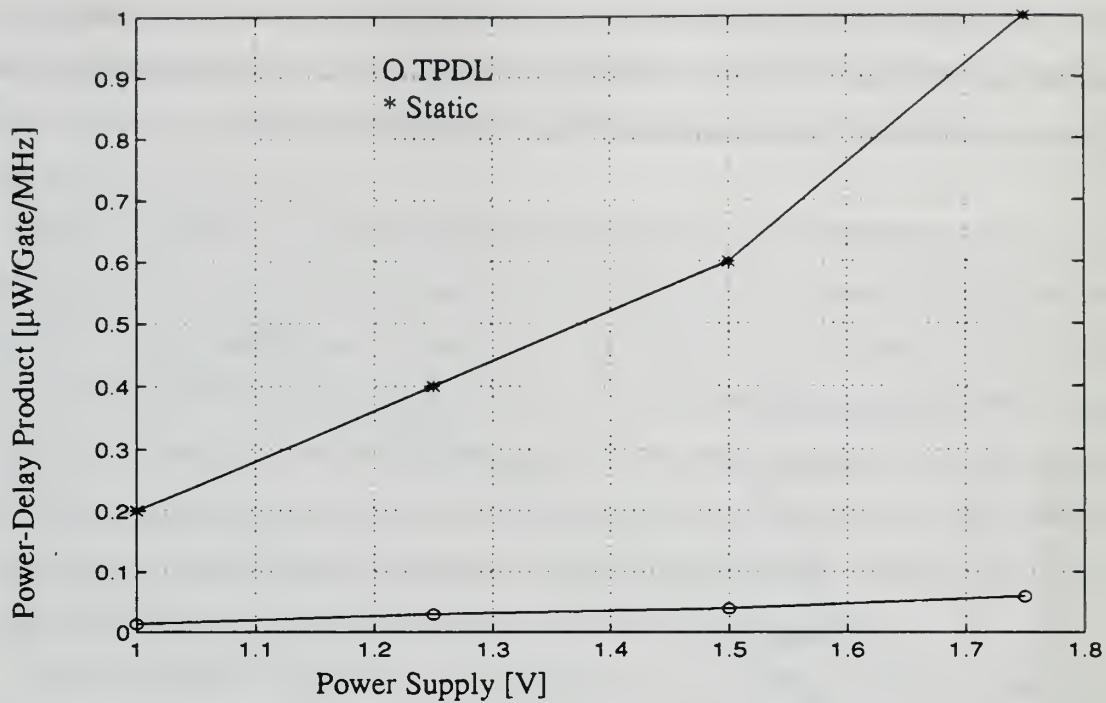
Figure 6.16: Power-Delay Product of 4-Bit CLAs
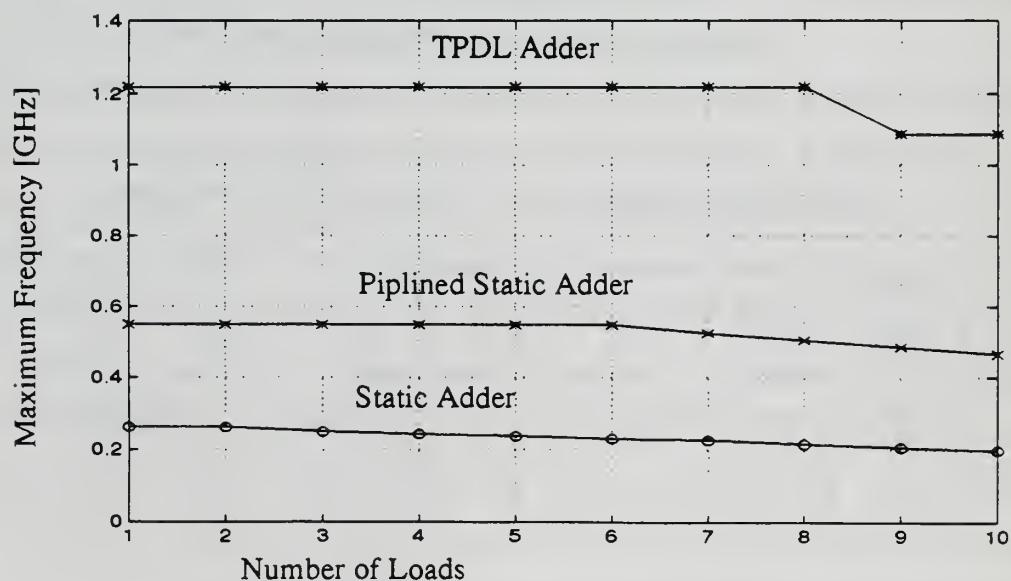
Figure 6.17: Loading Effects on CGaAs 4-Bit CLAs

146

VII. COMPLEMENTARY GaAs CIRCUIT IMPLEMENTATIONS AND TEST RESULTS

This chapter discusses the implementation (layout) of the circuits that have been designed, analyzed and optimized in the previous chapters. All circuits have been laid out using CADENCE tools and a proprietary CGaAs technology file supplied by Motorola Semiconductor. All layouts have passed the design rule check. The technology file used for the design rule checking is also proprietary. Seven integrated circuits have been implemented, translated into the GDSII format and forwarded to Motorola for fabrication.

All the implemented circuits use output drivers that are designed to drive a 50 Ω load and up to 15 pf of parasitic capacitance. The circuits implemented will be discussed in the following sections. Six of the designed circuits are compatible with the Micromanipulator corp. Analytical Probe Station model 6100, which is available at the NPS for die probing. Due to the limited number of high frequency test probes that can be used simultaneously and the difficulty of generating off-chip, multi-bit, test vectors at high speed, it was required that the number of high frequency I/O pins be minimal. For this reason, a three-bit, Linear Feedback Shift Register (LFSR) was designed and implemented on-chip to generate the input vectors required for testing the functionality of the designed circuits. The LFSR has only one input, which is the clock signal, and generates three outputs that are used as inputs for the designed circuits. The seventh circuit is the TPDL Carry Lookahead Adder (CLA) and it will be packaged for testing after fabrication.

All implemented circuits have been simulated in HSPICE to test their functionality. The transistor model parameters used in the simulations were supplied by Motorola and are representative of the devices manufactured by the Motorola complementary GaAs fabrication processes. The parameters were extracted from actual wafer probing data. Also, the simulation tool (HSPICE) has superior convergence and modeling accuracy. Therefore, the simulation results should not deviate significantly from the actual measured results obtained after fabricating the chips. Full functionality is expected. Speed should not vary more than + or - 35%.

HSPICE simulation files for all the implemented circuits are presented in Appendix A. The layouts of the implemented circuits are attached at the end of this chapter. The layout of the implemented chips, including the input and output pads, are presented in Appendix B.

A. CGaAs INPUT RECEIVER AND OUTPUT DRIVER CIRCUITS

The input receiver circuit is designed to minimize the loading effect on the circuit that drives the receiver. The output driver circuit is designed to drive a load of 50 Ω with up to 15 pf of parasitic capacitance. The input receiver and output driver test circuit has been designed and implemented without any additional circuits in between the receiver and driver to test their functionality, drive capability and maximum operating frequency. The receivers and drivers are used with the other implemented circuits. The maximum operating frequency of the I/O test circuit is 0.9 GHz and is limited by the driver. The receiver will operate at 1.0 GHz. This will limit the maximum frequency of any circuit that employs the drivers to 0.9 GHz. The gate lengths of all transistors in the driver are 0.7 μm. The input receiver consists of four cascaded inverters with N- and P-channel transistor gate widths as follows; 6 μm and 5.6 μm for the first inverter, 12 μm and 12 μm for the second, and 36 μm and 36 μm for both the third and the fourth inverters, respectively. The output driver also consists of four inverters with N- and P-channel transistor gate widths as follows; 6 μm and 6 μm for the first inverter, 12 μm and 12 μm for the second, 24 μm and 24 μm for the third, and 90 μm and 60 μm for the fourth inverter, respectively. The circuit consumes an average power of 108 mW at 0.9 GHz from a 2.0 V power supply. The maximum operating frequency decreases to 0.76 GHz when decreasing the supply voltage to 1.75 V and the average consumed power drops to 69 mW at this frequency. The input and output waveforms of the circuit, with a supply voltage of 2.0 V, are shown in Figure 7.5. Layout of the circuit, including all pads, is shown in Appendix B.

B. CGaAs STATIC 3-BIT LFSR CIRCUIT

In this section, the implementation of a three-bit LFSR is detailed. The LFSR circuit was required to minimize the number of input and output terminals of the implemented circuits described in the next sections. The design and optimization of the static 3-Bit LFSR is explained in Chapter IV. The circuit has one input (clock) and generates three outputs. The three outputs represent seven states (all the states except state 000) and is shown in Chapter IV, Table 4.1. These outputs are used as inputs for the static function generator (three-input circuit explained in the next section). The LFSR circuit consists of three D Flip-Flops and one XOR gate and is shown in Chapter IV, Figure 4.7. The circuit was laid out with an input receiver connected to the input and an output driver connected to each output of the circuit (three outputs). The maximum operating frequency of the implemented circuit is 0.55 GHz. The total power consumption (including the power consumption of the driver circuits) at the maximum operating frequency is 214 mW. The power consumption of the LFSR circuit by itself is explained in Chapter IV. Input and output waveforms of the implemented circuit are shown in Figure 7.6. The HSPICE simulation file for the circuit is included in Appendix A.2. The layout of the circuit is shown in Figure 7.14, while the layout of the entire circuit, including input and output pads, is presented in Appendix B.

C. CGaAs STATIC TWO-LEVEL FUNCTION GENERATION

In this section, a static logic circuit to generate the logic function $F_1 = (\overline{(\overline{A+B})+C})$, and explained in Chapter V, is implemented. The logic diagram of the implemented circuit is shown in Figure 7.1. The maximum operating frequency of the implemented circuit is limited by the maximum frequency of the LFSR (previous section) to 0.55 GHz. The circuit consumes an average power of 85.5 mW from a 2.0 V power supply at the maximum frequency. The input and output waveforms of the circuit, operating at maximum frequency, is shown in Figure 7.7. The HSPICE simulation file of the circuit is included in Appendix A.3. The layout of the function F_1 is shown in Figure

149

7.15, while the layout of the entire circuit, including the input and output pads, is shown in Appendix B.
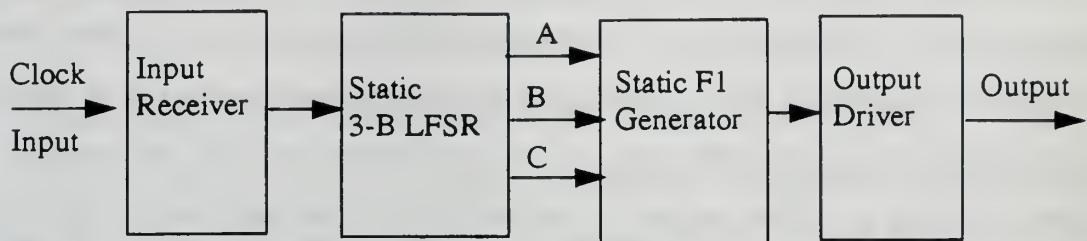
Figure 7.1: Logic Diagram of Static Logic Function F_1 Generator

D. CGaAs NON-OVERLAPING TWO-PHASE CLOCK GENERATOR

In this section, the implementation of the clock generator designed in Section C of Chapter III is described. The circuit has a clock input and generates the non-overlapped clock phases Φ_1 and Φ_2 (non overlapped in the logic low level) and their complements. These clock phases are required for the proper operation of the Two-Phase Dynamic FET Logic (TPDL) circuits. The maximum operating frequency of the implemented circuit is 0.9 GHz (limited by the maximum operating frequency of the driver circuits). The total power consumption of the circuit at the maximum operating frequency, when powered from a 2.0 V power supply, is 339 mW (including the power consumption of the driver circuits). The HSPICE simulation file of the implemented circuit is included in Appendix A.4. Input and output waveforms of the circuit operating at the maximum frequency is shown in Figure 7.8. The layout of the clock generator is shown in Figure 7.16, while the layout of the entire circuit, including all input and output pads, is presented in Appendix B.

E. CGaAs TPDL 3-BIT LFSR CIRCUIT

In this section, the implementation of the TPDL 3-Bit LFSR, designed in Section E of Chapter IV, is described. The LFSR design was required to minimize the number of input and output pins of the designed TPDL circuits. The logic diagram of the implemented circuit is shown in Figure 7.2. The circuit has one input (clock input) and three outputs. The

generated output sequence is shown in Table 4.1. The outputs are used as a test pattern to the inputs for the TPDL 3-input circuit explained in the next section. The LFSR circuit consists of two TPDL D Flip-Flops and one dynamic XOR (DXOR) gate. The DXOR gate, used as a separate stage, reduces the required number of D Flip-Flops by one. The maximum operating frequency of the implemented circuit is limited by the maximum frequency of the drivers to 0.9 GHz. The circuit consumes an average power of 320 mW from a 2.0 V power supply at the maximum operating frequency (including the power consumption of the on-chip drivers and clock generator). The power consumption of the LFSR circuit by itself is explained in Chapter IV. The HSPICE simulation file of the implemented circuit is presented in Appendix A.5. The input and output waveforms of the circuit are shown in Figure 7.9. The layout of the LFSR circuit is shown in Figure 7.17, while the layout of the entire circuit, including all the pads, is presented in Appendix B.
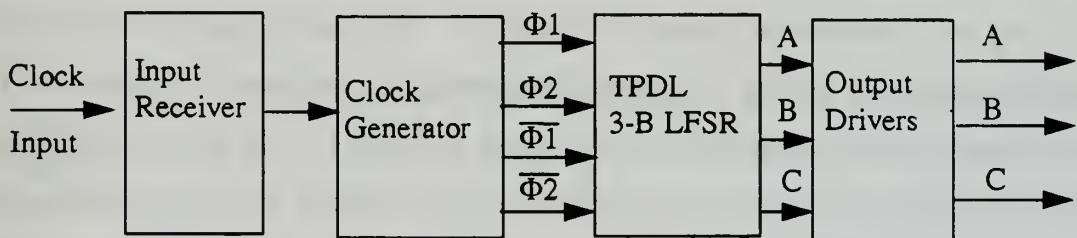
Figure 7.2: Logic Diagram of TPDL 3-Bit LFSR

F. CGaAs TPDL TWO-LEVEL FUNCTION GENERATION

In this section, the implementation of the TPDL circuit that generates the logic function $F_1 = (\overline{(A+B)+C})$, designed in Chapter IV, is discussed. The three inputs of the circuit are generated by a 3-bit LFSR. The maximum operating frequency of the implemented circuit is limited by the maximum frequency of the drivers to 0.9 GHz. The power consumption of the circuit at the maximum frequency, when powered from a 2.0 V power supply, is 172 mW (including the on-chip drivers, clock generator and the LFSR power consumption). The logic diagram of the implemented circuit is shown in Figure 7.3,

151

while the HSPICE simulation file of the circuit is presented in Appendix A.6. The input and output waveforms of the circuit are shown in Figure 7.10. The layout of the logic function F1 generator circuit is shown in Figure 7.18, while layout of the entire circuit, including all pads, is presented in Appendix B.
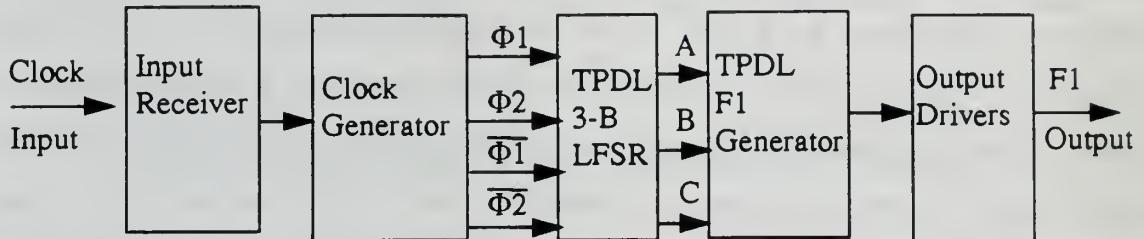
Figure 7.3: Logic Diagram of TPDL Logic Function F_1 Generator

G. CGaAs TPDL 4-BIT CARRY LOOKAHEAD ADDER CIRCUIT

The design and optimization of the TPDL four-Bit Carry Lookahead Adder (TPDL 4-Bit CLA) was presented in Chapter VI, Section C. The implementation of the circuit, including the drivers and the two-phase clock generator, is presented in this section. The logic diagram of the implemented circuit is shown in Figure 7.4. The maximum frequency of the circuit is limited by the drivers (static circuit) to 0.92 GHz. The circuit, including the clock generator and the drivers, consumes an average power of 800 mW from a 1.75 V power supply at the maximum operating frequency. The HSPICE simulation file is presented in Appendix A.7. The input and output waveforms of the circuit operating at the maximum frequency are shown in Figure 7.11. The layout of logic function F_1 is shown in Figure 7.19, while the layout of the entire circuit is presented in Appendix B.
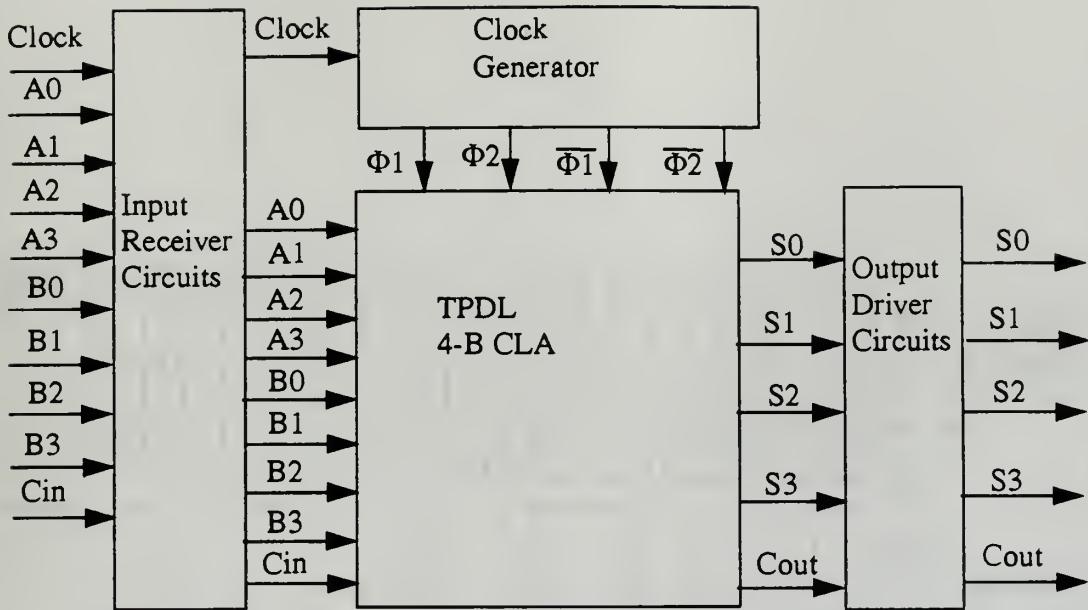
Figure 7.4: Logic Diagram of TPDL 4-Bit CLA
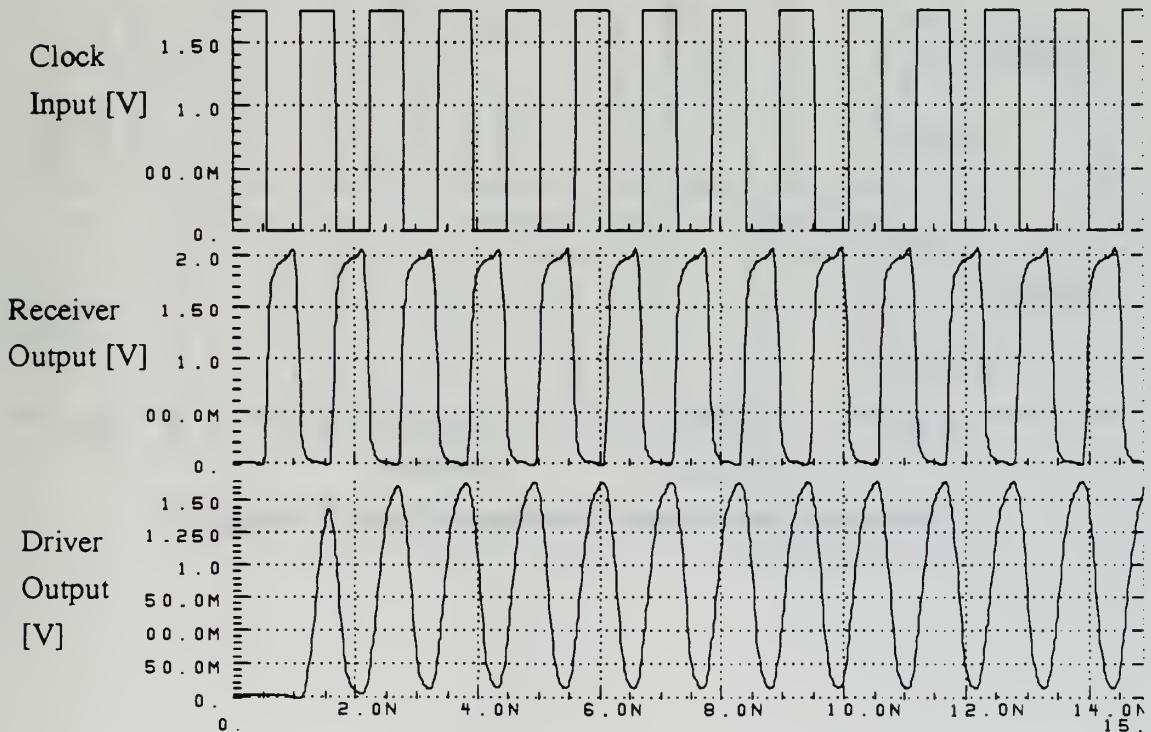
Figure 7.5: Input-Output Waveforms of Input Receiver and Output Driver IC

153
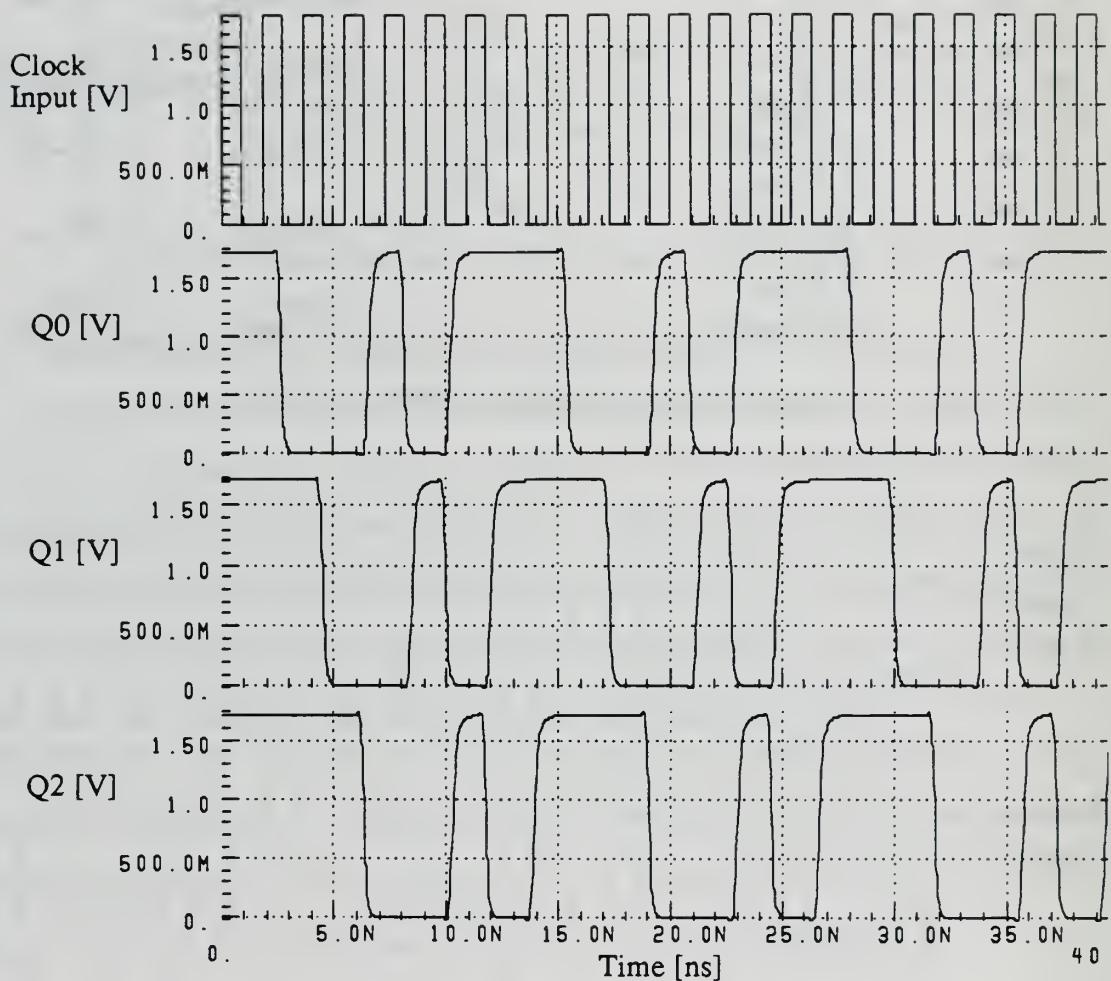
Figure 7.6: Input-Output Waveforms of Static 3-Bit LFSR IC

154
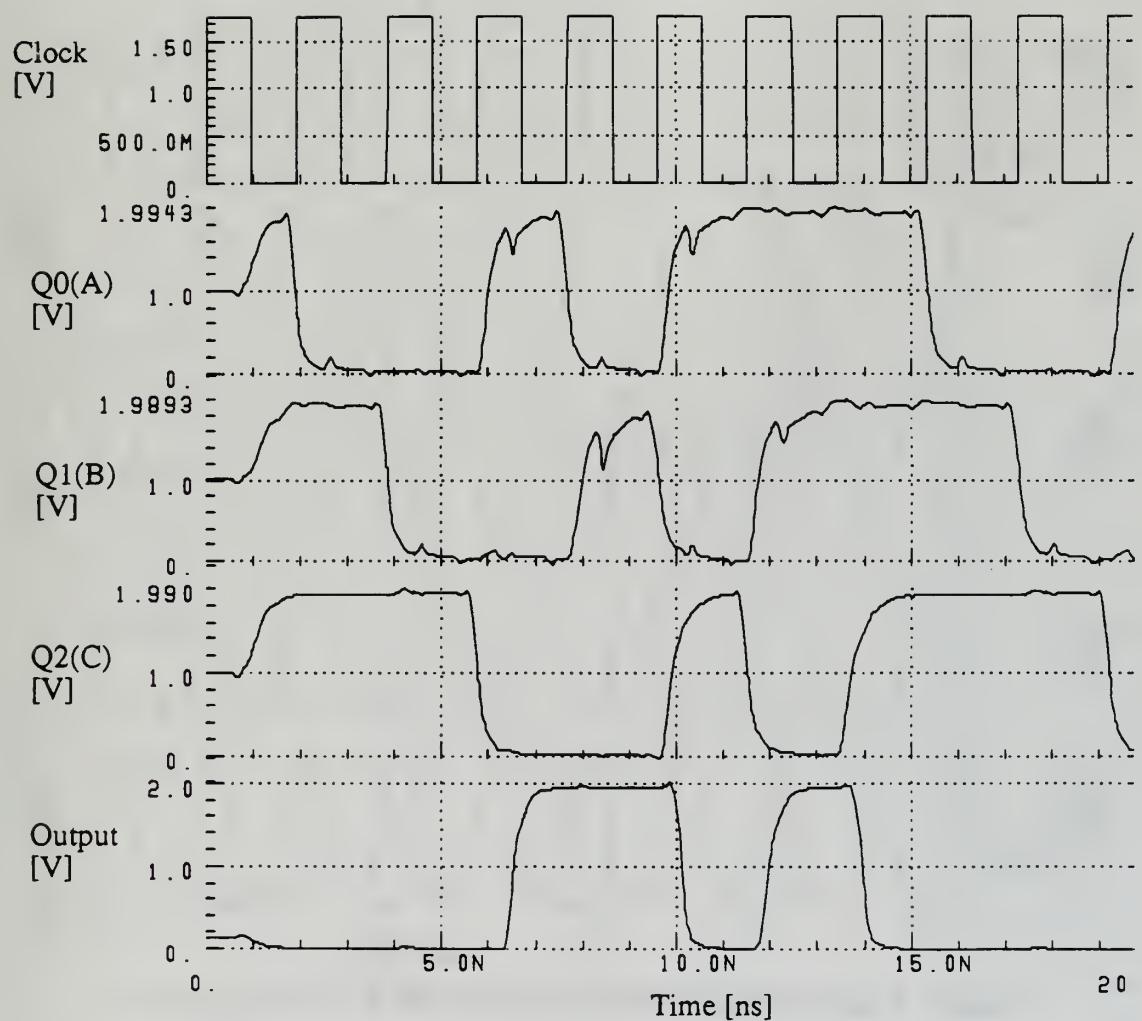
Figure 7.7: Input-Output Waveforms of Static Function F_1 IC

155
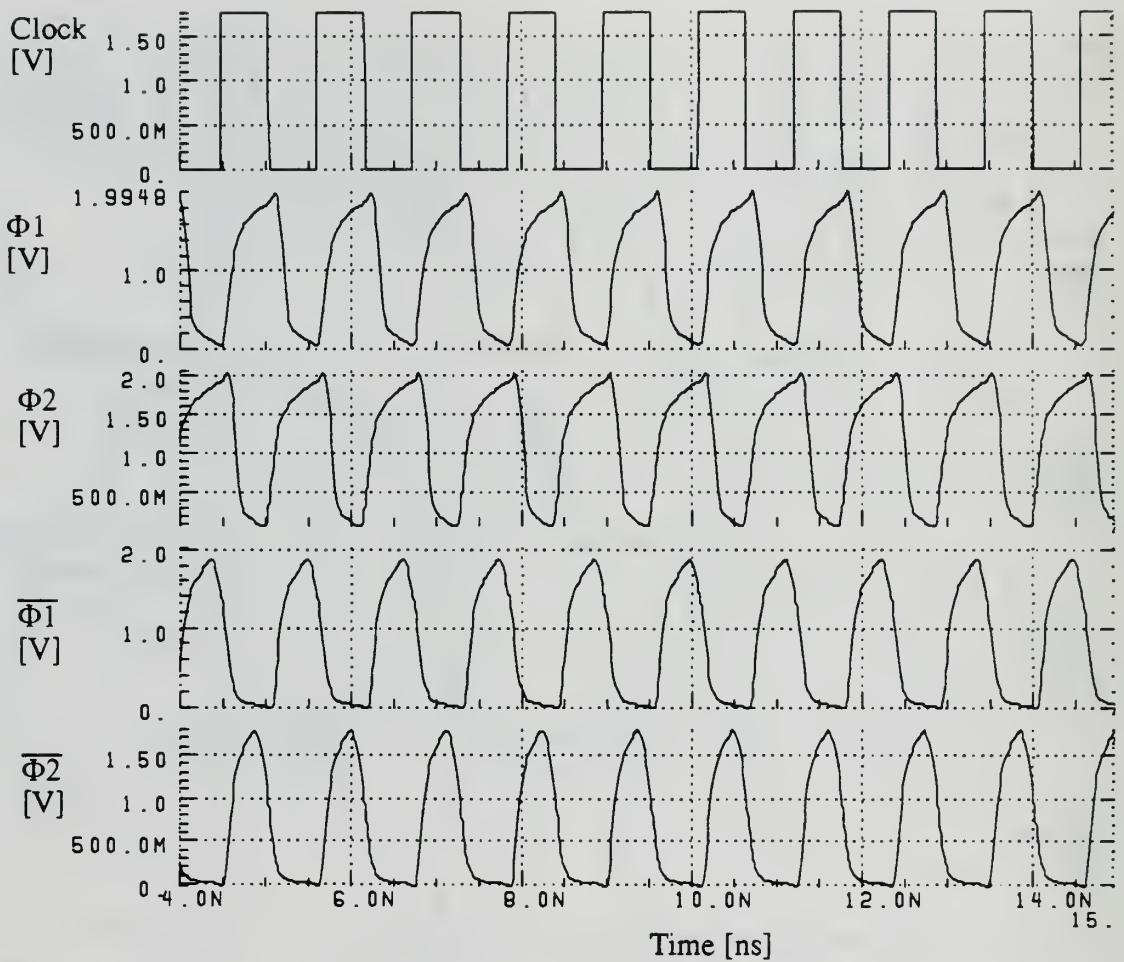
Figure 7.8: Input-Output Waveforms of Two-Phase Clock Generator IC
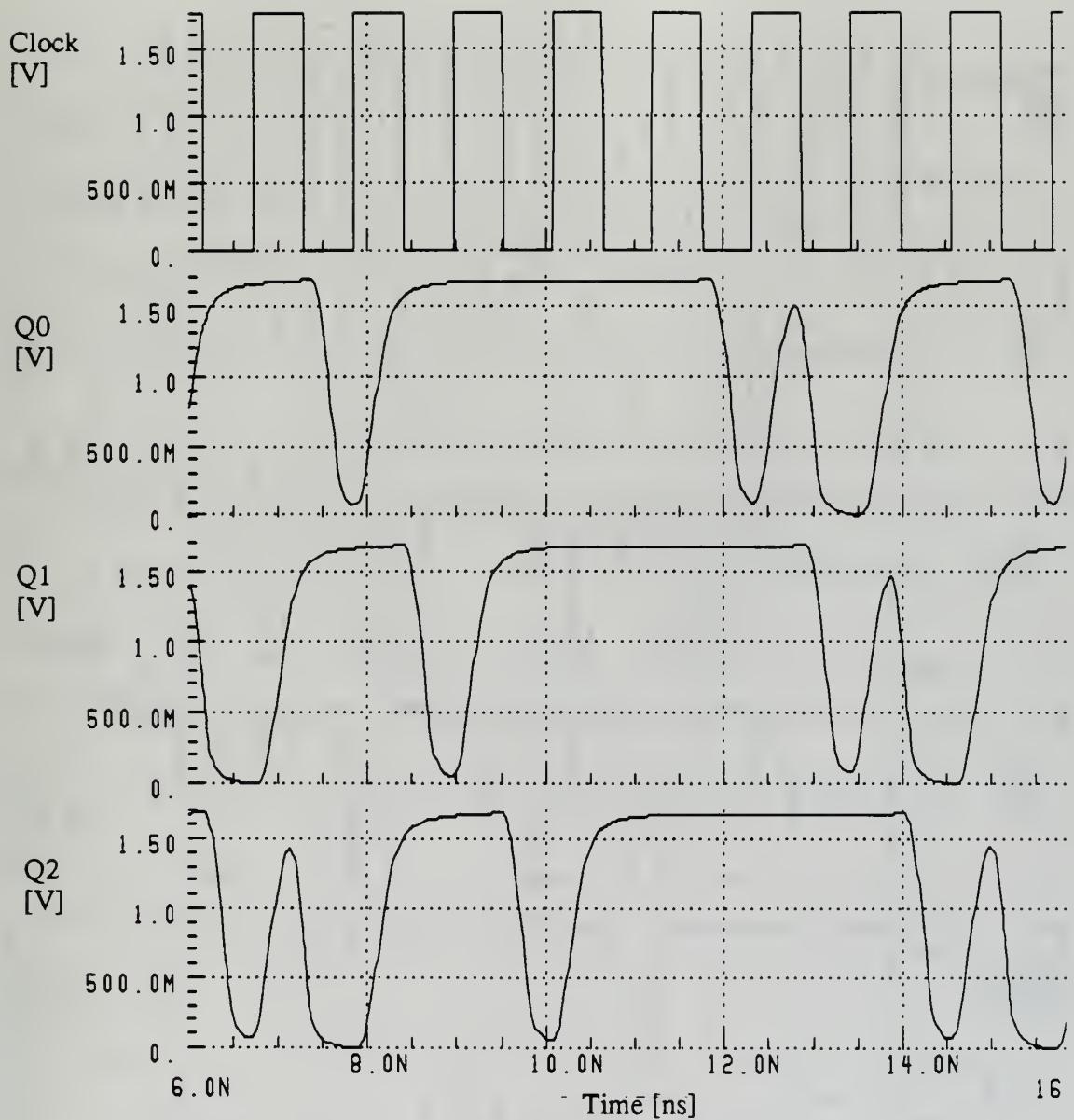
Figure 7.9: Input-Output Waveforms of TPDL 3-Bit LFSR IC

157
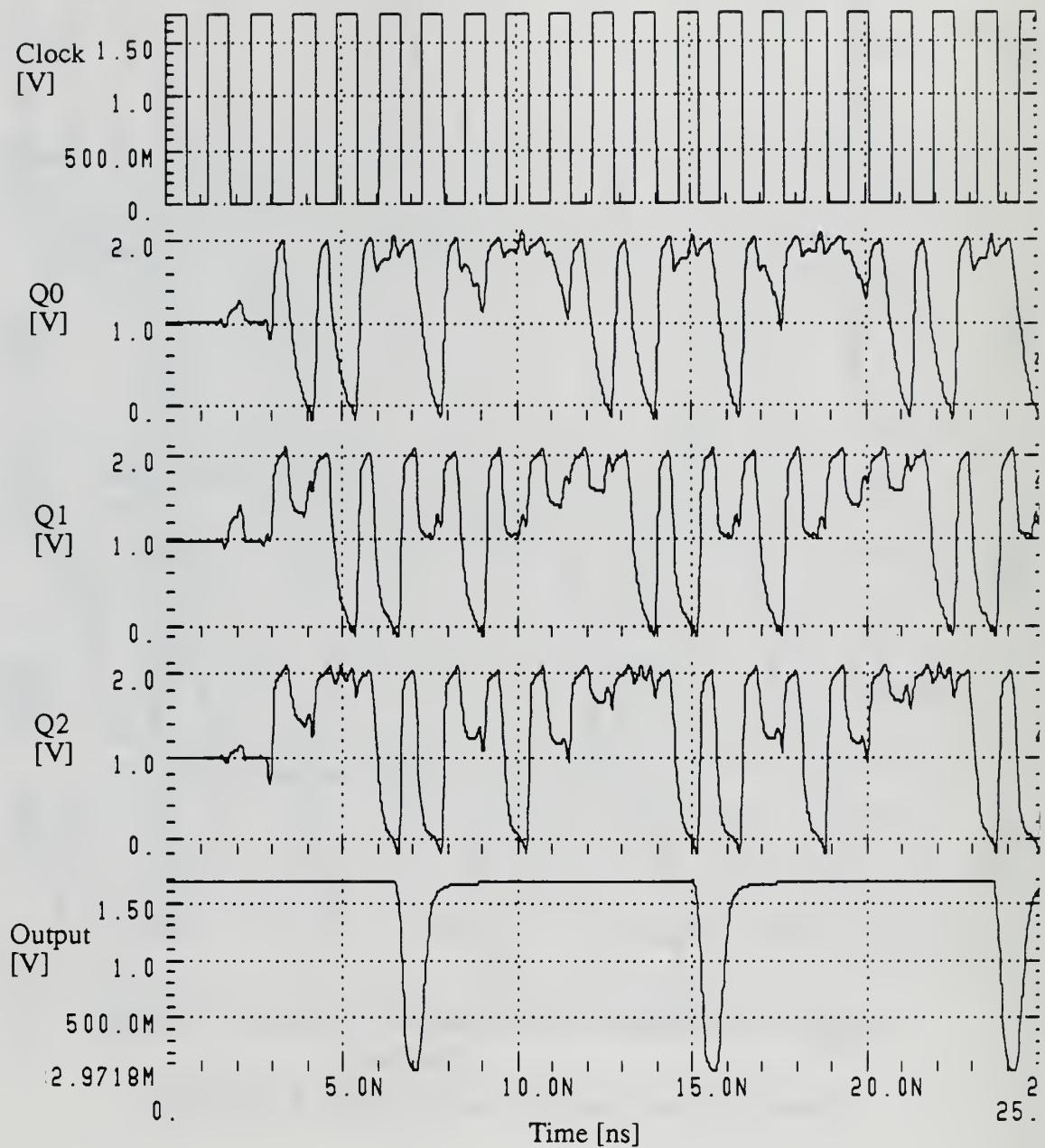
Figure 7.10: Input-Output Waveforms of TPDL Function F_1 IC

158
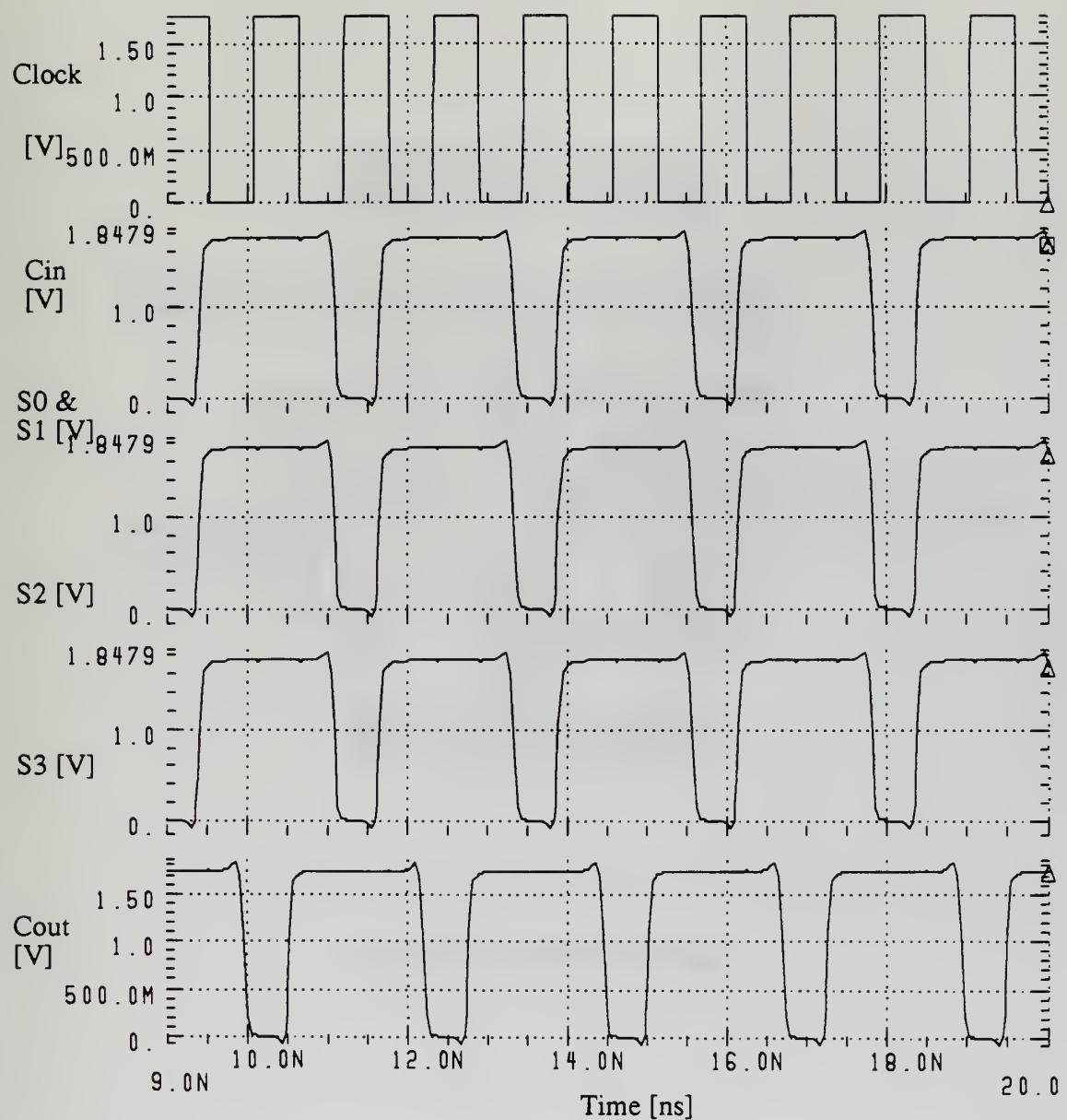
Figure 7.11: Input-Output Waveforms of TPDL 4-Bit CLA

159
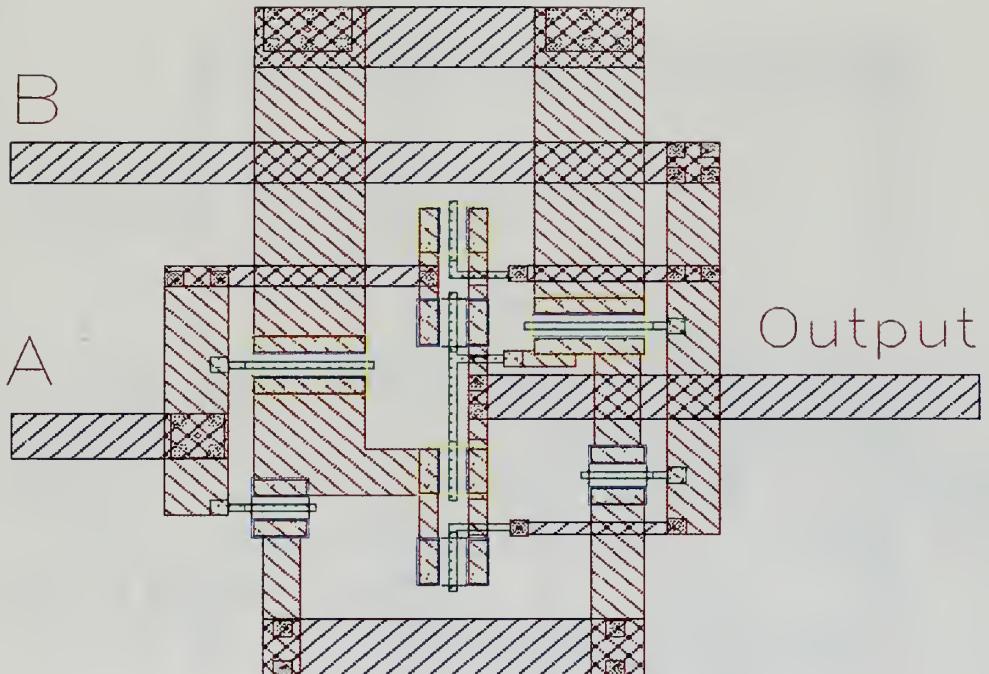
Figure 7.12: Static XOR Gate
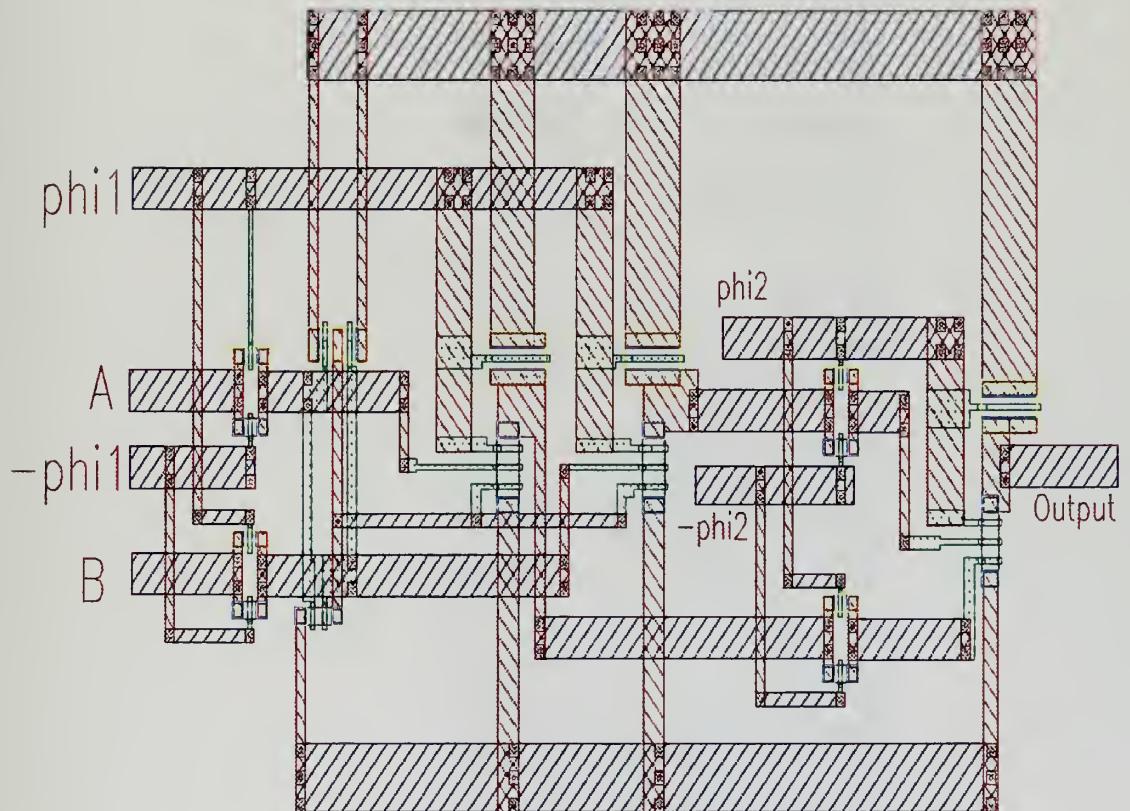
Figure 7.13: TPDL XOR Gate
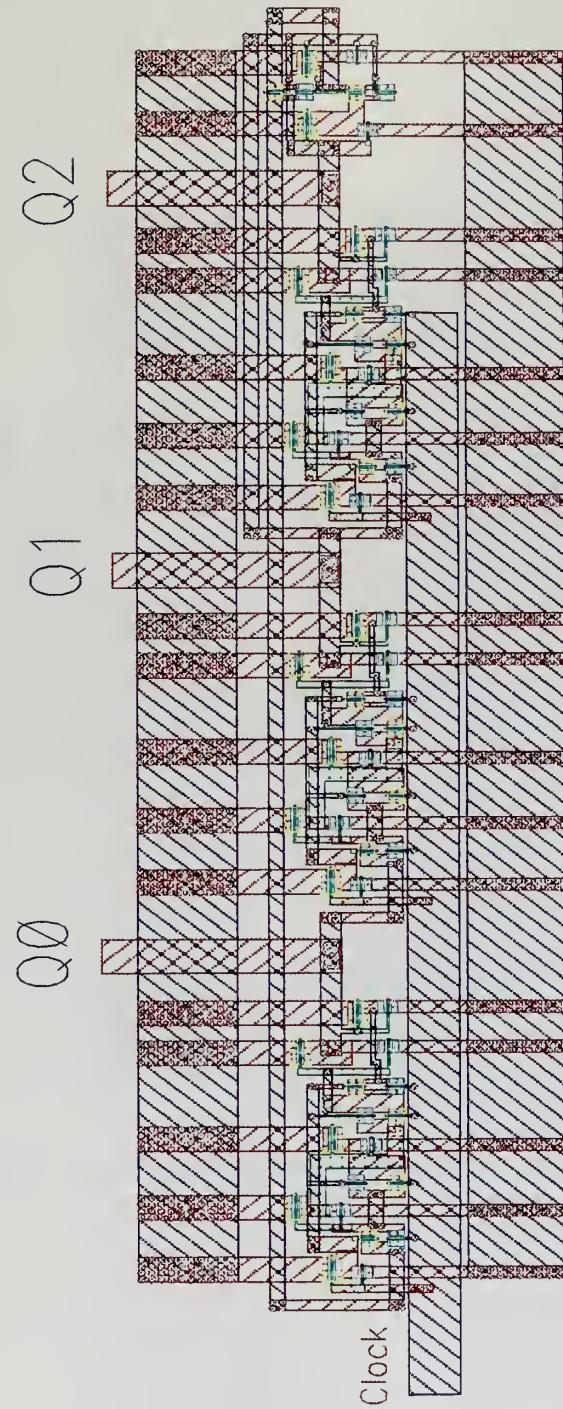
Figure 7.14: Static 3-Bit LFSR
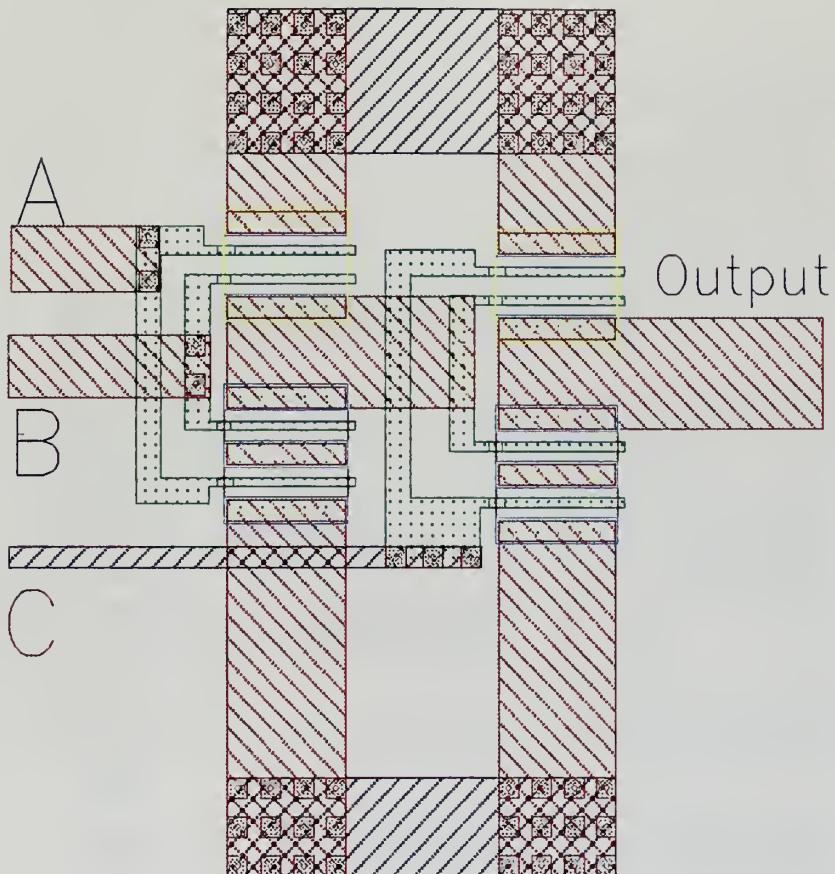
Figure 7.15: Static Function F_1 Generator
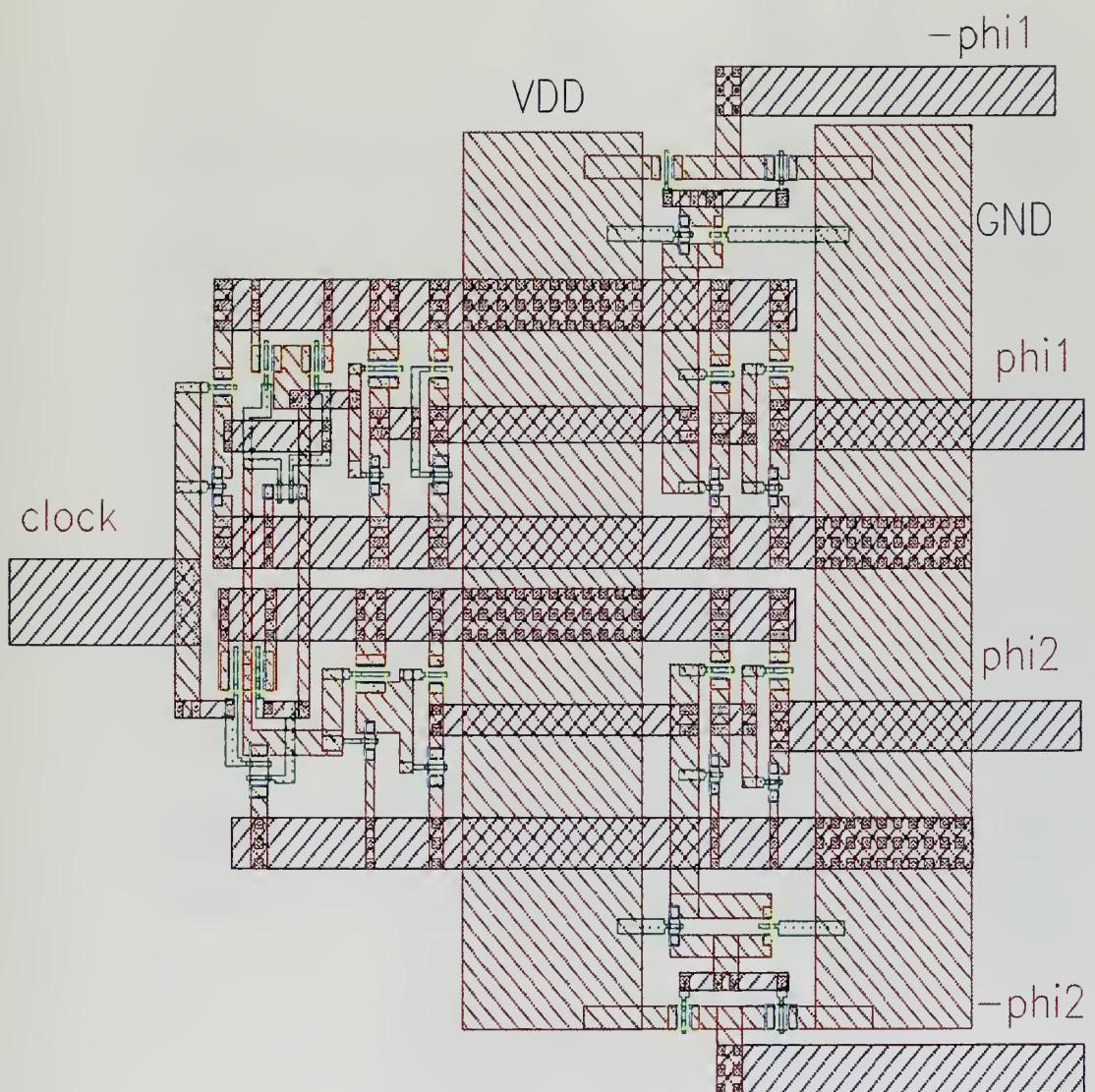
Figure 7.16: Two-Phase Clock Generator
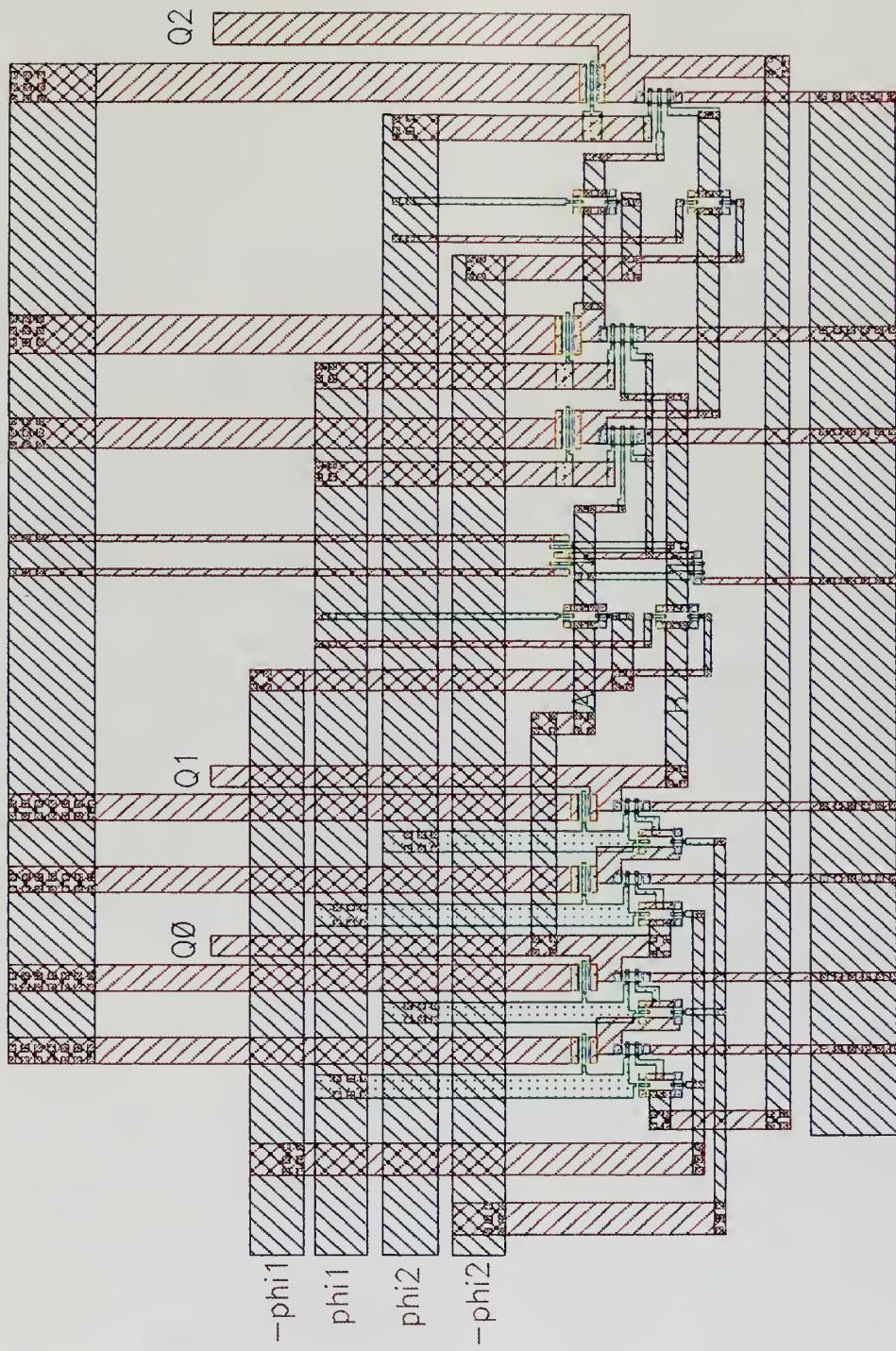
Figure 7.17: TPDL 3-Bit LFSR

165
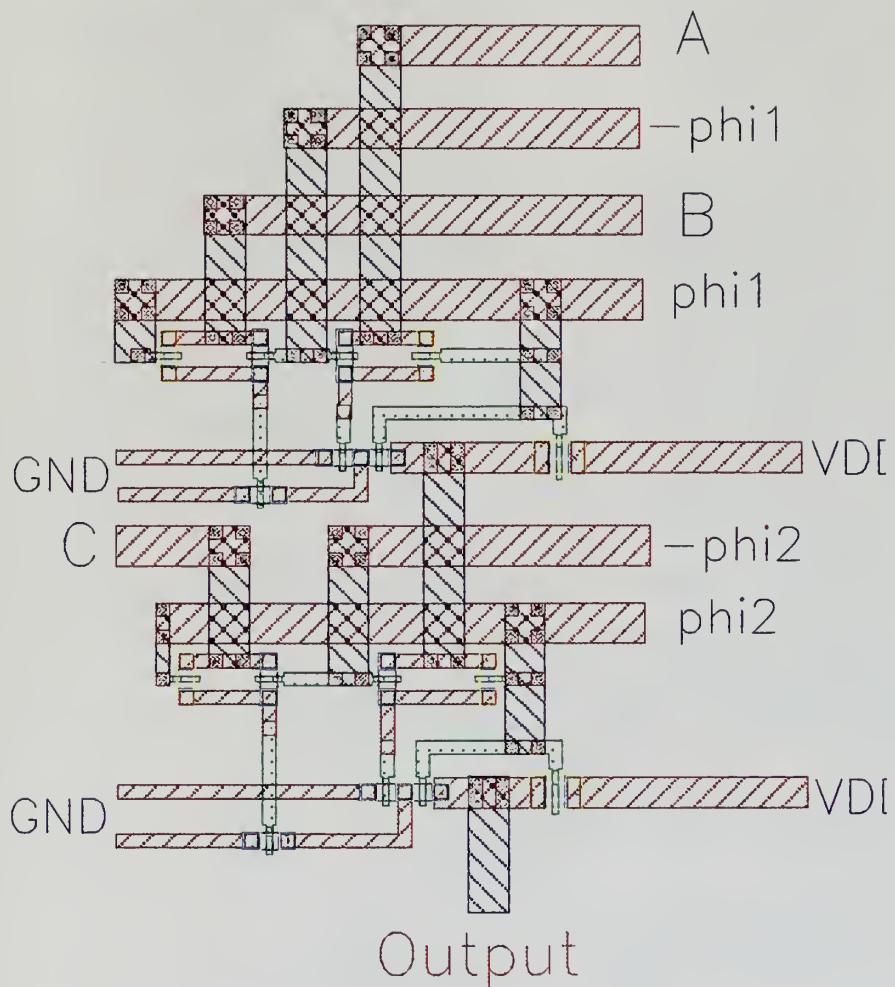
Figure 7.18: TPDL Function F_1 Generator

166
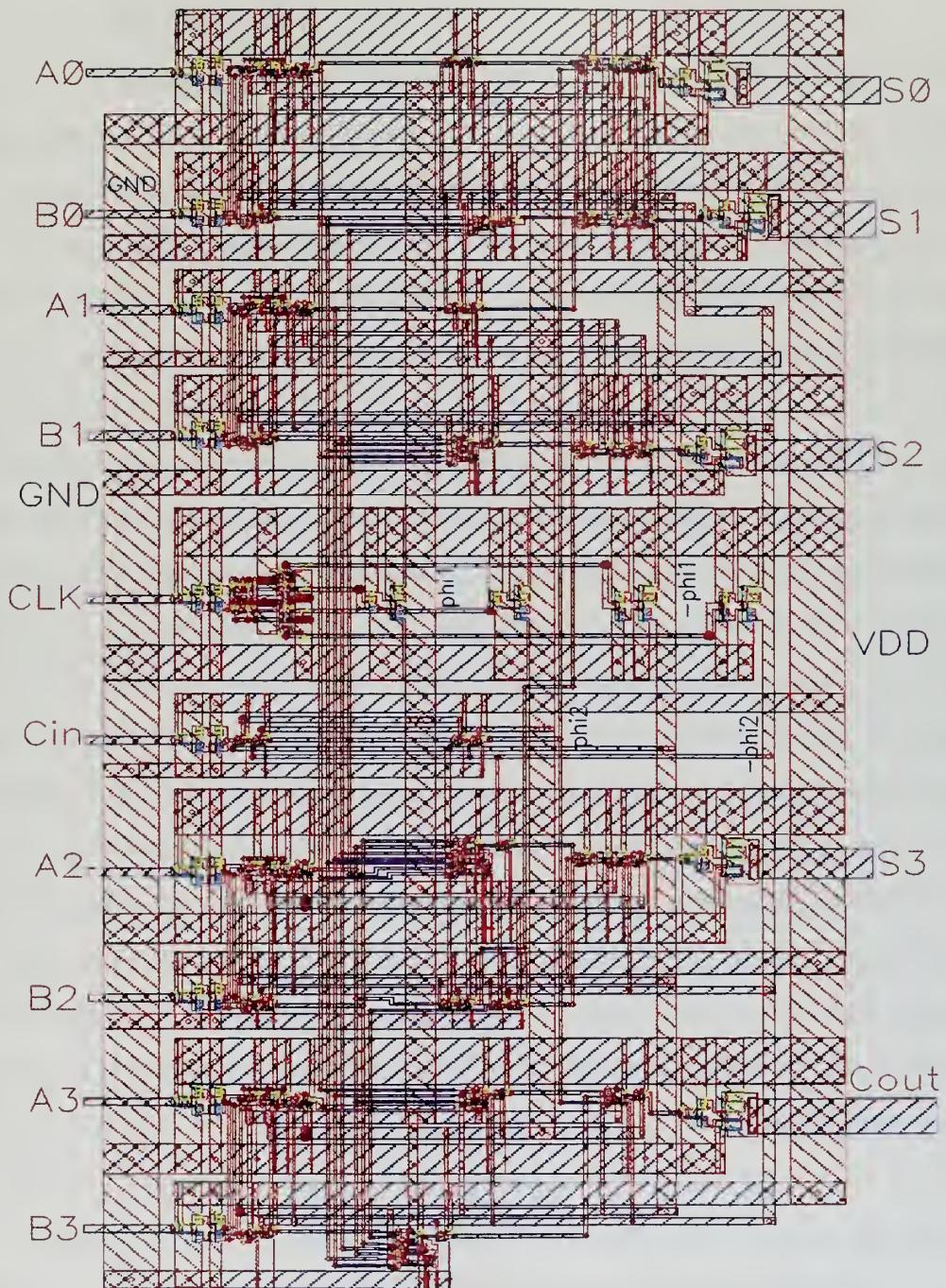
Figure 7.19: TPDL 4-Bit CLA

167

VIII. CONCLUSIONS AND CONTINUATION OF WORK

A. CONCLUSIONS

In this dissertation, the design, analysis and implementation of different experimental Complementary Galium Arsenide (CGaAs) dynamic logic circuits has been documented. The designed circuits are compatible with existing CGaAs fabrication process and design tools. Dynamic logic circuits offer several advantages over typical static logic circuits. They have a higher speed than GaAs MESFET Directly Couple FET Logic (DCFL) and lower power consumption than complementary logic. The non-ratioed nature of dynamic logic reduces the layout area.

In the first part of this dissertation, Two-Phase Dynamic FET Logic (TPDL), a new dynamic logic family for CGaAs was presented and implemented. Also, Domino and N-P Domino dynamic logic were implemented in CGaAs. Four different logic functions were designed and implemented using static and dynamic logic families for comparison purposes. The transistor source-drain leakage current limits the power supply voltage for all circuits to 2.0 V. The transistor gate-leakage current limits the peak-to-peak input signal transitions to 1.75 V. Beyond these voltage levels, the power consumption of the circuits increases dramatically with a small improvement in the maximum operating frequency.

CGaAs static logic designs are similar to the designs of silicon CMOS circuits. It is the simplest logic design because it has established design procedures. The maximum operating frequency of the implemented circuits in static logic is 620 MHz. Domino dynamic logic circuits have the smallest layout area. The use of a static inverter in Domino logic gates increases the power consumption. Also, only non-inverting functions can be implemented using Domino logic. The maximum operating frequency of the designed Domino logic circuits is 1.6 GHz. N-P Domino logic uses the slow P-channel transistor in evaluating the function, which enhances the disadvantage of GaAs and limits the maximum operating frequency of the designed circuits to 820 MHz.

TPDL uses only the fast N-channel transistors in evaluating the logic function. The slow P-channel transistors are used only to precharge the output nodes. Because of the pass gates in front of each evaluating circuit, TPDL designs are self latching and are suitable for pipelined architectures. Therefore, any circuit can be pipelined to reach the maximum frequency of operation without adding any storage elements (pipeline registers). The maximum frequency of the designed TPDL logic circuits is 2.38 GHz.

In the second part of the dissertation, the basic combinational logic gates (Inverter, NAND gate, NOR gate, XOR gate and XNOR gate) are designed and implemented in TPDL and static logic. These gates are used in the design and the fabrication of more complex circuits. TPDL gates have a maximum operating frequency of 2.38 GHz, while the static logic gates operate up to 1.2 GHz. The power consumption of TPDL gates is less than one-fourth that of the static logic gates when powered from the same power supply and having the same fan-out. The layout area of the TPDL logic gates is about one-half that of the static logic gates. Also, the D Flip Flop (D-FF) and Linear Feedback Shift Registers (LFSRs) are designed and implemented in TPDL and static logic. The comparison in performance between these circuits is also documented.

In the last part of this dissertation, a four-Bit Carry Lookahead Adder (4-Bit CLA) was designed and implemented in static logic, pipelined static logic and TPDL. The designed static 4-Bit CLA circuit has a maximum frequency of 260 MHz and consumes an average power of 26 mW from a 1.75 V power supply at this frequency. Its layout area is 989 μm^2. The maximum frequency is limited by the propagation delay through the entire circuit. A three-stage, pipelined, Static, 4-Bit CLA was designed to overcome this problem. The maximum operating frequency is 550 MHz and the power consumption at this frequency is 77 mW. The layout area is 1853 μm^2. The maximum frequency of this circuit is limited by the longest stage propagation delay. The added pipeline registers between stages increased the power consumption and the layout area. The TPDL 4-Bit CLA operates correctly up to 1.2 GHz and consumes an average power of 61 mW from a 1.75 V power

supply at this frequency. The layout area is $1109 \mu m^2$. Comparing these designs, the TPDL circuit consumes about half of the power consumption of the pipelined static circuit at the same frequency. The TPDL adder maximum operating frequency is more than double that of the pipelined static adder.

The comparison in performance among all the studied dynamic and static logic families is completed through the implemented circuits. TPDL circuits have the highest maximum operating frequency and the lowest power consumption ever reported in this technology. Also, the layout area is about half that of the static logic circuit and about the same as that of the Domino and N-P Domino logic circuits. The power consumption of the TPDL circuits is less than one-fourth that of the static logic circuits and less than one-half that of the Domino and N-P Domino logic circuits implementing the same logic function and powered from the same supply voltage. However, TPDL circuits can function properly up to the maximum operating frequency of the other logic designs with lower power supply voltages and less power consumption. The main disadvantage of the TPDL design is that it requires two non overlapped clock phases and their complements for proper operation. Also, routing these four clock phases to all of the circuit increases the design complexity. A 1.0 GHz clock generator is designed and implemented in this dissertation. It generates the two non overlapped clock phases and their complements required for the operation of the TPDL circuits.

Loading effects on the maximum frequency of all the designed circuits is also studied. In TPDL circuits, loads are isolated from the circuit outputs by the pass gates. Thus, increasing the output load will increase the output capacitance of all the designed logic circuits except for TPDL. Therefore, TPDL circuits are the least effected by increasing the output load. Also, the effects of changing the power supply on the maximum frequency and the power consumption of all the designed circuits are studied. The results presented in this dissertation show that the TPDL circuits are the best performing circuits over all the studied logic families when reducing the power supply voltage down to 1.0 V.

This dissertation concludes that the TPDL circuits are the candidate for the next generation of high speed, high density and low power CGaAs ICs. The results of the described research allow CGaAs technology to be used for implementing VLSI ICs for the first time.

B.   CONTINUATION OF WORK

As can be seen from this dissertation, TPDL circuits have the highest operating frequency with the lowest power consumption. Also, they have a reduced layout area compared with the other designs. This introduces the CGaAs technology into the LSI and VLSI era.

Testing the functionality of the designed and fabricated circuits will confirm the simulation results presented in this dissertation. The maximum operating frequency and the power consumption of the fabricated circuits are the principle parameters to be measured. Also, testing should include the effects of changing the power supply voltage on the maximum operating frequency and the power consumption of all fabricated circuits. The performance comparisons between the complementary static and the TPDL circuits also needs to be performed. Comparing the test results against the simulation results presented in this dissertation should also be done. The effects of radiation on both the static and TPDL circuits is also of interest. After finishing the test phase, the design and implementation of more complex TPDL logic functions, such as used on a high-speed, pipelined DSP ASIC (Application Specific IC), like a FIR filter or a digital communication integrated circuit should be attempted.

APPENDIX A: HSPICE SIMULATION FILES

This appendix contains the HSPICE simulation files of all the implemented complementary GaAs integrated circuits.

A.1   CGaAs INPUT/OUTPUT DRIVER IC

* File name   : inout.sp

* Directory name   : shehata/thesis/run1/inout

* Minimum clock time : 1.02ns

* Total average power : 115mW

* Last correction date : Dec./12/95

* File name   : inout.sp

* File directory : shehata/thesis/run1/inout

*Min clock time=1.02ns , total average power= 115mW

.include /home5/shehata/thesis/run1/parameters

*power supply

vdd vdd 0 2.0

* input signal

vin clock 0 pulse(0 1.75 0ns 0.01ns 0.01ns 0.5ns 1.02ns)

****

**   INPUT RECEIVER CIRCUIT   **

****

.SUBCKT INVI1 in out vdd 0

J0 out in vdd vdd tp0.7x10 L=0.7U W=6.0U

J1 out in 0 0 tn0.7x10 L=0.7U W=5.6U

.ENDS INVI1

.SUBCKT INVI2 in out vdd 0

J0 out in vdd vdd tp0.7x10 L=0.7U W=6.0U

J1 out in 0 0 tn0.7x10 L=0.7U W=6.0U

J2 out in vdd vdd tp0.7x10 L=0.7U W=6.0U

J3 out in 0 0 tn0.7x10 L=0.7U W=6.0U

.ENDS INVI2

174

```
.SUBCKT INVI3 in out vdd 0
J0 out in vdd vdd tp0.7x10 L=0.7U W=6.0U
J1 out in 0 0 tn0.7x10 L=0.7U W=6.0U
J2 out in vdd vdd tp0.7x10 L=0.7U W=6.0U
J3 out in 0 0 tn0.7x10 L=0.7U W=6.0U
J4 out in vdd vdd tp0.7x10 L=0.7U W=6.0U
J5 out in 0 0 tn0.7x10 L=0.7U W=6.0U
J6 out in vdd vdd tp0.7x10 L=0.7U W=6.0U
J7 out in 0 0 tn0.7x10 L=0.7U W=6.0U
J8 out in vdd vdd tp0.7x10 L=0.7U W=6.0U
J9 out in 0 0 tn0.7x10 L=0.7U W=6.0U
J10 out in vdd vdd tp0.7x10 L=0.7U W=6.0U
J11 out in 0 0 tn0.7x10 L=0.7U W=6.0U
.ENDS INVI3


.SUBCKT INPUTDRIVER in out vdd 0
X1 in 4 vdd 0 INVI1
X2 4 5 vdd 0 INVI2
X3 5 6 vdd 0 INVI3
X4 6 out vdd 0 INVI3
.ENDS INPUTDRIVER
**********************************************************
**              OUTPUT DRIVER CIRCUIT              **
**********************************************************
.SUBCKT INVO1 in out vdd 0
J0 out in vdd vdd tp0.7x10 L=0.7U W=6.0U
J1 out in 0 0 tn0.7x10 L=0.7U W=6.0U
```

.ENDS INVO1

.SUBCKT INVO2 in out vdd 0
J0 out in vdd vdd tp0.7x10 L=0.7U W=6U
J1 out in 0 0 tn0.7x10 L=0.7U W=6U
J2 out in vdd vdd tp0.7x10 L=0.7U W=6U
J3 out in 0 0 tn0.7x10 L=0.7U W=6U
.ENDS INVO2

.SUBCKT INVO3 in out vdd 0
J0 out in vdd vdd tp0.7x10 L=0.7U W=6U
J1 out in 0 0 tn0.7x10 L=0.7U W=6U
J2 out in vdd vdd tp0.7x10 L=0.7U W=6U
J3 out in 0 0 tn0.7x10 L=0.7U W=6U
J4 out in vdd vdd tp0.7x10 L=0.7U W=6U
J5 out in 0 0 tn0.7x10 L=0.7U W=6U
J6 out in vdd vdd tp0.7x10 L=0.7U W=6U
J7 out in 0 0 tn0.7x10 L=0.7U W=6U
J8 out in vdd vdd tp0.7x10 L=0.7U W=6U
J9 out in 0 0 tn0.7x10 L=0.7U W=6U
J10 out in vdd vdd tp0.7x10 L=0.7U W=6U
J11 out in 0 0 tn0.7x10 L=0.7U W=6U
.ENDS INVO3

.SUBCKT INVO4 in out vdd 0
J0 out in vdd vdd tp0.7x10 L=0.7U W=10U
J1 out in vdd vdd tp0.7x10 L=0.7U W=10U
J2 out in vdd vdd tp0.7x10 L=0.7U W=10U

J3 out in vdd vdd tp0.7x10 L=0.7U W=10U

J4 out in vdd vdd tp0.7x10 L=0.7U W=10U

J5 out in vdd vdd tp0.7x10 L=0.7U W=10U

J6 out in vdd vdd tp0.7x10 L=0.7U W=10U

J7 out in vdd vdd tp0.7x10 L=0.7U W=10U

J8 out in vdd vdd tp0.7x10 L=0.7U W=10U

J9 out in 0 0 tn0.7x10 L=0.7U W=10U

J10 out in 0 0 tn0.7x10 L=0.7U W=10U

J11 out in 0 0 tn0.7x10 L=0.7U W=10U

.ENDS INVO4

*Output driver subcircuit

.SUBCKT OUTDRIVER in out vdd 0

X1 in 3 vdd 0 INVO1

X2 3 4 vdd 0 INVO2

X3 4 5 vdd 0 INVO3

X4 5 out vdd 0 INVO4

c1 out 0 5pf

R1 out 0 50

.ENDS OUTDRIVER

****

**   main circuit   **

****

X1 clock input_rec._out vdd 0 INPUTDRIVER

X2 input_rec._out output_driver_out vdd 0 OUTDRIVER

*Type of analysis

.option dcon=1 post

```
.tran 10ps 15ns
*measurements
.MEAS avg_power avg power
*.MEAS rms_power rms power
.end
```

A.2   CGaAs STATIC 3-BIT LFSR IC

```
* File name          : slfsr.sp
* Directory name      : shehata/thesis/run1/slfsr
* Minimum clock time  : 1.82ns
* Total average power : 214.48mW
* Last correction date : Dec./12/95
.include /home5/shehata/thesis/run1/parameters
*power supply
vdd vdd 0 2.0
*input signals
vclk_in clock 0 pulse(0 1.75 0ns 0.01ns 0.01ns 0.9ns 1.82ns)

*********************************************************
**              INPUT DRIVER CIRCUIT              **
*********************************************************

.SUBCKT INVI1 in out vdd 0
J0 out in vdd vdd tp0.7x10 L=0.7U W=6.0U
J1 out in 0 0 tn0.7x10 L=0.7U W=5.6U
.ENDS INVI1


.SUBCKT INVI2 in out vdd 0
J0 out in vdd vdd tp0.7x10 L=0.7U W=6.0U
J1 out in 0 0 tn0.7x10 L=0.7U W=6.0U
J2 out in vdd vdd tp0.7x10 L=0.7U W=6.0U
J3 out in 0 0 tn0.7x10 L=0.7U W=6.0U
.ENDS INVI2


.SUBCKT INVI3 in out vdd 0
J0 out in vdd vdd tp0.7x10 L=0.7U W=6.0U
```

J1 out in 0 0 tn0.7x10 L=0.7U W=6.0U

J2 out in vdd vdd tp0.7x10 L=0.7U W=6.0U

J3 out in 0 0 tn0.7x10 L=0.7U W=6.0U

J4 out in vdd vdd tp0.7x10 L=0.7U W=6.0U

J5 out in 0 0 tn0.7x10 L=0.7U W=6.0U

J6 out in vdd vdd tp0.7x10 L=0.7U W=6.0U

J7 out in 0 0 tn0.7x10 L=0.7U W=6.0U

J8 out in vdd vdd tp0.7x10 L=0.7U W=6.0U

J9 out in 0 0 tn0.7x10 L=0.7U W=6.0U

J10 out in vdd vdd tp0.7x10 L=0.7U W=6.0U

J11 out in 0 0 tn0.7x10 L=0.7U W=6.0U

.ENDS INVI3

.SUBCKT INPUTDRIVER in out vdd 0

X1 in 4 vdd 0 INVI1

X2 4 5 vdd 0 INVI2

X3 5 6 vdd 0 INVI3

X4 6 out vdd 0 INVI3

.ENDS INPUTDRIVER

****
**   3 Bits LFSR CIRCUIT   **
****

.SUBCKT INVB in out vdd 0

J0 out in vdd vdd tp0.7x10 L=0.7U W=10.0U

J1 out in 0 0 tn0.7x10 L=0.7U W=5.0U

.ENDS INVB

```
.SUBCKT TGB in clockn clockp out vdd 0
J0 out clockp in vdd tp0.7x10 L=0.7U W=5.0U
J1 in clockn out 0 tn0.7x10 L=0.7U W=5.0U
.ENDS TGB


.SUBCKT DFFB D clock Q vdd 0
X1 clock clockbar vdd 0 INVB
X2 D clock clockbar 4 vdd 0 TGB
X3 4 6 vdd 0 INVB
X4 6 7 vdd 0 INVB
X5 7 clockbar clock 4 vdd 0 TGB
X6 6 clockbar clock 10 vdd 0 TGB
X7 9 clock clockbar 10 vdd 0 TGB
X8 10 Q vdd 0 INVB
X9 Q 9 vdd 0 INVB
.ENDS DFFB


.SUBCKT XORB A B out vdd 0
X1 A Abar vdd 0 INVB
X2 B Bbar vdd 0 INVB
X3 A Bbar B out vdd 0 TGB
X4 Abar B Bbar out vdd 0 TGB
.ENDS XORB


.SUBCKT SLFSR clock Q0 Q1 Q2 vdd 0
X1 2 clock Q0 vdd 0 DFFB
X2 Q0 clock Q1 vdd 0 DFFB
X3 Q1 clock Q2 vdd 0 DFFB
```

X4 Q1 Q2 2 vdd 0 XORB

.ENDS SLFSR

****

*   OUTPUT DRIVER CIRCUIT   **

****

.SUBCKT INVO1 in out vdd 0

J0 out in vdd vdd tp0.7x10 L=0.7U W=6.0U

J1 out in 0 0 tn0.7x10 L=0.7U W=6.0U

.ENDS INVO1

.SUBCKT INVO2 in out vdd 0

J0 out in vdd vdd tp0.7x10 L=0.7U W=6U

J01 out in vdd vdd tp0.7x10 L=0.7U W=6U

J1 out in 0 0 tn0.7x10 L=0.7U W=6U

J11 out in 0 0 tn0.7x10 L=0.7U W=6U

.ENDS INVO2

.SUBCKT INVO3 in out vdd 0

J0 out in vdd vdd tp0.7x10 L=0.7U W=6U

J01 out in vdd vdd tp0.7x10 L=0.7U W=6U

J02 out in vdd vdd tp0.7x10 L=0.7U W=6U

J03 out in vdd vdd tp0.7x10 L=0.7U W=6U

J1 out in 0 0 tn0.7x10 L=0.7U W=6U

J11 out in 0 0 tn0.7x10 L=0.7U W=6U

J12 out in 0 0 tn0.7x10 L=0.7U W=6U

J13 out in 0 0 tn0.7x10 L=0.7U W=6U

.ENDS INVO3

```
.SUBCKT INVO4 in out vdd 0
J0 out in vdd vdd tp0.7x10 L=0.7U W=10U
J01 out in vdd vdd tp0.7x10 L=0.7U W=10U
J02 out in vdd vdd tp0.7x10 L=0.7U W=10U
J03 out in vdd vdd tp0.7x10 L=0.7U W=10U
J04 out in vdd vdd tp0.7x10 L=0.7U W=10U
J05 out in vdd vdd tp0.7x10 L=0.7U W=10U
J06 out in vdd vdd tp0.7x10 L=0.7U W=10U
J07 out in vdd vdd tp0.7x10 L=0.7U W=10U
J08 out in vdd vdd tp0.7x10 L=0.7U W=10U
J1 out in 0 0 tn0.7x10 L=0.7U W=10U
J11 out in 0 0 tn0.7x10 L=0.7U W=10U
J12 out in 0 0 tn0.7x10 L=0.7U W=10U
J13 out in 0 0 tn0.7x10 L=0.7U W=10U
J14 out in 0 0 tn0.7x10 L=0.7U W=10U
J15 out in 0 0 tn0.7x10 L=0.7U W=10U
.ENDS INVO4


.SUBCKT OUTDRIVER in out vdd 0
X1 in 3 vdd 0 INVO1
X2 3 4 vdd 0 INVO2
X3 4 5 vdd 0 INVO3
X4 5 out vdd 0 INVO4
c1 out 0 5pf
R1 out 0 50
.ENDS OUTDRIVER
*****************************************************
*              main circuit                    **
```

```
*************************************************
vdd1 vdd1 0 2.0
X1 clock 3 vdd 0 INPUTDRIVER
X2 3 Q0 Q1 Q2 vdd1 0 SLFSR
X3 Q0 Q0out vdd 0 OUTDRIVER
X4 Q1 Q1out vdd 0 OUTDRIVER
X5 Q2 Q2out vdd 0 OUTDRIVER

*Type of analysis
.option dcon=1 post
.tran 100ps 20ns
*.tran (increment time) (stop time)
.MEAS avg_power avg power
.PLOT DC power P(vdd) P(vclk_in)
.end
```

A.3   CGaAs STATIC F1 GENERATOR IC

* Function   : (-(-(A + B) + C))

* File name   : f1loaded.sp

* Directory name   : shehata/thesis/run1/sfunction

* Minimum clock time   : 1.92ns

* Total average power   : 85.64mW

* Last correction date   : Dec./12/95

* Minimum clock time=1.92ns, Total Average Power=85.64mW

.include /home5/shehata/thesis/run1/parameters

*power supply

vdd vdd 0 2.0

*input signals

vclk_in clock 0 pulse(0 1.75 0ns 0.01ns 0.01ns 0.95ns 1.92ns)

****

**   INPUT DRIVER CIRCUIT   **

****

.SUBCKT INVI1 in out vdd 0

J0 out in vdd vdd tp0.7x10 L=0.7U W=6.0U

J1 out in 0 0 tn0.7x10 L=0.7U W=5.6U

.ENDS INVI1

.SUBCKT INVI2 in out vdd 0

J0 out in vdd vdd tp0.7x10 L=0.7U W=6.0U

J1 out in 0 0 tn0.7x10 L=0.7U W=6.0U

J2 out in vdd vdd tp0.7x10 L=0.7U W=6.0U

J3 out in 0 0 tn0.7x10 L=0.7U W=6.0U

.ENDS INVI2

.SUBCKT INVI3 in out vdd 0

J0 out in vdd vdd tp0.7x10 L=0.7U W=6.0U

J1 out in 0 0 tn0.7x10 L=0.7U W=6.0U

J2 out in vdd vdd tp0.7x10 L=0.7U W=6.0U

J3 out in 0 0 tn0.7x10 L=0.7U W=6.0U

J4 out in vdd vdd tp0.7x10 L=0.7U W=6.0U

J5 out in 0 0 tn0.7x10 L=0.7U W=6.0U

J6 out in vdd vdd tp0.7x10 L=0.7U W=6.0U

J7 out in 0 0 tn0.7x10 L=0.7U W=6.0U

J8 out in vdd vdd tp0.7x10 L=0.7U W=6.0U

J9 out in 0 0 tn0.7x10 L=0.7U W=6.0U

J10 out in vdd vdd tp0.7x10 L=0.7U W=6.0U

J11 out in 0 0 tn0.7x10 L=0.7U W=6.0U

.ENDS INVI3

.SUBCKT INPUTDRIVER in out vdd 0

X1 in 4 vdd 0 INVI1

X2 4 5 vdd 0 INVI2

X3 5 6 vdd 0 INVI3

X4 6 out vdd 0 INVI3

.ENDS INPUTDRIVER

****
**   3 Bits LFSR CIRCUIT   **
****

.SUBCKT INVB in out vdd 0

J0 out in vdd vdd tp0.7x10 L=0.7U W=10.0U

J1 out in 0 0 tn0.7x10 L=0.7U W=5.0U

.ENDS INVB

.SUBCKT TGB in clockn clockp out vdd 0

J0 out clockp in vdd tp0.7x10 L=0.7U W=5.0U

J1 in clockn out 0 tn0.7x10 L=0.7U W=5.0U

.ENDS TGB

.SUBCKT DFFB D clock Q vdd 0

X1 clock clockbar vdd 0 INVB

X2 D clock clockbar 4 vdd 0 TGB

X3 4 6 vdd 0 INVB

X4 6 7 vdd 0 INVB

X5 7 clockbar clock 4 vdd 0 TGB

X6 6 clockbar clock 10 vdd 0 TGB

X7 9 clock clockbar 10 vdd 0 TGB

X8 10 Q vdd 0 INVB

X9 Q 9 vdd 0 INVB

.ENDS DFFB

.SUBCKT XORB A B out vdd 0

X1 A Abar vdd 0 INVB

X2 B Bbar vdd 0 INVB

X3 A Bbar B out vdd 0 TGB

X4 Abar B Bbar out vdd 0 TGB

.ENDS XORB

.SUBCKT SLFSR clock Q0 Q1 Q2 vdd 0

X1 2 clock Q0 vdd 0 DFFB

X2 Q0 clock Q1 vdd 0 DFFB

X3 Q1 clock Q2 vdd 0 DFFB

X4 Q1 Q2 2 vdd 0 XORB

.ENDS SLFSR

****

*   CIRCUIT GENERATING F1   **

****

.SUBCKT INVF in out vdd 0

J0 out in vdd vdd tp0.7x10 L=0.7U W=10.0U

J1 out in 0 0 tn0.7x10 L=0.7U W=10.0U

.ENDS INVF

.SUBCKT SF1 A B C out vdd 0

J0 6 A vdd vdd tp0.7x10 L=0.7U W=10.0U

J1 7 A 0 0 tn0.7x10 L=0.7U W=10.0U

J2 7 B 6 vdd tp0.7x10 L=0.7U W=10.0U

J3 7 B 0 0 tn0.7x10 L=0.7U W=10.0U

J4 8 C vdd vdd tp0.7x10 L=0.7U W=10.0U

J5 out C 0 0 tn0.7x10 L=0.7U W=10.0U

J6 out 7 8 vdd tp0.7x10 L=0.7U W=10.0U

J7 out 7 0 0 tn0.7x10 L=0.7U W=10.0U

.ENDS SF1

****

*   OUTPUT DRIVER CIRCUIT   **

****

.SUBCKT INVO1 in out vdd 0

J0 out in vdd vdd tp0.7x10 L=0.7U W=6.0U

J1 out in 0 0 tn0.7x10 L=0.7U W=6.0U

.ENDS INVO1

.SUBCKT INVO2 in out vdd 0

J0 out in vdd vdd tp0.7x10 L=0.7U W=6U

J01 out in vdd vdd tp0.7x10 L=0.7U W=6U

J1 out in 0 0 tn0.7x10 L=0.7U W=6U

J11 out in 0 0 tn0.7x10 L=0.7U W=6U

.ENDS INVO2

.SUBCKT INVO3 in out vdd 0

J0 out in vdd vdd tp0.7x10 L=0.7U W=6U

J01 out in vdd vdd tp0.7x10 L=0.7U W=6U

J02 out in vdd vdd tp0.7x10 L=0.7U W=6U

J03 out in vdd vdd tp0.7x10 L=0.7U W=6U

J04 out in vdd vdd tp0.7x10 L=0.7U W=6U

J1 out in 0 0 tn0.7x10 L=0.7U W=6U

J11 out in 0 0 tn0.7x10 L=0.7U W=6U

J12 out in 0 0 tn0.7x10 L=0.7U W=6U

.ENDS INVO3

.SUBCKT INVO4 in out vdd 0

J0 out in vdd vdd tp0.7x10 L=0.7U W=10U

J01 out in vdd vdd tp0.7x10 L=0.7U W=10U

J02 out in vdd vdd tp0.7x10 L=0.7U W=10U

J03 out in vdd vdd tp0.7x10 L=0.7U W=10U

J04 out in vdd vdd tp0.7x10 L=0.7U W=10U

J05 out in vdd vdd tp0.7x10 L=0.7U W=10U

J06 out in vdd vdd tp0.7x10 L=0.7U W=10U

J07 out in vdd vdd tp0.7x10 L=0.7U W=10U

J08 out in vdd vdd tp0.7x10 L=0.7U W=10U

J1 out in 0 0 tn0.7x10 L=0.7U W=10U

J11 out in 0 0 tn0.7x10 L=0.7U W=10U

J12 out in 0 0 tn0.7x10 L=0.7U W=10U

.ENDS INVO4

.SUBCKT OUTDRIVER in out vdd 0

X1 in 3 vdd 0 INVO1

X2 3 4 vdd 0 INVO2

X3 4 5 vdd 0 INVO3

X4 5 out vdd 0 INVO4

c1 out 0 5pf

R1 out 0 50

.ENDS OUTDRIVER

****
*   main circuit   **
****

X1 clock 3 vdd 0 INPUTDRIVER

X2 3 Q0 Q1 Q2 vdd 0 SLFSR

X3 Q0 Q1 Q2 out vdd 0 SF1

X4 out outout vdd 0 OUTDRIVER

*Type of analysis

.option dcon=1 post

.tran 100ps 20ns

.MEAS avg_power avg power

.PLOT DC power P(vdd) P(vclk_in)

.end

A.4   CGaAs TWO-PHASE CLOCK GENERATOR IC

* DRIVERS USING C-HIGFET

* File name   : genloaded.sp

* Directory name   : shehata/thesis/run1/dgen

* Minimum clock time : 1.02ns

* Total average power: 349.18mW

* Last correction date: Dec./12/95

.include /home5/shehata/thesis/run1/parameters

*power supply

vdd vdd 0 2.0

*Input signal

vin clock 0 pulse(0 1.75 0ns 0.01ns 0.01ns 0.5ns 1.02ns)

```
**************************************************************
**            INPUT DRIVER CIRCUIT                      **
**************************************************************
```

.SUBCKT INVI1 in out vdd 0

J0 out in vdd vdd tp0.7x10 L=0.7U W=6.0U

J1 out in 0 0 tn0.7x10 L=0.7U W=5.6U

.ENDS INVI1

.SUBCKT INVI2 in out vdd 0

J0 out in vdd vdd tp0.7x10 L=0.7U W=6.0U

J1 out in 0 0 tn0.7x10 L=0.7U W=6.0U

J2 out in vdd vdd tp0.7x10 L=0.7U W=6.0U

J3 out in 0 0 tn0.7x10 L=0.7U W=6.0U

.ENDS INVI2

.SUBCKT INVI3 in out vdd 0

J0 out in vdd vdd tp0.7x10 L=0.7U W=6.0U

J1 out in 0 0 tn0.7x10 L=0.7U W=6.0U

J2 out in vdd vdd tp0.7x10 L=0.7U W=6.0U

J3 out in 0 0 tn0.7x10 L=0.7U W=6.0U

J4 out in vdd vdd tp0.7x10 L=0.7U W=6.0U

J5 out in 0 0 tn0.7x10 L=0.7U W=6.0U

J6 out in vdd vdd tp0.7x10 L=0.7U W=6.0U

J7 out in 0 0 tn0.7x10 L=0.7U W=6.0U

J8 out in vdd vdd tp0.7x10 L=0.7U W=6.0U

J9 out in 0 0 tn0.7x10 L=0.7U W=6.0U

J10 out in vdd vdd tp0.7x10 L=0.7U W=6.0U

J11 out in 0 0 tn0.7x10 L=0.7U W=6.0U

.ENDS INVI3

.SUBCKT INPUTDRIVER in out vdd 0

X1 in 4 vdd 0 INVI1

X2 4 5 vdd 0 INVI2

X3 5 6 vdd 0 INVI3

X4 6 out vdd 0 INVI3

.ENDS INPUTDRIVER

****

**   GENERATOR CIRCUIT   **

****

.SUBCKT INVG in out vdd 0

J0 out in vdd vdd tp0.7x10 L=0.7U W=4.0U

J1 out in 0 0 tn0.7x10 L=0.7U W=2.0U

.ENDS INVG

```
.SUBCKT INVG1 in out vdd 0
J0 out in vdd vdd tp0.7x10 L=0.7U W=6.0U
J1 out in 0 0 tn0.7x10 L=0.7U W=2.0U
.ENDS INVG1


.SUBCKT INVG2 in out vdd 0
J0 out in vdd vdd tp0.7x10 L=0.7U W=3.0U
J1 out in 0 0 tn0.7x10 L=0.7U W=3.0U
.ENDS INVG2


.SUBCKT INVG3 in out vdd 0
J0 out in vdd vdd tp0.7x10 L=0.7U W=4.0U
J1 out in 0 0 tn0.7x10 L=0.7U W=2.0U
.ENDS INVG3


.SUBCKT INVG4 in out vdd 0
J0 out in vdd vdd tp0.7x10 L=0.7U W=4.0U
J1 out in 0 0 tn0.7x10 L=0.7U W=4.0U
.ENDS INVG4


.SUBCKT NANDG1 A B out vdd 0
J0 out A vdd vdd tp0.7x10 L=0.7U W=4.0U
J1 out B vdd vdd tp0.7x10 L=0.7U W=4.0U
J2 out B 4 0 tn0.7x10 L=0.7U W=2.0U
J3 4 A 0 0 tn0.7x10 L=0.7U W=2.0U
.ENDS NANDG1


.SUBCKT NANDG2 A B out vdd 0
```

J0 out A vdd vdd tp0.7x10 L=0.7U W=6.4U

J1 out B vdd vdd tp0.7x10 L=0.7U W=6.4U

J2 out B 4 0 tn0.7x10 L=0.7U W=3.6U

J3 4 A 0 0 tn0.7x10 L=0.7U W=3.6U

.ENDS NANDG2

.SUBCKT PHI1PHI2 clock_in phi1_out phi2_out vdd 0

X1 clock_in 3 vdd 0 INVG

X2 5 3 4 vdd 0 NANDG1

X5 4 clock_in 5 vdd 0 NANDG2

X6 4 6 vdd 0 INVG1

X7 5 7 vdd 0 INVG1

X8 6 phi1_out vdd 0 INVG2

X9 7 phi2_out vdd 0 INVG2

.ENDS PHI1PHI2

.SUBCKT TG in out vdd 0

J0 in 0 out vdd tp0.7x10 L=0.7U W=2.0U

J1 out vdd in 0 tn0.7x10 L=0.7U W=2.0U

.ENDS TG

.SUBCKT PHI-PHI phi_in phi_out phibar_out vdd 0

X1 phi_in 4 vdd 0 TG

X2 phi_in 3 vdd 0 INVG

X3 3 phi_out vdd 0 INVG3

X4 4 phibar_out vdd 0 INVG4

.ENDS PHI-PHI

```
.SUBCKT GEN clock phi1 phi2 phi1bar phi2bar vdd 0
X1 clock 3 4 vdd 0 PHI1PHI2
X2 3 phi1 phi1bar vdd 0 PHI-PHI
X3 4 phi2 phi2bar vdd 0 PHI-PHI
.ENDS GEN

*************************************************************
*           OUTPUT DRIVER CIRCUIT FOR PHI SIGNAL         **
*************************************************************
.SUBCKT INVO1 in out vdd 0
J0 out in vdd vdd tp0.7x10 L=0.7U W=6.0U
J01 out in vdd vdd tp0.7x10 L=0.7U W=6.0U
J1 out in 0 0 tn0.7x10 L=0.7U W=2.0U
.ENDS INVO1


.SUBCKT INVO2 in out vdd 0
J0 out in vdd vdd tp0.7x10 L=0.7U W=6U
J01 out in vdd vdd tp0.7x10 L=0.7U W=6U
J02 out in vdd vdd tp0.7x10 L=0.7U W=6U
J03 out in vdd vdd tp0.7x10 L=0.7U W=6U
J04 out in vdd vdd tp0.7x10 L=0.7U W=6U
J1 out in 0 0 tn0.7x10 L=0.7U W=4U
J11 out in 0 0 tn0.7x10 L=0.7U W=4U
J12 out in 0 0 tn0.7x10 L=0.7U W=4U
.ENDS INVO2


.SUBCKT INVO3 in out vdd 0
J0 out in vdd vdd tp0.7x10 L=0.7U W=6U
J01 out in vdd vdd tp0.7x10 L=0.7U W=6U
```

195

J02 out in vdd vdd tp0.7x10 L=0.7U W=6U

J03 out in vdd vdd tp0.7x10 L=0.7U W=6U

J04 out in vdd vdd tp0.7x10 L=0.7U W=6U

J05 out in vdd vdd tp0.7x10 L=0.7U W=6U

J06 out in vdd vdd tp0.7x10 L=0.7U W=6U

J07 out in vdd vdd tp0.7x10 L=0.7U W=6U

J1 out in 0 0 tn0.7x10 L=0.7U W=4U

J11 out in 0 0 tn0.7x10 L=0.7U W=4U

J12 out in 0 0 tn0.7x10 L=0.7U W=4U

J13 out in 0 0 tn0.7x10 L=0.7U W=4U

.ENDS INVO3

.SUBCKT INVO4 in out vdd 0

J0 vdd in out vdd tp0.7x10 L=0.7U W=10U

J01 vdd in out vdd tp0.7x10 L=0.7U W=10U

J02 vdd in out vdd tp0.7x10 L=0.7U W=10U

J03 vdd in out vdd tp0.7x10 L=0.7U W=10U

J04 vdd in out vdd tp0.7x10 L=0.7U W=10U

J05 vdd in out vdd tp0.7x10 L=0.7U W=10U

J06 vdd in out vdd tp0.7x10 L=0.7U W=10U

J07 vdd in out vdd tp0.7x10 L=0.7U W=10U

J08 vdd in out vdd tp0.7x10 L=0.7U W=10U

J09 vdd in out vdd tp0.7x10 L=0.7U W=10U

J1 out in 0 0 tn0.7x10 L=0.7U W=10U

J11 out in 0 0 tn0.7x10 L=0.7U W=10U

J12 out in 0 0 tn0.7x10 L=0.7U W=10U

.ENDS INVO4

* Φ Output driver subcircuit

.SUBCKT OUTDRIVER in out vdd 0

X1 in 3 vdd 0 INVO1

X2 3 4 vdd 0 INVO2

X3 4 5 vdd 0 INVO3

X4 5 out vdd 0 INVO4

c1 out 0 5pf

R1 out 0 50

.ENDS OUTDRIVER

****

*   OUTPUT DRIVER CIRCUIT FOR PHIBAR SIGNAL   **

****

.SUBCKT INVOBAR1 in out vdd 0

J0 out in vdd vdd tp0.7x10 L=0.7U W=6.0U

J1 out in 0 0 tn0.7x10 L=0.7U W=6.0U

.ENDS INVOBAR1

.SUBCKT INVOBAR2 in out vdd 0

J0 out in vdd vdd tp0.7x10 L=0.7U W=6U

J01 out in vdd vdd tp0.7x10 L=0.7U W=6U

J02 out in vdd vdd tp0.7x10 L=0.7U W=6U

J03 out in vdd vdd tp0.7x10 L=0.7U W=6U

J1 out in 0 0 tn0.7x10 L=0.7U W=4U

J11 out in 0 0 tn0.7x10 L=0.7U W=4U

J12 out in 0 0 tn0.7x10 L=0.7U W=4U

.ENDS INVOBAR2

.SUBCKT INVOBAR3 in out vdd 0

JO out in vdd vdd tp0.7x10 L=0.7U W=6U

J01 out in vdd vdd tp0.7x10 L=0.7U W=6U

J02 out in vdd vdd tp0.7x10 L=0.7U W=6U

J03 out in vdd vdd tp0.7x10 L=0.7U W=6U

J1 out in 0 0 tn0.7x10 L=0.7U W=6U

J11 out in 0 0 tn0.7x10 L=0.7U W=6U

J12 out in 0 0 tn0.7x10 L=0.7U W=6U

J13 out in 0 0 tn0.7x10 L=0.7U W=6U

J14 out in 0 0 tn0.7x10 L=0.7U W=6U

.ENDS INVOBAR3

.SUBCKT INVOBAR4 in out vdd 0

JO vdd in out vdd tp0.7x10 L=0.7U W=10U

J01 vdd in out vdd tp0.7x10 L=0.7U W=10U

J02 vdd in out vdd tp0.7x10 L=0.7U W=10U

J03 vdd in out vdd tp0.7x10 L=0.7U W=10U

J04 vdd in out vdd tp0.7x10 L=0.7U W=10U

J05 vdd in out vdd tp0.7x10 L=0.7U W=10U

J06 vdd in out vdd tp0.7x10 L=0.7U W=10U

J07 vdd in out vdd tp0.7x10 L=0.7U W=10U

J08 vdd in out vdd tp0.7x10 L=0.7U W=10U

J1 out in 0 0 tn0.7x10 L=0.7U W=10U

J11 out in 0 0 tn0.7x10 L=0.7U W=10U

J12 out in 0 0 tn0.7x10 L=0.7U W=10U

.ENDS INVOBAR4

* $\overline{\Phi}$ Output driver subcircuit

.SUBCKT OUTBARDRIVER in out vdd 0

X1 in 3 vdd 0 INVOBAR1

X2 3 4 vdd 0 INVOBAR2

X3 4 5 vdd 0 INVOBAR3

X4 5 out vdd 0 INVOBAR4

c1 out 0 5pf

R1 out 0 50

.ENDS OUTBARDRIVER

****

*   main circuit   **

****

X1 clock 3 vdd 0 INPUTDRIVER

X2 3 phi1 phi2 phi1bar phi2bar vdd 0 GEN

X3 phi1 phi1out vdd 0 OUTDRIVER

X4 phi2 phi2out vdd 0 OUTDRIVER

X5 phi1bar phi1barout vdd 0 OUTBARDRIVER

X6 phi2bar phi2barout vdd 0 OUTBARDRIVER

*Type of analysis

.option dcon=1 post

.tran 10ps 15ns

*measurements

.MEAS avg_power avg power

.end

A.5   CGaAs TPDL 3-BIT LFSR IC

* File name   : genlfsr.sp

* Directory name   : shehata/thesis/run1/dlfsr

* Minimum clock time : 1.12ns

* Total average power: 320mW

* Last correction date: Dec./12/95

.include /home5/shehata/thesis/run1/parameters

*power supply

vdd vdd 0 2.0

*input and output signals

vclock_in clock 0 pulse(0 1.75 0ns .01ns .01ns 0.55ns 1.12ns)

****

**   INPUT DRIVER CIRCUIT   **

****

.SUBCKT INVI1 in out vdd 0

J0 out in vdd vdd tp0.7x10 L=0.7U W=6.0U

J1 out in 0 0 tn0.7x10 L=0.7U W=5.6U

.ENDS INVI1

.SUBCKT INVI2 in out vdd 0

J0 out in vdd vdd tp0.7x10 L=0.7U W=6.0U

J1 out in 0 0 tn0.7x10 L=0.7U W=6.0U

J2 out in vdd vdd tp0.7x10 L=0.7U W=6.0U

J3 out in 0 0 tn0.7x10 L=0.7U W=6.0U

.ENDS INVI2

.SUBCKT INVI3 in out vdd 0

J0 out in vdd vdd tp0.7x10 L=0.7U W=6.0U

J1 out in 0 0 tn0.7x10 L=0.7U W=6.0U

J2 out in vdd vdd tp0.7x10 L=0.7U W=6.0U

J3 out in 0 0 tn0.7x10 L=0.7U W=6.0U

J4 out in vdd vdd tp0.7x10 L=0.7U W=6.0U

J5 out in 0 0 tn0.7x10 L=0.7U W=6.0U

J6 out in vdd vdd tp0.7x10 L=0.7U W=6.0U

J7 out in 0 0 tn0.7x10 L=0.7U W=6.0U

J8 out in vdd vdd tp0.7x10 L=0.7U W=6.0U

J9 out in 0 0 tn0.7x10 L=0.7U W=6.0U

J10 out in vdd vdd tp0.7x10 L=0.7U W=6.0U

J11 out in 0 0 tn0.7x10 L=0.7U W=6.0U

.ENDS INVI3

.SUBCKT INPUTDRIVER in out vdd 0

X1 in 4 vdd 0 INVI1

X2 4 5 vdd 0 INVI2

X3 5 6 vdd 0 INVI3

X4 6 out vdd 0 INVI3

.ENDS INPUTDRIVER

****
**   GENERATOR CIRCUIT   **
****

.SUBCKT INVG in out vdd 0

J0 out in vdd vdd tp0.7x10 L=0.7U W=4.0U

J1 out in 0 0 tn0.7x10 L=0.7U W=2.0U

.ENDS INVG

.SUBCKT INVG1 in out vdd 0

J0 out in vdd vdd tp0.7x10 L=0.7U W=6.0U

J1 out in 0 0 tn0.7x10 L=0.7U W=2.0U

.ENDS INVG1

.SUBCKT INVG2 in out vdd 0

J0 out in vdd vdd tp0.7x10 L=0.7U W=3.0U

J1 out in 0 0 tn0.7x10 L=0.7U W=3.0U

.ENDS INVG2

.SUBCKT INVG3 in out vdd 0

J0 out in vdd vdd tp0.7x10 L=0.7U W=5.0U

J1 out in 0 0 tn0.7x10 L=0.7U W=3.0U

.ENDS INVG3

.SUBCKT INVG4 in out vdd 0

J0 out in vdd vdd tp0.7x10 L=0.7U W=6.0U

J1 out in 0 0 tn0.7x10 L=0.7U W=4.0U

.ENDS INVG4

.SUBCKT NANDG1 A B out vdd 0

J0 out A vdd vdd tp0.7x10 L=0.7U W=4.0U

J1 out B vdd vdd tp0.7x10 L=0.7U W=4.0U

J2 out B 4 0 tn0.7x10 L=0.7U W=2.0U

J3 4 A 0 0 tn0.7x10 L=0.7U W=2.0U

.ENDS NANDG1

.SUBCKT NANDG2 A B out vdd 0

J0 out A vdd vdd tp0.7x10 L=0.7U W=7.5U

J1 out B vdd vdd tp0.7x10 L=0.7U W=7.5U

J2 out B 4 0 tn0.7x10 L=0.7U W=3.8U

J3 4 A 0 0 tn0.7x10 L=0.7U W=3.8U

.ENDS NANDG2

.SUBCKT PHI1PHI2 clock_in phi1_out phi2_out vdd 0

X1 clock_in 3 vdd 0 INVG

X2 5 3 4 vdd 0 NANDG1

X5 4 clock_in 5 vdd 0 NANDG2

X6 4 6 vdd 0 INVG1

X7 5 7 vdd 0 INVG1

X8 6 phi1_out vdd 0 INVG2

X9 7 phi2_out vdd 0 INVG2

.ENDS PHI1PHI2

.SUBCKT TGG in out vdd 0

J0 in 0 out vdd tp0.7x10 L=0.7U W=2.0U

J1 out vdd in 0 tn0.7x10 L=0.7U W=2.0U

.ENDS TGG

.SUBCKT PHI-PHI phi_in phi_out phibar_out vdd 0

X1 phi_in 4 vdd 0 TGG

X2 phi_in 3 vdd 0 INVG

X3 3 phi_out vdd 0 INVG3

X4 4 phibar_out vdd 0 INVG4

.ENDS PHI-PHI

.SUBCKT GEN clock phi1 phi2 phi1bar phi2bar vdd 0

X1 clock 3 4 vdd 0 PHI1PHI2

X2 3 phi1 phi1bar vdd 0 PHI-PHI

X3 4 phi2 phi2bar vdd 0 PHI-PHI

.ENDS GEN

****

**   3 BITS DYNAMIC LFSR CIRCUIT   **

****

.SUBCKT TG in phi phibar out vdd 0

J0 in phi out vdd tp0.7x10 L=0.7U W=2.0U

J1 out phibar in 0 tn0.7x10 L=0.7U W=2.0U

.ENDS TG

.SUBCKT DINV in phi out vdd 0

J0 out phi vdd vdd tp0.7x10 L=0.7U W=7.0U

J1 out phi 5 0 tn0.7x10 L=0.7U W=2.0U

J2 5 in 0 0 tn0.7x10 L=0.7U W=2.5U

.ENDS DINV

.SUBCKT DNAND A B phi out vdd 0

J0 out phi vdd vdd tp0.7x10 L=0.7U W=10.0U

J1 out phi 5 0 tn0.7x10 L=0.7U W=3.0U

J2 5 A 7 0 tn0.7x10 L=0.7U W=4.0U

J3 7 B 0 0 tn0.7x10 L=0.7U W=4.0U

.ENDS DNAND

.SUBCKT DNAND1 A B phi out vdd 0

J0 out phi vdd vdd tp0.7x10 L=0.7U W=10.0U

J1 out phi 5 0 tn0.7x10 L=0.7U W=3.0U

J2 5 A 7 0 tn0.7x10 L=0.7U W=3.0U

J3 7 B 0 0 tn0.7x10 L=0.7U W=3.0U

.ENDS DNAND1

.SUBCKT SNAND A B out vdd 0

J0 out A vdd vdd tp0.7x10 L=0.7U W=4.0U

J1 out B vdd vdd tp0.7x10 L=0.7U W=4.0U

J2 5 A 0 0 tn0.7x10 L=0.7U W=2.0U

J3 out B 5 0 tn0.7x10 L=0.7U W=2.0U

.ENDS SNAND

.SUBCKT DFF D phi1 phi1bar phi2 phi2bar out vdd 0

X1 D phi1 phi1bar 8 vdd 0 TG

X2 8 phi1 9 vdd 0 DINV

X3 9 phi2 phi2bar 10 vdd 0 TG

X4 10 phi2 out vdd 0 DINV

.ENDS DFF

.SUBCKT DXOR A B phi1 phi1bar phi2 phi2bar out vdd 0

X1 A phi1 phi1bar 9 vdd 0 TG

X2 B phi1 phi1bar 10 vdd 0 TG

X3 9 10 11 vdd 0 SNAND

X4 9 11 phi1 12 vdd 0 DNAND

X5 10 11 phi1 13 vdd 0 DNAND

X6 12 phi2 phi2bar 14 vdd 0 TG

X7 13 phi2 phi2bar 15 vdd 0 TG

X8 14 15 phi2 out vdd 0 DNAND1

.ENDS DXOR

.SUBCKT SINV in out vdd 0

J0 out in vdd vdd tp0.7x10 L=0.7U W=4.0U

J1 out in 0 0 tn0.7x10 L=0.7U W=2.0U

.ENDS SINV

.SUBCKT DLFSR phi1 phi1bar phi2 phi2bar Q0 Q1 Q2 vdd 0

X1 Q0 phi1 phi1bar phi2 phi2bar Q1 vdd 0 DFF

X2 Q1 phi1 phi1bar phi2 phi2bar Q2 vdd 0 DFF

X3 Q1 Q2 phi1 phi1bar phi2 phi2bar Q0 vdd 0 DXOR

.ENDS DLFSR

****

*   OUTPUT DRIVER CIRCUIT FOR Q SIGNALS   **

****

.SUBCKT INVO1 in out vdd 0

J0 out in vdd vdd tp0.7x10 L=0.7U W=6.0U

J1 out in 0 0 tn0.7x10 L=0.7U W=6.0U

.ENDS INVO1

.SUBCKT INVO2 in out vdd 0

J0 out in vdd vdd tp0.7x10 L=0.7U W=6U

J01 out in vdd vdd tp0.7x10 L=0.7U W=6U

J1 out in 0 0 tn0.7x10 L=0.7U W=6U

J11 out in 0 0 tn0.7x10 L=0.7U W=6U

.ENDS INVO2

.SUBCKT INVO3 in out vdd 0

J0 out in vdd vdd tp0.7x10 L=0.7U W=6U

J01 out in vdd vdd tp0.7x10 L=0.7U W=6U

J02 out in vdd vdd tp0.7x10 L=0.7U W=6U

J03 out in vdd vdd tp0.7x10 L=0.7U W=6U

J1 out in 0 0 tn0.7x10 L=0.7U W=6U

J11 out in 0 0 tn0.7x10 L=0.7U W=6U

J12 out in 0 0 tn0.7x10 L=0.7U W=6U

J13 out in 0 0 tn0.7x10 L=0.7U W=6U

.ENDS INVO3

.SUBCKT INVO4 in out vdd 0

J00 vdd in out vdd tp0.7x10 L=0.7U W=10U

J01 vdd in out vdd tp0.7x10 L=0.7U W=10U

J02 vdd in out vdd tp0.7x10 L=0.7U W=10U

J03 vdd in out vdd tp0.7x10 L=0.7U W=10U

J04 vdd in out vdd tp0.7x10 L=0.7U W=10U

J05 vdd in out vdd tp0.7x10 L=0.7U W=10U

J06 vdd in out vdd tp0.7x10 L=0.7U W=10U

J07 vdd in out vdd tp0.7x10 L=0.7U W=10U

J1 out in 0 0 tn0.7x10 L=0.7U W=10U

J11 out in 0 0 tn0.7x10 L=0.7U W=10U

J12 out in 0 0 tn0.7x10 L=0.7U W=10U

J13 out in 0 0 tn0.7x10 L=0.7U W=10U

J14 out in 0 0 tn0.7x10 L=0.7U W=10U

.ENDS INVO4

.SUBCKT OUTDRIVER in out vdd 0

X1 in 3 vdd 0 INVO1

X2 3 4 vdd 0 INVO2

X3 4 5 vdd 0 INVO3

X4 5 out vdd 0 INVO4

c1 out 0 5pf

R1 out 0 50

.ENDS OUTDRIVER

****

*   SHAPING CIRCUIT   **

****

.SUBCKT INVS1 in out vdd 0

J0 out in vdd vdd tp0.7x10 L=0.7U W=6U

J01 out in vdd vdd tp0.7x10 L=0.7U W=6U

*J02 out in vdd vdd tp0.7x10 L=0.7U W=6U

J1 out in 0 0 tn0.7x10 L=0.7U W=4U

J11 out in 0 0 tn0.7x10 L=0.7U W=4U

.ENDS INVS1

.SUBCKT INVS2 in out vdd 0

J0 out in vdd vdd tp0.7x10 L=0.7U W=6U

J01 out in vdd vdd tp0.7x10 L=0.7U W=6U

J02 out in vdd vdd tp0.7x10 L=0.7U W=6U

J03 out in vdd vdd tp0.7x10 L=0.7U W=6U

J1 out in 0 0 tn0.7x10 L=0.7U W=6U

J11 out in 0 0 tn0.7x10 L=0.7U W=6U

J12 out in 0 0 tn0.7x10 L=0.7U W=6U

J13 out in 0 0 tn0.7x10 L=0.7U W=6U

J14 out in 0 0 tn0.7x10 L=0.7U W=6U

.ENDS INVS2

.SUBCKT INVS1BAR in out vdd 0

J0 out in vdd vdd tp0.7x10 L=0.7U W=4U

J01 out in vdd vdd tp0.7x10 L=0.7U W=4U

J1 out in 0 0 tn0.7x10 L=0.7U W=6U

J11 out in 0 0 tn0.7x10 L=0.7U W=6U

.ENDS INVS1BAR

.SUBCKT INVS2BAR in out vdd 0

J0 out in vdd vdd tp0.7x10 L=0.7U W=6U

J01 out in vdd vdd tp0.7x10 L=0.7U W=6U

J02 out in vdd vdd tp0.7x10 L=0.7U W=6U

J1 out in 0 0 tn0.7x10 L=0.7U W=6U

J11 out in 0 0 tn0.7x10 L=0.7U W=6U

J12 out in 0 0 tn0.7x10 L=0.7U W=6U

J13 out in 0 0 tn0.7x10 L=0.7U W=6U

.ENDS INVS2BAR

****

**   main circuit   **

****

X1 clock 3 vdd 0 INPUTDRIVER

X2 3 phi1 phi2 phi1bar phi2bar vdd 0 GEN

X3 phi1 phi11 vdd 0 INVS1

X4 phi2 phi21 vdd 0 INVS1

X5 phi1bar phi11bar vdd 0 INVS1BAR

X6 phi2bar phi21bar vdd 0 INVS1BAR

X7 phi11 phi12 vdd 0 INVS2

X8 phi21 phi22 vdd 0 INVS2

X9 phi11bar phi12bar vdd 0 INVS2BAR

X10 phi21bar phi22bar vdd 0 INVS2BAR

X11 phi12 phi12bar phi22 phi22bar Q0 Q1 Q2 vdd 0 DLFSR

X12 Q0 Q0out vdd 0 OUTDRIVER

X13 Q1 Q1out vdd 0 OUTDRIVER

X14 Q2 Q2out vdd 0 OUTDRIVER

*Type of analysis

.option dcon=1 post

.tran 100ps 16ns

.MEAS avg_power avg power

.end

A.6   CGaAs TPDL F1 GENERATOR IC

$* F_1 = (\overline{\overline{(A+B)}+C})$

*proceeded by the input receiver then clock generator then DLFSR

* and followed by the output driver

* File name   : df1loaded.sp

* Directory name   : shehata/thesis/run1/dfunction

* Minimum clock time   : 1.22ns

* Total average power : 172mW

* Last correction date : Dec./12/95

.include /home5/shehata/thesis/run1/parameters

*power supply

vdd vdd 0 2.0

*input and output signals

vclock_in clock 0 pulse(0 1.75 0ns .01ns .01ns 0.6ns 1.22ns)

****

**   INPUT DRIVER CIRCUIT   **

****

.SUBCKT INVI1 in out vdd 0

J0 out in vdd vdd tp0.7x10 L=0.7U W=6.0U

J1 out in 0 0 tn0.7x10 L=0.7U W=5.6U

.ENDS INVI1

.SUBCKT INVI2 in out vdd 0

J0 out in vdd vdd tp0.7x10 L=0.7U W=6.0U

J1 out in 0 0 tn0.7x10 L=0.7U W=6.0U

J2 out in vdd vdd tp0.7x10 L=0.7U W=6.0U

J3 out in 0 0 tn0.7x10 L=0.7U W=6.0U

.ENDS INVI2

.SUBCKT INVI3 in out vdd 0
J0 out in vdd vdd tp0.7x10 L=0.7U W=6.0U
J1 out in 0 0 tn0.7x10 L=0.7U W=6.0U
J2 out in vdd vdd tp0.7x10 L=0.7U W=6.0U
J3 out in 0 0 tn0.7x10 L=0.7U W=6.0U
J4 out in vdd vdd tp0.7x10 L=0.7U W=6.0U
J5 out in 0 0 tn0.7x10 L=0.7U W=6.0U
J6 out in vdd vdd tp0.7x10 L=0.7U W=6.0U
J7 out in 0 0 tn0.7x10 L=0.7U W=6.0U
J8 out in vdd vdd tp0.7x10 L=0.7U W=6.0U
J9 out in 0 0 tn0.7x10 L=0.7U W=6.0U
J10 out in vdd vdd tp0.7x10 L=0.7U W=6.0U
J11 out in 0 0 tn0.7x10 L=0.7U W=6.0U
.ENDS INVI3

.SUBCKT INPUTDRIVER in out vdd 0
X1 in 4 vdd 0 INVI1
X2 4 5 vdd 0 INVI2
X3 5 6 vdd 0 INVI3
X4 6 out vdd 0 INVI3
.ENDS INPUTDRIVER
****
**   GENERATOR CIRCUIT   **
****
.SUBCKT INVG in out vdd 0
J0 out in vdd vdd tp0.7x10 L=0.7U W=4.0U

J1 out in 0 0 tn0.7x10 L=0.7U W=2.0U

.ENDS INVG

.SUBCKT INVG1 in out vdd 0

J0 out in vdd vdd tp0.7x10 L=0.7U W=6.0U

J1 out in 0 0 tn0.7x10 L=0.7U W=2.0U

.ENDS INVG1

.SUBCKT INVG2 in out vdd 0

J0 out in vdd vdd tp0.7x10 L=0.7U W=3.0U

J1 out in 0 0 tn0.7x10 L=0.7U W=3.0U

.ENDS INVG2

.SUBCKT INVG3 in out vdd 0

J0 out in vdd vdd tp0.7x10 L=0.7U W=5.0U

J1 out in 0 0 tn0.7x10 L=0.7U W=3.0U

.ENDS INVG3

.SUBCKT INVG4 in out vdd 0

J0 out in vdd vdd tp0.7x10 L=0.7U W=6.0U

J1 out in 0 0 tn0.7x10 L=0.7U W=4.0U

.ENDS INVG4

.SUBCKT NANDG1 A B out vdd 0

J0 out A vdd vdd tp0.7x10 L=0.7U W=4.0U

J1 out B vdd vdd tp0.7x10 L=0.7U W=4.0U

J2 out B 4 0 tn0.7x10 L=0.7U W=2.0U

J3 4 A 0 0 tn0.7x10 L=0.7U W=2.0U

.ENDS NANDG1

.SUBCKT NANDG2 A B out vdd 0
J0 out A vdd vdd tp0.7x10 L=0.7U W=7.5U
J1 out B vdd vdd tp0.7x10 L=0.7U W=7.5U
J2 out B 4 0 tn0.7x10 L=0.7U W=3.8U
J3 4 A 0 0 tn0.7x10 L=0.7U W=3.8U
.ENDS NANDG2

.SUBCKT PHI1PHI2 clock_in phi1_out phi2_out vdd 0
X1 clock_in 3 vdd 0 INVG
X2 5 3 4 vdd 0 NANDG1
X5 4 clock_in 5 vdd 0 NANDG2
X6 4 6 vdd 0 INVG1
X7 5 7 vdd 0 INVG1
X8 6 phi1_out vdd 0 INVG2
X9 7 phi2_out vdd 0 INVG2
.ENDS PHI1PHI2

.SUBCKT TGG in out vdd 0
J0 in 0 out vdd tp0.7x10 L=0.7U W=2.0U
J1 out vdd in 0 tn0.7x10 L=0.7U W=2.0U
.ENDS TGG

.SUBCKT PHI-PHI phi_in phi_out phibar_out vdd 0
X1 phi_in 4 vdd 0 TGG
X2 phi_in 3 vdd 0 INVG
X3 3 phi_out vdd 0 INVG3

X4 4 phibar_out vdd 0 INVG4

.ENDS PHI-PHI

.SUBCKT GEN clock phi1 phi2 phi1bar phi2bar vdd 0

X1 clock 3 4 vdd 0 PHI1PHI2

X2 3 phi1 phi1bar vdd 0 PHI-PHI

X3 4 phi2 phi2bar vdd 0 PHI-PHI

.ENDS GEN

****
**   3 BITS DYNAMIC LFSR CIRCUIT   **
****

.SUBCKT TG in phi phibar out vdd 0

J0 in phi out vdd tp0.7x10 L=0.7U W=2.0U

J1 out phibar in 0 tn0.7x10 L=0.7U W=2.0U

.ENDS TG

.SUBCKT DINV in phi out vdd 0

J0 out phi vdd vdd tp0.7x10 L=0.7U W=7.0U

J1 out phi 5 0 tn0.7x10 L=0.7U W=2.0U

J2 5 in 0 0 tn0.7x10 L=0.7U W=2.5U

.ENDS DINV

.SUBCKT DNAND A B phi out vdd 0

J0 out phi vdd vdd tp0.7x10 L=0.7U W=10.0U

J1 out phi 5 0 tn0.7x10 L=0.7U W=3.0U

J2 5 A 7 0 tn0.7x10 L=0.7U W=4.0U

J3 7 B 0 0 tn0.7x10 L=0.7U W=4.0U

.ENDS DNAND

.SUBCKT DNAND1 A B phi out vdd 0

J0 out phi vdd vdd tp0.7x10 L=0.7U W=10.0U

J1 out phi 5 0 tn0.7x10 L=0.7U W=3.0U

J2 5 A 7 0 tn0.7x10 L=0.7U W=3.0U

J3 7 B 0 0 tn0.7x10 L=0.7U W=3.0U

.ENDS DNAND1

.SUBCKT SNAND A B out vdd 0

J0 out A vdd vdd tp0.7x10 L=0.7U W=4.0U

J1 out B vdd vdd tp0.7x10 L=0.7U W=4.0U

J2 5 A 0 0 tn0.7x10 L=0.7U W=2.0U

J3 out B 5 0 tn0.7x10 L=0.7U W=2.0U

.ENDS SNAND

.SUBCKT DFF D phi1 phi1bar phi2 phi2bar out vdd 0

X1 D phi1 phi1bar 8 vdd 0 TG

X2 8 phi1 9 vdd 0 DINV

X3 9 phi2 phi2bar 10 vdd 0 TG

X4 10 phi2 out vdd 0 DINV

.ENDS DFF

.SUBCKT DXOR A B phi1 phi1bar phi2 phi2bar out vdd 0

X1 A phi1 phi1bar 9 vdd 0 TG

X2 B phi1 phi1bar 10 vdd 0 TG

X3 9 10 11 vdd 0 SNAND

X4 9 11 phi1 12 vdd 0 DNAND

X5 10 11 phi1 13 vdd 0 DNAND

X6 12 phi2 phi2bar 14 vdd 0 TG

X7 13 phi2 phi2bar 15 vdd 0 TG

X8 14 15 phi2 out vdd 0 DNAND1

.ENDS DXOR

.SUBCKT SINV in out vdd 0

J0 out in vdd vdd tp0.7x10 L=0.7U W=4.0U

J1 out in 0 0 tn0.7x10 L=0.7U W=2.0U

.ENDS SINV

.SUBCKT DLFSR phi1 phi1bar phi2 phi2bar Q0 Q1 Q2 vdd 0

X1 Q0 phi1 phi1bar phi2 phi2bar Q1 vdd 0 DFF

X2 Q1 phi1 phi1bar phi2 phi2bar Q2 vdd 0 DFF

X3 Q1 Q2 phi1 phi1bar phi2 phi2bar Q0 vdd 0 DXOR

.ENDS DLFSR

****

**   DYNAMIC FUNCTION GENERATOR CIRCUIT   **

****

.SUBCKT TGF in phi phibar out vdd 0

J0 in phi out vdd tp0.7x10 L=0.7U W=2.0U

J1 out phibar in 0 tn0.7x10 L=0.7U W=2.0U

.ENDS TGF

.SUBCKT FUNC A B phi out vdd 0

J0 out phi vdd vdd tp0.7x10 L=0.7U W=4.0U

J1 out phi 12 0 tn0.7x10 L=0.7U W=2.0U

J2 12 A 0 0 tn0.7x10 L=0.7U W=2.0U

J3 12 B 0 0 tn0.7x10 L=0.7U W=2.0U

.ENDS FUNC

.SUBCKT DF1 A B C phi1 phi2 phi1bar phi2bar out vdd 0

X1 A phi1 phi1bar 10 vdd 0 TGF

X2 B phi1 phi1bar 11 vdd 0 TGF

X3 10 11 phi1 13 vdd 0 FUNC

X4 C phi2 phi2bar 15 vdd 0 TGF

X5 13 phi2 phi2bar 14 vdd 0 TGF

X6 14 15 phi2 out vdd 0 FUNC

.ENDS DF1

****

**   OUTPUT DRIVER CIRCUIT FOR Q SIGNALS   **

****

.SUBCKT INVO1 in out vdd 0

J0 out in vdd vdd tp0.7x10 L=0.7U W=6.0U

J1 out in 0 0 tn0.7x10 L=0.7U W=6.0U

.ENDS INVO1

.SUBCKT INVO2 in out vdd 0

J0 out in vdd vdd tp0.7x10 L=0.7U W=6U

J01 out in vdd vdd tp0.7x10 L=0.7U W=6U

J1 out in 0 0 tn0.7x10 L=0.7U W=6U

J11 out in 0 0 tn0.7x10 L=0.7U W=6U

.ENDS INVO2

.SUBCKT INVO3 in out vdd 0

J0 out in vdd vdd tp0.7x10 L=0.7U W=6U

J01 out in vdd vdd tp0.7x10 L=0.7U W=6U

J02 out in vdd vdd tp0.7x10 L=0.7U W=6U

J03 out in vdd vdd tp0.7x10 L=0.7U W=6U

J1 out in 0 0 tn0.7x10 L=0.7U W=6U

J11 out in 0 0 tn0.7x10 L=0.7U W=6U

J12 out in 0 0 tn0.7x10 L=0.7U W=6U

J13 out in 0 0 tn0.7x10 L=0.7U W=6U

.ENDS INVO3

.SUBCKT INVO4 in out vdd 0

J0 vdd in out vdd tp0.7x10 L=0.7U W=10U

J01 vdd in out vdd tp0.7x10 L=0.7U W=10U

J02 vdd in out vdd tp0.7x10 L=0.7U W=10U

J03 vdd in out vdd tp0.7x10 L=0.7U W=10U

J04 vdd in out vdd tp0.7x10 L=0.7U W=10U

J05 vdd in out vdd tp0.7x10 L=0.7U W=10U

J06 vdd in out vdd tp0.7x10 L=0.7U W=10U

J07 vdd in out vdd tp0.7x10 L=0.7U W=10U

J1 out in 0 0 tn0.7x10 L=0.7U W=10U

J11 out in 0 0 tn0.7x10 L=0.7U W=10U

J12 out in 0 0 tn0.7x10 L=0.7U W=10U

J13 out in 0 0 tn0.7x10 L=0.7U W=10U

J14 out in 0 0 tn0.7x10 L=0.7U W=10U

.ENDS INVO4

.SUBCKT OUTDRIVER in out vdd 0

X1 in 3 vdd 0 INVO1

X2 3 4 vdd 0 INVO2

X3 4 5 vdd 0 INVO3

X4 5 out vdd 0 INVO4

c1 out 0 5pf

R1 out 0 50

.ENDS OUTDRIVER

****

**   SHAPING CIRCUIT   **

****

.SUBCKT INVS1 in out vdd 0

J0 out in vdd vdd tp0.7x10 L=0.7U W=6U

J01 out in vdd vdd tp0.7x10 L=0.7U W=6U

J1 out in 0 0 tn0.7x10 L=0.7U W=4U

J11 out in 0 0 tn0.7x10 L=0.7U W=4U

.ENDS INVS1

.SUBCKT INVS2 in out vdd 0

J0 out in vdd vdd tp0.7x10 L=0.7U W=6U

J01 out in vdd vdd tp0.7x10 L=0.7U W=6U

J02 out in vdd vdd tp0.7x10 L=0.7U W=6U

J03 out in vdd vdd tp0.7x10 L=0.7U W=6U

J1 out in 0 0 tn0.7x10 L=0.7U W=6U

J11 out in 0 0 tn0.7x10 L=0.7U W=6U

J12 out in 0 0 tn0.7x10 L=0.7U W=6U

J13 out in 0 0 tn0.7x10 L=0.7U W=6U

J14 out in 0 0 tn0.7x10 L=0.7U W=6U

.ENDS INVS2

.SUBCKT INVS1BAR in out vdd 0

220

J0 out in vdd vdd tp0.7x10 L=0.7U W=4U

J01 out in vdd vdd tp0.7x10 L=0.7U W=4U

J1 out in 0 0 tn0.7x10 L=0.7U W=6U

J11 out in 0 0 tn0.7x10 L=0.7U W=6U

.ENDS INVS1BAR

.SUBCKT INVS2BAR in out vdd 0

J0 out in vdd vdd tp0.7x10 L=0.7U W=6U

J01 out in vdd vdd tp0.7x10 L=0.7U W=6U

J02 out in vdd vdd tp0.7x10 L=0.7U W=6U

J1 out in 0 0 tn0.7x10 L=0.7U W=6U

J11 out in 0 0 tn0.7x10 L=0.7U W=6U

J12 out in 0 0 tn0.7x10 L=0.7U W=6U

J13 out in 0 0 tn0.7x10 L=0.7U W=6U

.ENDS INVS2BAR

****
**   main circuit   **
****

X1 clock 3 vdd 0 INPUTDRIVER

X2 3 phi1 phi2 phi1bar phi2bar vdd 0 GEN

X3 phi1 phi11 vdd 0 INVS1

X4 phi2 phi21 vdd 0 INVS1

X5 phi1bar phi11bar vdd 0 INVS1BAR

X6 phi2bar phi21bar vdd 0 INVS1BAR

X7 phi11 phi12 vdd 0 INVS2

X8 phi21 phi22 vdd 0 INVS2

X9 phi11bar phi12bar vdd 0 INVS2BAR

X10 phi21bar phi22bar vdd 0 INVS2BAR

221

X11 phi12 phi12bar phi22 phi22bar Q0 Q1 Q2 vdd 0 DLFSR

X12 Q0 Q1 0 phi12 phi22 phi12bar phi22bar out vdd 0 DF1

X13 out outout vdd 0 OUTDRIVER

*Type of analysis

.option dcon=1 post

.tran 100ps 25ns

.MEAS avg_power avg power

.end

A.7   CGaAs STATIC 4-BIT CLA CIRCUIT

* File name   : scla.sp

* Directory name   : shehata/thesis/cla_adder/static

* Minimum clock time   : 3.82ns (0.26 GHz)

* Total average power : 26mW

* Last correction date : April,23, 96

.include /home5/shehata/thesis/cla_adder/parameters

*power supply

vdd vdd 0 1.75

vdd1 vdd1 0 1.75

*Input vectors

vinA0 A0 0 1.75

*vinA0 A0 0 pulse(0 1.75 0ns 0.01ns 0.01ns 1.7ns 3.42ns)

vinB0 B0 0 0.0

*vinB0 B0 0 pulse(0 1.75 0ns 0.01ns 0.01ns 1.7ns 3.42ns)

vinA1 A1 0 0.0

*vinA1 A1 0 pulse(0 1.75 0ns 0.01ns 0.01ns 1.7ns 3.42ns)

vinB1 B1 0 1.75

*vinB1 B1 0 pulse(0 1.75 0ns 0.01ns 0.01ns 1.7ns 3.42ns)

vinA2 A2 0 0.0

*vinA2 A2 0 pulse(0 1.75 0ns 0.01ns 0.01ns 1.7ns 3.42ns)

vinB2 B2 0 1.75

*vinB2 B2 0 pulse(0 1.75 0ns 0.01ns 0.01ns 1.7ns 3.42ns)

vinA3 A3 0 0.0

*vinA3 A3 0 pulse(0 1.75 0ns 0.01ns 0.01ns 1.7ns 3.42ns)

vinB3 B3 0 1.75

*vinB3 B3 0 pulse(0 1.75 0ns 0.01ns 0.01ns 1.7ns 3.42ns)

*vinCin Cin 0 0.0

223

vinCin Cin 0 pulse(0 1.75 0ns 0.01ns 0.01ns 1.90ns 3.82ns)

.SUBCKT SINV in out vdd 0
J0 out in vdd vdd tp0.7x10 L=0.7U W=8.0U
J1 out in 0 0 tn0.7x10 L=0.7U W=4.0U
.ENDS SINV

.SUBCKT SNAND A B out vdd 0
J0 out A vdd vdd tp0.7x10 L=0.7U W=8.0U
J1 out B vdd vdd tp0.7x10 L=0.7U W=8.0U
J2 5 A 0 0 tn0.7x10 L=0.7U W=4.0U
J3 out B 5 0 tn0.7x10 L=0.7U W=4.0U
.ENDS SNAND

.SUBCKT SAND A B out vdd 0
X1 A B 5 vdd 0 SNAND
X2 5 out vdd 0 SINV
.ENDS SAND

.SUBCKT SXOR A B out vdd 0
.
X1 A B 5 vdd 0 SNAND
X2 A 5 6 vdd 0 SNAND
X3 5 B 7 vdd 0 SNAND
X4 6 7 out vdd 0 SNAND
.ENDS SXOR

.SUBCKT PG A0 B0 A1 B1 A2 B2 A3 B3 P0 G0 P1 G1 P2 G2 P3 G3 vdd 0
X1 A0 B0 P0 vdd 0 SXOR

224

X2 A0 B0 G0 vdd 0 SAND

X3 A1 B1 P1 vdd 0 SXOR

X4 A1 B1 G1 vdd 0 SAND

X5 A2 B2 P2 vdd 0 SXOR

X6 A2 B2 G2 vdd 0 SAND

X7 A3 B3 P3 vdd 0 SXOR

X8 A3 B3 G3 vdd 0 SAND

.ENDS PG

.SUBCKT CZERO Cin P0 G0 out vdd 0

J0 6 Cin vdd vdd tp0.7x10 L=0.7U W=8.0U

J1 6 P0 vdd vdd tp0.7x10 L=0.7U W=8.0U

J2 5 G0 6 vdd tp0.7x10 L=0.7U W=8.0U

J3 5 P0 7 0 tn0.7x10 L=0.7U W=3.0U

J4 7 Cin 0 0 tn0.7x10 L=0.7U W=4.0U

J5 5 G0 0 0 tn0.7x10 L=0.7U W=4.0U

X1 5 out vdd 0 SINV

.ENDS CZERO

.SUBCKT CONE G1 G0 P1 P0 Cin out vdd 0

J0 8 P0 vdd vdd tp0.7x10 L=0.7U W=8.0U

J1 8 Cin vdd vdd tp0.7x10 L=0.7U W=8.0U

J2 8 P1 vdd vdd tp0.7x10 L=0.7U W=8.0U

J3 9 G0 8 vdd tp0.7x10 L=0.7U W=8.0U

J4 9 P1 8 vdd tp0.7x10 L=0.7U W=8.0U

J5 7 G1 9 vdd tp0.7x10 L=0.7U W=8.0U

J6 7 P0 10 0 tn0.7x10 L=0.7U W=2.0U

J7 10 Cin 11 0 tn0.7x10 L=0.7U W=3.0U

J8 11 P1 0 0 tn0.7x10 L=0.7U W=4.0U

J9 7 P1 12 0 tn0.7x10 L=0.7U W=3.0U

J10 12 G0 0 0 tn0.7x10 L=0.7U W=4.0U

J11 7 G1 0 0 tn0.7x10 L=0.7U W=4.0U

X1 7 out vdd 0 SINV

.ENDS CONE

.SUBCKT CTWO G2 G1 G0 P2 P1 P0 Cin out vdd 0

J0 10 P2 vdd vdd tp0.7x10 L=0.7U W=8.0U

J1 10 P1 vdd vdd tp0.7x10 L=0.7U W=8.0U

J2 10 P0 vdd vdd tp0.7x10 L=0.7U W=8.0U

J3 10 Cin vdd vdd tp0.7x10 L=0.7U W=8.0U

J4 11 P2 10 vdd tp0.7x10 L=0.7U W=8.0U

J5 11 P1 10 vdd tp0.7x10 L=0.7U W=8.0U

J6 11 G0 10 vdd tp0.7x10 L=0.7U W=8.0U

J7 12 P2 11 vdd tp0.7x10 L=0.7U W=8.0U

J8 12 G1 11 vdd tp0.7x10 L=0.7U W=8.0U

J9 9 G2 12 vdd tp0.7x10 L=0.7U W=8.0U

J10 9 P2 13 0 tn0.7x10 L=0.7U W=2.0U

J11 13 P1 14 0 tn0.7x10 L=0.7U W=3.0U

J12 14 P0 15 0 tn0.7x10 L=0.7U W=4.0U

J13 15 Cin 0 0 tn0.7x10 L=0.7U W=4.0U

J14 9 P2 16 0 tn0.7x10 L=0.7U W=2.0U

J15 16 P1 17 0 tn0.7x10 L=0.7U W=3.0U

J16 17 G0 0 0 tn0.7x10 L=0.7U W=4.0U

J17 9 P2 18 0 tn0.7x10 L=0.7U W=3.0U

J18 18 G1 0 0 tn0.7x10 L=0.7U W=4.0U

J19 9 G2 0 0 tn0.7x10 L=0.7U W=4.0U

```
X1 9 out vdd 0 SINV
.ENDS CTWO


.SUBCKT PASTRIC P3 P2 P1 P0 out vdd 0
J0 6 P3 vdd vdd tp0.7x10 L=0.7U W=8.0U
J1 6 P2 vdd vdd tp0.7x10 L=0.7U W=8.0U
J2 6 P1 vdd vdd tp0.7x10 L=0.7U W=8.0U
J3 6 P0 vdd vdd tp0.7x10 L=0.7U W=8.0U
J4 6 P3 7 0 tn0.7x10 L=0.7U W=2.0U
J5 7 P2 8 0 tn0.7x10 L=0.7U W=3.0U
J6 8 P1 9 0 tn0.7x10 L=0.7U W=4.0U
J7 9 P0 0 0 tn0.7x10 L=0.7U W=4.0U
X1 6 out vdd 0 SINV
.ENDS PASTRIC


.SUBCKT GASTRIC G3 G2 G1 G0 P3 P2 P1 out vdd 0
J0 10 G0 vdd vdd tp0.7x10 L=0.7U W=8.0U
J1 10 P1 vdd vdd tp0.7x10 L=0.7U W=8.0U
J2 10 P2 vdd vdd tp0.7x10 L=0.7U W=8.0U
J3 10 P3 vdd vdd tp0.7x10 L=0.7U W=8.0U
J4 11 G1 10 vdd tp0.7x10 L=0.7U W=8.0U
J5 11 P2 10 vdd tp0.7x10 L=0.7U W=8.0U
J6 11 P3 10 vdd tp0.7x10 L=0.7U W=8.0U
J7 12 G2 11 vdd tp0.7x10 L=0.7U W=8.0U
J8 12 P3 11 vdd tp0.7x10 L=0.7U W=8.0U
J9 9 G3 12 vdd tp0.7x10 L=0.7U W=8.0U
J10 9 G3 0 0 tn0.7x10 L=0.7U W=4.0U
J11 9 P3 18 0 tn0.7x10 L=0.7U W=3.0U
```

J12 18 G2 0 0 tn0.7x10 L=0.7U W=4.0U

J13 9 P3 16 0 tn0.7x10 L=0.7U W=2.0U

J14 16 P2 17 0 tn0.7x10 L=0.7U W=3.0U

J15 17 G1 0 0 tn0.7x10 L=0.7U W=4.0U

J16 9 P3 13 0 tn0.7x10 L=0.7U W=2.0U

J17 13 P2 14 0 tn0.7x10 L=0.7U W=3.0U

J18 14 P1 15 0 tn0.7x10 L=0.7U W=4.0U

J19 15 G0 0 0 tn0.7x10 L=0.7U W=4.0U

X1 9 out vdd 0 SINV

.ENDS GASTRIC

.SUBCKT COUT1 GAST PAST Cin out vdd 0

J0 6 PAST vdd vdd tp0.7x10 L=0.7U W=8.0U

J1 6 Cin vdd vdd tp0.7x10 L=0.7U W=8.0U

J2 5 GAST 6 vdd tp0.7x10 L=0.7U W=8.0U

J3 5 PAST 7 0 tn0.7x10 L=0.7U W=3.0U

J4 7 Cin 0 0 tn0.7x10 L=0.7U W=4.0U

J5 5 GAST 0 0 tn0.7x10 L=0.7U W=4.0U

X1 5 out vdd 0 SINV

.ENDS COUT1

.SUBCKT COUT G3 G2 G1 G0 P3 P2 P1 P0 Cin out vdd 0

X1 G3 G2 G1 G0 P3 P2 P1 12 vdd 0 GASTRIC

X2 P3 P2 P1 P0 13 vdd 0 PASTRIC

X4 12 13 Cin out vdd 0 COUT1

.ENDS COUT

****

*   main circuit   **

228

```
**************************************************

X1 A0 B0 A1 B1 A2 B2 A3 B3 P0 G0 P1 G1 P2 G2 P3 G3 vdd1 0 PG

X2 Cin P0 G0 C0 vdd1 0 CZERO

X3 19 G0 P1 P0 Cin C1 vdd1 0 CONE

X4 G2 G1 G0 P2 P1 P0 Cin C2 vdd1 0 CTWO

X5 G3 G2 G1 G0 P3 P2 P1 P0 Cin Cout vdd1 0 COUT

X6 Cin P0 S0 vdd1 0 SXOR

X7 C0 P1 S1 vdd1 0 SXOR

X8 C1 P2 S2 vdd1 0 SXOR

X9 C2 P3 S3 vdd1 0 SXOR


*loading circuit

X10 S0 S00 vdd 0 SINV

X11 S1 S10 vdd 0 SINV

X12 S2 S20 vdd 0 SINV

X13 S3 S30 vdd 0 SINV

X14 Cout Cout0 vdd 0 SINV

X15 S0 S01 vdd 0 SINV

X16 S1 S11 vdd 0 SINV

X17 S2 S21 vdd 0 SINV

X18 S3 S31 vdd 0 SINV

X19 Cout Cout1 vdd 0 SINV


*Type of analysis

.option dcon=1 post

.tran 100ps 25ns

*.DC vinA 0 1.8 .01
```

```
*measurements
.MEAS avg_power avg power
.MEAS TRAN Avg_P_VDD AVG P(vdd) FROM=0.0ns TO=20ns
.MEAS TRAN Avg_P_VDD1 AVG P(vdd1) FROM=0.0ns TO=25ns
.MEAS TRAN Avg_P_VC AVG P(vinCin) FROM=0.0ns TO=20ns
.MEAS TRAN Avg_P_VA AVG P(vinA0) FROM=0.0ns TO=20ns
.MEAS TRAN Avg_P_VB AVG P(vinB0) FROM=0.0ns TO=20ns

.MEAS TRAN Avg_I_VDD AVG I(vdd) FROM=0.0ns TO=15ns
.MEAS TRAN Avg_I_VDD1 AVG I(vdd1) FROM=0.0ns TO=15ns
.MEAS TRAN Avg_I_VA AVG I(vinCin) FROM=0.0ns TO=15ns
.MEAS TRAN Avg_I_VB AVG I(vinB) FROM=0.0ns TO=15ns

.MEAS max_power max power
.MEAS rms_power rms power
.MEAS tphls3 trig v(cin) val='0.85' rise=2
+targ v(s3) val='0.85' fall=2
.MEAS tplhs3 trig v(cin) val='0.85' fall=2
+targ v(s3) val='0.85' rise=2
.MEAS tphlcout trig v(cin) val='0.85' rise=2
+targ v(cout) val='0.85' rise=2
.MEAS tplhcout trig v(cin) val='0.85' fall=2
+targ v(cout) val='0.85' fall=2
.end
```

A.8   CGaAs TPDL 4-BIT CLA IC

* File name   : cla.sp

* Directory name   : shehata/thesis/cla_adder/2phase

* Minimum clock time : 0.82ns (1.22 GHz)

* Total average power: 61.79 mW

* Last correction date: April,23, 96

.include /home5/shehata/thesis/cla_adder/parameters

*power supply

vdd vdd 0 1.75

vdd1 vdd1 0 1.75

* Input clocks

vinphi1 phi1 0 pulse(0 1.75 0ns .01ns .01ns 0.45ns 0.82ns)

vin-phi1 phi1bar 0 pulse(1.75 0 0ns .01ns .01ns 0.45ns 0.82ns)

vinphi2 phi2 0 pulse(0 1.75 0.41ns .01ns .01nus 0.45ns 0.82ns)

vin-phi2 phi2bar 0 pulse(1.75 0 0.41ns .01ns .01ns 0.45ns 0.82ns)

*Input vectors

vinA0 A0 0 1.75

*vinA0 A0 0 pulse(0 1.75 0.2ns 0.01ns 0.01ns 0.81ns 1.64ns)

vinB0 B0 0 0.0

*vinB0 B0 0 pulse(0 1.75 0.2ns 0.01ns 0.01ns 0.81ns 1.64ns)

vinA1 A1 0 0.0

*vinA1 A1 0 pulse(0 1.75 0.2ns 0.01ns 0.01ns 0.81ns 1.64ns)

vinB1 B1 0 1.75

*vinB1 B1 0 pulse(0 1.75 0.2ns 0.01ns 0.01ns 0.81ns 1.64ns)

vinA2 A2 0 1.75

*vinA2 A2 0 pulse(0 1.75 6.0ns 0.01ns 0.01ns 0.81ns 1.64ns)

vinB2 B2 0 0.0

*vinB2 B2 0 pulse(0 1.75 0.2ns 0.01ns 0.01ns 0.81ns 1.64ns)

231

vinA3 A3 0 0.0

*vinA3 A3 0 pulse(0 1.75 0.2ns 0.01ns 0.01ns 0.81ns 1.64ns)

vinB3 B3 0 1.75

*vinB3 B3 0 pulse(0 1.75 0.5ns 0.01ns 0.01ns 0.81ns 1.64ns)

*vinCin Cin 0 1.75

vinCin Cin 0 pulse(0 1.75 0.2ns 0.01ns 0.01ns 0.81ns 1.64ns)

****

**   CLA GENERATOR CIRCUIT   **

****

.SUBCKT TG in phi phibar out vdd 0

J0 in phi out vdd tp0.7x10 L=0.7U W=2.0U

J1 out phibar in 0 tn0.7x10 L=0.7U W=2.0U

.ENDS TG

.SUBCKT DNAND A B phi out vdd 0

J0 out phi vdd vdd tp0.7x10 L=0.7U W=10.0U

J1 out phi 5 0 tn0.7x10 L=0.7U W=2.0U

J2 5 A 7 0 tn0.7x10 L=0.7U W=4.0U

J3 7 B 0 0 tn0.7x10 L=0.7U W=4.0U

.ENDS DNAND

.SUBCKT SNAND A B out vdd 0

J0 out A vdd vdd tp0.7x10 L=0.7U W=4.0U

J1 out B vdd vdd tp0.7x10 L=0.7U W=4.0U

J2 5 A 0 0 tn0.7x10 L=0.7U W=2.0U

J3 out B 5 0 tn0.7x10 L=0.7U W=2.0U

.ENDS SNAND

```
.SUBCKT DINV in phi out vdd 0
J0 out phi vdd vdd tp0.7x10 L=0.7U W=10.0U
J1 out phi 5 0 tn0.7x10 L=0.7U W=2.0U
J2 5 in 0 0 tn0.7x10 L=0.7U W=2.0U
.ENDS DINV


.SUBCKT SINV in out vdd 0
J0 out in vdd vdd tp0.7x10 L=0.7U W=4.0U
J1 out in 0 0 tn0.7x10 L=0.7U W=2.0U
.ENDS SINV


.SUBCKT DXOR A B phi1 phi1bar phi2 phi2bar out vdd 0
X1 A phi1 phi1bar 9 vdd 0 TG
X2 B phi1 phi1bar 10 vdd 0 TG
X3 9 10 11 vdd 0 SNAND
X4 9 11 phi1 12 vdd 0 DNAND
X5 10 11 phi1 13 vdd 0 DNAND
X6 12 phi2 phi2bar 14 vdd 0 TG
X7 13 phi2 phi2bar 15 vdd 0 TG
X8 14 15 phi2 out vdd 0 DNAND
.ENDS DXOR


.SUBCKT DAND A B phi1 phi1bar phi2 phi2bar out vdd 0
X1 A phi1 phi1bar 9 vdd 0 TG
X2 B phi1 phi1bar 10 vdd 0 TG
X3 9 10 phi1 11 vdd 0 DNAND
X4 11 phi2 phi2bar 12 vdd 0 TG
X5 12 phi2 out vdd 0 DINV
```

.ENDS DAND

.SUBCKT DELAY 2 4 5 6 7 10 vdd 0

X1 2 4 5 3 vdd 0 TG

X2 3 4 8 vdd 0 DINV

X3 8 6 7 9 vdd 0 TG

X6 9 6 10 vdd 0 DINV

.ENDS DELAY

.SUBCKT PG A0 B0 A1 B1 A2 B2 A3 B3 phi1 phi1bar phi2 phi2bar P0 P1 P2 P3 G0
G1 G2 G3 vdd 0

X1 A0 B0 phi1 phi1bar phi2 phi2bar P0 vdd 0 DXOR

X2 A1 B1 phi1 phi1bar phi2 phi2bar P1 vdd 0 DXOR

X3 A2 B2 phi1 phi1bar phi2 phi2bar P2 vdd 0 DXOR

X4 A3 B3 phi1 phi1bar phi2 phi2bar P3 vdd 0 DXOR

X5 A0 B0 phi1 phi1bar phi2 phi2bar G0 vdd 0 DAND

X6 A1 B1 phi1 phi1bar phi2 phi2bar G1 vdd 0 DAND

X7 A2 B2 phi1 phi1bar phi2 phi2bar G2 vdd 0 DAND

X8 A3 B3 phi1 phi1bar phi2 phi2bar G3 vdd 0 DAND

.ENDS PG

.SUBCKT CZERO P0 G0 Cin phi1 phi1bar phi2 phi2bar out vdd 0

X1 G0 phi1 phi1bar 10 vdd 0 TG

X2 Cin phi1 phi1bar 11 vdd 0 TG

X3 P0 phi1 phi1bar 12 vdd 0 TG

J0 13 phi1 vdd vdd tp0.7x10 L=0.7U W=10.0U

J1 13 phi1 14 0 tn0.7x10 L=0.7U W=2.0U

234

J2 14 10 0 0 tn0.7x10 L=0.7U W=2.0U

J3 14 11 15 0 tn0.7x10 L=0.7U W=3.0U

J4 15 12 0 0 tn0.7x10 L=0.7U W=3.0U

X4 13 phi2 phi2bar 16 vdd 0 TG

X5 16 phi2 out vdd 0 DINV

.ENDS CZERO

.SUBCKT CONE P0 P1 G0 G1 Cin phi1 phi1bar phi2 phi2bar out vdd 0

X1 Cin phi1 phi1bar 12 vdd 0 TG

X2 P0 phi1 phi1bar 13 vdd 0 TG

X3 G0 phi1 phi1bar 14 vdd 0 TG

X4 P1 phi1 phi1bar 15 vdd 0 TG

X5 G1 phi1 phi1bar 16 vdd 0 TG

J0 21 phi1 vdd vdd tp0.7x10 L=0.7U W=10.0U

J1 21 phi1 17 0 tn0.7x10 L=0.7U W=2.0U

J2 17 16 0 0 tn0.7x10 L=0.7U W=2.0U

J3 17 15 18 0 tn0.7x10 L=0.7U W=3.0U

J4 18 14 0 0 tn0.7x10 L=0.7U W=3.0U

J5 17 15 19 0 tn0.7x10 L=0.7U W=3.0U

J6 19 13 20 0 tn0.7x10 L=0.7U W=3.0U

J7 20 12 0 0 tn0.7x10 L=0.7U W=3.0U

X6 21 phi1 phi2bar 22 vdd 0 TG

X7 22 phi2 out vdd 0 DINV

.ENDS CONE

.SUBCKT CTWO P0 P1 P2 G0 G1 G2 Cin phi1 phi1bar phi2 phi2bar out vdd 0

X1 Cin phi1 phi1bar 13 vdd 0 TG

X2 P0 phi1 phi1bar 14 vdd 0 TG

X3 G0 phi1 phi1bar 15 vdd 0 TG

X4 P1 phi1 phi1bar 16 vdd 0 TG

X5 G1 phi1 phi1bar 17 vdd 0 TG

X6 P2 phi1 phi1bar 18 vdd 0 TG

X7 G2 phi1 phi1bar 19 vdd 0 TG

J0 27 phi1 vdd vdd tp0.7x10 L=0.7U W=10.0U

J1 27 phi1 20 0 tn0.7x10 L=0.7U W=2.0U

J2 20 19 0 0 tn0.7x10 L=0.7U W=2.0U

J3 20 18 21 0 tn0.7x10 L=0.7U W=3.0U

J4 21 17 0 0 tn0.7x10 L=0.7U W=3.0U

J5 20 18 22 0 tn0.7x10 L=0.7U W=4.0U

J6 22 16 23 0 tn0.7x10 L=0.7U W=4.0U

J7 23 15 0 0 tn0.7x10 L=0.7U W=4.0U

J8 20 18 24 0 tn0.7x10 L=0.7U W=2.0U

J9 24 16 25 0 tn0.7x10 L=0.7U W=2.0U

J10 25 14 26 0 tn0.7x10 L=0.7U W=4.0U

J11 26 13 0 0 tn0.7x10 L=0.7U W=4.0U

X8 27 phi2 phi2bar 28 vdd 0 TG

X9 28 phi2 out vdd 0 DINV

.ENDS CTWO

.SUBCKT PASTRIC P0 P1 P2 P3 phi1 phi1bar phi2 phi2bar out vdd 0

X1 P0 phi1 phi1bar 11 vdd 0 TG

X2 P1 phi1 phi1bar 12 vdd 0 TG

X3 P2 phi1 phi1bar 13 vdd 0 TG

X4 P3 phi1 phi1bar 14 vdd 0 TG

J0 15 phi1 vdd vdd tp0.7x10 L=0.7U W=10.0U

J1 15 phi1 16 0 tn0.7x10 L=0.7U W=2.0U

J2 16 11 17 0 tn0.7x10 L=0.7U W=4.0U

J3 17 12 18 0 tn0.7x10 L=0.7U W=4.0U

J4 18 13 19 0 tn0.7x10 L=0.7U W=4.0U

J5 19 14 0 0 tn0.7x10 L=0.7U W=4.0U

X5 15 phi2 phi2bar 20 vdd 0 TG

X6 20 phi2 out vdd 0 DINV

.ENDS PASTRIC

.SUBCKT GASTRIC G0 G1 G2 G3 P1 P2 P3 phi1 phi1bar phi2 phi2bar out vdd 0

X1 G3 phi1 phi1bar 13 vdd 0 TG

X2 P3 phi1 phi1bar 14 vdd 0 TG

X3 G2 phi1 phi1bar 15 vdd 0 TG

X4 P2 phi1 phi1bar 16 vdd 0 TG

X5 G1 phi1 phi1bar 17 vdd 0 TG

X6 P1 phi1 phi1bar 18 vdd 0 TG

X7 G0 phi1 phi1bar 19 vdd 0 TG

J0 20 phi1 vdd vdd tp0.7x10 L=0.7U W=10.0U

J1 20 phi1 21 0 tn0.7x10 L=0.7U W=2.0U

J2 21 13 0 0 tn0.7x10 L=0.7U W=2.0U

J3 21 15 22 0 tn0.7x10 L=0.7U W=3.0U

J4 22 14 0 0 tn0.7x10 L=0.7U W=3.0U

J5 21 17 23 0 tn0.7x10 L=0.7U W=4.0U

J6 23 16 24 0 tn0.7x10 L=0.7U W=4.0U

J7 24 14 0 0 tn0.7x10 L=0.7U W=4.0U

J8 21 19 25 0 tn0.7x10 L=0.7U W=4.0U

J9 25 16 26 0 tn0.7x10 L=0.7U W=4.0U

J10 26 18 27 0 tn0.7x10 L=0.7U W=4.0U

J11 27 14 0 0 tn0.7x10 L=0.7U W=4.0U

X8 20 phi2 phi2bar 28 vdd 0 TG

X9 28 phi2 out vdd 0 DINV

.ENDS GASTRIC

.SUBCKT COUT1 GAST PAST Cin phi1 phi1bar phi2 phi2bar out vdd 0

X1 GAST phi1 phi1bar 9 vdd 0 TG

X2 PAST phi1 phi1bar 10 vdd 0 TG

X3 Cin phi1 phi1bar 11 vdd 0 TG

J0 12 phi1 vdd vdd tp0.7x10 L=0.7U W=10.0U

J1 12 phi1 13 0 tn0.7x10 L=0.7U W=2.0U

J2 13 9 0 0 tn0.7x10 L=0.7U W=2.0U

J3 13 10 14 0 tn0.7x10 L=0.7U W=3.0U

J4 14 11 0 0 tn0.7x10 L=0.7U W=3.0U

X4 12 phi2 phi2bar 15 vdd 0 TG

X6 15 phi2 out vdd 0 DINV

.ENDS COUT1

* subcircuit to calculate Cout from Pi, Gi and Cin

* (P0)(P1)(P2)(P3)(G0)(G1)(G2)(G3)(Cin)(phi1)(-phi1)(phi2)(-phi2)(Cout)

.SUBCKT COUT P0 P1 P2 P3 G0 G1 G2 G3 Cin phi1 phi1bar phi2 phi2bar out vdd 0

X1 P0 P1 P2 P3 phi1 phi1bar phi2 phi2bar 16 vdd 0 PASTRIC

X2 G0 G1 G2 G3 P1 P2 P3 phi1 phi1bar phi2 phi2bar 17 vdd 0 GASTRIC

X3 Cin phi1 phi1bar phi2 phi2bar 15 vdd 0 DELAY

X4 17 16 15 phi1 phi1bar phi2 phi2bar out vdd 0 COUT1

.ENDS COUT

****

**   main circuit   **

****

238

X1 A0 B0 A1 B1 A2 B2 A3 B3 phi1 phi1bar phi2 phi2bar 15 16 17 18 19 20 21 22 vdd1 0 PG

X2 Cin phi1 phi1bar phi2 phi2bar 23 vdd1 0 DELAY

X3 23 phi1 phi1bar phi2 phi2bar 24 vdd1 0 DELAY

X4 15 19 23 phi1 phi1bar phi2 phi2bar 29 vdd1 0 CZERO

X5 15 16 19 20 23 phi1 phi1bar phi2 phi2bar 30 vdd1 0 CONE

X6 15 16 17 19 20 21 23 phi1 phi1bar phi2 phi2bar 31 vdd1 0 CTWO

X7 15 phi1 phi1bar phi2 phi2bar 25 vdd1 0 DELAY

X8 16 phi1 phi1bar phi2 phi2bar 26 vdd1 0 DELAY

X9 17 phi1 phi1bar phi2 phi2bar 27 vdd1 0 DELAY

X10 18 phi1 phi1bar phi2 phi2bar 28 vdd1 0 DELAY

X11 25 24 phi1 phi1bar phi2 phi2bar S0 vdd1 0 DXOR

X12 26 29 phi1 phi1bar phi2 phi2bar S1 vdd1 0 DXOR

X13 27 30 phi1 phi1bar phi2 phi2bar S2 vdd1 0 DXOR

X14 28 31 phi1 phi1bar phi2 phi2bar S3 vdd1 0 DXOR

X15 15 16 17 18 19 20 21 22 23 phi1 phi1bar phi2 phi2bar Cout vdd1 0 COUT

****

**   Loading circuit   **

****

X16 S0 phi1 phi1bar phi2 phi2bar S00 vdd 0 DELAY

X17 S0 phi1 phi1bar phi2 phi2bar S01 vdd 0 DELAY

X18 S1 phi1 phi1bar phi2 phi2bar S10 vdd 0 DELAY

X19 S1 phi1 phi1bar phi2 phi2bar S11 vdd 0 DELAY

X20 S2 phi1 phi1bar phi2 phi2bar S20 vdd 0 DELAY

X21 S2 phi1 phi1bar phi2 phi2bar S21 vdd 0 DELAY

X22 S3 phi1 phi1bar phi2 phi2bar S30 vdd 0 DELAY

X23 S3 phi1 phi1bar phi2 phi2bar S31 vdd 0 DELAY

X24 Cout phi1 phi1bar phi2 phi2bar Cout0 vdd 0 DELAY

X25 Cout phi1 phi1bar phi2 phi2bar Cout1 vdd 0 DELAY

*Type of analysis
.option dcon=1 post
.tran 100ps 50ns
*.DC vinA 0 1.5 .01

*measurements
.MEAS avg_power avg power
.MEAS TRAN Avg_P_VDD AVG P(vdd) FROM=0.0ns TO=15ns
.MEAS TRAN Avg_P_VDD1 AVG P(vdd1) FROM=20.0ns TO=50ns
.MEAS TRAN Avg_P_VC AVG P(vinCin) FROM=0.0ns TO=15ns
.MEAS TRAN Avg_P_VA AVG P(vinA0) FROM=0.0ns TO=15ns
.MEAS TRAN Avg_P_VB AVG P(vinB0) FROM=0.0ns TO=15ns
.end

APPENDIX B: INTEGRATED CIRCUIT LAYOUTS

This appendix contains the CADENCE/VIRTUOSO layout of all the implemented chips
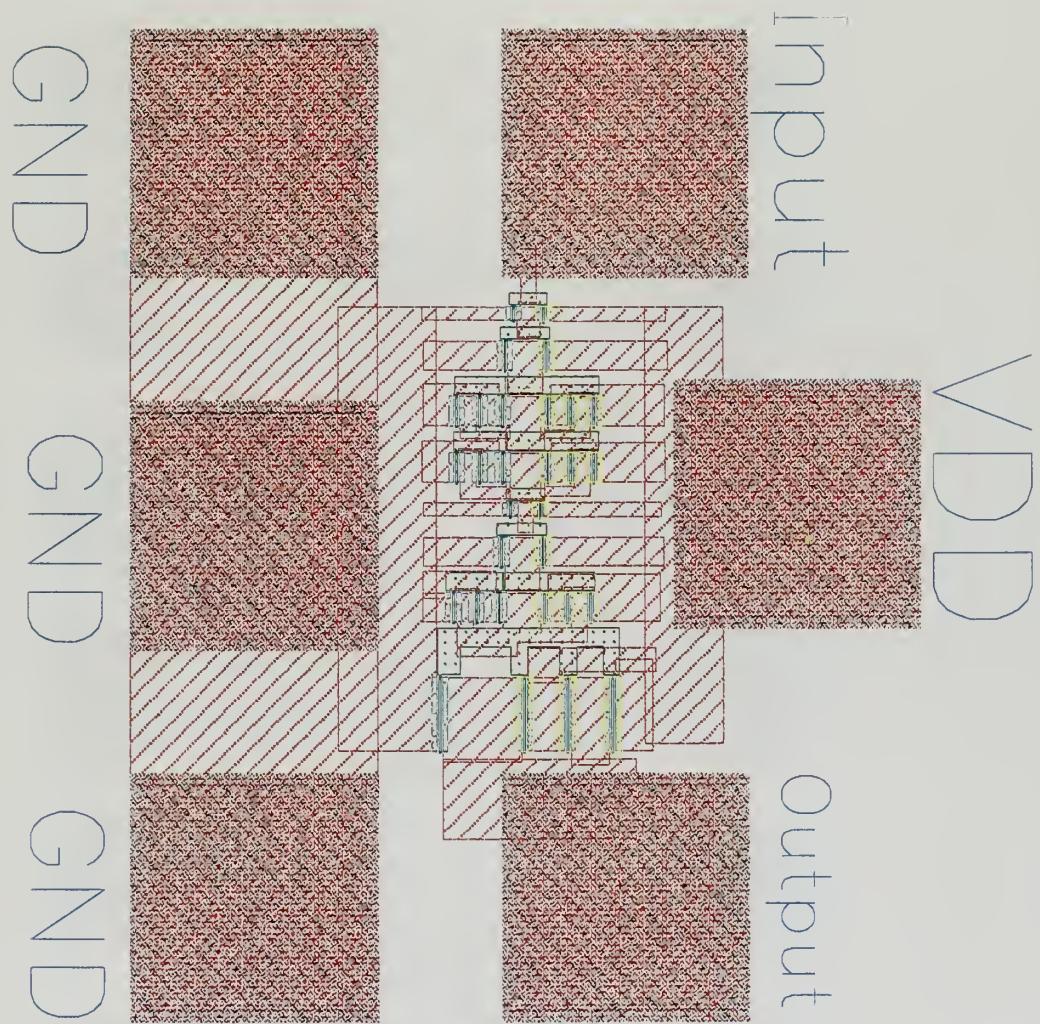
Static Linear Feedback Shift Register
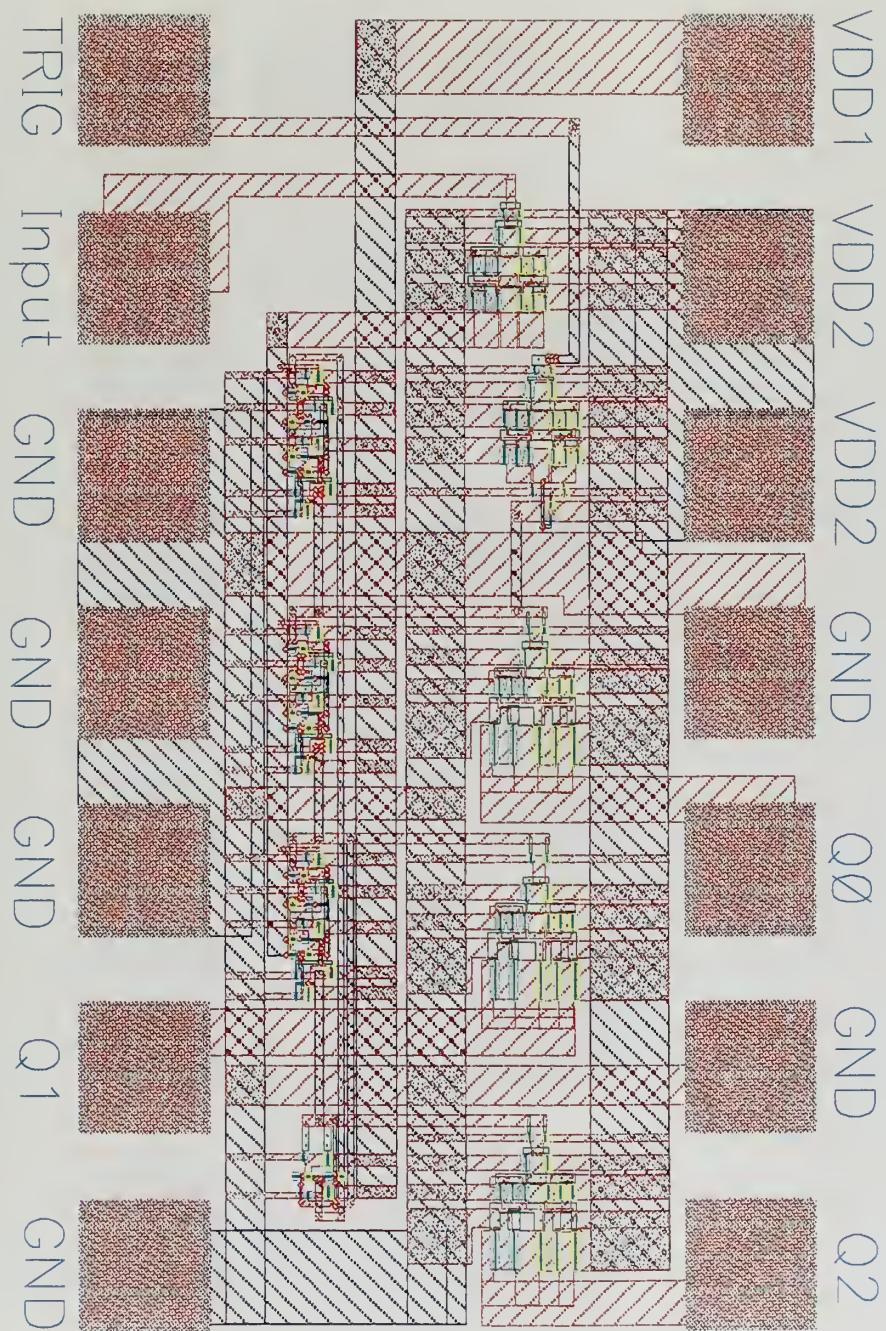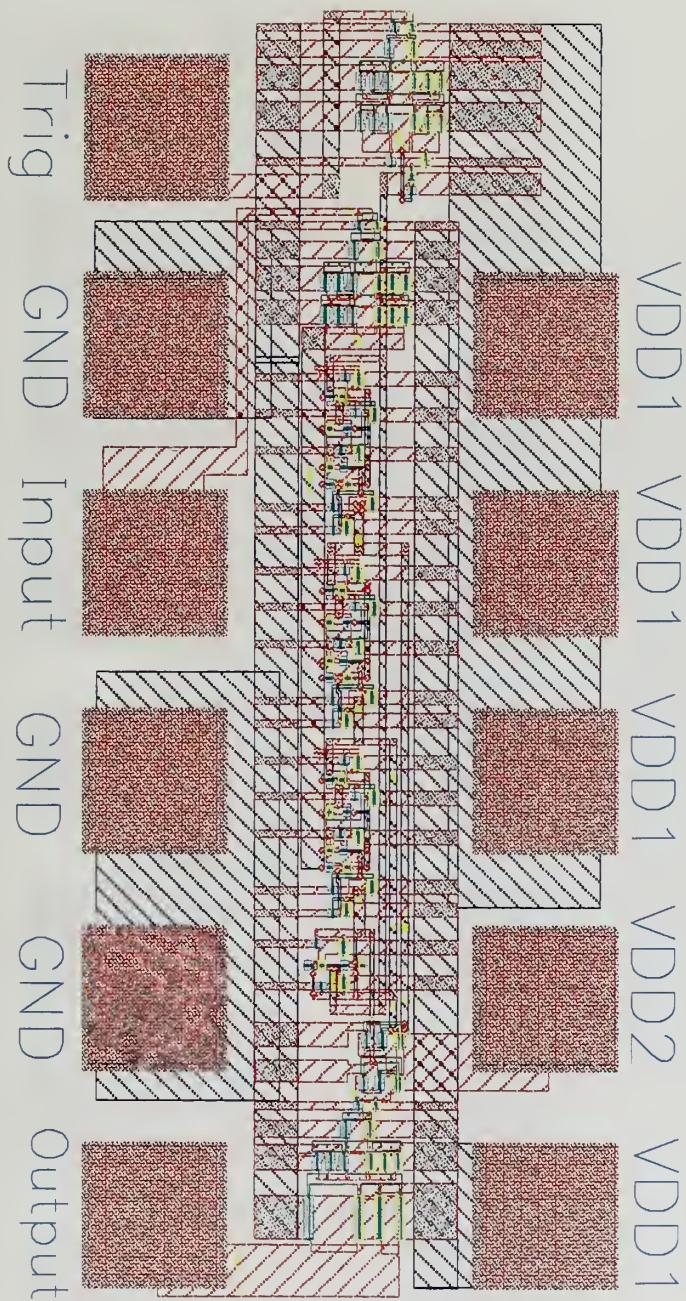
VDD1 VDD2 VDD2 GND Q0 GND Q1 GND Q2

TRIG Input GND GND GND Q1 GND

Static Logic Logic Function

Trig   GND   Input   GND   GND   Output

VDD1   VDD1   VDD1   VDD1   VDD2   VDD1

Clock Generator

Input
GND
GND
GND
phi1
GND
GND
phi2

VDD2
VDD1
–phi1
GND
VDD2
–phi2
GND
VDD2

245

TPDL Linear Feedback Shift Register

246

TPDL Function Generator

GND GND GND GND GND GND GND GND GND

Input

VDD1 VDD1 VDD1 VDD1 VDD1 VDD1 VDD2 Trig VDD1

Input

Out

247
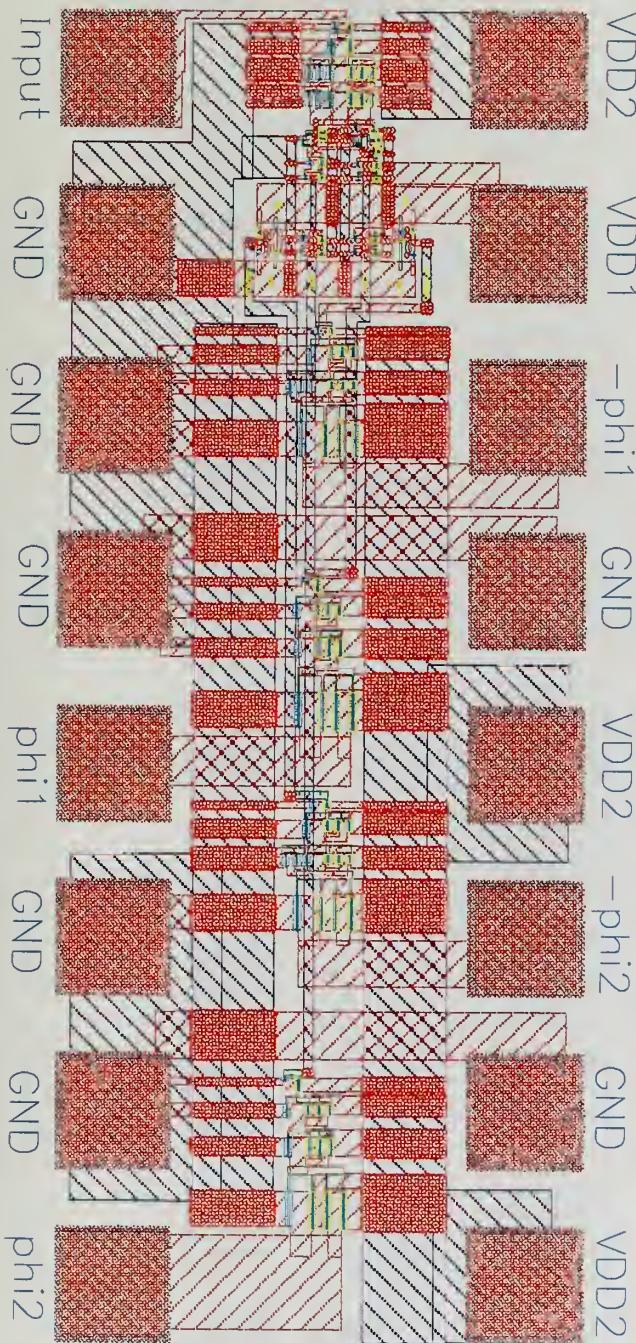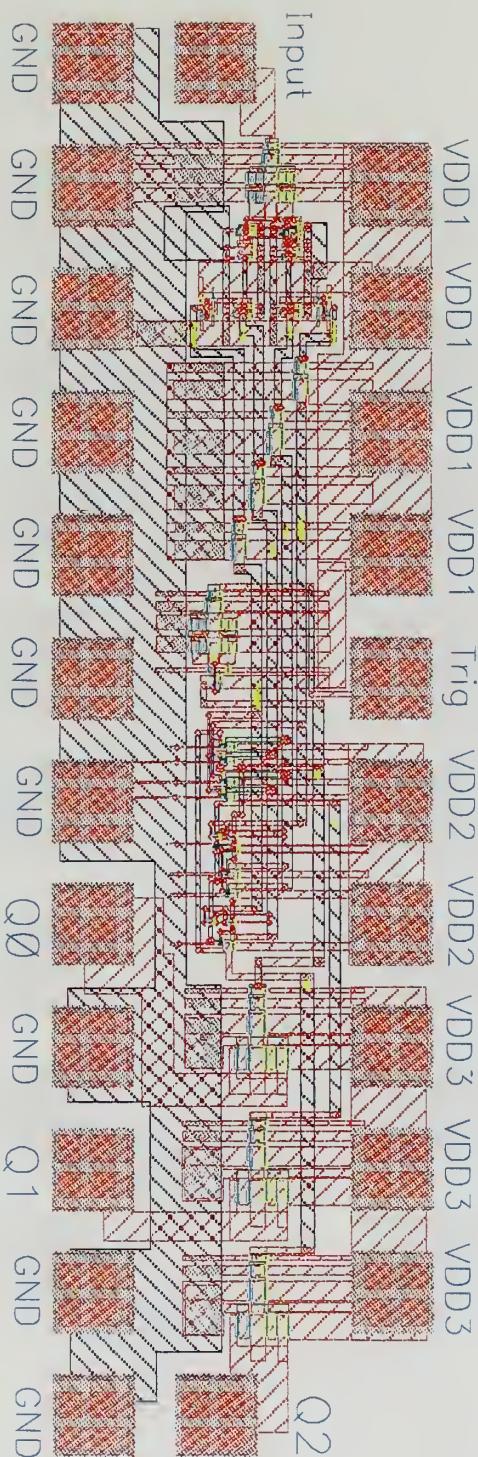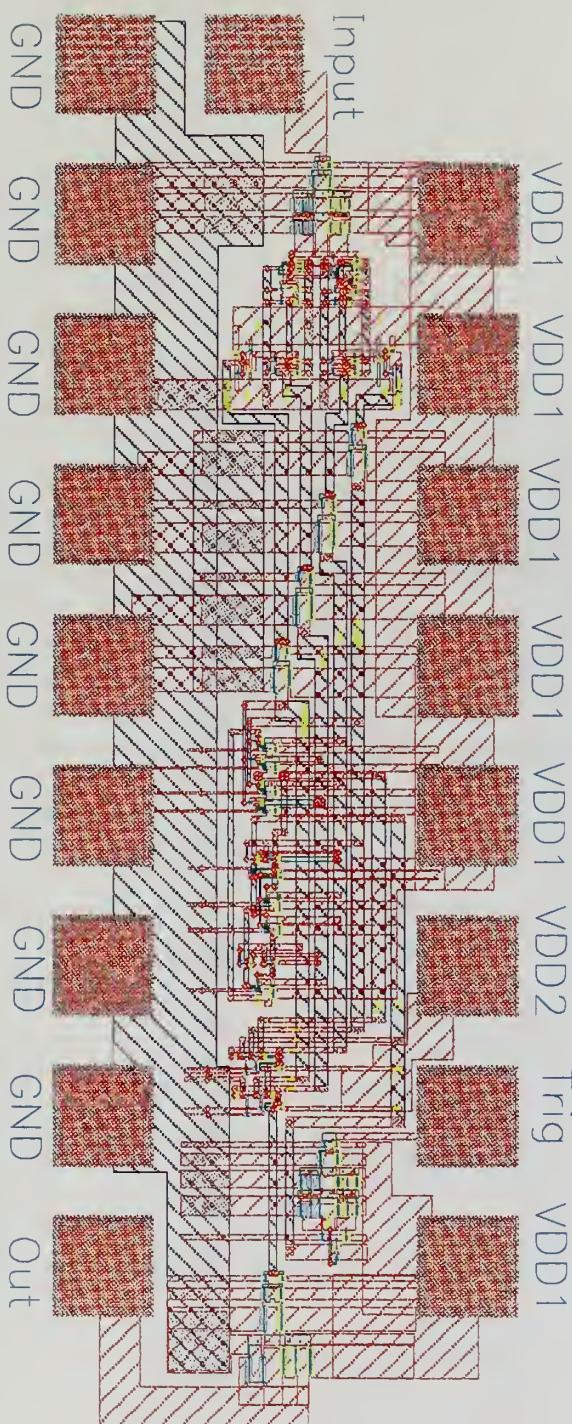
TPDL 4—Bit CLA
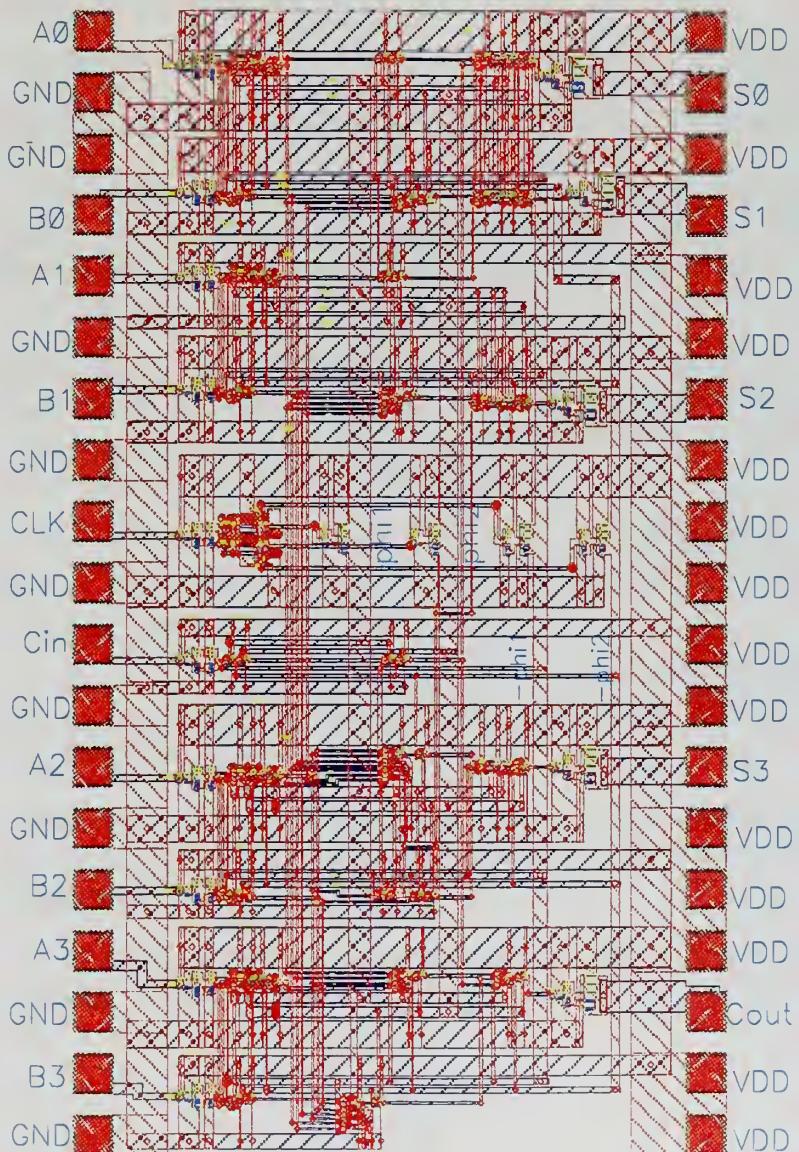
LIST OF REFERENCES

1.	P. Flahive, W. Clemetson, P. O'Connor, A. Dori, and S. C. Shunk, "A GaAs DCFL Chip set for multiplexer and demultiplexer applications at gigabit/sec. data rates," *IEEE GaAs IC Symposium Technical Digest*, pp. 7-10, October 1984.

2.	H. Nakamora, K. Tanaka, K. Inokuchi, T. Saito, Y. Kawakami, Y. Sano, M. Akiyama, and K. Kaminishi, "2 GHz multiplexer and demultiplexer using DCFL/SBFL circuit and the precise Threshold voltage control process," *IEEE GaAs IC Symposium Technical Digest*, pp. 151-154, October 1986.

3.	M. McDonald and G. McCormack, "A 12:1 Multiplexer and demultiplexer chip set for use in fiber optic communication system," *IEEE GaAs IC Symposium Technical Digest*, pp. 229-232, October 1986.

4.	T. Suzuki, S. Shikata, S. Nakajima, N. Herakata, Y. Mikamura, and T. Sugawa, "GaAs IC family for high speed optical communication systems," *IEEE GaAs IC Symposium Technical Digest*, pp. 225-228, October 1986.

5.	N. Kotera, K. Yamashita, Y. Hatta, T. Kinoshita, M. Miyakazi, and M. Maeda, "Laser driver and receiver amplifiers for 2.4 Gbit/s optical transmission using WSi-gate GaAs MESFETs," *IEEE GaAs IC Symposium Technical Digest*, pp. 103-106, October 1987.

6.	S. Notomi, Y. Asona, M. Kosugi, T. Nagata, K. Kosemura, M. Ono, N. Kobayashi, H. Ishiwari, K. Odani, T. Mimura and M. Abe, "A high speed 1K X 4-Bit static RAM using 0.5 um-gate HEMTs," *IEEE GaAs IC Symposium Technical Digest*, pp. 177-180, October 1987.

7.	M. Ino, H. Suto, H. Kata, H. Yamazaki, "A 1.2 ns GaAs 4kb Read Only Memory fabricated by 0.5 um-gate BP-SAINT," *IEEE GaAs IC Symposium Technical Digest*, pp. 189-192, October 1987.

8.	R. V. Gauthier, J. Weissman, and B. E. Peterson, "A 150 MOPS GaAs 8-bit slice processor," *IEEE International Solid State Circuits Conference Technical Digest*, pp. 32-33, February1988.

9.	E. Delhaye, C. Rocher, M. Fichelson, and I. Lecuru, "A 3.0 ns, 350 nW 8 x 8 Booth's Multiplier," *IEEE GaAs IC Symposium Technical Digest*, pp. 249-252, October 1987.

10.	J. S. Blakemore, "Semiconducting and other major Properties of Gallium Arsenide," *Journal of Applied Physics*, vol. 53, pp. R123-R181, October 1982.

11.   J. R. Chelikowsky, and M. L. Cohen, "Nonlocal Pseudopotential calculations for the electronic structure of eleven Diamond and Zinc-Blende semiconductors," *Physics Review*, vol. B14, pp556, 1976.

12.   S. I. Long and S. E. Butner, Gallium Arsenide Digital Integrated Circuit Design, McGraw-Hill, New York, NY, 1990.

13.   S. J. Harrold, An Introduction to GaAs IC Design, Prentice Hall, New York, NY, 1993

14.   Omar Wing, Gallium Arsenide Digital Circuits, Kluwer Academic Publishers, Boston, MA, 1990.

15.   Robert Soares, GaAs MESFET circuit design, Artech house, Boston, MA, 1988.

16.   C. Y. Chang and Francis Kai, GaAs high-speed devices physics, technology and circuit applications, Wiley-Interscience, New York, NY, 1994.

17.   R. Zuleeg and K. Lehovec, "Radiation effects in GaAs JFET devices," *IEEE Transaction Nuclear Science*, NS-27, pp.1343-1354, 1980.

18.   R. Zuleeg. J. K. Northof, and G. L. Troeger, "Channel and substrate currents in GaAs FETs due to ionizing radiation," *IEEE Transaction Nuclear Science*, NS-30, pp. 4151-4156, 1983.

19.   R. E. Lundgren, C. F. Crumm, and R. F. Lohr, "Enhancement mode GaAs MESFET Logic," *IEEE GaAs IC symposium Technical Digest*, Lake Tahoe, CA, September, 1979.

20.   L. Yang, A. T. Yuen and S. I. Long, "A simple method to improve the noise margin of III-V DCFL digital circuit, coupling diode FET logic," *IEEE Electron Device Letters*, vol. EDL-7 pp. 75-78, March 1986.

21.   R. Van Tuyl, and C. Liechti, "High speed integrated logic with GaAs MESFETs," *IEEE Journal Solid State Circuits*, vol. SC-9, pp. 269-276, 1974.

22.   R. C. Eden, B. M. Welch, and R. Zucca, "Low power GaAs digital ICs using Schottky diode-FET logic," *IEEE International Solid State Circuit Conference Proceedings*, San Francisco, CA, pp. 68-69, February, 1978.

23.   M. J. Helix, S. A. Jamison, C. Chao, M. S. Shur, "Fan out and speed of GaAs SDFL logic," *IEEE Journal Solid State Circuits*, vol. SC-17, pp. 1226-231, December 1982.

24.   R. C. Eden, F. S. Lee, S. I. Long, B. M. Welch, and R. Zucca, "Multi-level logic gate implementation in GaAs IC's using Schottky diode FET logic," *International Solid State Circuits Conference Proceedings*, pp. 122-123, February 1980.

25.   T. Vu, P. Roberts, R. Nelson, G. Lee, B. Hanzal, N. Zafar, D. Lamb, M. Helix, S. Jamison, S. Hanka, J. Brown, and M. Shur, "A Gallium Arsenide Gate Array with on-Chip RAM," *IEEE Transaction Electron Devices*, ED-31, pp. 144-156, 1984.

26.   A. Tamura, et al, "High speed GaAs SCFL Divider," *IEEE Electron Device Letters*, vol. 21, pp.605-606, July 1985.

27.   S. Katsu, S. Shemano, and G. Kano, "A source coupled FET logic - A new current mode approach to GaAs logics," *IEEE Transaction Electron Devices*, vol. ED-32, pp. 1114-1118, June 1985.

28.   P. Mellor, and A. Livingstone, "Capacitor-coupled logic using GaAs depletion mode FETs," *IEEE Electron Device Letters*, vol. 16, pp. 749, 1980.

29.   A. Livingstone, and D. Welbourn, "Design considerations of coupling capacitors in GaAs integrated circuits," *Journal Applied Physics*. Japan, Suppl. 22-1, pp. 393-396, 1983.

30.   R. C. Eden, "Capacitor diode FET logic (CDFL) circuit approach for GaAs D-MESFETs ICs," *IEEE GaAs IC Symposium Technical Digest*, Boston, MA, pp. 11-14, October 1984.

31.   K.Tanaka, H. Nakamura, Y. Kawakami, T. Ishida, and K. Kamanishi, "Super buffer FET logic (SBFL) for GaAs gate arrays," *IEEE Custom Integrated Circuits Conference Proceedings*, Portland, OR, pp. 425-428, May 1985.

32.   Neil H. E. Weste, Principles of CMOS VLSI Design a system perspective, Addison Wesely, New York, NY, 1993.

33.   R. H. Krabeck, and C. Lee, H. Law, "High speed compact circuits with CMOS," *IEEE Journal Solid State Circuits*, vol. SC-17, pp. 614-619, June 1982.

34.   V. Friedman, and S. Liu, "Dynamic logic CMOS circuits," *IEEE Journal Solid State Circuits*, vol. SC19, pp. 263-266, April 1984.

35.   N. Gonclaves, and H. DeMan, "NORA: a race-free dynamic CMOS technique for pipelined logic structures," *IEEE Journal Solid State Circuits*, vol. SC-18, pp. 261-266, June 1983.

36. C. Lee, and E. Szeto, "zipper CMOS," *IEEE Circuits and Systems Magazine*, pp. 10-16, May 1986.

37. M. Rocchi, and B. Gabillard, "GaAs digital dynamic IC's for applications up to 10 GHz," *IEEE Journal Solid State Circuits*, vol. SC-18, pp. 369-376, June 1983.

38. J. Jasen, L. Salmon, D. Deakin, and M. Delaney, "26 GHz room temperature dynamic divider circuit," *IEEE GaAs IC symposium Technical Digest*, Portland, OR, pp. 201-204, October 1987.

39. M. Namordi, P. Newman, A. Cappon, L. Hanes, and H. Statz, "A 2.2 GHz transmission gate GaAs shift register," *IEEE International Solid State Circuits Conference Proceedings*, pp. 218-219, 1985.

40. R. Yang, and S. Long, "A high speed dynamic Domino circuit implemented with GaAs MESFETs," *IEEE Journal Solid State Circuits*, vol. SC-22, pp. 874-879, October 1987.

41. H. David, and C. Salama, "Dynamic GaAs Copulatively Coupled Domino Logic (CCDL)," *IEEE Journal Solid State Circuits*, vol. SC-26, pp. 844-849, June 1991.

42. H. David, and C. Salama, "GaAs Trickle Transistor Dynamic Logic (TTDL)," *IEEE Journal Solid State Circuits*, vol. SC-26, pp. 1441-1448, October 1991.

43. Nary, Kavin, "Gallium Arsenide Metal-Semiconductor Field Effect Transistor Dynamic Logic Gate Topology," *Ph.D. Dissertation*, University of California, Santa Barbra, 1993.

44. Kavin R. Nary and Stephen I. Long, "Two-Phase Dynamic FET Logic: An Extremely Low Power, High Speed Logic Family for GaAs VLSI," *IEEE GaAs IC symposium Technical Digest*, pp. 83-86, 1991.

45. Kavin R. Nary and Stephen I. Long, "A 1 mW 500 MHz 4-Bit adder Using Two-Phase Dynamic FET Logic Gates," *IEEE GaAs IC symposium Technical Digest*, pp. 97-100, 1992.

46. Kavin R. Nary and Stephen I. Long, "GaAs Two-Phase Dynamic FET Logic: A Low-Power Logic Family for VLSI," *IEEE Journal Solid State Circuits*, vol. 27, no. 10, pp. 1364-1371, October 1992.

47. Peter S. Lassen, Stephen I. Long and Kavin R. Nary, "Ultra Low-Power GaAs MESFET MSI Circuits Using Two-Phase Dynamic FET Logic," *IEEE Journal Solid State Circuits*, vol. 28, no. 10, pp. 1038-1045, October 1992.

48.   J. Pastimak, and C. Salama, "GaAs MESFET Differential Pass-Transistor Logic," *IEEE Journal Solid State Circuits*, vol. SC-26, pp. 1309-1316, September 1991.

49.   Khaled A. Shehata and D. J. Fouts, "Two-Phase Dynamic Logic Circuits For Complementary GaAs Processes," to be Published, *Thirtieth Annual Asilomar Conference on Signals, Systems, and Computers*, November, 1996.

50.   Khaled A. Shehata and D. J. Fouts, "Low-Power High-Speed Complementary GaAs Dynamic Logic," to be Published, *IEEE International Electron Devices Meeting*, December, 1996.

51.   Khaled A. Shehata and D. J. Fouts, "A CGaAs TPDL 1.0 GHz 4-Bit Carry Lookahead Adder," to be Published, *IEEE International Symposium on Circuits and Systems*, December, 1996.

52.   Bruce Bernhardt, M. LaMacchia, J. Abrokwath, J. Hallmark, R. Lucero, B. Mathes, B. Crawforth, D. Foster, K. Clauss, S. Emmert, T. Lien, E. Lopez, V. Mazzotta and B. Oh, "Complementary GaAs: A High Speed BiCMOS Alternative," *IEEE GaAs IC Symposium Technical Digest*, San Diego, Cal. Invited Paper, pp. 18-21, October 1995.

53.   P. P. Ruden, Michael Shur, David K. Arch, R. R> Danials, David E. Grider and Thomas E. Nohava, "Quantum-Well p-channel AlGaAs/InGaAs/GaAs Hetrostructure Insulated Gate Field Effect Transistors", *IEEE Transaction on Electron Devices*, Vol. ED-36, No. 11, pp.2371-2378, November 1989.

54.   D. E. Grider, P. P. Ruden, J. C. Nohava, I. R. Mactaggart, J. J. Stronozer and R. H. Tran, "0.7 Micron Gate Length Complementary $Al_{0.75}Ga_{0.25}As/In_{0.25}Ga_{0.75}As/GaAs$ HIGFET Technology for High Speed/Low Power Digital Circuits" *IEEE International Electron Devices Meeting Technical Digest*, pp. 331-334, 1992.

55.   P. P. Ruden, A. I. Akinwande, D. Narum, D. E. Grider and J. Nohava, "High Performance Complementary Logic Based on GaAs/InGaAs/AlGaAs HIGFETs," *IEEE International Electron Devices Meeting Technical Digest*, pp. 117-120, 1989.

56.   D. E. Grider, A. I. Akinwande, R. Mactaggart, P. P. Ruden, J. C. Nohava, T. E. Nohava, J. E. Breezley, P. Joslyn and D. Tetzlaff, "Development of Static Random Access Memories using Complementary Hetrostructure Isolated Gate Field Effect Transistor Technology," *IEEE GaAs IC symposium Technical Digest*, 1990.

57. D. E. Grider, R. Mactaggart, J. C. Nohava, J. J. Stronozer, P. P. Ruden, T. E. Nohava, D. Fulkerson and D. Tetzlaff, "A 4 K Bit Synchronous Static Random Access Memory Based Upon Delta-Doped Complementary Hetrostructure Insulated Gate Field Effect Transistor Technology," *IEEE GaAs IC symposium Technical Digest*, pp. 71-74, 1991.

58. P. P. Ruden, Michael Shur, A. I. Akinwande, J. C Nohava, D. E. Grider, Junho Baek, "AlGaAs/InGaAs/GaAs Quantum Well Doped Channel Hetrostructure Field Effect Transistors," *IEEE Transaction on Electron Devices*, Vol. 37, No. 10, pp.2171-2175, October 1990.

59. D. E. Grider, P. P. Ruden. J. C. Nohava, I. R. Mactaggart, J. J. Stronozer, T. E. Nohava and S. S. Swirhun, "Delta-Doped Complementary Hetrostructure FETs with High Y-Value Pseudomorphic $In_yGa_{1-y}As$ Channels for Ultra-low-power Digital IC Applications," *IEEE International Electron Devices Meeting Technical Digest*, pp. 235-238, 1991.

60. A. I. Akinwande, P. P> Ruden, D. E. Grider, J. C. Nohava, T. E. Nohava, P. D. Joslyn and J. E. Breezley, "Complementary III-V Hetrostructure FETs for Low Power Integrated Circuits," *IEEE International Electron Devices Meeting Technical Digest*, pp. 983-985, 1990.

61. R. R. Danials, R. Mactaggart, J. K. Abrokwah, M. Shur, J. Beek and B. Jenkins, "Complementary hetrostructure insulated gate FET circuits for high-speed, low-power VLSI," *IEEE International Electron Devices Meeting Technical Digest*, pp. 448-451, 1986.

62. Thomas J. Cunningham, Eric R. Fossum and Steven M. Baier, "Noise and current-voltage characterization of complementary hetrojunction field-effect transistor (CHFET) structure below 8 K," *Proceedings of SPIE Infrared Readout Electronics*, vol. 1684, pp. 84-92, 1992.

63. P. O' Neil, B. Bernhardt, F. Nikpourian, C. Della, Y. Abad, Greg Hansell, "GaAs Integrated Circuit Fabrication at Motorola," *IEEE GaAs IC Symposium Technical Digest*, pp. 123-126, 1993.

64. J. Abrokwath, J. Huang, C. Shurboff, J. Hallmark, R. Lucero, Motorola PCRL and J. Gilbert, B. Bernhardt, G. Hansell, Motorola CS-1, "A Manufacturable Complementary GaAs Process," *IEEE GaAs IC Symposium Technical Digest*, pp. 127-130, 1993.

INITIAL DISTRIBUTION LIST

1. Defense Technical Information Center   2
   8725 John J. Kingman Rd., STE 0944
   Ft. Belvoir, VA 22060-6218

2. Dudley Knox Library   2
   Naval Postgraduate School, 411 Dyer Rd.
   Monterey, CA 93943-5101

3. Chairman, Code EC   1
   Department of Electrical and Computer Engineering
   Naval Postgraduate School
   Monterey, CA 93943-5121

4. Prof. Douglas Fouts, Code EC/Fs   1
   Department of Electrical and Computer Engineering
   Naval Postgraduate School
   Monterey, CA 93943-5121

5. Prof. Sherif Michael, Code EC/Mi   1
   Department of Electrical and Computer Engineering
   Naval Postgraduate School
   Monterey, CA 93943-5121

6. Prof. Herschel H. Loomis, Jr., Code EC/Lm   1
   Department of Electrical and Computer Engineering
   Naval Postgraduate School
   Monterey, CA 93943-5121

7. Prof. Yutaka Kanayama, Code CS/Ka   1
   Department of Computer Science
   Naval Postgraduate School
   Monterey, CA 93943-5118

8. Prof. Rick Howard, Code AA/Ho   1
   Department of Aeronautics and Astronautics
   Naval Postgraduate School
   Monterey, CA 93943-5106

9.   Maj. Hazem F. Abdel Hamid   2
      SGC # 3078, NPS
      Monterey, CA 93943

10.   LTC. Nabil Khalil   1
      SGC # 3079, NPS
      Monterey, CA 93943

11.   Khaled Ali Shehata   5
      Nahia, Embaba, Giza
      Egypt

12.   Osman Mohamed Ibrahim   2
      Apartment # 23
      15 Officers Housing, Mazrat El-Haram
      El-Haram, Giza
      Egypt

13.   Egyptian Armament Authority, Training Dept.   3
      c/o American Embassy (Cairo, Egypt)
      Office of Military Cooperation
      Box 29 (TNG)
      FPO, NY 09257-0051

14.   David Foster   1
      Motorola Inc.
      Government System Division
      8201 E. McDowell Rd.,
      Scottsdale, AZ 85257
      MS-H1021

15.   John Abrokwah   1
      Motorola Inc.
      Corporate Research Laboratory
      2100 E Elliot Rd.
      Tempe, AZ 85284
      MS-EL508

16. Brian Crawforth   1
    Motorola Inc.
    Government System Division
    8201 E. McDowell Rd.,
    Scottsdale, AZ 85257
    MS-H1021

17. Michael LaMacchia   1
    Motorola Inc.
    Government System Division
    8201 E. McDowell Rd.,
    Scottsdale, AZ 85252-1417
    MS-H1021

18. Jeff Ingles   1
    R22, Rand E Building
    National Security Agency
    9800 Savage Rd., Suite 6516
    Ft. George C. Meads, MD 20755-6516

19. Brian Weeks   1
    R22, Rand E Building
    National Security Agency
    9800 Savage Rd., Suite 6516
    Ft. George C. Meads, MD 20755-6516

20. Bill Schneider   1
    Naval Research Laboratory
    14675 Lee Rd.
    Chantilly, VA 20151-1715
    Room 41B18E

21. Bill Sharp   1
    V-34 / FANX3
    National Security Agency
    9800 Savage Rd., Suite 6516
    Ft. George C. Meads, MD 20755-6000

22. Dr. Stephen I. Long   1
    Dept. of Elect. and Comp. Eng.,
    Univ. of Calif.
    Santa Barbra, CA 93106

23. Dr. Steven E. Butner
    Dept. of Elect. and Comp. Eng.
    Univ. of Calif.
    Santa Barbra, CA 93106   1

24. Dr. Kevin Nary
    Rockwell Science Center
    1049 Dos Rios
    Thound Oaks, CA 91358   1

25. Dr. Richard Brown
    Dept. of Elect. Eng. and Comp. Sci.
    Univ. of Michigan
    Ann Arbor, MI 48109   1

26. Dr. Allen Ross, Code EC/
    Department of Electrical and Computer Engineering
    Naval Postgraduate School
    Monterey, CA 93943-5121   1

27. Andrew Fox, Code 8110
    Naval Research Laboratory
    4555 Overlook Ave., S. W.
    Washington, D.C. 20375   1